EKLF-MEDIATED TRANSCRIPTION OF ERYTHROID GENES

AURELIE D. C. DESGARDIN

KINGSTON UNIVERSITY
&
THE UNIVERSITY OF CHICAGO

This thesis is being submitted in partial fulfillment of the requirements of the University for a Ph.D degree

May 31, 2010

IN MEMORIAM

Antoine, Jean, Michel DESGARDIN

1952-2010

I would like to dedicate this work to the most valuable persons in my life, without whom it would never have been accomplished.

First and foremost, my parents, Antoine and Martine Desgardin, for teaching me to be strong, persistent and allowing me to pursue my dreams. My thesis is most particularly dedicated to my father who fought his hardest to stay with us but who unfortunately did not live to see the final product. It was his wish that I complete this work and make him proud.

Lastly, I would like to dedicate this work to my uncle and his wife, Fabrice and Khadija Desgardin, as well as my brother Benjamin, for showing me what family and unity are all about.

ACKNOWLEDGEMENTS

I would like to thank my advisors, Dr John Cunningham and Dr Andrew Jewell, whose encouragement, guidance and support from the initial to the final level enabled me to develop as a scientist.

I would also like to thank my examiners, Dr John Peacock and Prof Swee Lay Thein. Their comments and suggestions have been extremely useful in shaping my thesis.

I would like to express my deepest gratitude towards every member of the Cunningham lab, past and present, for helping and participating in my training as a scientist, and for creating a congenial and fun work environment. A special thanks to Tatiana Abramova and Jenny Lin who contributed more than fairly to the completion of this project.

Lastly, I offer my regards and blessings to all of those who supported me in any way during the completion of the project and most particularly my best friend Daniel Sowu, for his unwavering support and encouragement.

TABLE OF CONTENTS

ABSTRACT

Erythroid Krüppel-like factor (EKLF) is an erythroid specific transcription factor that binds to the proximal β-globin gene promoter and is essential for high level expression. In addition, EKLF binds to the far upstream enhancer commonly referred to as the Locus Control Region (LCR). The nature of these two events, their relationship to other events at the multigene β-globin locus and the precise and required interaction of these *cis*-acting sequences remains unclear. Equally, the mode of action of EKLF at other erythroid-specific gene loci that are not regulated by an LCR has not yet been reported. These targets include chaperones, membrane-bound proteins, and enzymes of the heme biosynthesis pathway that are essential for red blood cell function. To elucidate the role of EKLF at the multigene locus, and at other erythroid genes, we monitored the temporal EKLF-directed events across the β-globin locus, at the AHSP and Dematin as well as the ALAD promoter using a unique 4-OH-Tamoxifen EKLF-inducible erythroid cell line (JH31), developed in the laboratory, chromatin immunoprecipitation (ChIP) studies, and DNaseI hypersensitivity assays.

We demonstrate here that EKLF is not required for priming of the β-globin locus for expression. However, EKLF is essential for maximal erythroid factor occupancy, recruitment of chromatin-modifying enzymes, and effective recruitment of the RNA Polymerase II complex. We show that EKLF recruits these complexes first to the LCR prior to the β-globin promoter, suggesting that the LCR serves as a docking element. Finally we provide evidence that the LCR/promoter interacting factor, Ldb-1, is recruited to the β-promoter in an EKLF-dependent manner. We extend our observations to several EKLF-regulated genes outside the β-globin cluster, demonstrating not only the kinetics of transcriptional activation, but also a previously unknown mechanism of chromatin remodeling that implicates histone eviction. Finally, we report a discrepancy between the roles of the histone acetyltransferases CBP and p300 at EKLF target gene promoters, challenging conservative notions of basic transcriptional events. Together, our observations

deepen our understanding of the mechanisms of action of EKLF, and provide a platform for additional studies.

-CHAPTER 1-

GENERAL INTRODUCTION

I- OVERVIEW OF ERYTHROPOIESIS

Erythropoiesis constitutes the developmental process during which early erythroid progenitor cells differentiate into mature enucleated red blood cells. This pathway is integrated into the biological process of hematopoiesis which is best described as blood cell formation and development from a common pluripotent progenitor cell termed the Hematopoietic Stem Cell or HSC. The progeny of HSCs gradually differentiate into hematopoietic progenitors cells with less potential which ultimately transition into progenitor cells irreversibly committed to a single hematopoietic lineage (*1*). Commitment of progenitor cells to differentiation is regulated by cytokines as well as a variety of lineage-specific transcription factors (TFs) including SCL/TAL-1, LMO2, c-myb, PU.1, Gfi-1, GATA-1, GATA-2, NF-E2 and EKLF (*1-2*). An illustrated overview of hematopoiesis is represented in figure 1.1.

Fate decision in bi-potent megakaryocyte-erythroid progenitors (MEP), towards the erythroid lineage is modulated by the cytokines SCF, IL3, IL9 as well as transcription factors including GATA-1/GATA-2 and FOG-1(*2-6*). Once erythroid, differentiation is predominantly governed by erythropoietin leading to the formation of the hemoglobin producing proerythroblasts. Further transition of erythroblasts results in enucleation and the formation of RNA containing reticulocytes. Mature erythrocytes, also known as red blood cells, are a fully differentiated, enucleated end product of the pathway.

In mice, erythropoiesis occurs in two distinct developmental phases, each of

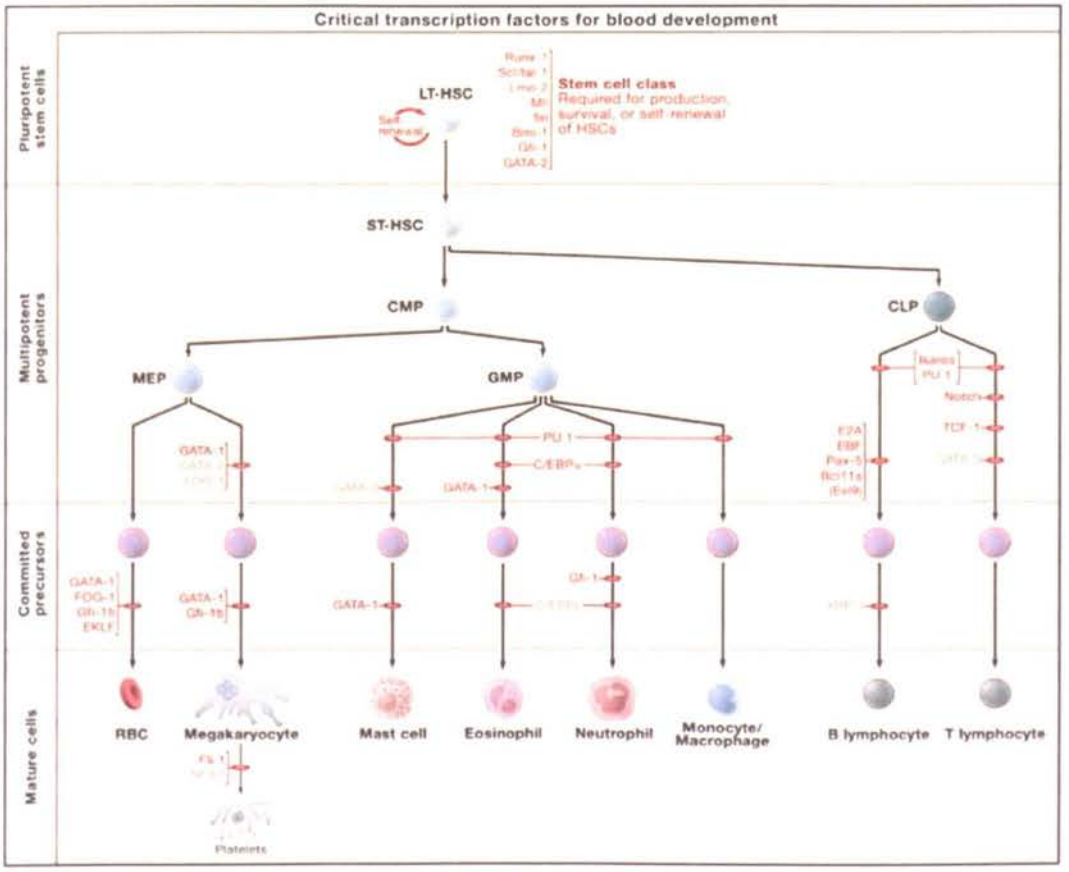

Figure 1.1. Overview of hematopoiesis. Derived from reference (*2*) Cells from the blood stream are derived from a common pluripotent stem cell. Their differentiation during ontogeny is regulated by critical transcription factors.

which is associated with specific primary sites of red blood cell production (*7-8*). The first phase of erythropoiesis, termed primitive erythropoiesis, originates in the yolk sac at embryonic day 7.5 (E7.5). HSCs are found shortly thereafter in the aorta-gonad mesonephros (AGM) region and the chorio-allantoic placenta. Primitive erythrocytes remain nucleated and express embryonic globin genes to produce Hemoglobin (Hb) consisting of variable combinations of ζ-, α-, ε-, and βh1-globin chains, which integrate a heme moiety to form the mature molecule (*9*). The onset of the second phase of erythropoiesis, termed definitive erythropoiesis, is established in the fetal liver by E10.5 and transitions to the bone marrow shortly before birth. Adult erythrocytes enucleate to form RBCs and produce large amounts of HbA which is formed of α- and β-globin chains and a heme moiety (α2β2) (*8, 10*). At this stage, genes encoding embryonic globin genes are silenced.

II- THE HEMOGLOBINIZED ADULT ERYTHROCYTE

The biological function of RBCs is entirely centered on the transport of oxygen from the lungs to the tissues via the formation of hemoglobin tetramers which efficiently and reversibly bind oxygen molecules. Appropriate function of RBCs is dependent upon its shape and deformability, appropriate formation of hemoglobin molecules and its ability to reduce oxidative stress to the hemoglobin molecule.

The red blood cell membrane

The particular biconcave discoid shape of RBCs is critical to its flexibility and allows the passage of the cell into the microvasculature. It also facilitates gaseous exchange by increasing the surface area to volume ratio of the cell. The combined

resistance and flexibility of the membrane of enucleated erythrocyte relies on its unique composition and structure. The plasma membrane constitutes its only structural component and is composed of equivalent amounts of cholesterol and phospholipids which are anchored to a flexible network of skeletal proteins via transmembrane proteins inserted into the lipid bilayer. A variety of cytoskeletal proteins tether to the cytoplasmic domain collaborate in the formation of tight but flexible junctions between the membrane protein and spectrin tetramers (*11*) (Figure 1.2).

The most relevant macromolecular complexes of the red blood cell membrane are based around Ankyrin and protein 4.1R (*12*). The tail end of β-spectrin is anchored to protein 4.1R via the complex interactions of several proteins including actin, tropomyosin, tropomodulin, adducin and dematin. This structure is often referred to as spectrin-actin junctions or junctional complex (*13*). Disruption of any protein in these complexes alters membrane stability and results in a defect termed hereditary spherocytosis (HS), hereditary elliptocytosis (HE) or hereditary ovalocytosis (HO) (*11, 14-19*).

The hemoglobin molecule

Hemoglobin is the most abundant molecule in RBCs. HbA represents the vast majority of hemoglobin in definitive erythroid cells. HbA is composed of two α-globin chains and two β-globin chains which bind to an iron-porphyrin compound, heme. Each α-chain combines with a β-chain to form a dimer which functions as a single unit within the hemoglobin tetramer. Recently, subtractive hybridization studies have led to the discovery of a α-globin chaperone (*20*). The Alpha-Hemoglobin-Stabilizing-Protein, AHSP, interacts with free α-globin chains to prevent their precipitation. The affinity of α-globin chains for AHSP is lesser

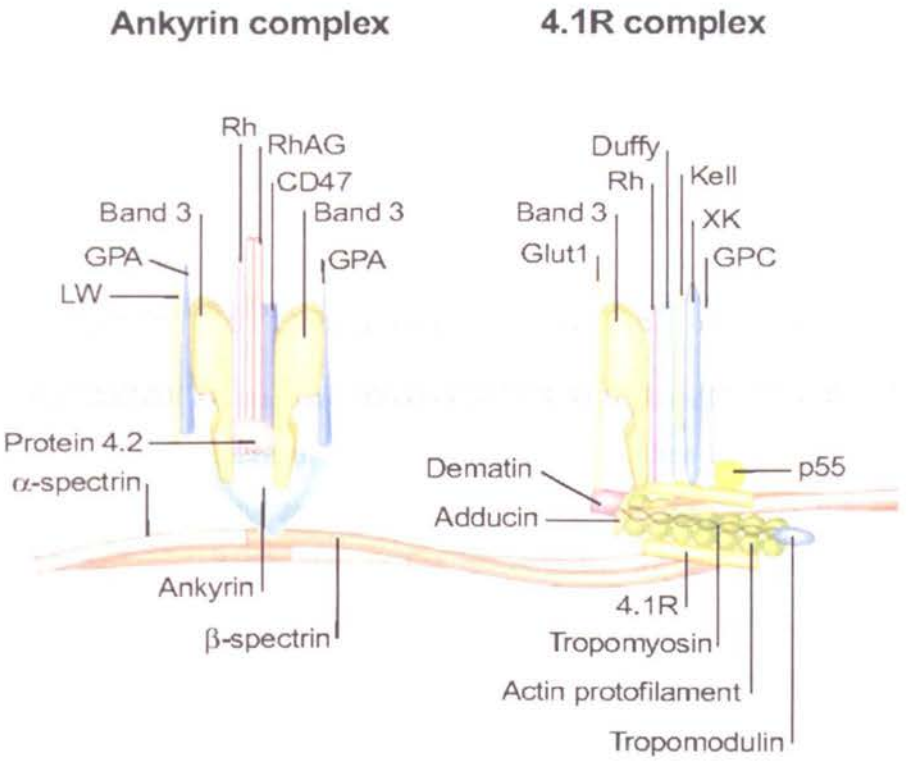

Figure 1.2. Diagram of the red cell membrane. Derived from reference (*21*). The red blood cell membrane is tethered to proteins of the cytoskeleton by a 2 dimensional system. Vertically, transmembrane protein macromolecular complexes are based around ankyrin and protein 4.1R both containing band 3 and glycoproteins. Horizontally, β-spectrin tetramers are linked at the 'head' region to ankyrin directly and stabilized with protein 4.2. The 'tail' region of β-spectrin is anchored to the 4.1R complex via a mesh of proteins including actin, tropomyosin, tropomodulin, p55, adducin and dematin which form the spectrin-actin junction complex or junctional complex.

than for β-globin chains, thereby favoring the formation of the tetramer. Structural and/or expression defects in any of the three components of the hemoglobin tetramer lead to anemia (*22-23*). A diagram of the steps of hemoglobin formation is represented in Figure 1.3.

Red blood cell metabolism

RBCs are devoid of nucleus, ribosomes and mitochondria and therefore are incapable of synthesizing proteins, or produce mitochondrialy derived energy. RBCs constantly catabolize glucose from the blood stream via the anaerobic glycolytic pathway. RBCs stay in the bloodstream for 120 days and therefore require protection against oxidative damage in order to maintain survival. Thus, the glycolytic pathway is essential to RBCs function as it produces ATP required by the membrane Na+-K+ pump to maintain cell volume.

This pathway also provides the main source of phosphorus through the production of 2,3 diphosphoglycerate (32,3 DPG). NADH is required to reconvert the oxidized hemoglobin to its native state and prevent oxidative damage and is derived from the glycolytic pathway as well as the Hexose-Monophosphate Shunt. Recently, proteins of the junctional complex have been reported to interact with the glucose-receptor 1 (GLUT-1) which therefore intimately links membrane structural integrity, deformability and metabolism. Thus, an integrated approach to synthesis of these proteins is critical for normal RBC homeostasis.

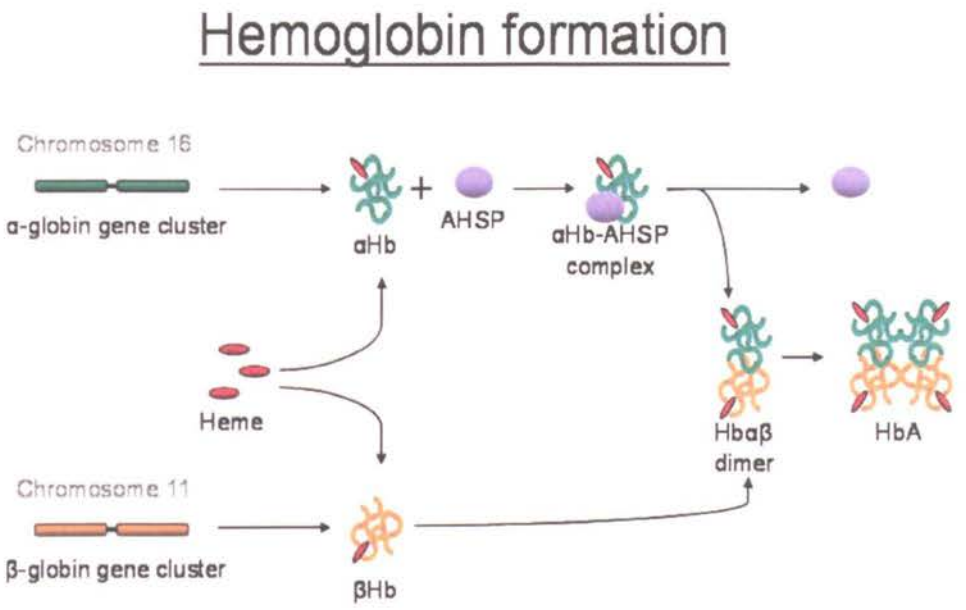

Figure 1.3. Diagram of hemoglobin formation. Adapted from (*24*). Hemoglobin chains separately bind heme. A-Hb is stabilized by AHSP and subsequently associates with β-Hb to form Hbαβ dimer. 2 Hbα dimmers assemble the hemoglobin tetramer.

III- OVERVIEW OF TRANSCRIPTION

In eukaryotes, protein-encoding genes are transcribed by the RNA polymerase II (RNA Pol-II) multiprotein enzyme complex. Gene transcription is a dynamic process which can be regulated in a tissue- and development-specific manner. For transcription to occur, an RNA Pol-II complex formed of RNA Pol-II and general transcription factors or GTFs (TFIIA, TFIIB, TFIID, TFIIE, TFIIF and TFIIH) has to recognize specific genomic sequences within the bulk of chromatin (*25*). In addition to being constricted within itself, DNA is perceived to have constitutively restrictive nature with regards to the transcription machinery, which implicates that DNA accessibility to RNA Pol-II as a regulated process (*26-27*). However, specific DNA sequences are more accessible to various proteins other than those of the transcription machinery. The transcriptional state is regulated by the combination of two types of elements which are defined as *cis*- or *trans*-regulatory elements. *Cis*-regulatory elements are located on the same DNA molecule as the controlled gene. In contrast, *trans*-regulatory elements, or *trans*-acting factors (TFs), are distinct from the gene-containing DNA molecule and can be either proteins or RNA.

Cis-regulatory element

Cis-regulatory regions can be categorized into four functionally distinct elements:

i) ***Core promoters*** are located approximately at -40 to +40 nucleotides relative to the transcriptional start site and harbor one or a combination of motifs recognized by the transcription initiation complex. These sequences are referred to as TATA box, TFIIB recognition element (BRE), initiator (Inr), motif ten element (MTE), downstream core element (DCE) and the downstream promoter element (DPE)(*28*). Upstream of these core elements lay several hundred nucleotides which encode motifs that can be recognized by a subset of sequence-specific TFs.

ii) Enhancer regions are defined as elements that increase transcription from a linked promoter. Enhancers are effective independently of their orientation and can modulate transcription from long distances (*29-30*). Not unlike promoters, enhancers are constituted of DNA binding motifs recognized by a subset of sequence-specific TFs.

Active promoters and enhancers can be detected by their hypersensitivity to DNaseI digestion. These hypersensitive sites or HS can be preferentially hydrolyzed due to their lack of nucleosomal structure (see below). Therefore, sensitivity to enzymatic digestion can be correlated to DNA accessibility (*31-32*). Active multigene loci will display a lower but general sensitivity to DNaseI that differs from the repressive chromatin characterized in regions that are not being transcribed.

iii) Locus control regions The first described Locus Control Region (LCR) was the β-globin LCR, and was defined as *cis*-regulatory elements which specify tissue specific, position-independent and copy-number-dependent expression of a linked transgene in mice (*33*). LCRs are powerful elements capable of driving transcription of a single copy of integrated transgene to levels comparable with the endogenous gene locus (*34*). Studies indicate that the LCR establishes DNA accessibility to RNA Pol-II even when the transgene is integrated in highly restrictive chromatin domains (*35-36*). LCRs can be detected as a series of HSs carrying multiple DNA binding motifs for sequence-specific transcription factors (*6, 34, 37-38*). They regulate multigene loci differentially during ontogeny.

iv) Insulators are also referred to as boundary elements. They are defined by their ability, when placed in between, to impede the effect of an enhancer on a promoter. To exert their function, insulators have to be placed appropriately, meaning they have to be located between a promoter and the potentially activating or silencing region. Insulators are characterized by the presence of motifs for specific DNA binding proteins such as CTCF (*39-40*). Insulators, like active

promoters, enhancers and LCRs, can be detected by its hypersensitivity to DNAseI digestion (*41*).

Trans-regulatory elements or *trans*-acting factors (TFs)

RNA Pol-II alone is incapable of driving transcription(*25*). This event requires the formation of a pre-initiation complex (PIC), composed of approximately 70 *trans*-acting factors is required for efficient transcription. The two key components of the complex are the TATA-binding protein (TBP) and RNA Pol-II.

RNA Pol-II is a protein complex of approximately 550KDa composed of 12 subunits. The carboxyl terminal domain (CTD) of its largest subunit is of critical importance to specify the stages of transcription (*42*). During PIC assembly, the CTD is hypophosphorylated. However, the CTD is rapidly phosphorylated upon transcriptional initiation (*43*). GTFs, although necessary for correct positioning and orientation of RNA Pol-II, are not sufficient to promote transcription of chromatinized templates *in vitro*, but are insufficient for *in vivo* function. Context-specific recruitment of sequence-specific transcription factors and co-factors are required.

Sequence-specific transcription factors are composed of several functional domains in addition to a DNA binding domain which recognizes a specific DNA motif (*44*). Additional domains include activation, repression, nuclear localization, ligand binding and chromatin remodeling structures. These domains have the capability to influence transcription via interaction with the RNA Pol-II complex either directly or indirectly, or by modulating the chromatin template.

The activity of many sequence-specific transcription factors is modulated by co-factors, many of which were initially identified by their ability to modify chromatin by enzymatic methods. These factors which have many similar functions to TFs but are unable to bind DNA in a sequence-specific manner. Most co-factors are known to affect the structure of chromatin by acting on the packaging of the DNA or by covalently modifying nucleosomal histones.

The best characterized class of chromatin remodeling complexes utilizes ATP to promote changes in the architecture of the chromatin (*45*). The SWI/SNF complex is an ATP-dependent chromatin remodeling complex of particular interest in the presented work. The complex is composed of 9 or more subunits and exhibit a minimum catalytic core containing INI1, BAF155/BAF170 combined with a conserved ATPase subunit Brg1 or Brm, which is critical to its chromatin remodeling function but dispensable for binding to nucleosomes (*46-48*). SWI/SNF complexes can slide, transfer as well as mobilize nucleosomes *in vitro* and have been implicated in promoter remodeling leading to activation or repression, elongation, splicing events and DNA loop formation *in vivo* (*49-58*). SWI/SNF complexes have been implicated in the regulation of various erythroid genes and are known co-factors of erythroid specific transcription factors (*49, 52, 59-63*).

Co-factors using histones as substrates to establish covalent modifications are also well characterized. Mostly, histone modifying enzymes acetylate, methylate, phosphorylate or ubiquitylate histones, although few other modifications have been reported. Histone acetylation and more recently methylation have been extensively studied in the context of transcription. Co-factors of importance in the presented work include Histone Acetyl Transferases (HATs) and Histone Methyl Transferases (HMTs). HATs of the KAT3 family, essentially CBP and p300, can

acetylate histones and non-histone proteins. Both co-factors have been implicated in the transcriptional regulation of erythroid genes although deficiencies in CBP and p300 preferentially affect other hematopoietic lineages (*59, 64-69*).

Chromatin structure

DNA is condensed in the nucleus as chromatin. Nucleosomes constitute the basic building blocks of chromatin and consist of 147bp of DNA wrapped around a histone octamer (*70-72*). Histone octamers are generally composed of two copies of histones H2A, H2B, H3 and H4. Histone variants can also be integrated into nucleosomes and are associated with specific functions (*73-74*). The tails of histones are N-terminal tails that extend from the histone core and are heavily modified throughout the genome and carry chemical moieties such as acetyl, methyl, ubiquitin and phosphate groups. Modifications of histone tails can influence transcription by affecting the higher order of chromatin structure (*72, 75*).

DNA stretching between histones is referred to as linker DNA. Nucleosomes together with linker DNA constitute the 10nm fiber and can be visualized as "beads on a string" by electron microscopy (*70, 72*). The next level of compaction of DNA involves linker histones which belong to the histone H1 family. Linker histones are absent from transcriptionally active chromatin and inhibit transcription *in vitro* most probably by restricting nucleosome mobility (*76-79*).

The existence of an additional order of chromatin, referred to as the 30nm fiber, is still an ongoing debate (*72, 75*). *In vitro* studies suggest that the density of the 30nm fiber is dependent upon CpG proteins and is independent of the

modification status of histone tails (*80*). In contrast, histone tail modifications such as acetylation have been associated with the relaxed conformation of the fiber which in turn facilitates transcription (*81*).

Epigenetic Regulation

This series of mechanisms modifies the base DNA sequence or the associated histone structure by chemical modification, with resultant alteration in rates of transcription.

Modification of the DNA itself is achieved by the methylation of cytosine residues of CpG dinucleotides and is commonly referred to as DNA methylation. CpG nucleotides are typically found in clusters referred to as CpG islands. DNA methylation is associated with repression of transcription (*82*).

In contrast, histone modifications can be associated with repression and/or activation of transcription. Core histones are known to be modified; however, histone tails carry the bulk of modifications. Numerous modifications have been reported so far and the multiple possible combinations of modifications have raised the idea of a "histone code" that determines the transcriptional state of associated genes (*83-85*). In addition, some modifications have been implicated in DNA replication and repair (*83, 85*).

A subset of histone modifications are very well characterized and can be associated with repressive or active chromatin states. Histone modifications can exert two functions in the context of transcription regulation. First, covalent

histone modifications can alter the structure of chromatin by influencing the interactions between adjacent nucleosomes or modifying the interaction between histones and DNA. Second, histone modifications can facilitate the recruitment of non-histone proteins. A number of co-factors encode domains known to recognize a specific histone tail modification (*85-89*). A summary of recorded histone tail modifications is represented in Figure 1.4. The best characterized histone modifications are located on histone H3 and H4. Acetylation and methylation of lysine and arginine residues are the most significant as there is an extensive body of work linking these modifications to the state of transcription (*85*). Of importance in this manuscript are the acetylation events affecting histone H3 (AcH3) and more specifically lysine 14 (H3K14Ac). These modifications have been associated with transcriptionally permissive chromatin (*90*). However, evidence for its absolute requirement for transcriptional initiation is lacking. The next set of modifications of importance is the methylation of histone H3 at lysine 4. Methylation is more complex than acetylation as a lysine residue can carry up to three methylation groups. Histone H3 methylation of lysine 4 (H3K4Me) is the most extensively studied modification as it has been proven to correlate with different status of chromatin domains. H3K4Me1 is represented at high levels at enhancer elements and has been recently used to identify novel elements across the genome (*91-94*). H3K4Me2 is associated with transcriptionally potent domains and promoters (*95*). In contrast, H3K4Me3 is established as a 'hallmark' of transcriptionally active genes and has recently been correlated with developmental genes (*90, 96-97*).

IV- TRANSCRIPTION FACTORS IN ERYTHROPOIESIS

The erythroid program is regulated by a web of lineage- and tissue-restricted transcription factors which are essential to erythropoiesis and work in combination to regulate erythroid genes in a developmental-specific manner. The

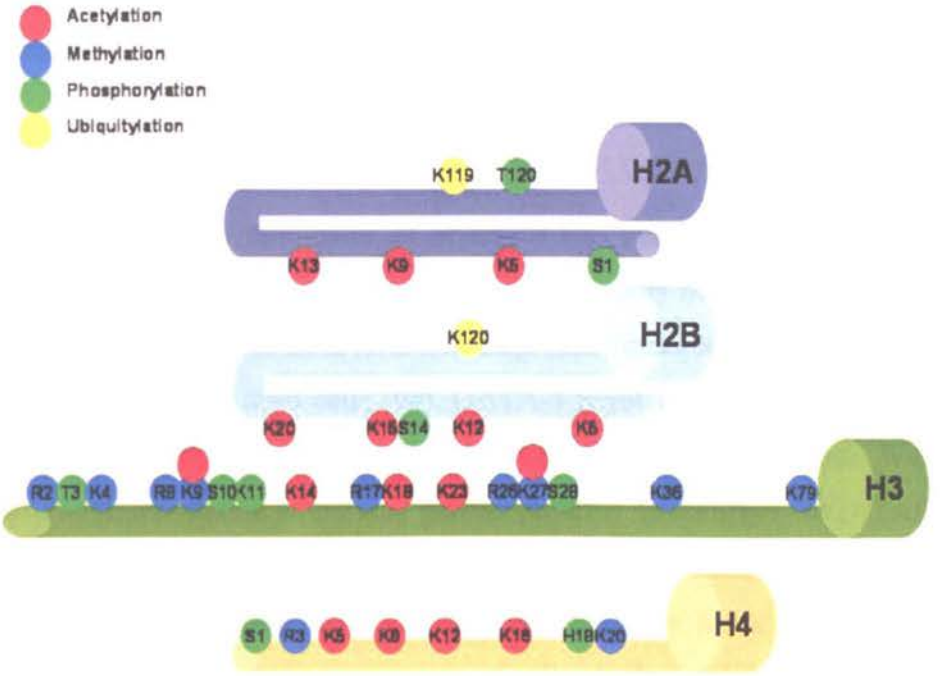

Figure 1.4. Histone modifications. Covalent histone modifications of each nucleosomal histone tail in mammalian cells.

expression pattern of these critical factors is tightly regulated throughout erythropoiesis to control cell proliferation, differentiation and survival.

GATA-1

GATA-1 is the key modulator of erythroid cell maturation and differentiation. GATA-1 is the founding member of the GATA family of zinc finger transcription factors and is expressed in several hematopoietic lineages such as erythroid cells, megakaryocytes and mast cells (*98*). GATA-1 regulates the expression of critical factors of erythropoiesis via binding to GATA consensus sequences, WGATAR, and through interaction with many partner proteins. In addition, WGATAR motifs are found at a majority, if not all, of *cis*-regulatory elements of erythroid genes and was first identified as by its DNA binding affinity to the human β-globin 3' enhancer and regulatory sequences of all chicken globin genes (*99-102*). Disruption in GATA-1 DNA binding ability or its interaction with well known co-binding proteins leads to severe blood disorders including anemia and thrombocytopenia (*103-105*).

GATA-1 null mice succumb by E11.5 due to severe anemia as primitive and definitive erythroid precursors fail to mature (*103*). Megakaryopoiesis is also severely impaired in GATA-1 null animals. ES cells however, can develop into other hematopoietic lineages, albeit at a lesser frequency, emphasizing on the critical role of GATA-1 in erythropoiesis and megakaryopoiesis (*106*).

GATA-1's ability to modulate transcription relies extensively on its interaction with additional transcription factors and co-factors including FOG-1, ZBP89 and the SCL/TAL-1 complex via its direct interaction with LMO2 (*60, 107-109*). In addition, GATA-1 has been reported to interact with a plethora of co-factors

including CBP, Brg1, MeCP1/NuRD among others (*8, 110*). GATA-1 regulates the expression of two essential erythroid TFs directly, FOG-1 and EKLF (*111*).

SCL/TAL-1

SCL/TAL-1 is a basic helix-loop-helix (bHLH) transcription factor which recognizes a short consensus DNA motif, CANNTG, most commonly known as E-box. Its expression in hematopoiesis is similar to that of GATA-1(*112-113*). SCL/TAL-1 ablation in mice has catastrophic consequences on hematopoiesis (*114-116*). Development-specific ablation of SCL/TAL-1 in adult hematopoietic progenitors results in the failure of erythropoiesis. Recently, GATA-1 and the SCL/TAL-1 complex have been reported to co-occupy promoters of GATA-1 activated genes (*117*).

SCL/TAL1 is the central protein of a well-characterized complex SCL/TAL-1-LMO2-Ldb1-E2A. Evidence suggests that the integrity of this pentameric complex is of critical importance in SCL/TAL-1 modulated gene regulation. The phenotype of LMO2 null mice is identical to that of SCL/TAL-1 null mice (*118*). In addition, ectopic co-expression of SCL/TAL-1, GATA-1 and LMO2 induced erythropoiesis in Xenopus embryos (*119-120*).

Further evidence of the role of this complex in erythropoiesis emerged from recent studies centered on Ldb1. Ldb1 knockdown using a morpholino approach in zebrafish led to defective erythropoiesis (*121*). Ldb1 knockdown in murine erythroid cell lines by shRNA strategies also resulted in abnormal erythropoiesis and more specifically the absence of β-globin gene expression due to impeded communication between the β-globin promoter and the β-globin LCR (*122*).

NF-E2

NF-E2 is a heterodimeric protein, consisting of the ubiquitously expressed 18 kDa Maf subunit and a lineage-specific 45kDA subunit (*123-125*). NF-E2 is required for high-level β-globin gene expression in erythroid cell lines (*126*). Surprisingly, p45 NF-E2 null mice do not exhibit a profound erythropoietic phenotype but display severe thrombocytopenia (*127-129*). p45NF-E2 can dimerize with several Maf proteins. Maf proteins can also dimerize with other NF-E2 related proteins. Therefore, the mild erythroid phenotype observed in p45 NF-E2 null mice is likely the result of functional redundancy (*130*).

IV-ERYTHROID KRUPPEL LIKE FACTOR: EKLF

Discovery of EKLF

EKLF was isolated from a subtractive hybridization screen between MEL cells and a murine-macrophage cell line, enriching for erythroid specific genes (*131*). MEL cells, or murine erythroleukemia cells, are erythroid progenitors cells immortalized with a Friend leukemia virus and respond to chemical induction to undergo erythroid differentiation (*132*).

Molecular properties of EKLF

EKLF maps to a region on mouse chromosome 8 (*133*) and human chromosome 19 (*131, 134*). The EKLF gene is composed of 3 exons spanning approximately 6.5kb. Two alternative transcriptional start sites, at nucleotides 41 and 55, promote the production of two major transcripts. Translation of the protein starts from methionine 19 and encodes a 358 amino acid polypeptide (37.755 Da) (*135*).

The structure of EKLF consists of a carboxyl-terminal DNA binding domain composed of three C2H2 type zinc fingers and a proline-rich amino domain which shares structural similarities with other transactivation domains. A schematic diagram of EKLF structure and associated covalent modifications is represented in Figure 1.5.

EKLF or KLF1 recognizes a DNA binding motif, CCNCNCCCN, present at many erythroid gene promoters and referred to as the CACC box (*135*). EKLF is the founding member of a 15 genes family which share identical DNA binding properties. The EKLF protein contains two nuclear localization signal (NLSs), localized to a region adjacent to the zinc finger DNA binding domain and within the zinc finger domain itself (*136-137*).

Expression of EKLF

Human and mouse EKLF show a high degree of homology with >90% similarity in the zinc finger domain and approximately 70% within the proline rich amino domain (*131, 134*). Human and murine EKLF expression is restricted to the erythroid lineage with higher levels in definitive erythroid progenitor cells (*131, 134-135*). Expression of EKLF is detected in the common myeloid progenitor (CMP) and megakaryocytic-erythroid progenitor (MEP) populations (*138*). In contrast, EKLF expression is absent in lymphoid cells as well as common lymphoid progenitors (CLP) and their progeny (*135, 138*).

During murine ontogeny, EKLF is expressed early at different anatomical sites (*139*). EKLF expression, as measured by mRNA detection, is detected first within the blood islands of the yolk sac at the neural plate stage (E7.5). EKLF expression is then detected within the hepatic tissue from the earliest stage of hepatic

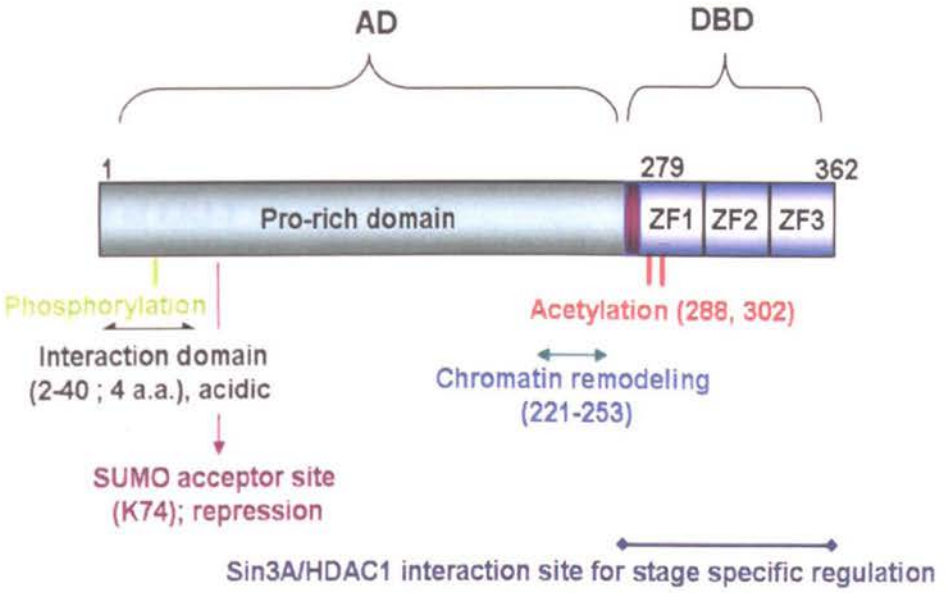

Figure 1.5. Schematic representation of the structure of human EKLF. The EKLF protein is composed of a proline rich activation domain, a chromatin remodeling domain and a zinc finger DNA binding domain. The protein is subjected to several post-translational modifications including phosphorylation, acetylation and sumoylation.

formation (E9) and continues until E14.5, at which time the liver becomes the only source of EKLF. Concomitantly with EKLF mRNA, EKLF protein is also detected in primitive cells and the fetal liver. In adult animals, EKLF expression is strictly localized to the red pulp of the spleen.

Regulation of EKLF

The expression of EKLF is tightly regulated in a stage- and lineage-specific manner. It is induced by Bmp4/Smad signaling and by the erythroid TF, GATA-1(*140-141*). However, regulation of EKLF activity is also modulated by post-translational modifications (Figure1.6.). First, the transcriptional activity of EKLF is dependent upon the phosphorylation status of its threonine residue located at position 23 (T23) (*142*). Similarly, acetylation of EKLF by CBP and p300 increases its affinity for DNA as well as for the components of SWI/SNF chromatin remodeling complexes *in vitro* (*59, 64*). The SWI/SNF chromatin remodeling complex has been suggested to induce chromatin remodeling at EKLF target gene promoters and more specifically the β-major promoter (*63, 143*). Acetylation of EKLF can also results in the inhibition of transcription via its recruitment of the co-repressor proteins Sin3a and histone deacetylases (HDACs) to target promoters, particularly those involved in megakaryocytic differentiation. In addition, sumoylation at lysine 74 of EKLF has been implicated in the transcriptional repression of megakaryopoiesis.

The role of EKLF in erythroid gene transcription

Since its discovery, EKLF has been extensively studied in the context of β-globin gene transcription. Disruption of the EKLF gene by homologous recombination has demonstrated its non-redundant role in erythropoiesis. EKLF-null embryos

succumb at E14.5-16.5 as a consequence of a severe defect in definitive erythropoiesis, with little evidence of an effect on other lineages (*144-145*). The lack of β-globin transcripts detectable in EKLF null mice was consistent with the idea that EKLF is essential for β-globin gene transcription.

Numerous studies have allowed gaining insight into the mechanisms by which EKLF and other factors modulate β-globin gene transcription. First, *in vitro* structure-function studies using chimeric proteins consisting of the EKLF domains linked to the DNA binding domain of the yeast zinc finger protein GAL4 have established two domains of EKLF with opposite functions (*146*). A domain encompassing amino acids 20 to 195 was determined as the activation domain of EKLF. In contrast, an internal domain (aa196-291) mediated transcriptional repression. Additional studies in our laboratory demonstrated that an internal domain of EKLF is sufficient to promote activation of the endogenous β-globin promoter, as opposed to heterologous promoters in the previous studies. However, it remains unclear what functions of EKLF are required for β-globin gene expression *in vivo* as well as what are the mechanisms involved.

Second, EKLF was the first factor implicated in establishing the DNaseI hypersensitivity profile of any promoter, in this case the β-globin promoter. Analysis of EKLF-null progenitor cells revealed a specific loss of a developmentally specific DNaseI hypersensitive site in the proximal β-globin promoter (*147*). An additional loss of hypersensitivity to DNaseI, but to lesser extent, was detected at the LCR HS3. This function of EKLF has been attributed to the recruitment of the SWI/SNF chromatin remodeling complex E-RC1 (*63*). The chromatin remodeling activity of EKLF can be separated from its transactivation domain. This activity resides within the last 141 amino acids of the proteins and includes the DNA binding domain for function *in vivo* (Jansen et al. in preparation) (*148*). Furthermore, EKLF is required for the acetylation of histone H3 at the β-globin promoter, presumably via its interaction with CBP

(*65*). Functional corroboration of EKLF-directed chromatin remodeling and histone modifications in primary erythroblasts has yet to be established.

More recently, EKLF has been implicated in the establishment of the communication between the β-globin promoter and the long distance LCR. Regulation of the β-globin locus is believed to occur in part by competition of globin gene promoters for direct interaction with the LCR. Direct support for the implication of EKLF in the stabilization of the LCR/β-globin promoter interaction arose from the application of the chromosome conformation capture (3C) technology in EKLF-null derived fetal liver erythroid progenitor cells (*149*). Basically, the 3C technique allows the detection of clustered *cis*-elements within the spatial organization of fixed chromatin. This assay has allowed the detection of the physical proximity between the LCR and the promoter of actively transcribed globin genes. This physical proximity promotes the establishment of a chromatin 'loop' termed the active chromatin loop (ACH) where the promoter of the active gene and the LCR constitute the base of the loop, keeping inactive promoters away from the LCR. 3C results in EKLF null fetal livers revealed the requirement for EKLF in the formation of the ACH and confirmed its necessity towards β-globin gene transcription (*150*). This observation was of critical significance; however, the mechanisms behind the EKLF-directed formation of the ACH and the activation of the β-globin promoter remain unclear.

More recently, studies of EKLF have shifted towards the regulation of additional target genes. Microarray analyses performed by two different groups have revealed a multitude of potential EKLF target genes, involved in cell cycle, membrane integrity, cytoskeleton integrity as well as other transcription factors (*151-152*). To date, the best established targets are AHSP, Dematin and the transcriptional repressor BKLF (*151, 153-154*). Outside of the detection of EKLF binding at the promoter of these genes, and EKLF-dependent formation of a

DNaseI hypersensitivity site at the AHSP promoter, the role of EKLF at these target genes has not been established.

PROJECT OUTLINE

EKLF is involved in the transcription of multiple genes, most importantly the β-globin gene. The β-globin gene serves as a paradigm to study developmental- and tissue-specific transcription. In addition, the β-globin locus includes the first described LCR and is established as a critical locus towards the exploration of the role of enhancers and more specifically the way LCRs communicate with promoters. So far, not much is known about the mode of action of EKLF at any target endogenous gene promoter. By way of determining the true mechanisms of EKLF-mediated transcription, we will be able to further dissect the complexity of *cis*-elements influence on transcription.

Specific Aim 1: *Determine the EKLF-dependent events across the β-globin locus and establish the temporal sequence of events across the locus upon transcriptional activation of the β-globin gene.*

The goal of this specific aim is to determine the series of EKLF dependent events at the β-globin locus leading to the transcriptional activation of the β-globin gene. This project will lead to a better understanding of the role of EKLF in β-globin gene transcription, as well as determine its broader role in the function of the LCR.

My hypothesis is that EKLF is required to recruit a specific subset of transcription factors and co-factors at the LCR and the β-globin promoter, leading to changes visible at the level of chromatin structure. In addition, I hypothesize that the role of EKLF at promoters differs from its role at enhancers.

Specific Aim 2: *To evaluate the role of EKLF at target gene loci devoid of long distance enhancers.* I propose to explore EKLF-directed events at target promoters that are not regulated by long distance enhancers. Studying the mechanisms of EKLF-modulated transcription in a relatively simpler chromatin context, I will be able to truly determine the direct effects of EKLF binding.

I hypothesize that the mechanism of action of EKLF at the AHSP and Dematin promoter differs from its role at the β-globin promoter.

Specific Aim 3: *To assess directly the role of EKLF in the heme biosynthesis synthesis pathway and explore its function as a co-factor.* Studies have reported a possible involvement of EKLF in the regulation of the genes from the heme biosynthesis pathway. However, all efforts to date have focused on the first enzyme of the pathway ALAS2. I propose to assess the direct role of EKLF at additional heme biosynthesis genes.

I hypothesize that EKLF is direct and specific modulator of erythroid-specific ALAD gene transcription.

-CHAPTER 2-

MATERIALS AND METHODS

Cell culture

i) *JH31 cells:* JH31 cells are transduced J2eΔ*eklf* cells (*155*) that express a tamoxifen-inducible, EKLF-mutant estrogen receptor (EKLF-ER) fusion protein under the influence of a Murine Stem Cell Virus (MSCV) 5'Long Terminal Repeat (LTR). Cells were maintained in the log phase of growth, between 0.2 and $1.5x10^6$ cells/ml, in D15puro (Dulbecco's modified Eagle's medium (DMEM) supplemented with 15% Fetal Calf Serum (FCS), 1% penicillin/Streptomycin and 1μg/ml of puromycin (Invivogen)) at 37°C, 5% CO_2. Cells were cultured for no more than 8 weeks. JH31 cells with a low passage number were expanded for 10 days and frozen on dry ice as stock vials of $10x10^6$ cells /ml in cold freezing medium (70% DMEM, 20% FCS and 10% DMSO). One stock vial was put back in culture for another 10 days. Cells were then frozen as working vials of $10x10^6$ cells/ml. Prior to the use of all working vials, a stock vial was put back in culture and expanded for 10 days in order to freeze an additional set of working vials. All frozen cells were stored at -190° F in a liquid nitrogen freezer. 2 units/ml of EPO (erythropoietin, supplied by the University of Chicago Hospitals pharmacy) was added directly to the cells 3 days prior to cell harvest. From this day on, cells were split 1:2 daily with D15puro. The nuclear translocalization of EKLF in JH31 cell was induced by the addition of 4-OH-Tamoxifen (4-OH-TAM) to a final concentration of 100nM directly into the media. The stock solution of 4-OH-TAM has a concentration of 1mM in absolute ethanol. Therefore, a first dilution of 1:100 in D15puro was freshly prepared prior to induction. Subsequently, 1ml of diluted 4-OH-TAM was added directly to 100ml of JH31 cells in culture at a concentration of $5x10^6$ cells/ml.

ii) *Mel cells:* Murine Erythroleukemia cells, commonly referred to as Mel cells, are maintained in DMEM supplemented with 10% FCS and 1% Penicillin/Streptomycin, at 37°C and 5% CO_2. The differentiation of Mel cells was induced by the addition of 2% DMSO (SIGMA) to $1x10^4$ cells/ml for 4 days.

Protein Analysis

Nuclear extracts from ethanol treated and 4-OH-Tamoxifen treated JH31 cells were obtained using a modified Dignam's protocol (*156*). Harvested cells ($5x10^5$ to 10^7) were washed twice in cold PBS by filling the tube to capacity. Cell pellets were resuspended in 400μl of cold hypotonic buffer (10mM HEPES-KOH pH7.9, 1.5mM MgCl2, 10mM KCL, 0.5 mM DTT) supplemented with protease inhibitors (Complete, EDTA-free protease inhibitor cocktail (ROCHE), 200mM PMSF (SIGMA)) and incubated on ice for 10min followed by a 10sec vortex at medium setting. Nuclei were collected by centrifugation at 12,500g for 2min at 4°C. Nuclei pellets were resuspended in cold 1% NP-40 lysis buffer (50mM Tris-HCl pH8.0, 150 mM NaCl, 1% NP40) supplemented with protease inhibitors (Complete, EDTA-free protease inhibitor cocktail (ROCHE), 100mM PMSF (SIGMA)). Cellular materials were discarded by quick centrifugation at room temperature and nuclear lysates were transferred to a chilled 1.5ml tube and stored on ice for no longer than 30 minutes until further processing. Protein concentration was assessed using the Bradford method (Bradford reagent (Biorad)) at 595nm using the SmartSpec spectrophotometer from Biorad. 50μg of nuclear lysate was diluted with 6X SDS-loading buffer(1.2% SDS, 0.6% bromophenol blue, 47% glycerol, 60mM Tris-Cl pH6.8, 0.6M DTT), denatured by boiling for 3 minutes and resolved on a 10% or 12% SDS-PAGE gel. Proteins were then transferred to a nitrocellulose membrane (Protran BA 83 0.2μm (Whatman)) by wet transfer procedure using the Biorad apparatus. The membrane was blocked in 5% milk in PBST (1X PBS, 0.1% Tween-20) for 1hr at room temperature with constant shaking and cut at the 100KD band from the protein size marker (Precision Plus, Biorad). Primary antibody incubation with relevant antibodies was carried out overnight at 4°C with constant shaking at a dilution of 1:500 of primary antibody in 5% milk in PBST followed by 3 individual washes in PBST of 10 min each, at room temperature with constant shaking. Secondary antibody incubation was carried out at a dilution of 1:3000 of anti-rabbit or anti-goat horseradish peroxidase (HRP) conjugated antibodies (Jackson Immunoresearch) in 5% milk in PBST for 1 hr. After 3 additional washes in PBST of 10 min each at room temperature with constant shaking, the peroxidase activity was detected by enhanced chemiluminescence (ECL) using detection reagents from Pierce followed by exposure to X-ray films. Antibodies used are described in the "Antibodies" section.

RNA analysis

Total RNA isolated from $2.5x10^6$ ethanol-treated or 4-OH-Tamoxifen treated JH31 cells was subjected to semi-quantitative RT-PCR analysis. RNA was extracted using the Trizol method and cDNA was prepared using the Superscript II First Strand System (Invitrogen) following the manufacturer's protocols. RNA pellets were air dried for 10min and resuspended in 50µl of DEPC treated water. RNA concentration was determined by absorbance at 260:280nm with a conversion ratio of 40µg/ml using the SmartSpec spectrophotometer from Biorad. In order to remove contaminating genomic DNA, RNA (10µg) was treated with Turbo DNase (Ambion) in a 50µl reaction following manufacturer's instructions. Subsequently, 2µg of DNase-treated RNA was used for first strand cDNA synthesis using Superscript II (Invitrogen) and following the manufacturer's instructions. The resulting cDNA was diluted 1:50 for mRNA analysis and 1:2 for primary transcripts analysis.

2µl of the synthesized cDNA was subjected to semi-quantitative analysis using Real-Time PCR (Applied Biosystems Prism 7900/7500 Fast) with the appropriate primer pairs. Products were quantified using SYBR green fluorescence (Applied Biosystems) in 15- or 20µl reactions in relation to a standard curve generated from 1:5 serial dilutions of cDNA synthesized from RNA isolated from induced Mel cells. Standards were given arbitrary values (625, 125, 25, 5 and 1). PCR efficiency and specificity was determined by analysis of the standard curve and the dissociation curve respectively. Primer pairs were designed using the Clone Manager software (see table 2.1.) or described in previous publications (see table 2.2.).

Amplified region	Forward (5'-3') Reversed (5'-3')
AHSP (intron 2)	tgaatcagcaggtgagtc gcaatgggattcgggaatac
ALAD (exon2-intron2)	gcctccaacctcatctatcc tcccattgcctgttccagtc
β-major (intron 2)	ccagtccttctctctctcct atcttccttgtcctctgagc
Dematin (intron 11-exon12)	cccaggtgaatgtaggtag tcacagtcagcgctcattg

Table 2.1. List of primers designed for Real-Time PCR primary transcripts analysis.

Region of amplification	Forward (5'-3') Reverse (5'-3')	Reference
ALAD	ctttgatctcaggactgctg aacagctgcggtgcaaagta	(*152*)
ALAS2	cacctatgcttaaggagcca cagaagcacacaggaaagca	(*152*)
GAPDH	gaaggtacggagtcaacggattt gaatttgaccatgggtggaat	(*152*)
HPRT	gcagtacagccccaaaatgg aacaaagtctggcctgtatccaa	(*151*)
PBGD	tacttctggcttccaagtgc caaggtgaggcatatcttcc	(*152*)
UROD	atccctgtgccttgtatgca aggttggcaattgagcgttg	(*152*)

Table 2.2. List of primers used for Real-Time PCR mRNA analysis

Chromatin Immunoprecipitation (ChIP)

i) *Basic protocol:* The chromatin immunoprecipitation technique was initially adapted from Boyd and Farnham by Forsberg et al. (*157-160*). ChIP assays were performed as previously described (*160-161*) with slight modifications. Briefly, protein-DNA and protein-protein crosslinking from ethanol treated or 4-OH-Tamoxifen treated JH31 cells at a density of $0.5x10^6$/ml was achieved by the addition of formaldehyde to a final concentration of 1% followed by a 10min incubation at room temperature with constant shaking. The reaction was quenched by the addition of glycine to a final concentration of 0.125M followed by an incubation of 5min at room temperature with constant shaking. Cells were then collected in 50ml conical tubes by centrifugation at 1,000rpm for 5min at 4°C and washed twice filling the tube to capacity with cold PBS. $1x10^7$ cells were transferred to a 1.5ml tube in cold PBS and spun quickly. After removal of the supernatant, cell pellets were snap frozen in a dry-ice/ethanol bath and stored at -80°C or at -190°C until further processing. Crosslinked were stored at -80°C for up to 3 months or -190°C for up to 6 months.

$1x10^7$ cells per immunoprecipitation condition were resuspended in cold cell lysis buffer (10mM Tris-HCl pH8.0, 10mM NaCl, 0.2% NP-40) supplemented with protease inhibitors (Complete, EDTA-free protease inhibitor cocktail (ROCHE), 100mM PMSF (SIGMA)) and incubated on ice for 10min. Cells were collected by centrifugation at 600rpm for 5min at 4°C. Nuclei were then resuspended in 300µl of cold nuclear lysis buffer (50mM Tris-HCl pH8.0, 10mM EDTA, 1% SDS) supplemented with protease inhibitors (Complete, EDTA-free protease inhibitor cocktail (ROCHE), 100mM PMSF (SIGMA)) and incubated for 10min at 4°C. Chromatin was sheared by sonication at high power for 10 cycles of 30sec ON/30sec OFF using the Bioruptor sonicator (Diagenode) to achieve an average DNA fragment size of 500-2000bp. DNA fragment size is evaluated at the end of the procedure by electrophoretic separation of input sample DNA on a 1% agarose gel in 1X TAE (40mM Tris acetate and 1mM EDTA) for 1h at 70mA. Soluble chromatin was collected by centrifugation at 12,500g for 5min at 4°C and diluted 1:4 with cold immunoprecipitation buffer (20mM Tris-HCl pH8.0, 2mM EDTA, 150mM NaCl, 1% Triton-X100, 0.1% SDS) supplemented with protease inhibitors (Complete,

EDTA-free protease inhibitor cocktail (ROCHE) , 100mM PMSF (SIGMA)). Samples were pre-cleared by adding 50µl of salmon sperm DNA/ protein A/G agarose beads (Millipore) as well as 5µl/ml of rabbit serum and allowed to rotate at 4°C for 1hr. Agarose beads were discarded by centrifugation at 1,000rpm at 4°C for 5min. 10% of the pre-cleared lysate (input) was removed and stored at -20°C overnight. 2 (histone marks) to 5µg of antibody (other targets), or appropriate normal IgG (control) were added to the remainder of the soluble chromatin (1.350ml) and allowed to rotate at 4°C overnight. When monoclonal antibodies were used, 1h incubation at 4°C with rotation in the presence of 5µg of secondary antibody was added. Immune complexes were adsorbed to 70µl of salmon sperm DNA/ protein A/G agarose beads (Millipore) for 2hrs at 4°C with constant rotation. Beads were washed twice in cold wash buffer 1 (20 mM Tris-HCl pH8.0, 2mM EDTA, 50mM NaCl, 1% Triton X-100, 0.1% SDS) followed by 1 wash with cold wash buffer 2 (10mM Tris-HCl pH8.0, 1mM EDTA, 250mM $liCl_2$, 1% NP-40, 1% Deoxycholic acid) and 2 washes with Tris-EDTA buffer. Protein-bound DNA was eluted from the beads by 2 subsequent incubations of 15min each with freshly prepared elution buffer (50mM $NaHCO_3$, 1%SDS). Crosslinks from immunoprecipitation samples and inputs were reversed by the addition of 1µl of 20mg/ml RNaseA (Ambion) followed by overnight incubation at 65°C.

DNA purification was carried out using a Qiaquick PCR purification kit (QIAGEN) following manufacturer's instruction. DNA was eluted twice with 50µl of ddH2O.

Analysis of the purified DNA was achieved by using Real-Time PCR (Applied Biosystems Prism 7900/7500 Fast/7900HT Fast) with the appropriate primer pairs. Products were quantified using SYBR green fluorescence (Applied Biosystems) in 15- or 20µl reactions in relation to a standard curve generated from 5 1:10 serial dilutions of an input sample. Standards were given arbitrary values (1000000, 100000, 10000, 1000 and 100). PCR efficiency and specificity was determined by standard curve and dissociation curve analysis respectively. Primer pairs were previously described or designed using the Clone Manager software to obtain PCR products of 50-150bp (table 2.3.).

Region of amplification	Forward (5'-3') Reverse (5'-3')	Reference
AHSP promoter	ctaactccagggaagcctcacc tttgtgtgtcttctgcactaagcg	(*162*)
AHSP upstream (-1.1kb)	cacaggttgtaactgtgagatcttgg tctcaccctgactctatctggtatgtagtag	Self designed
ALAD promoter 1b	ctcttgtgtcctgtgaagag caagcagctcagggcccaccttatc	Self designed
ALAD upstream (-1.3kb)	cctgtgcctcatacagtaac gtttggcccagaaacagttg	Self designed
Amylase promoter	ctccttgtacgggttggt aatgatgtgcacagctgaa	(*163*)
β-major promoter	gggagaaatatgcttgtcatc caactgatcctacctcacctt	(*163*)
Dematin promoter P2(E)	aatgagagggtgggtggttt cggaagacccccttcaac	(*151*)
Dematin upstream (-650bp)	gtttggatggccaattcg ccagcagagttcaagttagc	Self designed
Dematin (+1.28kb)	gccactaactcggtcaag aacggagtccgtctgttc	Self designed
HS3	ctttcagaaccaggaggc tttgctgttgttgttactgttc	(*163*)
HS2	ttccctgtggacttcctc gtcatgctgaggcttagg	(*163*)
Ivr5	gtatgctcaattcaaatgtaccttattttaa ttacctctttatttcacttttacacatagctaa	(*161*)

Table 2.3. List of ChIP primers used for Real-Time PCR.

ii) *Antibody validation:* Antibodies used in ChIP experiments were first validated using JH31 cells treated with ethanol or 4-OH-TAM for 6 hours. The assay was carried out as described in the "*basic protocol*" section of this chapter. Antibodies were selected for further application towards kinetic studies when the signal intensity was at least 2 folds over the IgG control. The β-globin promoter was consistently amplified to a lesser degree when compared to other studied regions. Therefore, in cases where several

assessed antibodies targeted an identical protein, the main criterion of antibody selection was the signal intensity at the β-globin promoter. The antibody leading to the greatest enrichment was selected for further use. Test ChIPs for antibody selection were performed once only, along with anti-HA antibody ChIP as a positive control.
The validation data of the Brg1 antibody used in the presented ChIP studies is described as an example of routine antibody testing and is represented in figure 2.1.

iii) *Kinetic analysis:* Essentially, ChIP experiments assessing the kinetics of factor recruitment to target regions were carried out as described previously with a few additional considerations. Each Kinetic study required a large number of cells that were processed as batches. JH31 cells maintained in the log phase of growth from multiple tissue culture flasks are combined for the purpose of cell counting. Once counted using a Neubauer hemocytometer, JH31 cells were dispatched at a concentration of $0.5x10^6$ cells/ml in D15puro, among a minimum of 6 large tissue culture flasks (1 per time point) and in a total volume of 100, 150 or 200ml (equivalent to 5 reactions, 7.5 reactions and 10 reactions respectively). Total culture volumes were consistent within all tissue culture flasks of a kinetic batch. After 2 hours in the incubator (37°C, 5% CO_2), cells were treated with 4-OH-TAM for either 30min, 1h, 2h, 4h and 6h. The 0h time point consisted of a flask of JH31 cells treated with ethanol for 6h, since ethanol is the solvent used in the preparation of the 4-OH-TAM stock solution.

iv) *Cell batch validation:* To ensure that all batches of JH31 cells responded to 4-OH-TAM induction with similar kinetics, $2.5x10^6$ cells from each tissue culture flask of each time point were harvested and processed for RNA extraction followed by cDNA synthesis as described in the "RNA analysis" section of this chapter. The transcriptional induction of the β-globin, AHSP and Dematin genes was then assessed by quantitative Real-Time PCR using a standard curve consisting of 5 1:5 serial dilutions of synthesized cDNA from isolated RNA of DMSO induced MEL cells. Induction curves were then compared to previous cell batches and either discarded or stored in liquid nitrogen until further processing for kinetic analysis of ChIP studies. Discarded cell batch preparations usually exhibited slower induction profiles for all three target genes with a transcriptional

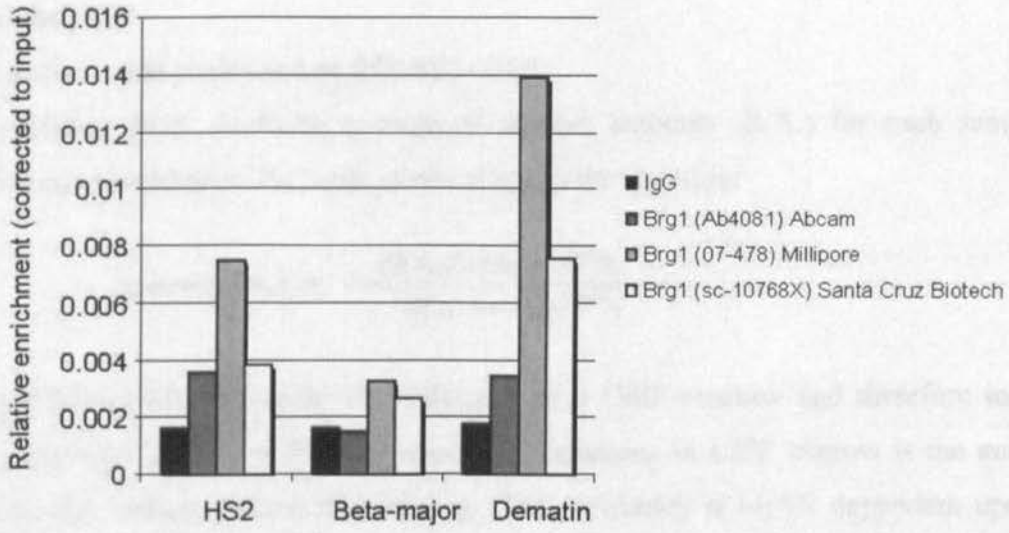

Figure 2.1. Data analysis methodology of kinetic ChIP studies.

The control anti-HA ChIP is not displayed in this figure.

plateau being reached at a later time point when compared to the majority of other preparations.

Data analysis:

Data analysis was performed as followed (*164*):

The real-time PCR duplicate average of relative amounts (R.A.) for each sample or control was corrected to 2% input as described in the equation:

$$\textbf{Corrected R.A.} = \frac{(\textbf{R.A. Average}^{\textbf{Sample}})}{(\textbf{R.A. Average}^{\textbf{Input}})}$$

Several factors may influence the efficiency of a ChIP reaction and therefore increase data variations. The most frequent source of variations in ChIP outputs is the antibody used for the immunoprecipitation step as ChIP efficiency is highly dependent upon the affinity of the antibody towards its target protein and thus may vary with changes in antibody lots. Since large quantities of antibodies were used towards the evaluation of factor recruitment kinetics by ChIP assay, multiple lots of a specific antibody were required.

In addition, fluctuations in the manipulation of samples and reagents equally affect the outcome of the ChIP assay.

As a result, overall signal intensities obtained by ChIP assays applied to kinetic studies of factor recruitment to target regions are variable from ChIP experiment to ChIP experiment as well as from cell batch to cell batch. However, overall trends of binding kinetics are similar. To circumvent high variations in overall signal intensities between kinetic studies and graph a representative kinetic curve of factor recruitment, the maximal detected signal intensity of each kinetic study was set to 100 and signal intensities from additional ChIP reactions within the study were corrected accordingly. By doing so, each kinetic study can be graphed on a common scale of signal intensity ranging from 0 to 100, where 100 represents the maximal enrichment detected within a study of 6 time points. Data analysis for kinetic studies is best described in the equation:

$$\textbf{Factor Occupancy (\% of maximal)} = \frac{[\,(\text{R.A. Average}^{\text{Sample}}) / (\text{R.A. Average}^{\text{Input}})\,]}{\textbf{(Corrected R.A. of Highest value)}} \times 100$$

An example of the stepwise analysis of ChIP results is represented in figure 2.2.

Each kinetic study was performed in a minimum of two separate cell batches and at least three times. The number of independent experiments, as described by the letter n in figure legends, was representative of the number of cell batches used towards a particular kinetic study and was not representative of the actual number of individual ChIPs for a specific antibody at a specific time point.

All samples were not taken into consideration for the final data analysis. Sample discrimination was based on one or more of the following sample's characteristics:

- Abnormal low signal intensities, as described as less than 50% of signal intensities of surrounding samples of the plateau section of the kinetic study. For earlier time points, these samples were determined based on their low signal intensities when compared to additional kinetic studies. Low signal intensities usually occurred as a result of mishandling of the samples (omission of primary antibody, secondary antibody or agarose beads).
- Abnormal high signal intensities, as described as more than 50% of signal intensities of surrounding samples of the plateau section of the kinetic study.
- Significant enrichment of the Amylase promoter region. Such samples usually also exhibited abnormal high signal intensities as the extent of the enrichment was the result of sample contamination.

Inconsistent enrichment at the control upstream region, highlighting an insufficient sonication. Samples such as RNA Pol-II and certain histone modifications may procure significant enrichment of upstream regions. Therefore, the lack of consistency of such signals was the determinant in classifying a sample as erroneous.

Correction 1: relative enrichment corrected to input

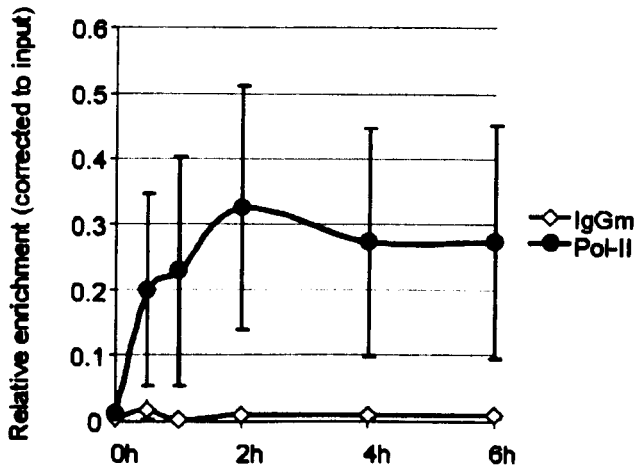

Correction 2: maximum signal intensity above IgG = 100

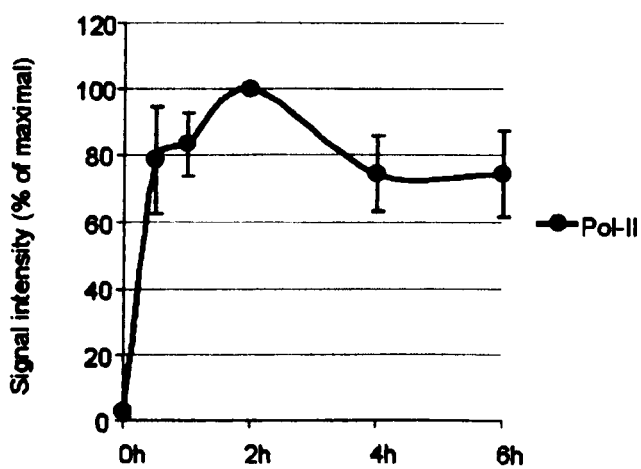

Figure 2.2. Data analysis methodology of kinetic ChIP studies.

Statistical Analysis

The choice of the statistical method used to analyze the data was decided upon review of previous publications of similar work in Tamoxifen inducible GATA-1 cells (G1E) from the Bresnick laboratory (*49, 60-61*). Average deviations (avedev) or standard error of the means (SEM), were calculated using the Microsoft Excel program. The statistical significance of the data was determined using a Student T test of the homoscedastic type (two-sample equal variance) with 1 distribution tail. A calculated p value, or probability associated with the Student t test, was considered significant when ≤ 0.05. Calculated probability values for factor occupancy at all kinetic time points with significant differences to the percentage of EKLF occupancy are displayed in the Appendix section (A7-10). Importantly, p values were also significant using the Student T test of the "two-sample unequal variance" type.

DNase I sensitivity assays

DNase I sensitivity assays were performed essentially as described by McArthur *et al.* (2001) with slight modifications. Briefly, fetal livers were harvested from E14.5 mouse embryos and made into single cell suspension by passing through a 70μm cell strainer flushed with DMEM complemented with 10% FCS. Fetal liver cells ($6x10^6$) or JH31 cells ($1.2x10^7$) were washed once with cold PBS and resuspended in 5 ml of buffer A (15mM Tris HCl (pH 7.6), 60mM KCl, 15mM NaCl, 1mM EDTA, 0.5mM EGTA, 0.5mM spermidine, 0.15mM spermine). Cells were lysed in the presence of 0.5% (v/v) NP40, and nuclei were collected and resuspended in 1.2ml of digestion buffer (buffer A supplemented with 3mM CaCl2, 75mM NaCl). 200μl of the nuclei mixture was added to 1.5ml tubes containing 50 μl of an enzymatic mix containing 0-18 units of DNaseI (ROCHE). DNaseI digestion was carried out at 37 °C for five minutes and terminated by the addition of an equal volume of stop buffer (0.1M NaCl, 0.1% (w/v) SDS, 50mM Tris-HCl (pH 8.0), and 100mM EDTA). The samples were subjected to proteinase K (500 μg/ml) treatment overnight at 55°C. DNA was recovered by extraction with phenol/chloroform using a phase lock gel (5prime) following manufacturer's instructions. DNA was further purified by ethanol precipitation in the presence of 1:10 (v: v) of 5M

NaCl. After centrifugation at 12,000g for 10min at 4°C and removal of the supernatant, the DNA pellet was dialyzed against two changes of TE buffer, re-precipitated as described above with an additional wash of the DNA pellet with 1ml of 75% ethanol followed by a quick vortex step and centrifugation at 7,500g for 5min at 4°C. The recovered DNA was diluted in water to a concentration of 10ng/µl. DNA analysis was performed using Real-Time PCR with SYBR green fluorescence detection in a 20µl reaction volume. Quantification of the undigested template was achieved in relation to a standard curve generated from 1:5 serial dilutions of undigested genomic DNA. Results were normalized to those obtained for a previously determined DNaseI insensitive gene, Nf-M (*165*). PCR efficiency and specificity was determined by the analysis of the standard and dissociation curves respectively. Control primers used for the assay areas were as followed:

Nf-M forward: 5'- GCTGGGTGATGCTTACGACC-3' and Nf-M reverse: 5'-GCGGCATTTGAACCCTCTT-3' (*165*) Additional primer pairs used for the assay were identical to those used for the ChIP studies (see Table 2.3).

Real-Time PCR analysis

Three different Real-Time PCR systems from Applied Biosystems were used in the presented studies; the Prism 7900, 7500 Fast and 7900HT Fast. The later can accommodate reactions set up in 384 well plates. Reactions were set up as followed:

7.5µl 2X SYBR mix		10µl 2X SYBR mix
0.06 µl primer mix (100 µM each)	or	0.08 µl primer mix (100 µM each)
5.44 µl ddH2O		7.92 µl ddH2O
2µl cDNA		2µl cDNA
15µl Total		20µl Total

Duplicate PCR reactions were set up in 96 or 384 well plates. In the case of the 7500 Fast Real-Time PCR system, method settings were as followed:

7500 Fast /Quantitative/SYBR/Standard run

The pre-set Real-Time PCR programs were identical on each Real-Time PCR system used with the exception of the melting curve step that needed to be added as the final step of the program for the 7900HT Fast. Real-Time PCR programs are described below.

	50°C 2:00	Holding Stage
	95°C 10:00	
40X {	95°C 0:15	Cycling Stage
	60°C 1:00	

Followed by :

95°C 0:15	Dissociation Stage (prism 7900/7500 Fast)
60°C 1:00	
95°C 0:30	
60°C 0:15	

or

95°C 0:15	Dissociation Stage (7900HT Fast)
60°C 0:15	
95°C 0:15	

The success of the PCR reactions was determined by standard curve as well as dissociation curve analysis. The standard curve characteristics indicate the PCR efficiency and define the linear range of amplification. The correlation coefficient (r) should be equal to or superior to 0.99. A progressive decrease in PCR efficiency after a few Real-Time PCR reactions indicated that primer sets used in the reaction were no longer stable. To avoid this issue, primer mix aliquots were prepared upon receipt and stored at -20°C. Multiple freeze and thaw cycles of primer mixes should be avoided and were generally limited to 6. However, some primer sets displayed extremely low stability. Freeze and thaw cycles for these sets were limited to 2. The specificity of the assay was determined upon analysis of the dissociation curve. A valid PCR reaction displayed a single peak of dissociation. Some primer pairs gave rise to a small dissociation peak followed by a much stronger one. While these were not ideal dissociation curves, the data was processed as all reactions displayed an identical pattern which did not affect the correlation coefficient the standard curve. In summary, valid data sets resulting from Real-Time PCR reactions should display good duplicate values within the

linear range of amplification determined by the standard curve and displayed one major dissociation peak.

Electrophoretic mobility shift assay (EMSA) or gel retardation assay or gel shift

Nuclear extracts from Murine erythroleukemia cells (Mel) cells were prepared as described in the "Protein Analysis" section. Protein concentrations were determined with the Bradford assay.

The EMSA was carried out using the LightShift® Chemiluminescent EMSA kit (Pierce), following the manufacturer's instructions. Double-stranded oligonucleotide – CCCAGGGGTGTGGTGGCAGGT- (CACC proximal probe) was used as the probe for EMSA. The 20μl EMSA reactions contained 5μg of Mel cells nuclear extracts, 2μl of 10X binding buffer provided in the kit, 2.5% Glycerol, 0.05% NP-40, 5mM $MgCl_2$, 20fmol of Biotin-End labeled probe and dH_2O to a final volume of 20μl. A separate control reaction was prepared omitting the nuclear extract. After 20min incubation at room temperature, 5μl of 5X loading buffer was added and samples were loaded onto a 5% polyacrylamide gel. Samples were separated by electrophoresis in 0.5X TBE buffer. To assess binding specificity, a second control was prepared adding a 200X molar excess of unlabeled CACC proximal probe for competition. A third control was prepared adding a 200X molar excess of the non-specific mutated CACC proximal probe – CCCAGGTTTGTGTTGGCAGGT-. Mutated nucleotides are underlined.

After transfer onto a 0.40μm nylon membrane (Pierce) at 380mA for 30min, DNA was crosslinked to the membrane using UV-light. For detection by chemiluminescence, the membrane was first blocked for 15min with gentle shaking in 20ml of blocking buffer provided in the kit prior to incubation for 15min with gentle shaking with 20ml of conjugate/blocking buffer containing a 1:300 dilution of stabilized Streptavidin-Horseradish Peroxidase conjugate (S-HRP). The membrane was washed a total of 4 times for 5min in 20ml of a 1:4 dilution of 4X wash solution provided in the kit. Finally, the membrane was equilibrated for 5min with gentle shaking in 30ml of substrate equilibration buffer provided in the kit.

Detection of the DNA was achieved by 5min incubation in a working solution containing 1:1 ratio of Luminol/Enhancer solution and stable peroxide solution both provided in the kit, followed by exposure to an X-ray film.

Antibodies

Antibodies used in western blots and ChIP assays are listed in table 2.4.

Antibody	Clone	Host	Type	Supplier
normal IgG		goat		SantaCruz Biotech
normal IgG		mouse		SantaCruz Biotech
normal IgG		rabbit		SantaCruz Biotech
normal IgG		rat		SantaCruz Biotech
HA	Y11	rabbit	polyclonal	SantaCruz Biotech
GATA-1	N16	rat	monoclonal	SantaCruz Biotech
Clim-2 (Ldb1)	N18	goat	polyclonal	SantaCruz Biotech
NF-E2	C19	rabbit	polyclonal	SantaCruz Biotech
CBP	A22	rabbit	polyclonal	SantaCruz Biotech
p300	N15	rabbit	polyclonal	SantaCruz Biotech
Brg1	*ND*	rabbit	polyclonal	Millipore
AcH3	*ND*	rabbit	polyclonal	Millipore
H3K14Ac	*ND*	rabbit	polyclonal	Millipore
H3K27Me	*ND*	mouse	monoclonal	Millipore
RNA Pol-II	4H8	mouse	monoclonal	Abcam
Ser5 RNA Pol-II	*ND*	rabbit	polyclonal	Abcam
H3	*ND*	rabbit	polyclonal	Abcam
H3K4Me1	*ND*	rabbit	polyclonal	Abcam
H3K4Me2	Y47	rabbit	polyclonal	Abcam
H3K4Me3	*ND*	rabbit	polyclonal	Abcam

ND = non disclosed

Secondary Antibody	Host	Type	Supplier
anti-mouse	rabbit	polyclonal	Jackson Immunoresearch
anti-rat	rabbit	polyclonal	Jackson Immunoresearch

Table 2.4. List of antibodies used in protein analysis and ChIP studies.

-CHAPTER 3-

EKLF-DEPENDENT MOLECULAR EVENTS AT THE MAMMALIAN β-GLOBIN LOCUS

INTRODUCTION

Mammalian β-globin gene clusters are ideal models to examine the mechanisms of tissue-specific gene transcription. The murine β-globin gene locus encodes four globin genes (5'–εγ-βh1-βmaj-βmin-3') that are positioned in the order of expression during ontogeny. Globin gene transcription is modulated by proximal and distal *cis*-regulatory elements that are characterized in erythroid cells by their hypersensitivity to DNaseI digestion, a marker of 'open chromatin'.

All β-globin like genes are immediately flanked by cis-regulatory regions that are similar, but not identical, in sequence. The promoter of each gene contains consensus binding sequences for a variety of ubiquitous, tissue-restricted and tissue-specific transcription factors. Of particular interest is the β-globin promoter CACC motif, which is required for high level transcription. The developmentally-specific transacting factor EKLF binds this motif specifically in erythroid cells, and is necessary for gene activation. Naturally occurring mutations of either the distal or proximal CACC boxes located at the β-globin promoter leads to β-thalassemia via disruption of EKLF binding (*166-168*). Similarly, cellular systems that recapitulate disruption of EKLF binding results in loss of β-globin transcription (*65*).

A long distance enhancer located 50kb upstream of the β-major globin gene, the locus control region, or LCR, is required for high level expression of all β-like globin genes (*33, 169*). This domain is composed of 6 functional lineage-specific DNaseI hypersensitive (HS) regions, the bulk of the enhancing activity of the LCR residing within HS2 and HS3. Core sequences of each HS encode cis-acting elements required for the recruitment of ubiquitous and tissue-specific transcription factors that are essential for globin gene expression. These include CACC boxes. Deletion of HS core regions affects β-globin gene expression drastically (*170-171*). While the deletion of HS2 inhibits

expression of all β-like globin genes throughout development, HS3 function is developmentally-specific, and enhances β-globin gene transcription specifically.

To date, the majority of globin gene regulation studies have focused on factors that have a broad impact on the specification and differentiation of all hematopoietic lineages, on cell fate/commitment, as well as on globin transcription. These factors include GATA-1, TAL-1/SCL and NFE2. In contrast, homozygous EKLF gene ablation in mice results in lethal anemia *in utero*. EKLF-null animals die at embryonic day 14.5-16.5 of gestation as a consequence of a severe defect in definitive erythropoiesis, with little evidence of an effect on other lineages (*144-145*). This thalassemic phenotype is characterized by a decrease in erythrocyte number, the absence of enucleated erythrocytes as well as a complete lack of β-globin gene expression. Detailed analysis of fetal liver-derived erythroblasts from EKLF null embryos at E14.5 revealed the loss of developmental-specific DNaseI hypersensitivity sites at the β-major promoter as well as within the HS3 of the LCR.

The mechanism of EKLF-directed transcriptional activation is unclear. Briefly, notions about EKLF mode of action revolve around its capability to remodel chromatin most likely via the recruitment of the SWI/SNF complex to *cis*-regulatory regions of the β-globin locus. In addition, EKLF has been shown to activate β-promoter function via a proline-rich amino-terminal domain. What is unclear is the temporal series of events that are mediated by EKLF, and required for gene activation at the endogenous locus.

In this study, we developed and validated a cellular system to investigate EKLF-dependent and -independent molecular events during terminal erythroid differentiation. Using this system, we were able to test the hypothesis that EKLF binding is indispensable to the temporal recruitment of a complex of transactivation factors and co-factors previously shown to be essential for β-globin transcription. Furthermore, we demonstrated EKLF-dependent and independent modifications of chromatin structure, and provided evidence of a role for EKLF in recruitment of the far upstream LCR. Taken together, we propose a model for EKLF function in transcriptional activation at the β-

globin locus, providing clues into the molecular cues that modulate β-globin promoter/LCR communication.

RESULTS

JH31: an EKLF-inducible cell system

To examine EKLF-directed transcription, we generated an erythroblast cell line model that does not express endogenous EKLF, but has integrated a retroviral construct allowing expression of ectopic human EKLF fused to a hemagglutinin (HA) epitope-tagged mutated estrogen element (ER^{TM}) domain at its amino terminal. Fetal liver progenitor cells from EKLF targeted mice were isolated and immortalized as described in (*155*). The cells were transduced with a vector supernatant encoding a murine stem cell virus (MSCV)-internal ribosome entry site (IRES) - puromycin resistance retroviral vector. Cells, in which the construct was integrated, were isolated by puromycin selection. These cells, designated JH31, express EKLF in the cytoplasm alone. Exposure of these cells to 4-OH-Tamoxifen (4-OH-TAM), a ligand for ER^{TM}, induces cytoplasm/nuclear translocation where EKLF can function as a transcription factor.

As shown in Figure 3.1.B, EKLF was detected at high levels in nuclear extracts from 4-OH-TAM treated cells, when compared to EtOH treated control (0h time point). Large amounts of the ER-fused EKLF protein were detected in the nucleus 30 min after induction, and as late as 6 hours post treatment. Importantly, extremely low protein levels were detected in nuclear extracts from uninduced cells. This demonstrated that EKLF was efficiently translocated to the nucleus upon 4-OH-TAM treatment.

The presence of EKLF in the nuclear compartment of the cells restores β-globin gene transcription. Primary transcripts, a measure of gene transcription, were detectable within 30min of induction, and reached a plateau between two and four hours post-treatment (Figure 3.1.C). Thus, JH31 cells treated with 4-OH-TAM demonstrated efficient translocation of EKLF to the nucleus with an associated rapid induction of β-globin gene transcription.

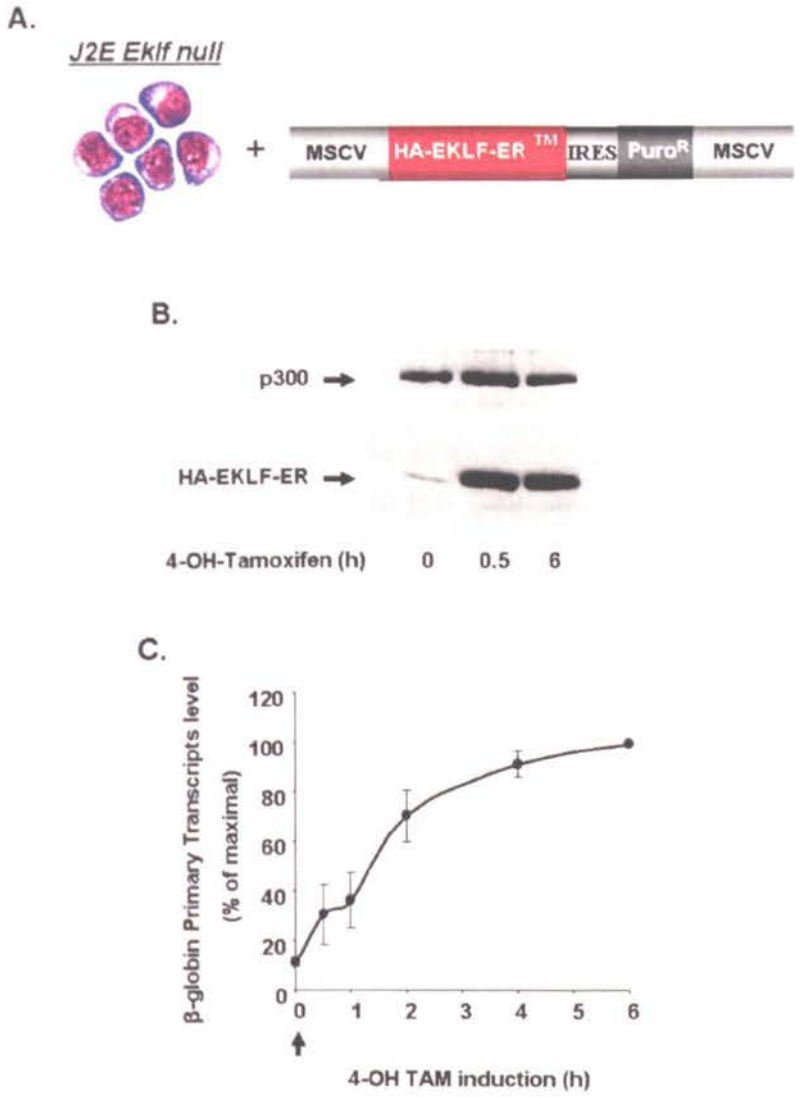

Figure 3.1. Tamoxifen Inducible EKLF Erythroid (JH31) cell system. (A) Description of the JH31 cell system with the construct used to create the cell line. (B). Western blot analysis from nuclear extracts derived from JH31 cells at 0, 0.5 and 6 hours of induction with 4-OH-Tamoxifen. An HA-tag antibody is used to detect the EKLF fusion protein (lower panel). Protein loading was estimated using an anti-p300 antibody (upper panel). (C). Primary transcripts analysis for the β-globin gene from 0 to 6 hours of induction with 4-OH-tamoxifen. Primary transcript levels were corrected to GAPDH levels. Data shown represents the average of 3 independent experiments (mean ± SEM)

The JH31 cell system is appropriate for evaluating the kinetics of transacting factor occupancy

EKLF binding at specific *cis*-regulatory regions of the β-globin locus was assessed by ChIP analysis using an anti-HA tag antibody (Figure 3.2.A). EKLF binding relative to IgG binding was detected at the HS3, HS2 and β-globin promoter regions after, but not prior to, induction of the cells with 4-OH-TAM. Interestingly, the relative enrichment of HS2 using the anti-HA antibody was significantly greater than both HS3 and β-major promoter regions.

A variety of controls were included in the assay. First, we demonstrated a lack of enrichment of a region located approximately 1kb upstream of the β-globin promoter by HA-ChIP. This control is critical to evaluate the efficiency of DNA shearing and therefore validates the sensitivity of the HA-ChIP. Importantly, no enrichment of the DNA was observed at the non-EKLF dependent amylase promoter, validating the specificity of the assay.

To study the consequences of EKLF binding to its target sequences at the β-globin locus, it would be ideal to follow the recruitment of factors, co-factors and chromatin modifications upon induction of JH31 cells with 4-OH-TAM in a temporal fashion. Since maximum levels of primary transcripts were reached prior to 6 hours post induction, we decided to follow the kinetics of EKLF binding during the first 6 hrs of treatment.

Crosslinking cells at various time points from 0 to 6 hours after 4-OH-TAM treatment, we were able to develop a picture of EKLF binding kinetics at cis-regulatory sequences within the β-globin locus. As depicted in Figure 3.2.B., EKLF was progressively recruited to the β-major promoter region reaching a plateau 2hrs into treatment. Although EKLF was detected at higher levels at HS2 than HS3, the kinetics of EKLF binding were comparable at both HSs. Intriguingly, EKLF binding at the LCR occurred more rapidly than at the β-major promoter. EKLF was recruited to the LCR within the first hour of 4-OH-TAM induction, with a majority of the recruitment being detectable within 30 min of induction. Together, our data suggests that EKLF is recruited preferentially at the LCR, and more particularly at HS2, upon 4-OH-TAM treatment in JH31 cells.

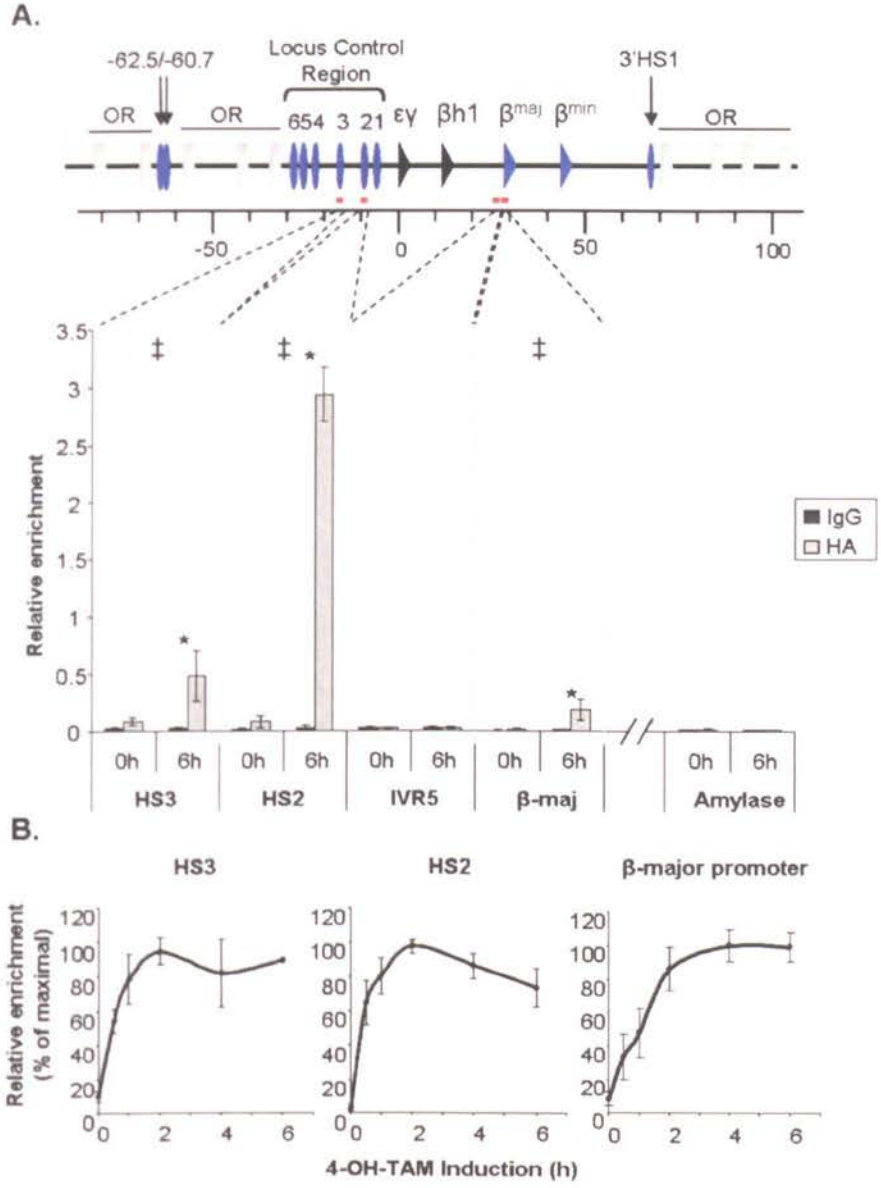

Figure 3.2. Binding of EKLF at the beta-globin locus in JH31 cells. EKLF binding across the beta-globin locus was determined by ChIP analysis using an anti- HA antibody and is represented as (A). Relative enrichment of EKLF corrected to input prior to, and 6hrs post treatment of JH31 cells with 4-OH-TAM. * p value<0.05 between IgG and corresponding sample. ‡ p value<0.05 between 0h and 6hr. (B). Relative enrichment of EKLF binding corrected to overall maximal signal intensity at 0, 0.5, 1, 2 and 6hours post treatment of JH31 cells with 4-OH-TAM. Data shown represents the average of at least 3 independent experiments (mean ± SEM)

EKLF-dependent binding of sequence-specific transcription factors at the β-globin promoter.

CACC elements are found in close proximity to GATA sites and E-boxes within *cis*-regulatory regions of the β-globin locus. The latter sites are critical for binding of the tissue restricted GATA-1 factor, and the SCL multiprotein complex respectively. In addition, a third hematopoietic restricted transacting factor, p45NF-E2 has been implicated in erythroid gene expression. Given the complex multistep nature of the gene transcriptional machinery and the essential role of several factors in maximal β-globin gene transcription, we hypothesized that EKLF may recruit a temporal series of multiprotein complexes to activate gene expression.

For example, EKLF interacts with GATA-1 *in vitro* and cooperates synergistically to induce transcription of a reporter gene (*172*). In contrast, although no direct interaction has been reported between EKLF and the SCL/TAL-1 -LMO2-Ldb1 complex, this heteromer is essential for globin gene transcription, the Ldb1 component mediating LCR/promoter interaction. Interestingly, a high frequency of GATA-1 and SCL/TAL-1-complex co-occupancy has been reported at GATA-1 activated genes (*173*).

Despite the lack of a recognizable binding site for NF-E2 at the β-major promoter, recruitment of this heterodimeric protein complex at both promoter and LCR is necessary for high-level expression of the β-globin gene (*126, 174-175*). Indeed, an NF-E2 multiprotein complex has been implicated in recruitment of the histone methyltransferase MLL2, with consequent induction of H3K4Me3 modification at the β-gene promoter.

As depicted in Figure 3.3.A., ChIP analysis using a GATA-1 specific antiserum revealed that the β-major promoter was enriched for GATA factor binding after, but not prior to, 4-OH-TAM induction. Thus, GATA-1 binding at the β-major promoter is strictly dependent upon EKLF.

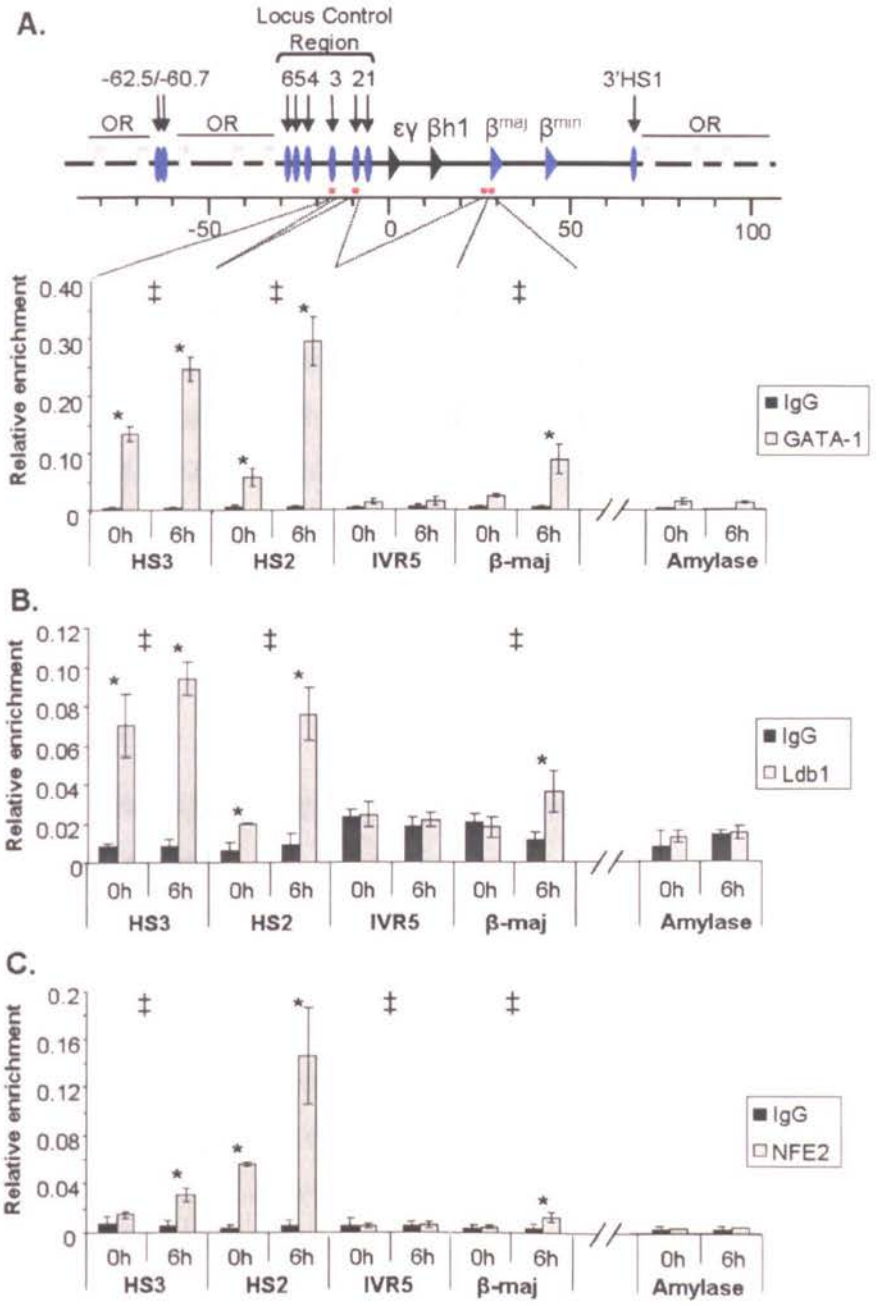

Figure 3.3.Binding of transcription factors across the β-globin locus in JH31 cells. Factor binding across the locus as determined by ChIP analysis using (A) GATA-1, (B) Ldb1 or (C) p45NFE2 antibodies at 0h and 6h post induction with 4-OH-TAM. * p value<0.05 between IgG and corresponding sample. ‡ p value<0.05 between 0h and 6hr. Data is representative of at least three individual experiments (± SEM).

Due to the profound defects associated with homozygous gene deletion in mice, it has been difficult to study the role of SCL/TAL-1 in the context of globin gene regulation. Using Ldb1 as a marker of the SCL/TAL-1-LMO2-Ldb1-E2A complex, we performed additional ChIP studies focused across the locus. Similar to GATA-1, Ldb1 was not recruited to the β-globin promoter in the absence of EKLF (Figure 3.3.B). Levels of enrichment of the promoter were similar using an anti-Ldb1 antibody or purified rabbit IgG prior to 4-OH-TAM induction. However, a significant increase in signal intensity was detected 6 hours post-induction. We can conclude that Ldb-1 recruitment at the β-major promoter requires the presence of EKLF. Finally, as depicted in Figure 3.3.C., data from ChIP analysis using an antibody directed against p45NFE2 demonstrates an EKLF-dependent recruitment of NFE2 mobilization at the β-major promoter. Enrichment of the promoter in ethanol treated control cells is equivalent to the IgG control. However, a significant increase in signal intensity is observed 6 hrs post induction using NFE2-specific antisera.

EKLF-dependent binding of sequence-specific transcription factors at other β-globin locus regulatory sites.

Unlike the β-major promoter, significant enrichment of the LCR was detected by ChIP in ethanol-treated control cells when tested for GATA-1, Ldb1 or NFE2 occupancy (Figure 3.3.A., B., and C. respectively). Specifically, high-level occupancy by GATA-1 and Ldb1 was detected at the HS3 prior to induction. In addition, significant low-level enrichment of HS2 is detected by ChIP assay specific for GATA-1 and the TAL-1/Ldb1 complex. In contrast, NFE2 mobilization at HS3 was strictly dependent upon 4-OH-TAM induction. Finally, high-levels of HS2 enrichment with NFE2 specific antisera were detected prior to EKLF translocation. Our data correlates with studies demonstrating that NF-E2's binding at the HS2 is a prerequisite for the erythroid-, but not developmentally-, specific formation of this HS (*159, 175-178*). Interestingly, NFE2 levels detected at HS2 were significantly higher than levels detected at HS3 both prior to, and post EKLF binding.

With EKLF binding, a statistically significant increase in signal intensity was detected at both HSs for all three factors. However, further analysis of the ChIP results obtained at

the LCR reveals differences in the behavior of factor occupancy between the two HSs of interest upon induction. Six hours post-induction, overall levels of GATA-1 and Ldb1 occupancy at HS2 reached levels comparable to those observed at HS3. Our data therefore indicates that high level binding of GATA-1 and Ldb1 at the HS3 occurs with little sensitivity to EKLF occupancy. HS2, we observed a significant dependence of maximal GATA-1 and Ldb1 recruitment on EKLF binding.

In conclusion, our experimental results demonstrate that unlike the β-promoter, recruitment of GATA-1 and the TAL-1/Ldb1 complex at the HS3 regulatory domain occurs independently of EKLF. In contrast, NF-E2 recruitment is EKLF-dependent. In contrast, although enrichment is detectable in its absence, EKLF enhances binding at HS2 of all three lineage-restricted transcription factors examined in this study.

EKLF-dependent ordered recruitment of transcription factors at the β-globin locus

To determine the tempo of recruitment of sequence-specific transcription factors to regulatory elements targeted by EKLF, we assayed GATA-1, Ldb1 and NF-E2 antisera-mediated enrichment of β-globin locus sequences at similar time points to that assayed for EKLF. Analysis of the kinetics of factor recruitment at each *cis*-element of interest revealed several important facts. First, the time of induction required for maximal occupancy of a factor is indicative of its relationship with EKLF. Secondly, the shape of the curve itself reveals valuable information about the manner in which a factor is being recruited. The initial response to EKLF binding can be categorized as early coupled or delayed in response and is measured by the slope of the curve as opposed to the actual percentage of factor occupancy. For the purpose of this manuscript, events at each individual target are presented first followed by a comparison of the data from each target to one another in order to emphasize similarities and differences between *cis*-elements.

Kinetic analyses for GATA-1, Ldb1 and NF-E2 across the β-globin locus are represented in Figure 3.4. At the β-major promoter, the kinetics of mobilization of GATA-1 and NF-

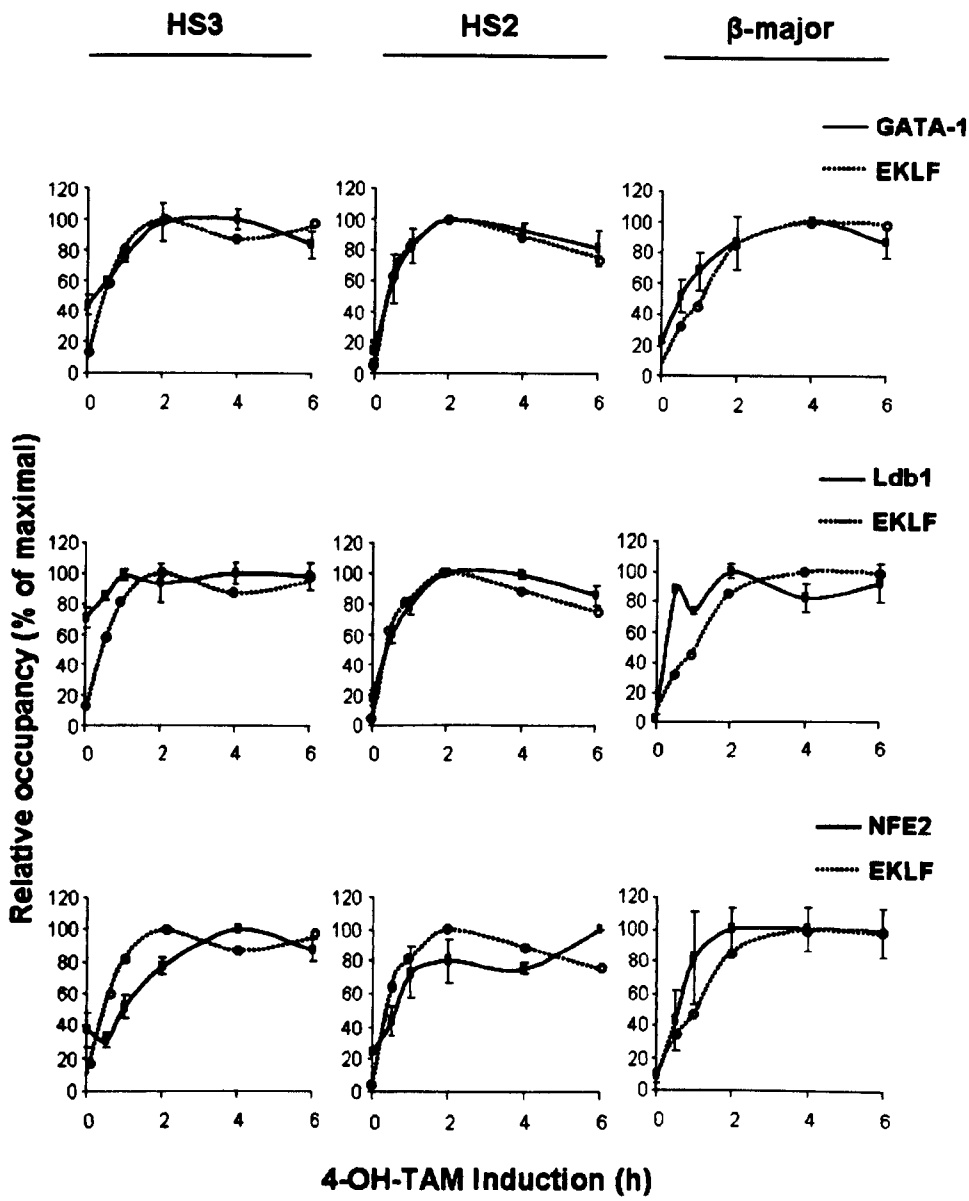

Figure 3.4. Kinetics of transcription factor binding at the beta-globin locus in JH31 cells. Transcription factor binding across the beta-globin locus was determined by ChIP analysis using an antibody raised against GATA-1, NFE2 and Ldb-1. Relative enrichment corrected to overall maximal signal intensity at 0, 0.5, 1, 2 and 6hours post treatment of JH31 cells with 4-OH-TAM. The broken line represents binding of EKLF for comparison. Data shown represents the average of at least 3 independent experiments (mean ± SEM)

E2 correlated closely with EKLF binding (broken line). In contrast, Ldb1 recruitment reached maximal occupancy prior to EKLF, suggesting that Ldb1 mobilization does not require interactions with other components of the EKLF multiprotein complex. This data suggests that appropriate SCL/TAL-1-E2A-LMO2-Ldb1 assembly at the β-globin promoter is a consequence of EKLF binding to its cognate CACC box rather than a physical recruitment by EKLF or GATA-1.

The fact that HS3 is highly occupied by GATA-1 and Ldb1 prior to EKLF binding renders the analysis of recruitment kinetics at HS3 difficult. Fluctuations were detected throughout the time course and allow us to state that a modest increase in GATA-1 recruitment at HS3 is coupled to EKLF binding. Intriguingly, NFE2 interaction at HS3 does not coincide exactly with EKLF mobilization. A clear delay in the response to induction was detected as NF-E2 levels remain unperturbed within the first 30min of induction, when more than 50% of maximal amounts of EKLF are measured. Our data suggest that NFE2 is recruited to HS3 by events subsequent to EKLF binding.

GATA-1, Ldb1 and NFE2 events at HS2 occurred rapidly, reaching 80% of maximum levels within an hour of induction. Recruitment of each factor was coincident with each other, as well as with EKLF binding. We can therefore conclude that recruitment of GATA-1, Ldb-1 and NF-E2 to HS2 is a direct consequence of EKLF binding.

EKLF–dependent and -independent histone modification at the β-globin locus

The chromatin state at a gene locus, determined in part by a variety of histone modifications, known as histone marks, modulate regulatory element function and gene activation. Currently, the role of EKLF in the establishment of these various histone modifications is not clear. Such a role is highly likely, given the closed chromatin structure at the of β-globin promoter delineated in EKLF-null primary erythroblasts, the essential requirement for EKLF in mediating β-globin gene transcription, and observations of interactions of EKLF with chromatin modifying enzymes. As an initial step in elucidating the role of EKLF in this process, we evaluated the acetylation and methylation status of core histones at EKLF targets sites within the locus.

i) Acetylation: Global histone acetylation across promoter regions serves as a universal marker of transcriptional activation (*179-181*). Domain-wide histone acetylation is representative of permissive chromatin and therefore priming of a domain for transcriptional activation. For example, acetylation of histone H3K14 residue is present at high levels throughout the β-globin locus prior to gene activation (*182*). Thus, in initial experiments, we focused our efforts on understanding the role of EKLF, if any in modulating levels of histone H3K14 acetylation. As shown in Figure 3.5.A, high levels of H3K14Ac are detected prior to EKLF binding and are maintained up to 6 hours post-induction. This particular modification is therefore established independently of EKLF.

In a second experiment, we determined global H3Ac levels in uninduced and induced cells. H3Ac levels, while detectable at the LCR prior to induction, increased across the locus with EKLF binding (Figure 3.5.B). Our data demonstrate that H3K14 acetylation across the locus does not require EKLF. However, EKLF triggers the acetylation of additional lysine residue(s) across the locus.

ii) Methylation: Differential histone H3K4 methylation identifies the transcriptional state of chromatin (*95, 183-184*). Enhancer elements are generally distinguished by a specific signature of H3K4 methylation which consists of high levels of H3K4Me1 in combination with low levels of H3K4Me3 (H3K4Me1+/H3K4Me3-) (*185*). H3K4Me2+/H3K4Me3- is a "hallmark" of developmentally poised genes, whereas H3K4Me3 is markedly increased at actively transcribed genes only (*95*).

To evaluate the role of EKLF on H3K4 methylation across the locus, we performed ChIP with isoform-specific antisera prior to, and 6 hours post induction of JH31 cells. Surprisingly, given its previous description as a marker of enhancer elements, high levels

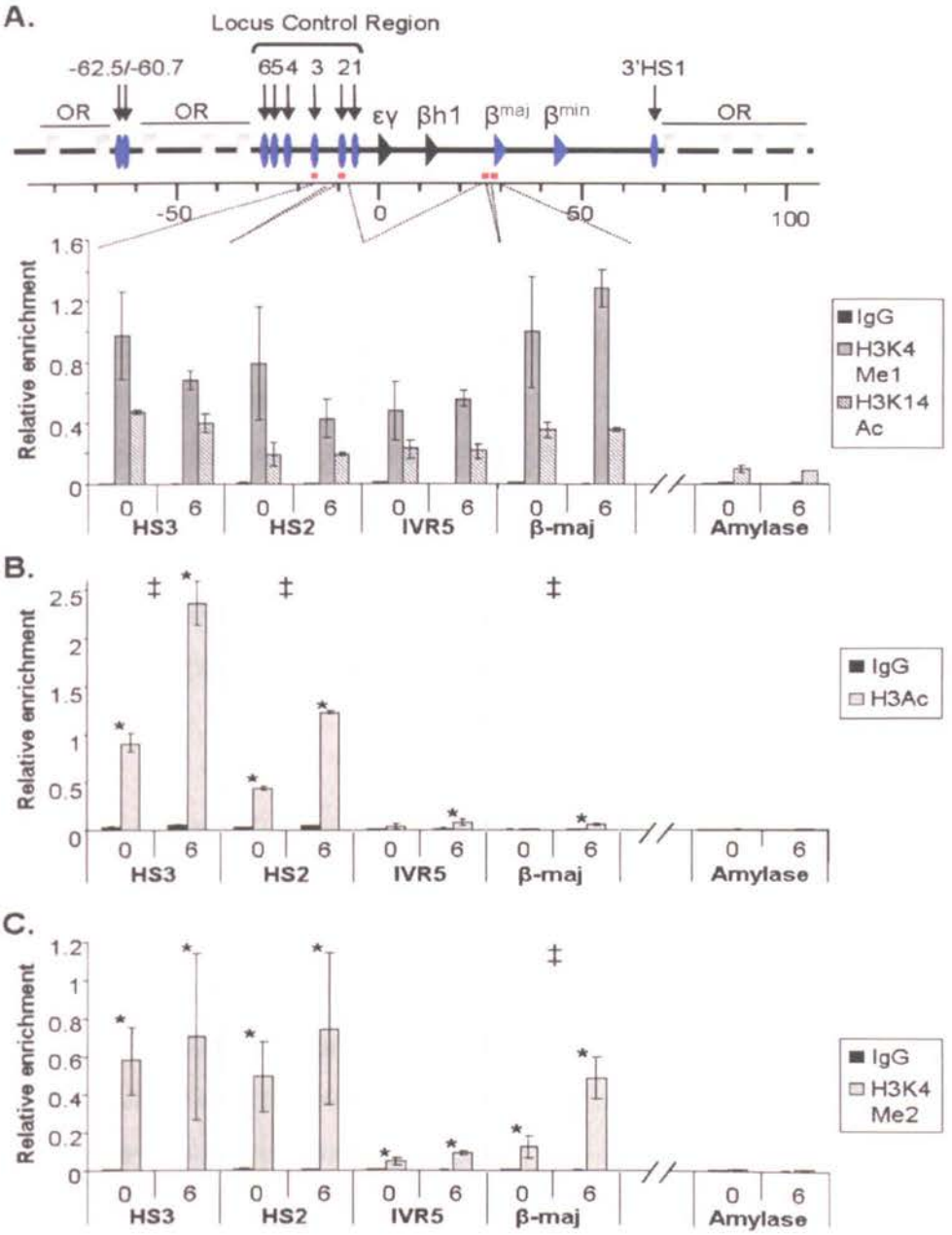

Figure 3.5. EKLF independent priming of the β-like globin genes locus. Schematic representation of the β-like globin genes locus where histone modification ChIP experiments were conducted for (A) H3K4Me1 and H3K14Ac, (B) H3Ac and (C) H3K4Me2. * p value<0.05 between IgG and corresponding sample. ‡ p value<0.05 between 0h and 6hr. Data is representative of a minimum of two individual experiments (± SEM).

of H3K4Me1 were not restricted to the LCR alone, but were observed across the locus (Figure 3.5.A.). Like H3K14Ac, H3K4Me1 marks were detected across the locus in an EKLF-independent manner. Similarly robust levels of H3K4Me2 (Figure 3.5.C) were detected throughout the locus in the absence of EKLF, restoration of factor activity by 4-OH-TAM inducing a significant increase in H3K4Me2 at the β-major promoter but not at the LCR.

In contrast to these events, trimethylation of H3K4 (H3K4Me3) was induced robustly, and in an EKLF dependent manner, at the β-globin gene promoter. In contrast, no significant change in this mark was observed at HS2-3 (Figure 3.6., and data not shown). High levels of H3K4Me3 coexist with H3Ac at the promoter of transcriptionally active genes. H3Ac demarks permissive chromatin domains regardless of the transcriptional status of a gene. However, there is no evidence to support the presence of high levels of H3K4Me3 at transcriptionally poised promoters or its requirement for transcriptional activation.

To explore the temporal relationship between EKLF binding and induction of trimethylation, we decided to monitor H3K4Me3 levels upon activation of the β-globin gene in JH31 cells. As depicted in figure 3.6.A, results from H3K4Me3 ChIP analysis demonstrated H3K4Me3 levels at the β-major promoter were not detected in the absence of EKLF, when the β-globin gene was not transcribed. Levels of H3K4Me3 increased significantly at the β-major promoter, but not at the non-EKLF dependent amylase promoter, upon 4-OH-TAM induction. Our data reinforces previous studies suggesting that H3K4Me3 is a marker of actively transcribed genes. However, the kinetics of H3K4Me3 occupancy at the β-globin promoter revealed a delay in the deposition of the H3K4Me3 mark with regards to EKLF binding and transcription (Figure 3.6.B.). Our data strongly argues that H3K4Me3 is not required for initial transcriptional events and is increasingly deposited with maximal transcriptional rates.

iii) Conclusion: Our data demonstrate that EKLF is not required for the priming of the β-globin locus as measured by H3K14 acetylation and H3K4 Me1-2 marks. However, its

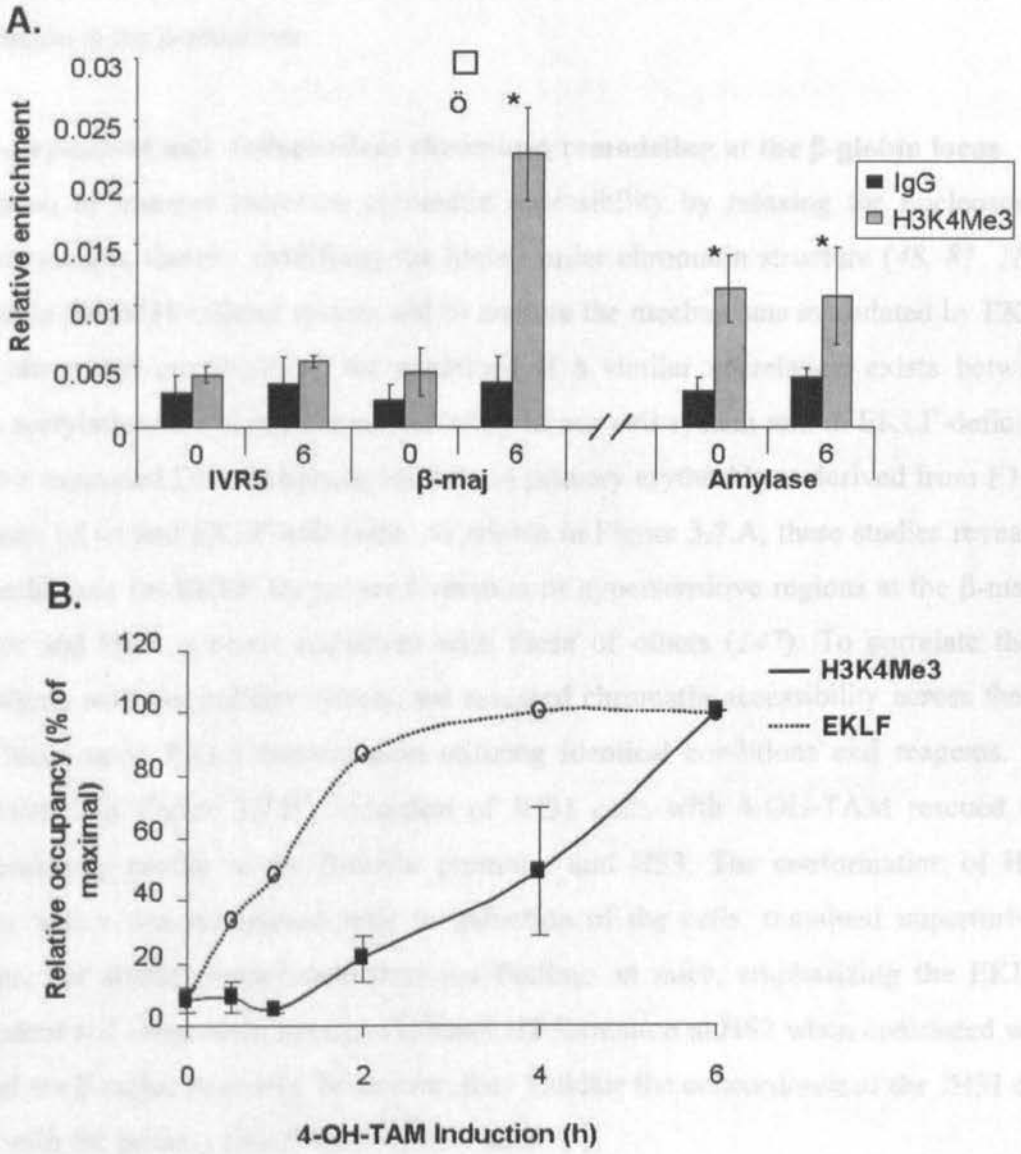

Figure 3.6. EKLF dependent H3K4Me3 at the β-globin promoter in JH31 cells. H3K4Me3 occupancy was determined by ChIP analysis using an anti-H3K4Me3 antibody and is represented as (A.) relative factor enrichment corrected to input prior to, and 6hrs post treatment of JH31 cells with 4-OH-TAM or (B.) kinetics of enrichment from 0 to 6h of induction of JH31 cells. * p value<0.05 between IgG and corresponding sample. ‡ p value<0.05 between 0h and 6hr. Data shown represents the average of at least 3 independent experiments (mean ± SEM)

translocation results in enhanced H3Ac marks across the locus, and specific H3K4Me3 modification at the β-promoter.

EKLF–dependent and -independent chromatin remodeling at the β-globin locus

Acetylation of histones increases chromatin accessibility by relaxing the nucleosome: DNA interaction, thereby modifying the higher order chromatin structure (*48, 81, 186*). To validate the JH31 cellular system and to explore the mechanisms modulated by EKLF during chromatin modification, we examined if a similar correlation exists between histone acetylation and chromatin accessibility in our cell system and in EKLF-deficient mice. We examined DNaseI hypersensitivity in primary erythroblasts derived from E14.5 fetal livers of wt and EKLF-null mice. As shown in Figure 3.7.A, these studies revealed an essential role for EKLF for proper formation of hypersensitive regions at the β-major promoter and HS3, a result consistent with those of others (*147*). To correlate these observations with our cellular system, we assessed chromatin accessibility across the β-globin locus upon EKLF translocation utilizing identical conditions and reagents. As demonstrated in Figure 3.7.B., induction of JH31 cells with 4-OH-TAM rescued the hypersensitivity profile of the β-major promoter and HS3. The conformation of HS2 element, which was remodeled prior to induction of the cells, remained unperturbed. Together, our studies recapitulate previous findings in mice, emphasizing the EKLF-independent and -dependent nature of DNaseI HS formation at HS2 when contrasted with HS3 and the β-major promoter. Moreover, they validate the concordance of the JH31 cell system with the primary EKLF-null erythroblasts.

EKLF-dependent recruitment of chromatin modifying enzymes to the β-globin locus

i) SWI/SNF activity: Having defined the histone modifications and chromatin remodeling that are associated with EKLF binding, we next evaluated the recruitment of chromatin-modifying co-factors, known to be recruited by EKLF. The SWI/SNF chromatin remodeling complex E-RC1 catalyzes remodeling of the β-major promoter *in vitro* via recruitment of its core ATPase subunit, Brg1, by EKLF. Subsequent studies have

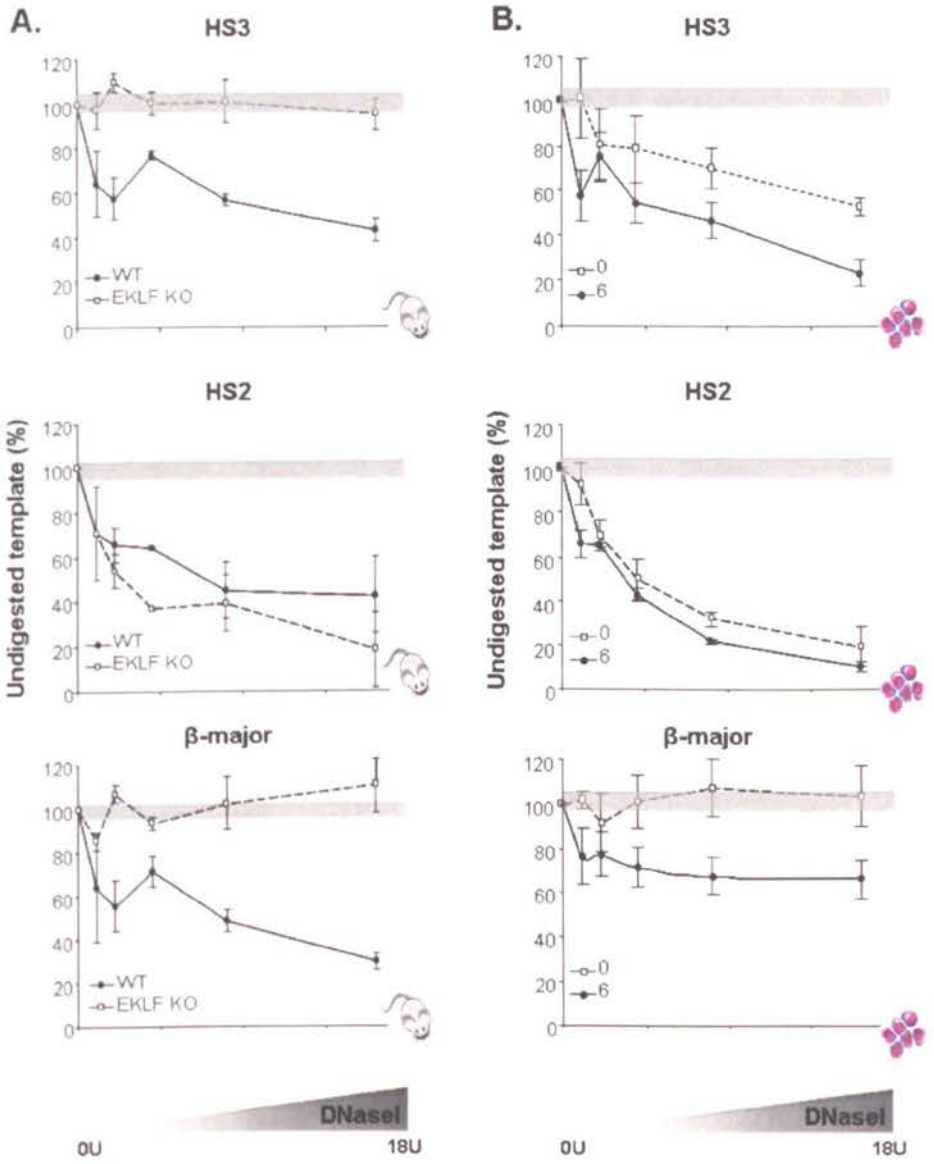

Figure 3.7.EKLF induces HS formation at the β-globin promoter and the LCR. DNaseI hypersensitivity assay in mice (A) and JH31 cells (B) at the HS3, HS2 and β-major promoter (higher, middle and lower panels respectively). Data shown represents the average of a minimum of 2 independent experiments (mean ± SEM).

demonstrated that the ATPase activity of Brg1 is required for appropriate formation of all HSs of the β-globin LCR *in vivo* (*47*). Interestingly, these studies have not demonstrated a requirement for Brg1 at the β-globin promoter! To clarify these observations in an *in vivo* setting, and to test the established model that EKLF recruits the E-RC1 complex at the β-globin locus, we performed ChIP assay in the JH31 cells, prior to and 6 hours post induction, using an antibody directed against Brg1. As depicted in figure 3.8.A., Brg1 was recruited to the β-globin promoter in the context of EKLF occupancy only. Importantly, no significant enrichment was observed at the non-EKLF dependent amylase promoter although significant enrichment was detected at the IVR5, 1 kb upstream the β-major promoter. Our data reinforces the idea that SWI/SNF mobilization at the β-major promoter is promoted by the recruitment of EKLF. In contrast to these observations, Brg1 was detected at low levels at the LCR in the absence of EKLF. A significant increase in Brg1 antisera-mediated enrichment of HS3 and HS2 sequences was detected 6 hours post-induction, indicating that Brg1 recruitment across the locus is enhanced in the presence of EKLF.

ii) CBP/p300: Specific lysine residues of histone proteins H3 and H4 tails are known substrates of HATs at transcriptionally activated loci (reviewed in (*187*)).The histone acetyl transferases CBP and p300 are known co-factors of EKLF. CBP- and p300-directed acetylation of EKLF modulates its transcriptional activity by increasing its DNA binding affinity as well as its transactivation activity *in vitro* (*59, 64-65*). HATs are also known interacting partners of other erythroid-specific transacting factors involved in globin gene regulation, including GATA-1 and NF-E2 (*188-189*). Thus, CBP and p300 may influence β-globin transcription via EKLF acetylation and/or histone lysine acetylation.

It is therefore interesting to decipher the relative recruitment of each HAT co-factor after EKLF binding, with the goal of dissecting their potential role(s), if any. Given our observations, that the murine β-globin locus histones are widely acetylated in the absence of EKLF, we would expect that CBP and/or p300 are efficiently recruited across the

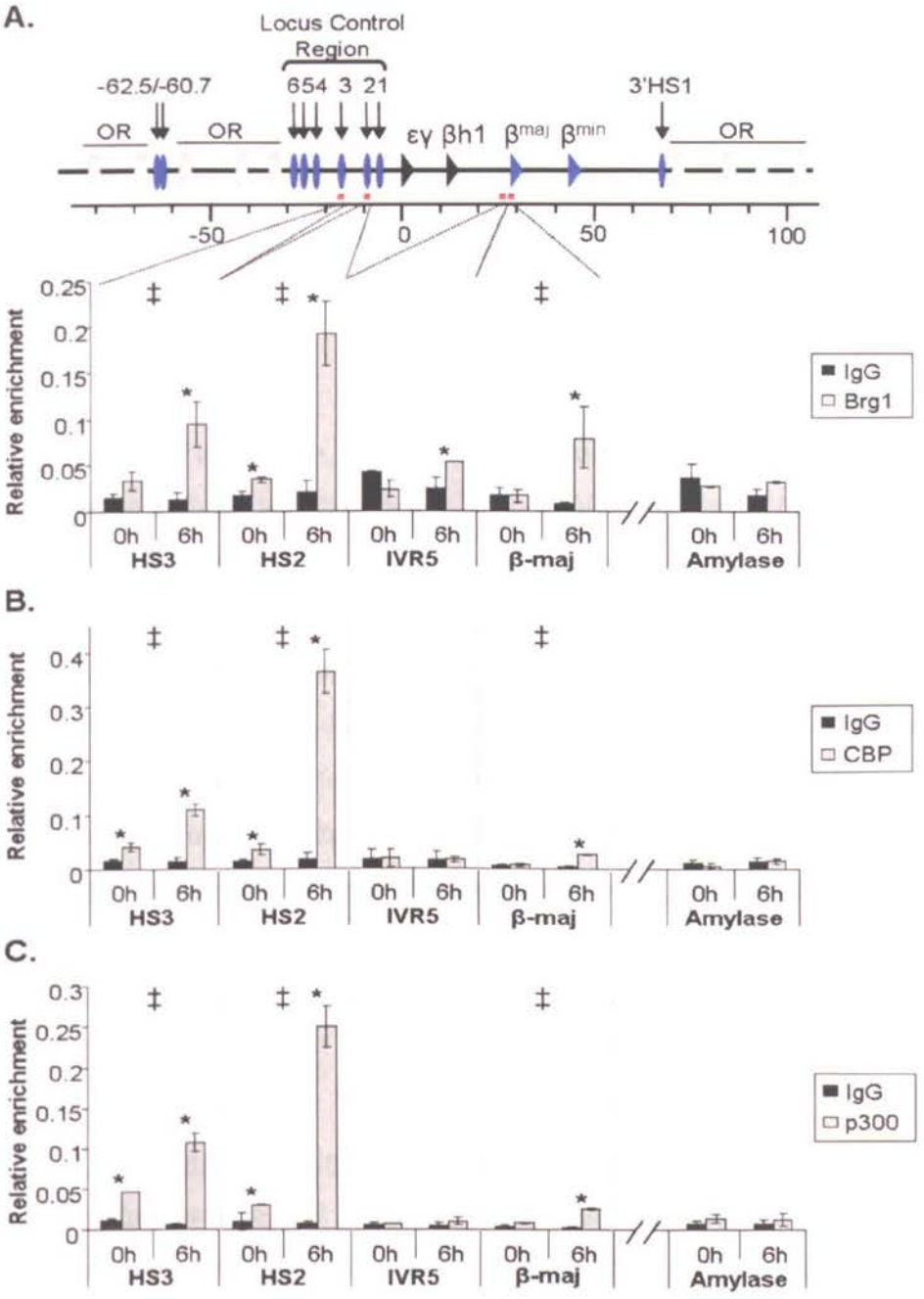

Figure 3.8. Binding of co-factors across the β-globin locus in JH31 cells. Factor binding across the locus as determined by ChIP analysis using (A) Brg1, (B) CBP or (C) p300 antibodies at 0h and 6h post induction with 4-OH-TAM. * p value<0.05 between IgG and corresponding sample.* p value<0.05 between 0h and 6hr. Data is representative of at least three individual experiments (± SEM).

locus prior to induction in JH31 cells. To test the hypothesis that EKLF is dispensable for CBP and/or p300 occupancy across the β-globin locus, we performed CBP and p300 ChIP analysis in the absence or presence of nuclear-localized EKLF (Figure 3.8.B., C. respectively). Surprisingly, significant enrichment of neither CBP nor p300 was detected at the β-major promoter prior to EKLF binding. This data contrasts with results obtained 6 hours post-induction, when both CBP and p300 are mobilized to the β-globin promoter. Our data strongly suggests that EKLF influences the recruitment of both HATs to the β-major promoter.

In agreement with our hypothesis, significant enrichment of HS3 and HS2 sequences with CBP and p300 antisera was detected prior to 4-OH-TAM induction. However, as a result of EKLF binding, our data indicates enhanced occupancy of both HATs at the LCR at 6 hours post induction. Interestingly, signal intensity measured for both CBP and p300 were more modest at the β-major promoter than at the LCR. Additionally, the fold increase in enrichment for both co-factors was also significantly greater at HS2 than HS3, suggesting that HATs are preferentially recruited to HS2 upon EKLF binding. Furthermore, our data indicates that EKLF binding enhances recruitment of CBP and p300 at the β-globin promoter. Both co-factors are preferentially recruited to the LCR in a semi-EKLF dependent manner, with a significantly higher affinity for HS2. ChIP analyses across the β-globin locus revealed strong similarities in occupancy patterns of the individual HATs.

iii) Kinetics of recruitment of chromatin remodeling enzymes to the β-globin locus: Using a similar approach to that described earlier in this Chapter, we analyzed the kinetics of recruitment of the co-factors of EKLF, namely Brg1, CBP and p300 at various time points post-4-OH-TAM treatment of JH31 cells. Interesting mobilization profiles emerged from these studies as represented in Figure 3.9. First, the rate of recruitment for HATs to the β-major promoter, were similar but not identical to the kinetics of EKLF binding. Although recruitment of both HATs is coupled to EKLF at all *cis*-regions studied, the shape of the curves for both factors differed significantly from each other at the β-major promoter. Recruitment of CBP to the promoter could be described as

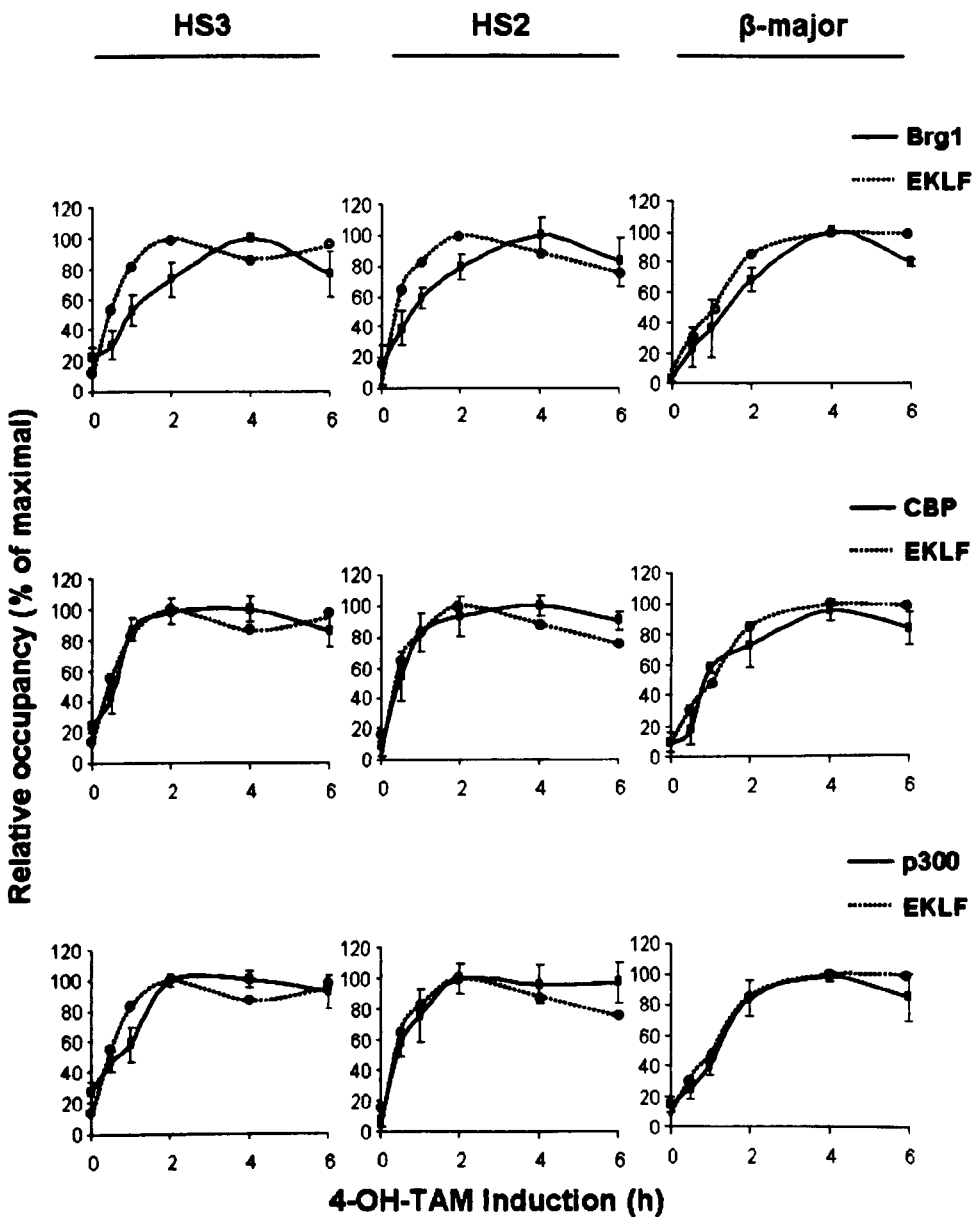

Figure 3.9. Kinetics of co-factor binding at the beta-globin locus in JH31 cells. Co-factor binding across the beta-globin locus was determined by ChIP analysis using an antibody raised against Brg1, CBP and p300. Relative enrichment corrected to overall maximal signal intensity at 0, 0.5, 1, 2 and 6hours post treatment of JH31 cells with 4-OH-TAM. The doted line represents binding of EKLF for comparison. Data shown represents the average of at least 3 independent experiments (mean ± SEM)

biphasic, with no significant binding in the first 30 minutes post-induction, but maximal binding by 1 hr post-induction. In contrast, p300 mobilization to the promoter occurred more gradually. Importantly, similar differences in recruitment profile of the two HATs were also detected at HS3. Our data suggests significant differences in the manner in which both HATs are recruited and may reflect distinct roles for each individual HAT in β-globin gene activation.

When the timing of Brg1 recruitment at the β-promoter and HS3 is evaluated, little significant binding occurs in the first hour post-induction, with a rapid increase to a plateau level beginning at two hours. In contrast, occupancy at HS2 is coincident with EKLF binding. Together, these observations suggest that Brg1 is recruited first to HS2, then HS3 and the β-major promoter.

EKLF-dependent activation of the β-globin gene is associated with recruitment of the basal transcription machinery

EKLF has previously been shown to function as a trans-activator. Furthermore, recent data suggests that EKLF is required in recruitment of the β-globin locus to RNA Pol-II-rich 'transcription factories'. To explore the mechanisms underpinning these observations, we extended our studies to explore the kinetics of RNA Pol-II recruitment. As shown in Figure 3.10.A., occupancy of RNA Pol-II was analyzed by ChIP assay in the JH31 cell system, using antisera that recognize unphosphorylated and phosphorylated forms of the enzyme. No significant enrichment of the β-major promoter was detected with RNA Pol-II antibody prior to 4-OH-TAM treatment, as opposed to a significant increase in signal intensity at 6 hours post- induction. Our data therefore demonstrates that EKLF is necessary for RNA Pol-II recruitment to the β-major promoter. A potential mechanism of recruitment relies on the ability of the LCR to act as a reserve for RNA Pol-II (*174, 190-195*). Analysis of (*196-197*) RNA Pol-II specific ChIP results at the LCR revealed enrichment of HS2 and HS3 sequences in ethanol-treated cells. RNA Pol-

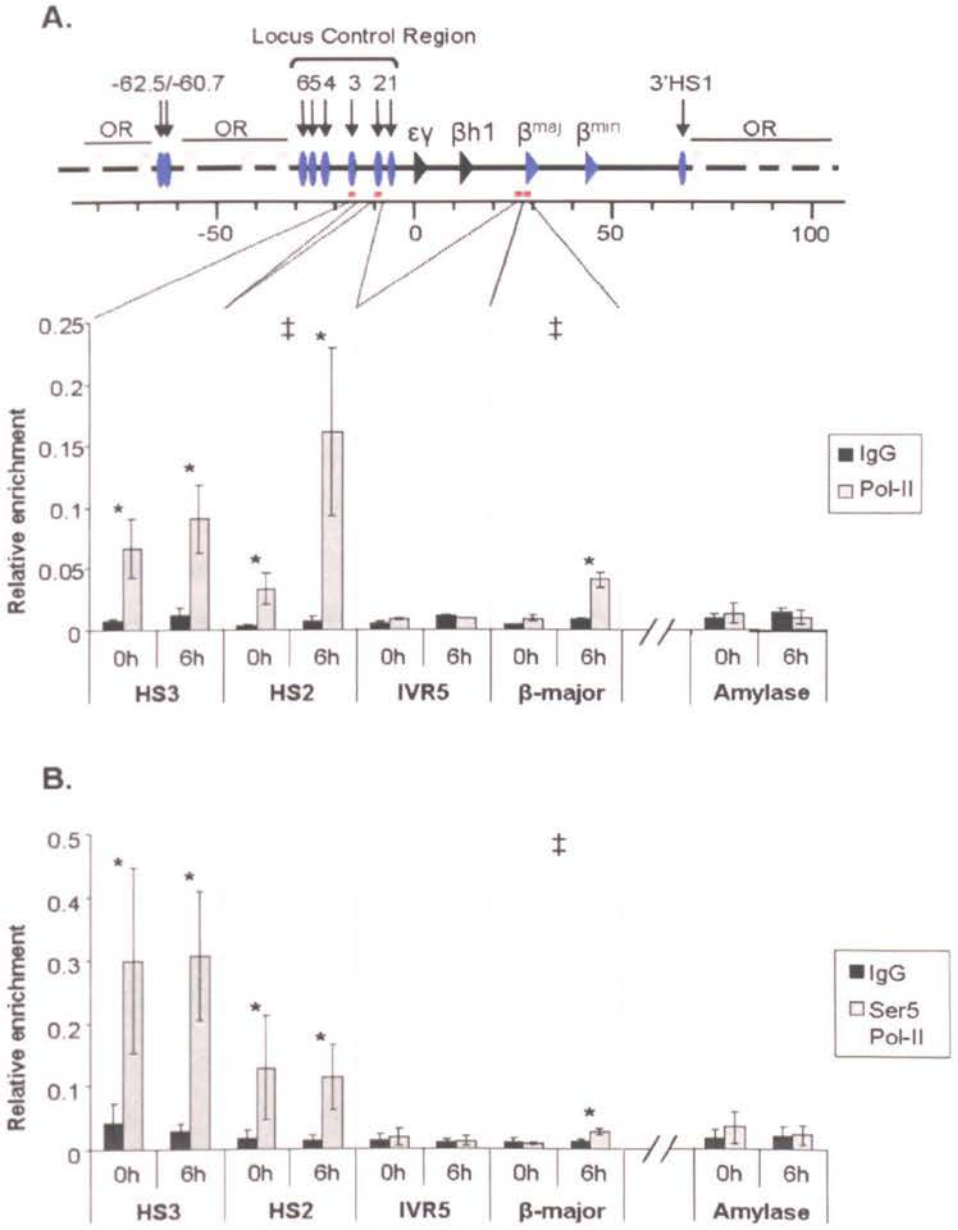

Figure 3.10. Binding of RNA polymerase II at the beta-globin locus in JH31 cells. RNA Pol-II binding across the beta-globin locus was determined by ChIP analysis using an anti- Pol-II antibody or an anti-Ser5Pol-II and is represented as relative factor enrichment corrected to input prior to, and 6hrs post treatment of JH31 cells with 4-OH-TAM. * p value<0.05 between IgG and corresponding sample. ‡ p value<0.05 between 0h and 6hr. Data shown represents the average of at least 3 independent experiments (mean ± SEM)

II levels detectable at the HS3 were similar pre- and post-induction. In contrast, further enrichment was observed with RNA Pol-II antisera of HS2 sequences, suggesting that EKLF binding is required for enhanced occupancy of the transcription machinery at the HS2.

We next considered the role of EKLF in RNA Pol-II activation. This event requires the phosphorylation of serine residues (Ser2 and Ser 5) in the carboxyl-terminal domain (CTD) of the core enzyme molecule (*198-199*). We chose to focus on the Ser5 moiety which, for the purpose of this manuscript, we will refer to as Ser5Pol-II. ChIP analysis allowed us to separate overall Pol-II occupancy from Ser5Pol-II occupancy across the locus (Figure 3.10.B.). Similar to overall Pol-II binding, Ser5Pol-II localization to the β-major promoter was strictly dependent, and enhanced, upon EKLF binding. In contrast we observed comparable Ser5Pol-II occupancy at HS2 and HS3 pre- and post-induction. However, given the increase in total Pol-II observed at HS2, the Ser5Pol-II/total Pol-II was reduced at this site. Our results are consistent with the idea that EKLF subserves context-specific functions in modulating RNA Pol-II across the locus.

EKLF-coupled Pol-II recruitment across the β-globin locus.

So far our data indicates that EKLF mediates the mobilization of the basal transcription machinery to the β-major promoter and HS2, but not HS3, 6 hours into 4-OH-TAM treatment of JH31 cells. Since the rate of β-globin transcription reaches a plateau by 6 hours of treatment, it is possible that our assay is biased towards these events. In addition, the assay design does not allow us to determine whether Pol-II recruitment is coupled directly to EKLF binding. In order to address these issues, we performed Pol-II and Ser5Pol-II ChIP analysis across the locus at various time points from 0 to 6 hours of induction in JH31 cells, as represented in figure 3.11.

First, we focused our attention at events at the β-globin promoter. Total Pol-II mobilization at the β-major promoter was not coupled with EKLF binding. Although EKLF binding was progressive at the β-major promoter, Pol-II occupancy did not

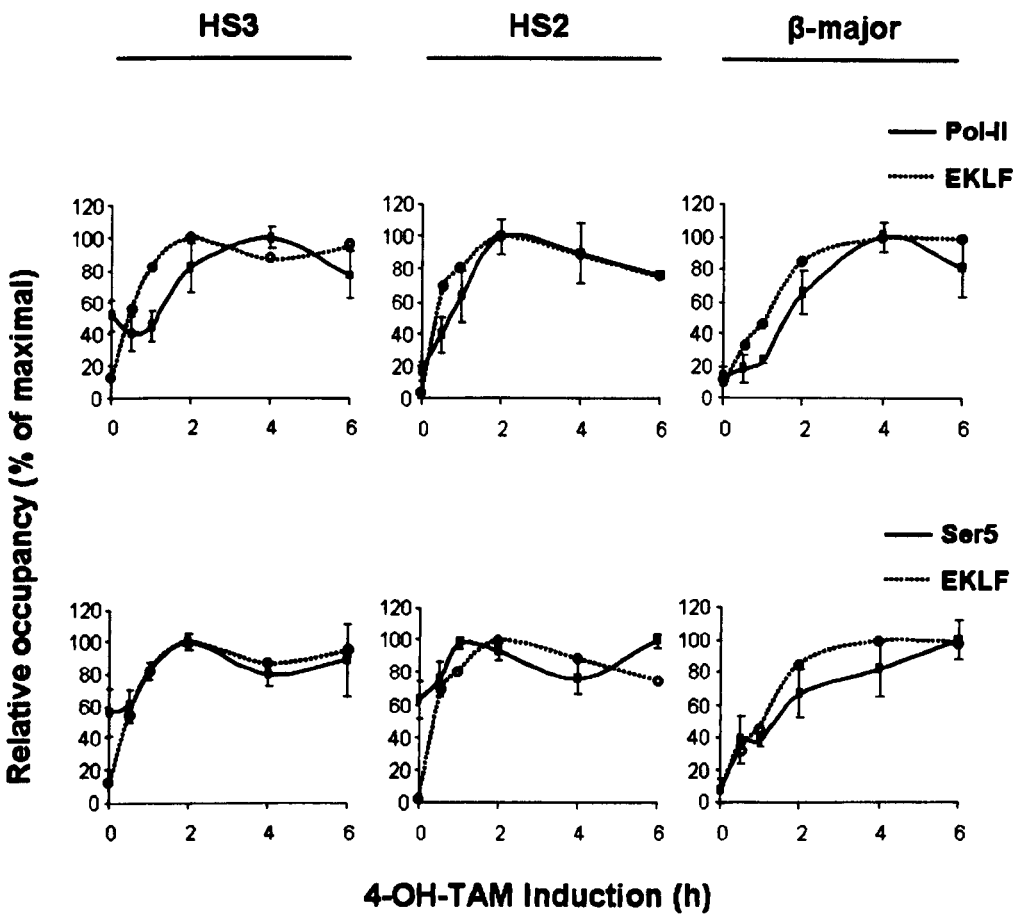

Figure 3.11. Kinetics of RNA Pol-II binding at the beta-globin locus in JH31 cells. RNA polymerase II binding across the beta-globin locus was determined by ChIP analysis using an antibody raised against Pol-II or Ser5Pol-II. Relative enrichment corrected to overall maximal signal intensity at 0, 0.5, 1, 2 and 6hours post treatment of JH31 cells with 4-OH-TAM. The doted line represents binding of EKLF for comparison. Data shown represents the average of at least 3 independent experiments (mean ± SEM)

significantly increase until 2 hours into treatment, when levels of EKLF were maximal. Therefore, Pol-II mobilization at the β-major promoter required an intermediary step subsequent to EKLF binding. In contrast, Ser5Pol-II recruitment correlated strongly with the kinetics of EKLF binding at the promoter as well as transcriptional kinetics of the β-globin gene. We can therefore conclude that a significant amount of Ser5Pol-II is recruited and/or modification coincides with EKLF binding to the β-major promoter.

The dynamics of Pol-II recruitment/modification at the LCR differ between HS3 and HS2. As expected, there was no significant difference after induction at HS3, although the amounts of Pol-II fluctuate somewhat between 0 and 6 hours. In contrast, there was preferential recruitment to the HS2. Thus, increase in Pol-II binding was detectable within 30min of induction and steadily increased at the HS2. Analysis of Ser5PolII modification demonstrated statistically significant differences at the LCR. A minor increase in Ser5PolII modification preceded changes in total Pol-II events at both HS3 and HS2. Indeed, the positive fluctuation of Ser5Pol-II occupancy at the HS3 was detectable prior to 1hour post induction. HS2 events follow a similar although noticeably more rapid pattern.

In conclusion, studies of Pol-II binding, and its activation, across the β-globin locus indicate that Pol-II recruitment is coupled closely to EKLF binding only at HS2, while EKLF-coupled Ser5Pol-II modification is detected at both β-major promoter and HS3. Thus, EKLF directly influences Pol-II density at the HS2, and Ser5Pol-II density at the β-globin promoter.

DISCUSSION

The EKLF-dependent erythroblast model, that we have validated and characterized here, provides an ideal template to explore the temporal mechanism(s) that modulate β-globin gene transcription. Our studies demonstrate not only clear effects of EKLF on chromatin structure and *trans*-activation at the murine β-major promoter and the LCR, but also context-specific differences in EKLF action at the proximal and distal *cis*-acting regulatory elements. For example, the tempo of EKLF binding varies between the promoter and LCR, suggesting that differences in the chromatinized template may determine the rate of interaction. Similarly, EKLF has differential effects on factor and co-factor recruitment at these elements, which, when coupled with the observations of others in primary murine erythroblasts, support a context-specific mechanism of action for this critical factor. We also show that the EKLF-naïve chromatin architecture of the promoter exists in a poised state, and that EKLF binding induces histone H3 trimethylation. The latter event occurs in a timeframe that suggests that it is not required for early initiation of transcription, but rather stabilizes the process when it is occurring at a maximal rate. Similarly, the lack of correlation between chromatin remodeling and Brg1 recruitment suggests, that unlike the LCR, Brg1 is necessary, but not sufficient, for chromatin remodeling at the endogenous promoter. In contrast, even the modest level of EKLF binding observed in the first hour after induction stimulates recruitment of Ldb1, a component of the TAL1 complex essential for LCR/promoter interaction. This observation provides the first physical evidence that EKLF modulates promoter/enhancer interaction. Finally, we show that EKLF binding induces rapid binding of the Ser5-Pol-II isoform of the RNA polymerase II multiprotein complex, a context-specific difference with the LCR, given the role of EKLF at increasing total Pol-II alone at HS2. Together, these studies provide novel insights into EKLF function, and provide an outstanding platform to dissect the roles of the functional domains of the EKLF molecule.

EKLF-dependent factor occupancy of the β-globin promoter

Factor occupancy at the actively transcribing β-globin promoter is largely dependent upon EKLF binding. Indeed, in the context of this study we demonstrate that the recruitment of transcription factors (GATA-1, NF-E2), bridging molecules (Ldb1), transcriptional complex (RNA Pol-II), cofactors and chromatin modifiers (CBP, p300) and finally chromatin remodeling complex (Brg1) to the promoter occurred as a consequence of EKLF binding.

One cannot eliminate the possibility that additional factors to those examined in this study are being recruited to, or lost from, the promoter in an EKLF-independent fashion. Some additional factors may be associated with transcriptional repression or chromatin remodeling in order to maintain the promoter in a DNaseI non-hypersensitive configuration. The requirement of factor occupancy for the recruitment of EKLF to its binding motifs cannot be excluded.

Our data correlates with factor occupancy studies at the β-globin promoter in erythrocytes derived from mice carrying a human β-globin locus transgene (*200*). We supplement the mentioned studies with the demonstration of the EKLF dependent recruitment of Ldb-1, p300 and Ser5Pol-II.

Importantly, our data significantly complements additional transcription factor dependency studies at the β-globin promoter. A similar strategy was used to evaluate GATA-1 directed molecular events and revealed that promoter occupancy by EKLF, NF-E2 and FOG-1 in addition to Brg1, CBP and RNA polymerase II requires the presence of GATA-1(*61*). Studies in CB3 cells where NF-E2 is not expressed revealed the requirement for the B-zip factor in the recruitment of Ser5-PolII as well as a MLL2 based histone methylase complex which itself is critical for high levels of H3K4Me3, a modification associated with actively transcribed genes (*201*). Our studies therefore highlight similarities between EKLF dependent, GATA-1 dependent and NF-E2 dependent events, suggesting an interdependency of all transcription factors to recruit the factors necessary to induce high level β-globin gene expression.

The lack of detectable occupancy of any of the studied factors in the absence of EKLF, in addition to the resistance to DNaseI at the β-major promoter explains in part the profound defect in β-globin synthesis observed in EKLF null mice and patients suffering from β-thalassemia resulting from a mutation of the CACCC element in the promoter.

EKLF independent occupancy of GATA-1, Ldb1 and NF-E2 at the β-globin LCR

Unlike factor recruitment at the β-globin promoter, factor occupancy at the LCR was not entirely dependent upon EKLF binding. High levels of GATA-1 and Ldb1, but not NF-E2, at the HS3 were proven to be EKLF-independent. It is interesting that factors involved in β-globin transcription were detected at the HS3 prior to EKLF binding. The data demonstrates that even though the HS3 is not hypersensitive to DNaseI in the absence of EKLF, GATA-1 and most probably TAL-1 binding motifs are accessible. The presence of both factors at the HS3 is therefore insufficient to increase its sensitivity to DNaseI and requires the recruitment of EKLF.

The data is in agreement with several studies linking HS3 formation and β-globin transcription to EKLF expression (*202*). In K562 cells, where EKLF is expressed at low levels and gamma-globin genes are expressed at the expense of the β-globin gene, the HS3 does not exhibit DNaseI hypersensitivity. In MEL cells however, where β-globin genes are expressed upon differentiation and EKLF is expressed at high levels, HS3 is hypersensitive to DNaseI cleavage.

In addition, the developmental specificity of the HS3 transcriptional regulation of the β-globin gene has been described in transgenic mice, where eGFP expression is under the influence of the HS3 (*203*). The hypersensitivity status of the HS3 in EKLF null mice, where β-globin transcription is impeded, is similar to that of K562 cells. Therefore, there is a strong correlation between EKLF expression, β-globin expression and HS3 hypersensitivity profile. All studies combined lead us to the likely hypothesis that HS3 activity as well as its accessibility to DNaseI depends upon EKLF binding.

Surprisingly, our data at the LCR only partially correlates with aforementioned experiments in mice carrying the human β-globin locus transgene. Both set of studies demonstrated the EKLF-dependent nature of histone modifications in addition to the mobilization of CBP and Brg1 at HS2. However, in contrast to the data from transgenic erythrocytes, we demonstrate enhanced occupancy of GATA-1 at HS2 in the presence of EKLF as well as p45NF-E2 binding at the HS2 in the absence of EKLF. Transgenic studies did not include a survey of factor occupancy at the HS3. The observed discrepancies may underlie mechanistic differences between the mouse and human β-globin loci. The application of distinct detection techniques for the ChIP experiments may also account for the noticeable inconsistencies.

It is interesting to notice the similarities between GATA-1 and SCL/TAL-1 occupancy at the β-globin locus in relation to EKLF. Our data is in agreement with studies describing GATA-1 as a potent recruiter of SCL/TAL-1(*173*). The fact that both GATA-1 and TAL1, core components of several multiprotein complexes linked to either activation or repression processes, suggests the presence of a repressor complex at the HS3. Developmental cues such as EKLF binding may induce a subunit switch that triggers change in the activity of the complex (es) whose core is composed of GATA-1 and TAL1. Such mechanism has been implicated in the regulation of β-globin transcription, where heme constitutes the developmental cue, leading to a switch in MafK dimerization partner from Bach1 to p45NF-E2 (*204*). Recent studies suggest that the combined presence of GATA-1 and SCL/TAL1 is associated with GATA-1 activated genes selectively (*117, 173*). The lack of SCL presence at GATA-1 repressed genes thus argues against the hypothesis of a GATA-1 repressive type complex docked at the β-globin HS3. Nonetheless, the mentioned study was carried out using a GATA-1 inducible erythroid cell line and may have therefore not detected intermediary stages of gene activation.

GATA-1 repression is associated with recruitment of the NuRD complex and low levels of histone acetylation. Although highly significant, levels of H3Ac are similar at HS3 and HS2 prior to induction of EKLF relocation and increase with EKLF binding. While this

observation does not provide a strong support for the proposed hypothesis, it is certainly not contradictory.

Despite the fact that it is technically challenging to determine the kinetics of chromatin remodeling we can propose that EKLF-dependent reconfiguration of the HS3 occurs prior to and is require for NF-E2 to be mobilized. In contrast to its EKLF-dependent nature at the HS3, NF-E2 binding to the core HS2 occurs independently of EKLF. About 50% of the maximal signal is detected prior to induction of the JH31 cells. Maximal levels are detected after EKLF binding to HS2 suggesting a facilitating process where EKLF recruits additional NF-E2 most probably through the recruitment of GATA-1. One striking observation is that the lack of efficient factor binding at the HS2 in the absence of EKLF does not correlate with its DNaseI accessibility status. The data strongly implies that EKLF is required for GATA-1 and TAL1 binding to their DNA binding motifs at the HS2. The data further favors the concept of separate GATA-1, TAL1 complexes at the LCR where a complex A is recruited in an EKLF-independent manner whereas the GATA-1, TAL1 containing complex (es) B requires EKLF to occupy the LCR at high levels.

Locus priming does not require EKLF directed chromatin reconfiguration

EKLF is required for the establishment of an active chromatin hub (ACH) consisting of a measurable decrease in proximity between the β-globin promoter and the HSs of the LCR (*150*). Nevertheless, the absence of EKLF does not perturb the spatial clustering of the individual HSs to each other, a configuration of the LCR that is tissue specific (*150, 205*). Our data, especially the EKLF-independent priming of the locus clearly suggests that EKLF is not involved in establishing the tissue-specific characteristics of the locus. However, the lack of β-globin transcription observed in EKLF null mice and in JH31 cells that are treated with ethanol suggest that EKLF's role is at a stage when the locus is already poised, as defined by LCR activity, and broad changes in histone modification that span the entire locus.

Improving our understanding of the relationship between the Locus Control Region and the active β-globin promoter.

Using EKLF as a limiting factor of globin gene transcription, we were able to distinguish between molecular events at the LCR and the β-globin promoter. Since EKLF-independent binding of several factors can be detected at the LCR (Pol-II, Ser5-PolII, GATA-1, Ldb1, NF-E2) as opposed to none measured at the promoter, we can conclude that some events at the LCR precede events at the β-promoter and occur prior to clustering of the promoter to the HSs.

Similar studies in the GATA-1 deficient G1E cell line led to comparable conclusions as Pol-II is detected at both HSs in a GATA-1 dependent manner, prior to EKLF binding (*61*) and that GATA-1 binding itself at the HS3 occurred prior to EKLF being detected. Additional data supporting this statement resides in the kinetic studies of factor occupancy at each *cis*-element. Indeed, the kinetics of factor recruitment at the HS2 were globally more rapid than at the β-globin promoter.

However, several clues direct to several potential LCR-dependent promoter events. Analysis of the phosphorylation status of the mobilized RNA pol-II revealed that the enzyme present at both the HS2 and the β-globin promoter was of similar nature and distinguished itself from the RNA Pol-II detected at the HS3. The LCR being involved in the elongation process taking place at the β-globin promoter, it is possible that the above observation is reflective of a transfer/communication from the HS2 to the promoter. Indeed, support for such a conclusion comes from the studies of Bresnick and colleagues (*193*). However, it is likely that the precise mechanism is more complex, given that recent studies in mice transgenic for the human β-globin locus suggest that deletion of the core HS2 has little effect on β-globin transcription (*206*).

Similarities between the HS3 and the β-globin promoter were also observed, suggesting that the promoter may communicate with HS3. The overall kinetics of factor recruitment at the HS3 has a significant resemblance to events occurring at the promoter. The data being mainly descriptive leaves much room for speculation. There is evidence for a

physical adjacency between the β-globin promoter with the LCR in β-globin expressing cells. However the HS2 and HS4 appear to be in closer physical proximity to the promoter than the HS3 (*207*). All together, the data strongly suggests that the HS3 and the β-major promoter elements share mechanistic properties adding to their developmentally-specific profile.

It is important to consider that the assays we have used to evaluate factor binding may have technical challenges that may misrepresent the physiological conditions during gene activation. Although ChIP analysis is widely applied in laboratories studying transcriptional mechanisms and is a powerful tool used to dissect molecular events *in vivo*, it is not a flawless technique, and may bias our results. The assay relies extensively on the antibody's capacity and efficiency to detect the target protein. Several factors may contribute to the decrease in the accessibility of the epitope including over-crosslinking as well as the nature and conformation of the protein complex. Previous studies have suggested a structural interaction between the 2 HSs that may constitute a blockade in the accessibility of the protein to the antibody (*208*). One could therefore link the relatively low detection in factor occupancy at the HS2 prior to recruitment of EKLF to restricted epitope access. Following the above scenario, it is entirely possible that the detected factors at the HS2 in untreated cells are actually present in higher amounts but remain undetected.

Another plausible interpretation of these studies is that the HS3 is blocking access to the HS2 for all factors excluding NF-E2 and that the chromatin reconfiguration resulting form EKLF binding leads to a shift in the overall configuration of the LCR holocomplex, permitting factor interaction at the HS2. Thus, it is unclear whether factor recruitment at the HS2 is a direct consequence of EKLF binding at the HS2 or a result of holocomplex reconfiguration by EKLF binding at the HS3.

Overall, our studies allowed us to establish a model of the temporal molecular events leading to β-globin gene expression. Our model is represented in figure 3.12. and distinguishes between the temporal events at the β-globin promoter, HS3 and HS2.

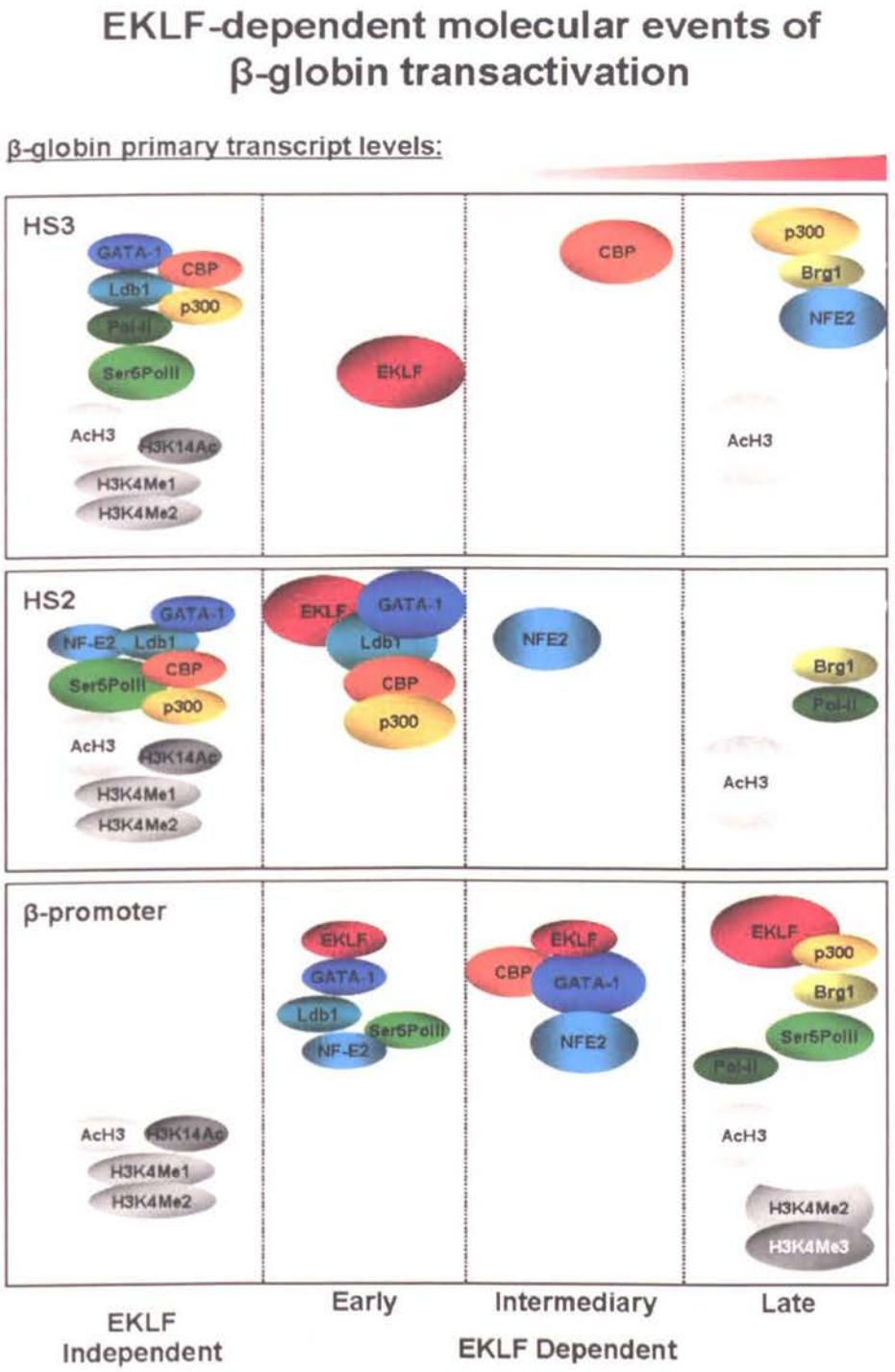

Figure 3.12. EKLF-dependent molecular events of β-globin transcriptional activation. Factor binding and histone modifications across the beta-globin locus upon EKLF binding in 4-OH-Tamoxifen treated JH31 cells. "Late" events represent events occurring when β-globin transcription is reaching a plateau.

-CHAPTER 4-

CONTEXT-SPECIFIC EKLF-MEDIATED TRANSCRIPTIONAL ACTIVATION OF THE ALPHA HEMAGLOBIN-STABILIZING PROTEIN (AHSP) AND DEMATIN GENES

INTRODUCTION

The role of EKLF in the activation of β-globin gene transcription has been well documented. Microarray analysis from EKLF-null fetal livers, and inducible cell lines, revealed the essential role of EKLF in the expression of multiple additional erythroid specific genes (*151-152*). EKLF target genes are involved in the regulation of various cellular processes including cell cycle regulation, membrane and cytoskeleton integrity as well as hemoglobin production. Of these EKLF-dependent genes, we decided to focus predominantly on the chaperone protein AHSP, and the membrane associated cytoskeleton protein dematin.

Although not an integral part of the hemoglobin tetramer, AHSP is one of the components required for its appropriate formation. The main function of the AHSP protein is to stabilize free alpha chains in erythroid cells, preventing their precipitation and subsequent induction of hemolysis. AHSP loss in alpha-thalassemic mice worsens the erythroid phenotype, implying that AHSP exerts additional functions which are still undefined (*209*). The AHSP gene, located on mouse chromosome 7, is constituted of 3 exons across a chromatin region spanning approximately 1kb (Figure 4.1.A.). AHSP expression is modulated by a promoter located immediately upstream of Exon 1. As described in Figure 4.1.B. and C., the AHSP promoter contains DNA binding elements for GATA factors and potential EKLF sites (CACC boxes). Of interest for this study, we noticed the absence of an E-box within the cluster of GATA and CACC boxes. E-boxes are often associated with GATA elements and are known to cooperate in regulating the transcription of several genes including the β-globin gene, protein 4.2 gene and the EKLF gene (*122, 140, 151, 173, 210-213*). Although additional functional elements reside within the promoter, we decided to focus on those which are erythroid-specific. Importantly, expression of AHSP does not appear to be influenced by a long distance enhancer, placing it in a different class to the more-studied globin gene loci.

A.

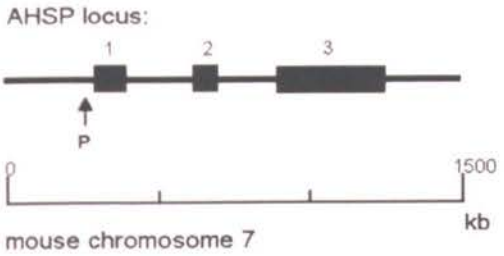

B.

```
-317  CCTTACCCAGCTTCTAAACTGTTATTAATATGGCAGCCATAGATTGGAGA

      AGCAACACCATTGCATTTTTGTATGGCGCAAAAGGTGCCCATTACCTAAT

-217  GTTAGTTTCCTTAGAATTCTGAGTCTGGTTGTAGGGTTGTAGGGTTGGGA

      AAGGGCAAGCTTATGTTCCTGGTTTGTTTCTTACATTTTCTGTCTTCATT

-117  TATCTATTTTTCTCCCGAGGTCTATCTTTCTAACTCCAGGGAAGCCTCAC
      GATA                    GATA
      CGCCCACCTTCTCCACCCTAGGATGACCTATCACACTCCTTCAGGACCAC
      CACCC     CACCC          GATA
-17   AAGGCAGGGCGTTGCCTtcttaagctaactcctgactgcctgcgtctcgc

      ttagtgcagaagacacacaaacccccgaggattgtggatgaggcgggctca

+83   gcaccattagacttgaaggtGAGCCCACACTTGTGAAAATGTAACTTCAG
                                  E-box
      AGCAGAGCGGGACTTGAAAGGTTTAGGGAAAGGGGTTCTCCTCTTTAATG
```

C.

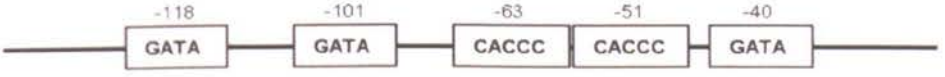

Figure 4.1. Structure of the mouse AHSP gene and transcription factor binding sites at the mouse AHSP promoter.

(A) Structure of the mouse AHSP gene (B) Nucleotide sequence of the mouse AHSP promoter. Positioning of nucleotides is relative the transcriptional start site in Exon 1. Underlined sequences represent consensus binding sequences for GATA factors or CACCC binding factors or previously undisclosed E-boxes (red). The exon 1 sequence is displayed in lower case. The broken upper line represents the region amplified for ChIP analysis. (C) Representative diagram of clustered transcription factor binding sites of the mouse AHSP promoter.

Membrane integrity and cell deformability are critical determinants of healthy erythrocytes. Defects in the composition and/or function of membrane protein complexes and cytoskeleton organization lead to changes in the shape, size and fragility of erythroid membrane. The dematin protein, or Erythrocyte Protein Band 4.9 (Epb4.9), is a trimeric complex composed of two 48KDa and one 52KDa isomeric subunits. Each factor encodes an actin binding sites in the headpiece and amino-terminal domains (*214*).

Together with ADD2, dematin modulates actin binding and bundling in the erythrocyte (*210, 215*). Mice expressing dematin proteins devoid of the headpiece domain are viable and display mild spherocytosis, indicating a role of dematin in cell shape (*215*). Further studies of the dematin headpiece-null fibroblasts suggest that dematin regulates cell shape and cytoskeleton rearrangements by modulating the activity of Rho GTPases (*216-217*). Both proteins are localized at spectrin/actin junctions and are associated with the GLUT-1 receptor which serves as an anchor for the junctional complex to the erythrocyte plasma membrane (*210, 218*). Interestingly, similar to dematin and ADD2, GLUT-1 is downregulated in EKLF null mice (*152*). The dematin gene, as with many other membrane-associated protein encoding genes that have unique erythroid phenotypes (ankyrin, β-spectrin, AE1, ADD2), contains an alternate erythroid-specific promoter (*219-222*).

The organization of the mammalian dematin genes are complicated by the use of alternative promoters and exons, resulting in a number of splice variants. As described in Figure 4.2.A., the dematin gene, located on mouse chromosome 14, comprises 15 exons stretching over approximately 30 kb. A tissue-specific transcript detectable in E14.5 fetal livers is regulated by an alternative erythroid-specific promoter referred to as P2 (E) for the purpose of this study (*151*).

Close sequence analysis of the P2 (E) promoter reveals the presence of multiple putative GATA and CACC elements along with 2 previously unreported E-boxes (Figure 4.2.B. and C.). This complex environment is simplified however as these regulatory elements

appear to be sufficient for high level expression; like AHSP no long range enhancer has been identified.

Both genes are involved in separate biological processes however, unlike the β-globin gene, the AHSP and dematin genes are not located at multi-gene loci. The independent state of these genes when compared to the β-globin locus renders both promoters attractive models to explore the mechanisms of EKLF-directed transcriptional activation at LCR-independent loci. We hypothesized that the mechanism of action of EKLF is distinct at LCR-independent loci when compared to the β-globin locus. Taking advantage of our inducible EKLF cell system, we determined the temporal events of EKLF-directed transcriptional activation. Our results increase the present knowledge of EKLF mode of action at target promoters and reveal additional clues about general transcription processes.

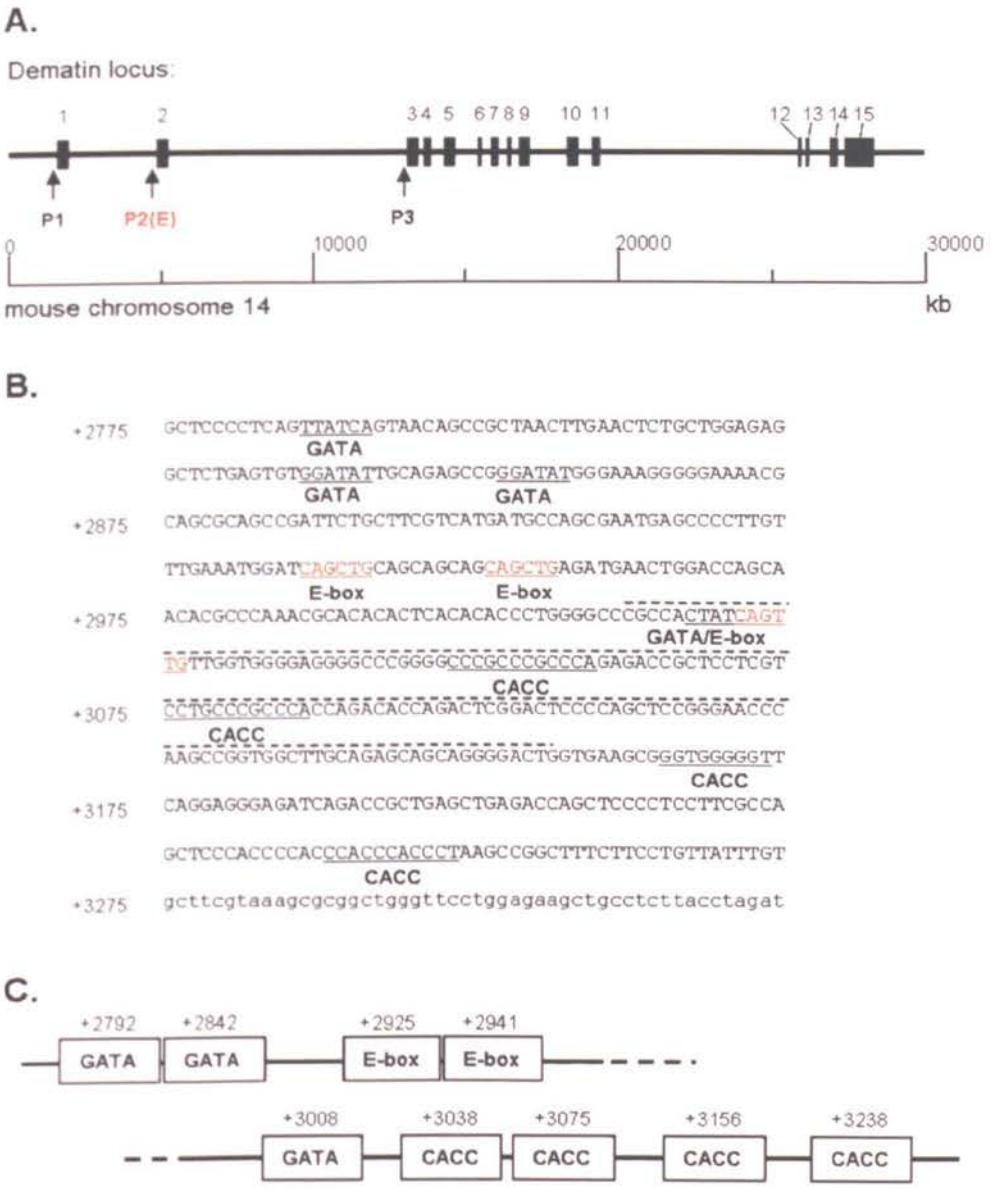

Figure 4.2. Transcription factor binding sites at the murine Dematin promoter.

(A) Structure of the mouse Dematin gene locus. P1, P2 (E) and P3 represent the three known alternate promoters. The erythroid promoter P2 (E) is the promoter of interest in this study. P3 is the original reported promoter (*223*). (B) Nucleotide sequence of the mouse AHSP promoter. Positioning of nucleotides is relative the transcriptional start site in Exon1. The erythroid specific transcript starts at position +3275. Underlined sequences represent consensus binding sequences for GATA factors or CACCC binding factors or previously undisclosed E-boxes (red). The broken upper line represents the region amplified for ChIP analysis. (C) Representative diagram of clustered transcription factor binding sites of the mouse Dematin promoter P2 (E).

RESULTS

Rapid induction of AHSP and dematin gene transcription upon EKLF binding

Previously, we described the JH31 cell system and demonstrated that β-globin gene expression is rescued upon induction of the EKLF transgene by exposure to 4-OH-TAM (see Chapter 3). Random integration of the retroviral construct used to express the HA-EKLF-mER fusion protein may affect the expression of some EKLF target genes. Therefore, in order to study EKLF-dependent transcription at the AHSP and dematin genes, we wanted to validate further the JH31 cell system and verify that the expression of both genes was rescued upon EKLF translocalization. Indeed, as illustrated in Figure 4.3, transcription of AHSP and dematin was initiated upon induction. Interestingly, primary transcripts of both genes reached high levels within an hour of 4-OH-TAM induction, with dematin transcription being the most responsive. In contrast, kinetics of β-globin reached about 75% of maximum by 2 hours of treatment. Our data indicated that the JH31 cell system is a valid system to study EKLF-dependent transcriptional activation of the AHSP and dematin genes. We also demonstrated within this system that transcription of both genes is highly responsive to EKLF translocation, its tempo being significantly more rapid than that observed at β-globin locus.

EKLF-coupled recruitment of GATA-1 and Ldb-1 at the AHSP and dematin promoter

EKLF binds directly to the CACC boxes located at the AHSP and dematin promoters (*151, 153, 162*). We decided to verify the transcriptional activation of both genes correlated with binding of EKLF. ChIP analysis in JH31 cells using an anti-HA antibody demonstrated EKLF occupancy at the AHSP and dematin promoters 6 hours post-induction with 4-OH-TAM (Figure 4.4.A.). Importantly, no enrichment was detected prior to induction. In addition, EKLF occupancy was not detected at upstream regions located approximately 1kb away from the promoters nor at

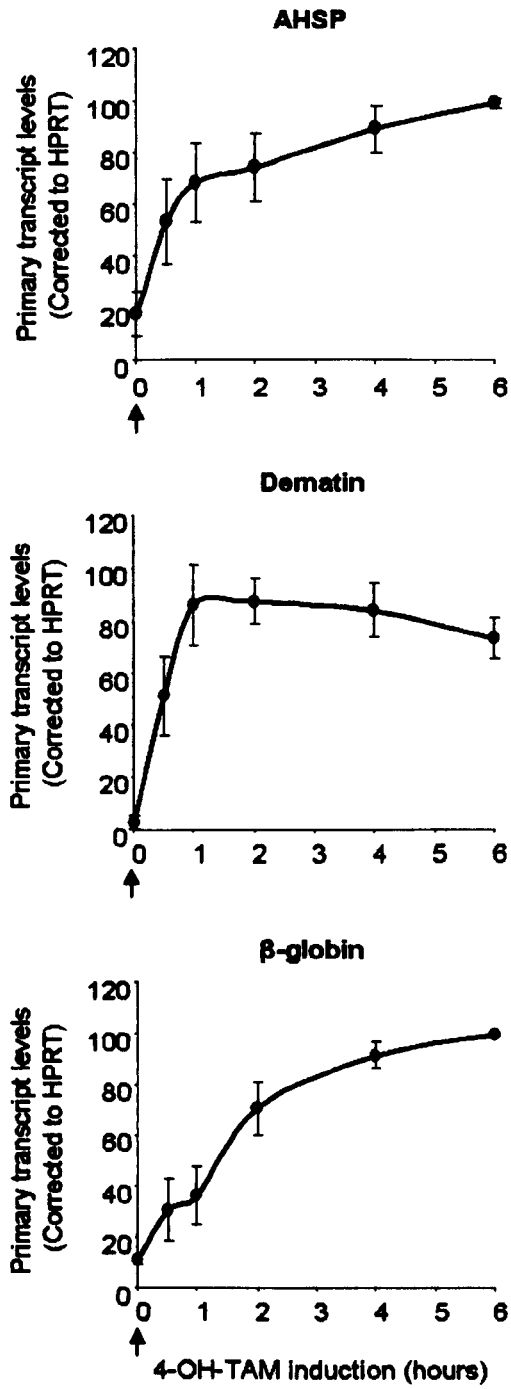

Figure 4.3. EKLF dependent transcriptional activation of AHSP, Dematin and β-globin in JH31 cells. Primary transcript levels following 4-OH-TAM induction of JH31 cells at 0, 0.5, 1, 2 and 6hours post treatment. Primary transcripts levels are corrected to HPRT levels and related to overall maximal signal intensity. Data shown represents the average of at least 3 independent experiments (mean ± SEM).

the non EKLF-dependent amylase promoter. Therefore, binding of EKLF directly correlates with transcription of the AHSP and dematin genes.

GATA-1 cooperates with EKLF in the regulation of β-globin gene expression and is known to modulate AHSP transcription (*20*). GATA binding motifs can be found within the promoter sequences of the AHSP and dematin genes. In addition, studies have demonstrated a critical role for GATA-1 in AHSP transcription (*61, 224-225*).We therefore decided to explore the hypothesis that EKLF and GATA-1 co-occupy both promoters. Using a ChIP approach in JH31 cells, we assessed the promoter occupancy by GATA-1 as depicted in Figure 4.4.B. Significant enrichment was detected at the AHSP promoter as well as the dematin promoter in ethanol treated control cells. However, signal intensity increased about 10 fold at the AHSP promoter and about 5 fold at the dematin promoter by 6 hours of treatment with 4-OH-TAM. Our data clearly demonstrated that EKLF binding enhances the mobilization of GATA-1 at both promoters and establishes the co-occupancy of the two transcription factors at the activated promoters. Interestingly, we report that EKLF is not required for low levels of GATA-1 occupancy at the promoter of both the AHSP and dematin genes.

ChIP studies combined with genome-wide high resolution massively parallel sequencing, or ChIP-seq, have revealed recently a frequent co-occupancy of GATA-1 and SCL/TAL-1 at GATA-1 activated genes (*173*). However, little is known about the manner in which each component of the complex is recruited to the promoter of GATA-1 target genes. Taking advantage of our JH31 cell system, we decided to address this issue by monitoring SCL/TAL-1 occupancy at the AHSP and dematin promoters in the absence and presence of nuclear EKLF. We hypothesized that, similarly to GATA-1, EKLF is required for the mobilization of the SCL/TAL-1 complex at the promoter of both genes. SCL/TAL-1 is found in complexes with LMO2, E2A and Ldb-1 in erythroid cells. Since no commercial TAL-1 antibody is available for ChIP applications, we decided to use Ldb-1 as a marker of the SCL/TAL-1 complex. ChIP studies using the Ldb-1 antibody are represented in Figure 4.4.C. and validate our hypothesis. Indeed, Ldb-1 occupancy

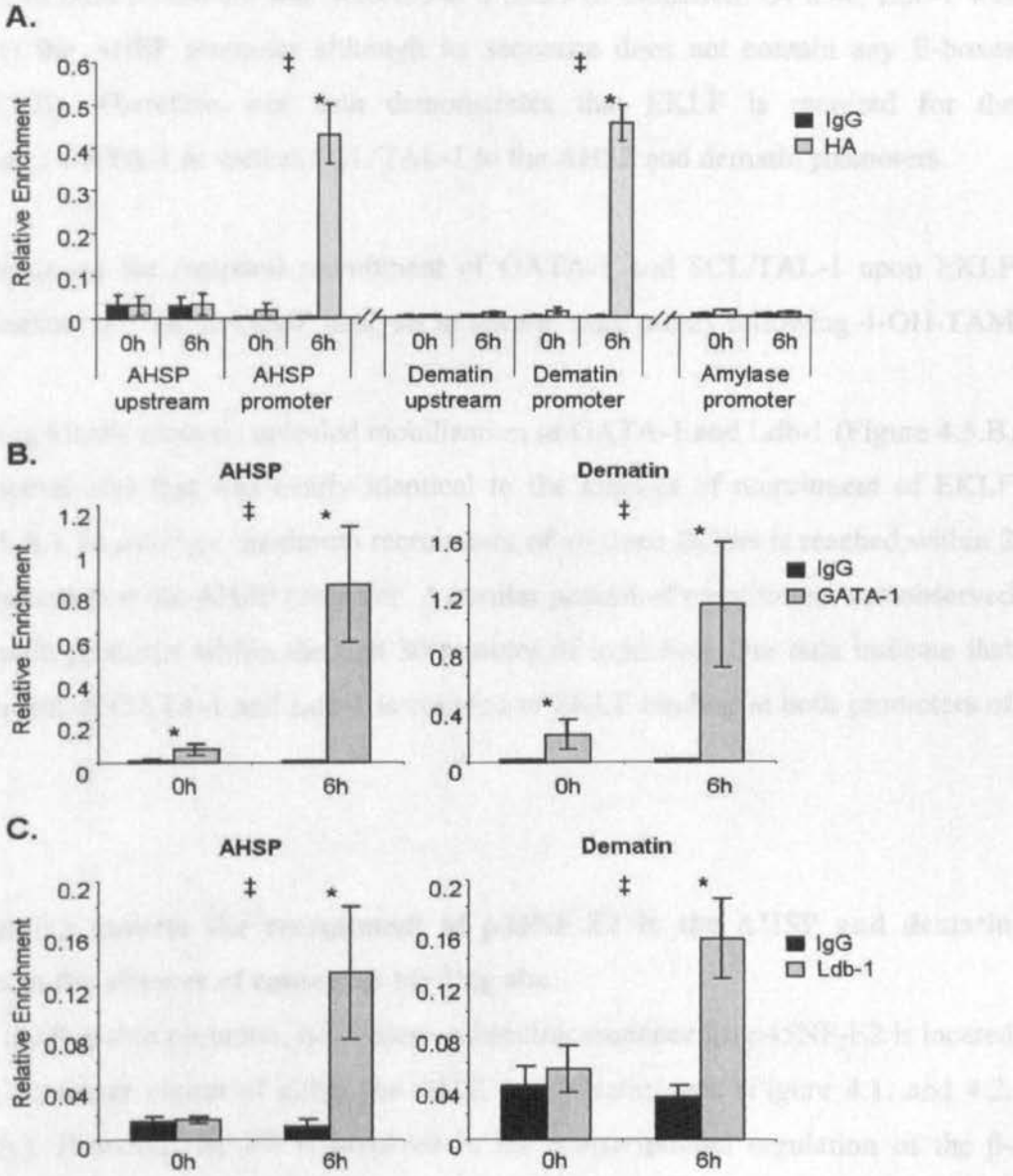

Figure 4.4. Binding of EKLF, GATA-1 and Ldb1 at the AHSP and Dematin promoters in JH31 cells. Transcription factor binding as determined by ChIP analysis is represented as (A). Relative enrichment of EKLF using an anti-HA antibody at the AHSP, Dematin and Amylase promoters respectively, prior to and 6 hrs post 4-OH-TAM treatment of JH31 cells. Upstream regions region are located within 1-2 Kb upstream of the corresponding promoter region. (B). Relative enrichment of GATA-1 and (C). Ldb1 at the AHSP and Dematin promoters respectively. Values for each factor were corrected to input prior to, and 6hrs post treatment of JH31 cells with 4-OH-TAM. * p value<0.05 between IgG and corresponding sample. ‡ p value<0.05 between 0h and 6hr. Data shown represents the average of at least 3 independent experiments (mean ± SEM)

was not detected at either promoter in the absence of EKLF. However, significant enrichment of both promoters was detected at 6 hours of induction. Of note, Ldb-1 was recruited to the AHSP promoter although its sequence does not contain any E-boxes (Figure 4.1.B). Therefore, our data demonstrates that EKLF is required for the recruitment of GATA-1 as well as SCL/TAL-1 to the AHSP and dematin promoters.

In order to assess the temporal recruitment of GATA-1 and SCL/TAL-1 upon EKLF translocalization, we applied ChIP analysis at several time points following 4-OH-TAM induction.

The resulting kinetic analysis revealed mobilization of GATA-1 and Ldb-1 (Figure 4.5.B. and C. respectively) that was nearly identical to the kinetics of recruitment of EKLF (Figure 4.5.A.). In addition, maximum recruitment of all three factors is reached within 2 hours of induction at the AHSP promoter. A similar pattern of recruitment was observed at the dematin promoter within the first 30 minutes of induction. Our data indicate that the recruitment of GATA-1 and Ldb-1 is coupled to EKLF binding at both promoters of interest.

EKLF binding induces the recruitment of p45NF-E2 to the AHSP and dematin promoters in the absence of consensus binding site

Similar to the β-globin promoter, no consensus binding sequence for p45NF-E2 is located within the promoter region of either the AHSP or dematin gene (Figure 4.1. and 4.2. respectively). However, NF-E2 is involved in the transcriptional regulation of the β-globin gene and is recruited to the promoter in an EKLF-dependent manner (see Chapter 3). In order to assess the potential role of NF-E2 in the regulation of AHSP and dematin expression, we decided to monitor NF-E2 occupancy at each promoter. Interestingly, NF-E2 ChIP assay results illustrated in Figure 4.6.A. indicate a small but significant enrichment of each promoter upon EKLF binding that is not detectable in ethanol-treated cells.

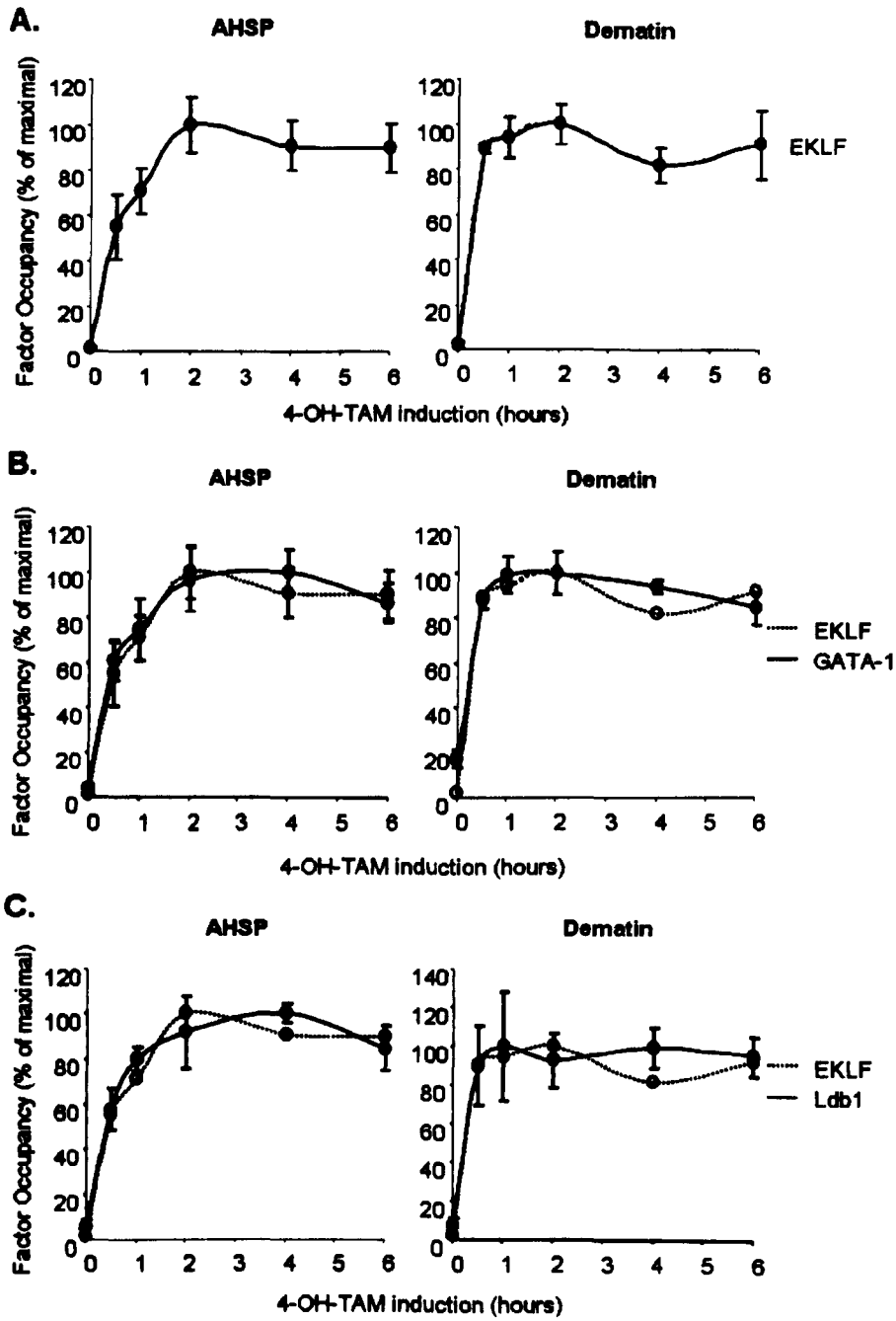

Figure 4.5. Kinetics of Transcription Factor binding at the AHSP and Dematin genes in JH31 cells. Transcription factor binding was determined by ChIP analysis of (A). EKLF, (B). GATA-1 and (C). Ldb1. Relative enrichment is corrected to overall maximal signal intensity at 0, 0.5, 1, 2 and 6 hours post treatment of JH31 cells with 4-OH-TAM. The doted line represents binding of EKLF for comparison. Data shown represents the average of at least 3 independent experiments (mean ± SEM)

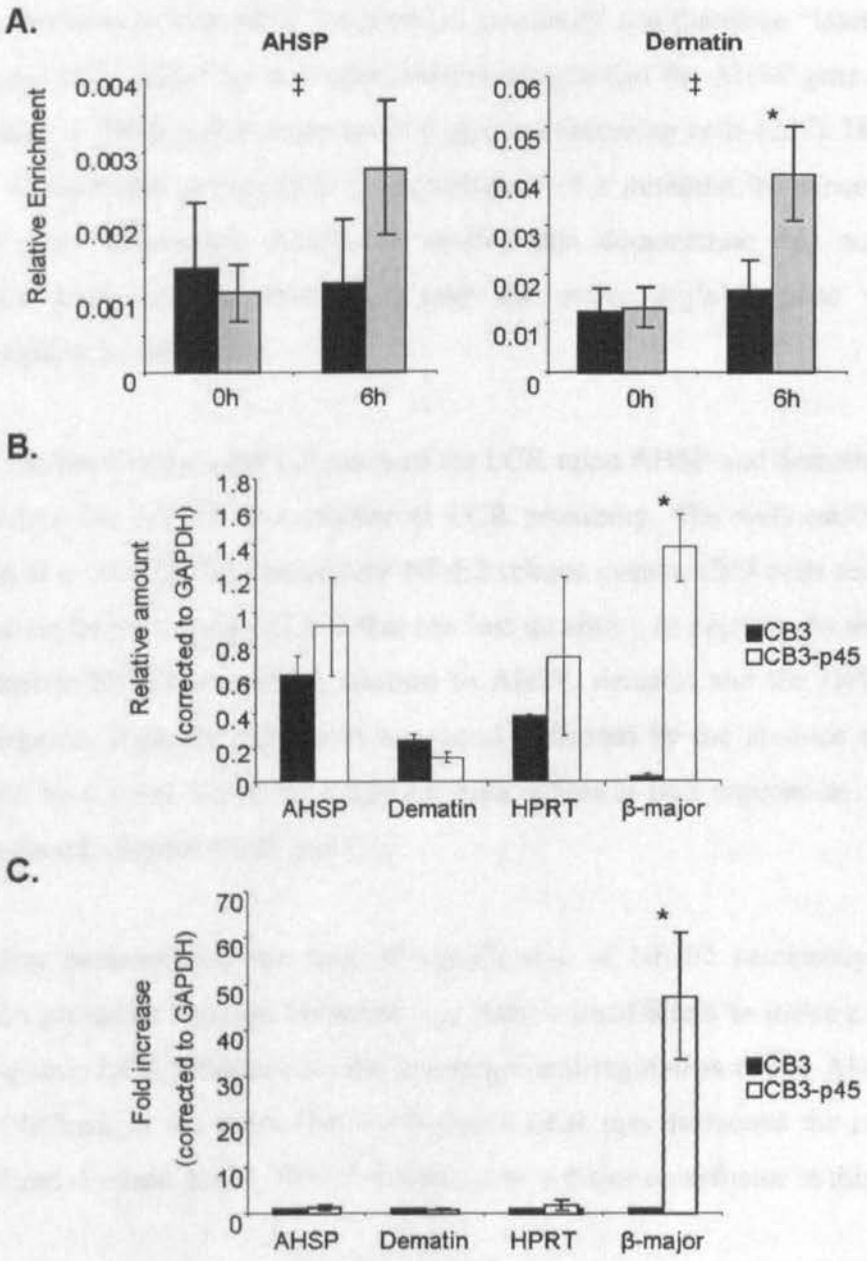

Figure 4.6. Binding and role of NF-E2 at the AHSP and Dematin promoters in JH31 cells. (A). NF-E2 binding as determined by ChIP analysis is represented as relative enrichment at the AHSP and Dematin promoters respectively, prior to and 6 hrs post 4-OH-TAM treatment of JH31 cells. Values were corrected to input.* p value<0.05 between IgG and corresponding sample. ‡ p value<0.05 between 0h and 6hr. Gene expression in CB3 or CB3-p45 cells corrected to GAPDH and represented as (A). Relative amount or (B). Fold increase relative to gene expression in CB3 cells. Data shown for each graph represents the average of at least 3 independent experiments (mean ± SEM).

Unlike EKLF, NF-E2 is not required for the formation of an active chromatin hub at the β-globin locus (*226*). Therefore, it has been proposed that NF-E2 occupancy at the β-major promoter is a result of the physical proximity and therefore "interaction" between the β-globin LCR and the promoter. Studies suggest that the AHSP gene is found in close proximity to the β-major promoter in β-globin expressing cells (*227*). However, it is not clear whether this proximity is a consequence of a potential influence of the LCR on AHSP gene expression. Additional studies also demonstrate that active AHSP and dematin genes tend to co-localize with the active β-globin gene within a shared transcription factory (*228*).

In an attempt to assess the influence of the LCR upon AHSP and dematin expression, we decided to use NF-E2 as a marker of LCR proximity. The well established CB3 cell system is a valuable tool to explore NF-E2 related events. CB3 cells are derived from a murine erythroleukemia cell line that has lost its ability to express the p45 component of the dimeric NF-E2 protein. In contrast to AHSP, dematin and the HPRT control gene transcription, β-globin expression is severely affected by the absence of NF-E2 and is rescued to a great extent in CB3-p45 cells where a p45 expression vector has been reintroduced. (Figure 4.6.B. and C.).

Our data demonstrated the lack of significance of NF-E2 occupancy on AHSP and dematin promoter activity. However, our data is insufficient to make a statement about the β-globin LCR influence on the transcriptional regulation of the AHSP and dematin genes. Indeed, in the event that the β-globin LCR may influence the expression of the AHSP and dematin genes, NF-E2 would not be a major contributor in this process.

EKLF modulates the structural reconfiguration of the AHSP and dematin promoters

The generation and expression of truncated mutants of EKLF *in vitro* and in EKLF null erythroid cells have clearly defined three functions of EKLF, encoded within three domains of the protein. First, a proline rich domain harbors the transactivation activity of EKLF. Second, its zinc fingers domain alone is sufficient and necessary for binding of

the transcription factor to DNA. Third, a few amino acids in addition to the DNA binding domain of EKLF are sufficient to remodel chromatin *in vitro* and *in vivo* (Jansen et al., in preparation). Thus, the EKLF protein modulates transcription via a dual mode of action. EKLF's activity combines classical transactivation properties to chromatin remodeling potential. However, it is unclear whether both functions are required and/or utilized towards appropriate expression of EKLF target genes.

One way to examine the effects of EKLF on chromatin structure is to assess the sensitivity of the target promoter to DNaseI digestion. The sensitivity of the chromatin to DNaseI digestion is measured as the extent of enzymatic cleavage with increasing amounts of enzyme. As described in Figure 4.7.A, the β-major promoter was hypersensitive to DNaseI digestion in wild type when compared to EKLF null fetal liver erythroblasts. A similar phenomenon was detected at the AHSP and dematin promoters. Our data reciprocates studies from others at the AHSP promoter but are novel for the dematin promoter (*162*).

To verify that the chromatin remodeling of the three promoters is a direct consequence of EKLF binding, we repeated the assay in our inducible cell system. As presented in Figure 4.7.B., promoter chromatin of all three genes was more sensitive to DNaseI in cells treated with 4-OH-Tam for 6 hours than in ethanol treated control cells. Our data therefore implies that EKLF binding is required to rescue the DNaseI hypersensitivity profile of the β-major, AHSP and dematin promoters. These experimental results indicate that EKLF chromatin remodeling activity is potentially utilized at each target promoter.

To analyze further the impact of EKLF binding on the configuration of chromatin, we decided to monitor the kinetics of chromatin structural changes and their correlation to EKLF binding. Technical difficulties hinder the application of the DNaseI protocol towards kinetic studies. However, we demonstrated throughout this study that the ChIP assay can be utilized successfully to monitor the kinetics of factor recruitment. An additional strategy to assess the fluctuations of chromatin architecture is to determine the density of nucleosomes along a defined stretch of chromatin. We therefore decided to

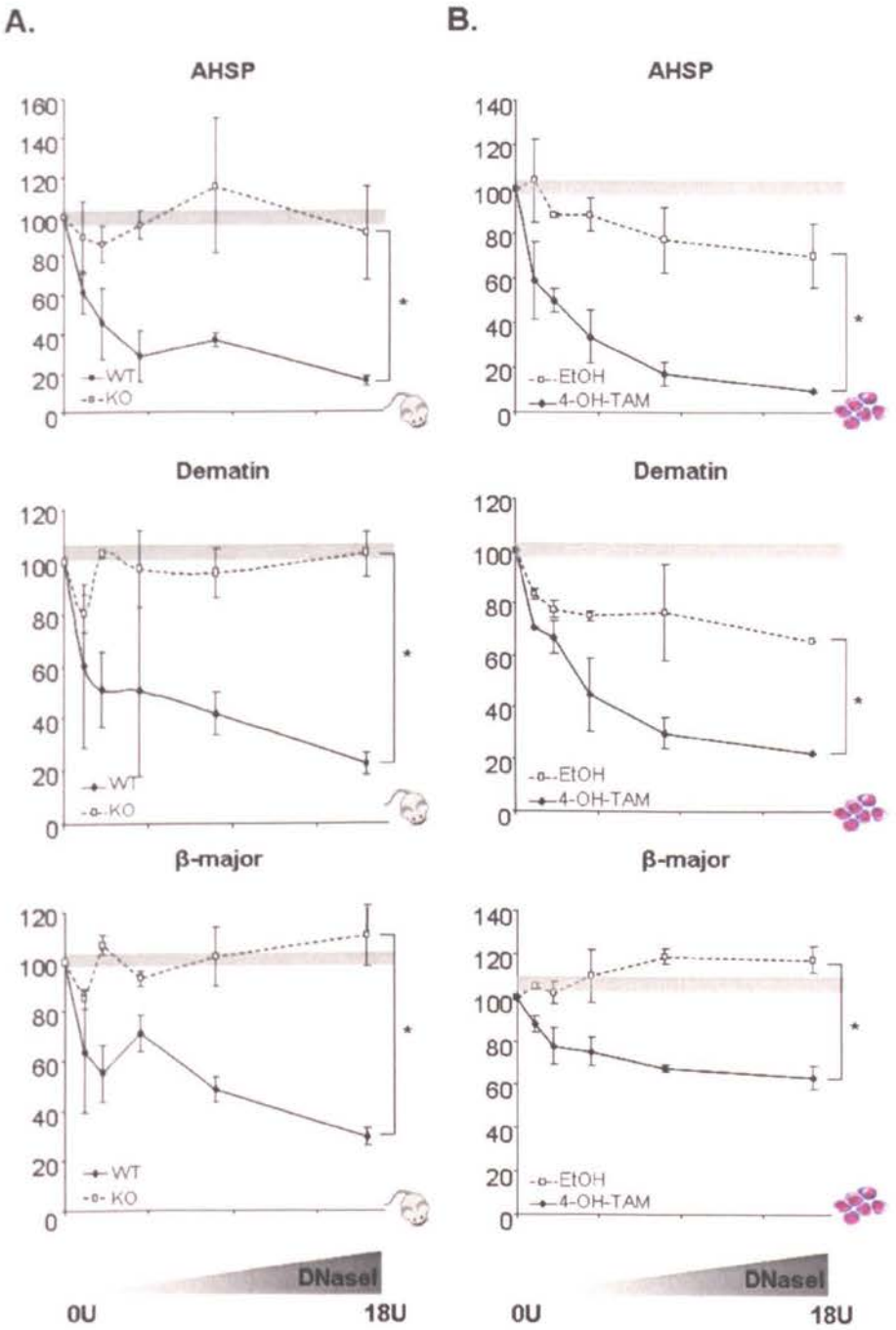

Figure 4.7.EKLF induces HS formation at the AHSP, Dematin and β-globin promoters. DNaseI hypersensitivity assay in mice (A) and JH31 cells (B) at the AHSP, Dematin and β-major promoter (higher, middle and lower panels respectively). Data shown represents the average of a minimum of 2 independent experiments (mean ± SEM).

apply the ChIP technique in JH31 cells using an antibody directed against histone H3, and validate the choice of this antibody. As described in Figure 4.8.A., H3 density decreased at all 3 EKLF-dependent promoters and was not significantly affected at the non EKLF-dependent amylase promoter upon induction.

Interestingly, the degree of H3 loss at each promoter was reflective of the DNaseI data described previously. Histone loss at the AHSP and dematin promoter proved to be more significant than at the β-major promoter. Similarly, DNaseI hypersensitivity analysis revealed the more accessible nature of the chromatin at the AHSP and dematin promoters when compared to the β-major promoter. Our data demonstrates that changes in H3 occupancy are an appropriate measure of chromatin architectural reconfiguration.

Considering H3 occupancy as a guide of chromatin remodeling, we carried out H3 ChIP at time points identical to those used in EKLF mobilization studies for comparison. As represented in Figure 4.8.B., H3 loss at the AHSP and dematin promoters occurred within the first 30 minutes of induction, indicating that EKLF triggers rapid remodeling of the chromatin at each promoter. In contrast, H3 occupancy at the β-globin promoter decreased gradually. This observation was surprising and pointed out evident differences in the effect of EKLF binding at the β-globin promoter when compared to the AHSP and dematin promoters.

Our data is further strengthened by studies of the Delta221 EKLF mouse strain established in our laboratory. The Delta 221 EKLF protein is a truncated form of EKLF that retains chromatin remodeling capability, while losing its transactivation activity (*148*). DNAseI hypersensitivity analysis using fetal livers cells from E14.5 Delta 221 embryos revealed that the Delta 221 protein remodels the chromatin structure at the β-major promoter. Most importantly, the chromatin configuration at the AHSP and dematin promoters remained unperturbed. Binding of the truncated protein at the β-major, AHSP and dematin promoters was confirmed by ChIP analysis (Jansen et al., in preparation). Therefore, we demonstrate the context-specificity of EKLF directed chromatin remodeling.

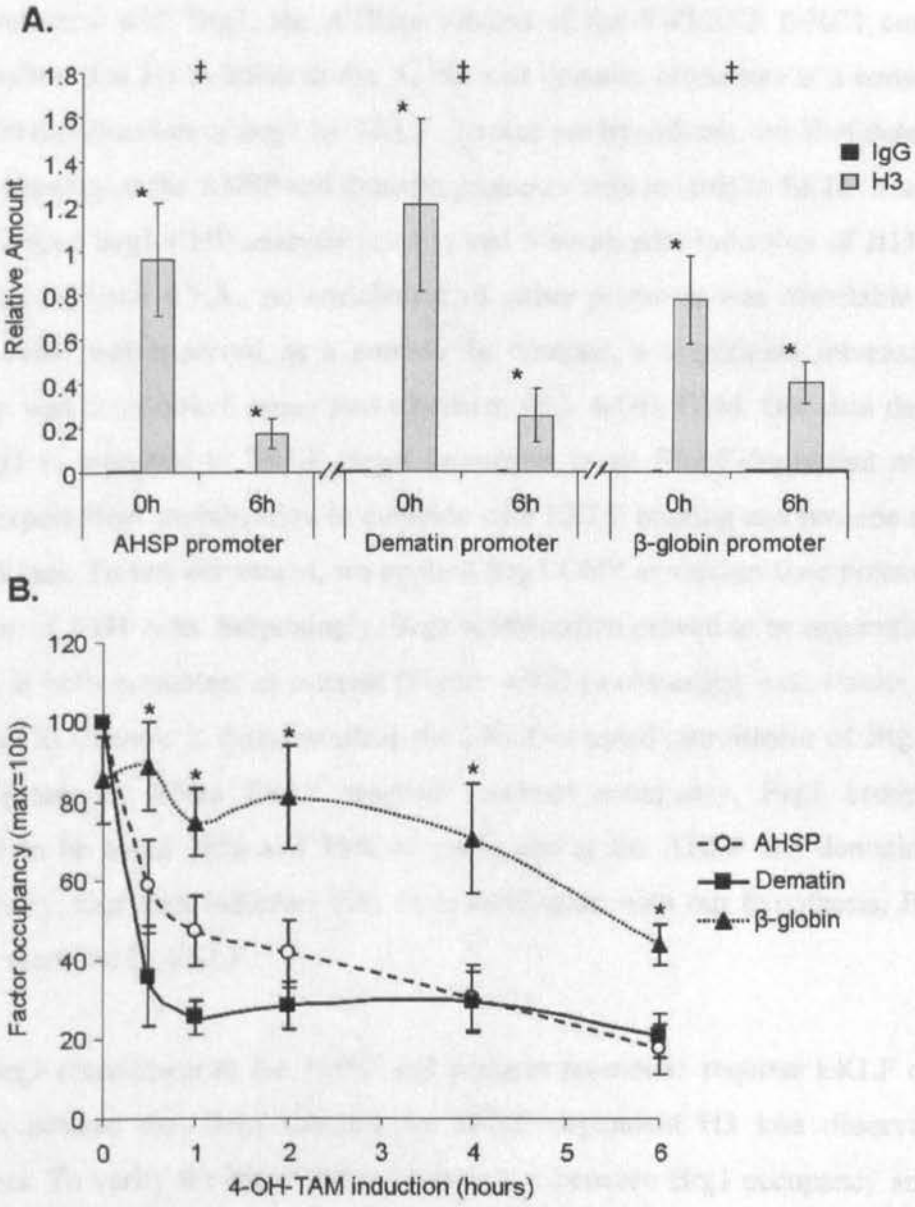

Figure 4.8. Histone H3 occupancy at the AHSP and Dematin genes in JH31 cells. H3 occupancy at the AHSP, Dematin and β-major promoters respectively was determined by ChIP analysis (A). Relative enrichment of H3 prior to and 6 hrs post 4-OH-TAM treatment of JH31 cells corrected to input. * p value<0.05 between IgG and corresponding sample. ‡ p value<0.05 between 0h and 6hr. (B). Kinetics of H3 occupancy corrected to overall maximal signal intensity at 0, 0.5, 1, 2 and 6 hrs post treatment of JH31 cells with 4-OH-TAM. The doted line represents binding of EKLF for comparison. * p value< 0.05 between value for β-major and values for both AHSP and Dematin. Data shown represents the average of at least 3 independent experiments (mean ± SEM).

Brg1 recruitment does not correlate to EKLF binding or H3 loss at the AHSP and dematin promoters

EKLF interacts with Brg1, the ATPase subunit of the SWI/SNF E-RC1 complex. We hypothesized that H3 eviction at the AHSP and dematin promoters is a consequence of the direct mobilization of Brg1 by EKLF. To test our hypothesis, we first determined the Brg1 occupancy at the AHSP and dematin promoter with regards to EKLF binding. Thus, we performed Brg1 ChIP analysis prior to and 6 hours post-induction of JH31 cells. As depicted on Figure 4.9.A., no enrichment of either promoter was detectable in ethanol treated cells, which served as a control. In contrast, a significant increase in signal intensity was detectable 6 hours into treatment with 4-OH-TAM. Our data demonstrates that Brg1 is recruited to EKLF target promoters in an EKLF-dependent manner. We would expect Brg1 mobilization to coincide with EKLF binding and precede or coincide with H3 loss. To test our model, we applied Brg1 ChIP at various time points following induction of JH31 cells. Surprisingly, Brg1 mobilization proved to be sequential to EKLF binding at both promoters of interest (Figure 4.9.B.) contrasting with results previously described in Chapter 1, demonstrating the EKLF-coupled recruitment of Brg1 at the β-globin promoter. When EKLF reached maximal occupancy, Brg1 occupancy was detected to be about 70% and 35% of maximum at the AHSP and dematin promoter respectively. Our data indicates that, in contradiction with our hypothesis, Brg1 is not directly recruited by EKLF.

Since Brg1 recruitment at the AHSP and dematin promoters requires EKLF occupancy, we hypothesized that Brg1 induces the EKLF dependent H3 loss observed at both promoters. To verify the hypothesized correlation between Brg1 occupancy and H3 loss, we compared the kinetics of both events. Unexpectedly, we were not able to significantly correlate Brg1 occupancy to H3 loss. As described in Figures 4.8.B. and 4.9.B, H3 loss and Brg1 occupancy do not reach similar levels in the first 30 minutes of induction. The discrepancy between histone eviction and Brg1 occupancy was more drastic at the dematin promoter than at the AHSP promoter. Against all expectations, our data strongly suggests that H3 eviction occurs prior to efficient Brg1 binding at the AHSP and dematin

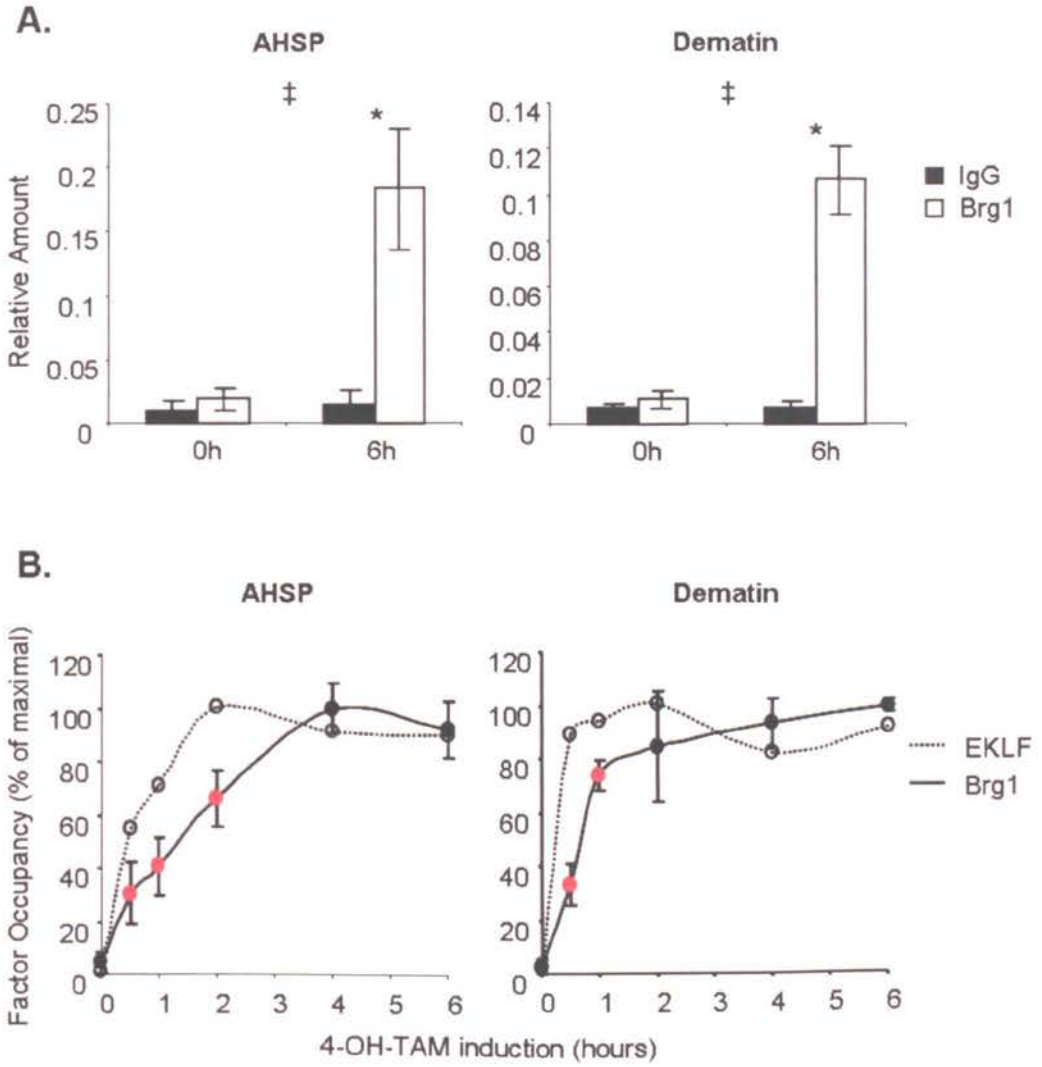

Figure 4.9. SWI/SNF recruitment at the AHSP and Dematin genes in JH31 cells. Brg1 mobilization at the AHSP and Dematin promoters respectively was determined by ChIP analysis (A). Relative enrichment of Brg1prior to and 6 hrs post 4-OH-TAM treatment of JH31 cells corrected to input. * p value<0.05 between IgG and corresponding sample. ‡ p value<0.05 between 0h and 6hr. (B). Kinetics of recruitment of Brg1 corrected to overall maximal signal intensity at 0, 0.5, 1, 2 and 6 hrs post treatment of JH31 cells with 4-OH-TAM. The doted line represents binding of EKLF for comparison. •p value< 0.05. Data shown represents the average of at least 3 independent experiments (mean ± SEM).

promoters. Therefore, we propose that the chromatin remodeling capability of EKLF is not limited to the recruitment of Brg1.

Interestingly, Brg1 has been reported to facilitate the transcription elongation process and has been detected across the transcribed region of several genes (*56, 58, 229-230*). In addition, the Brg1 paralog Brm has been implicated in the regulation of the elongation rate of RNA Pol-II *in vivo* (*56, 231*). Therefore, we decided to further investigate the potential role of Brg1 in dematin transcription. We propose that Brg1 is involved in the regulation of the transcriptional elongation at EKLF target genes. In order to assess the veracity of our hypothesis, we monitored RNA Pol-II and Brg-1 occupancy at a transcribed region located 1.5kb downstream of the dematin promoter. As described in Figure 4.13., preliminary results strongly indicated that Brg1 was involved in the transcription elongation process. ChIP analysis revealed that Brg-1 was detected along with RNA Pol-II at a transcribed region located downstream from the promoter (Figure 4.10.A and B.). Importantly, no significant enrichment was measured following ChIP analysis targeting the EKLF co-factor CBP (Figure 4.10.C).

EKLF-dependent acetylation of the AHSP and dematin promoters does not correlate with histone eviction

EKLF-dependent chromatin remodeling is accompanied by the acetylation of histones at the β-major promoter (see Chapter 3). However, gene promoters can harbor acetylated histones independently of transcription (*182*). It is unclear whether histone acetylation is a common mechanism by which EKLF achieves transcriptional activation. To address this issue, we monitored the promoter occupancy of acetylated histone H3 (AcH3) by ChIP analysis in JH31 cells. As shown in Figure 4.11.A., AcH3 was detected at significant levels prior to EKLF translocalization. Enhanced enrichment of the AHSP and dematin promoter was detected 6 hours post induction. Importantly, no significant enrichment of the EKLF-independent amylase promoter was detected in the presence or absence of nuclear EKLF. Since H3 is evicted upon EKLF binding, we determined the impact of EKLF on acetylation at the histone level by correcting the signal intensity of

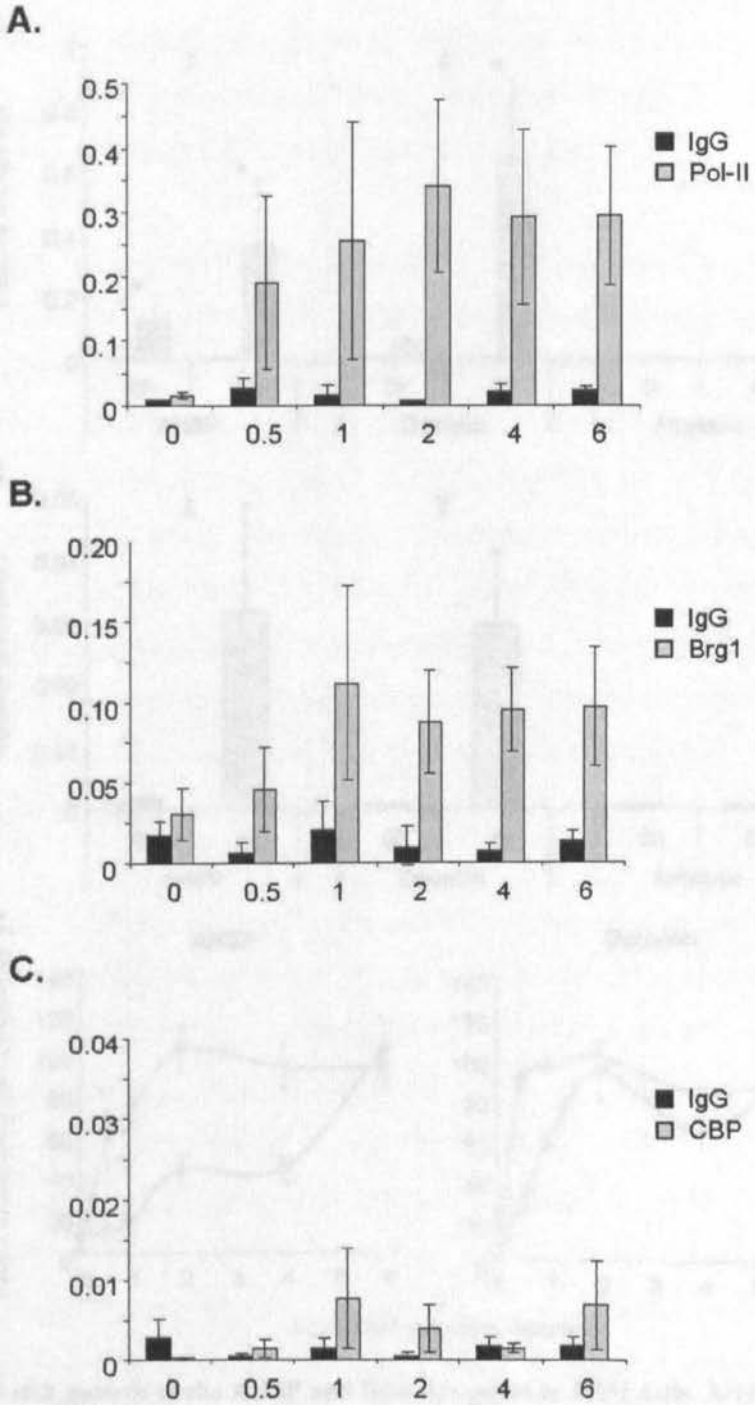

Figure 4.10. Binding of RNA Pol-II, Brg-1 and CBP downstream of the Dematin promoters in JH31 cells. Relative enrichment at a transcribed region located 1.5kb downstream of the Dematin erythroid promoter determined by ChIP analysis using antibodies against (A). RNA Pol-II, (B). Brg-1and (C). CBP. ChIP analysis was performed at 0, 0.5, 1, 2, 4, and 6 hours post induction with 4-OH-Tamoxifen of JH31 cells. Data shown represents the average of at least 2 independent experiments (mean ± SEM).

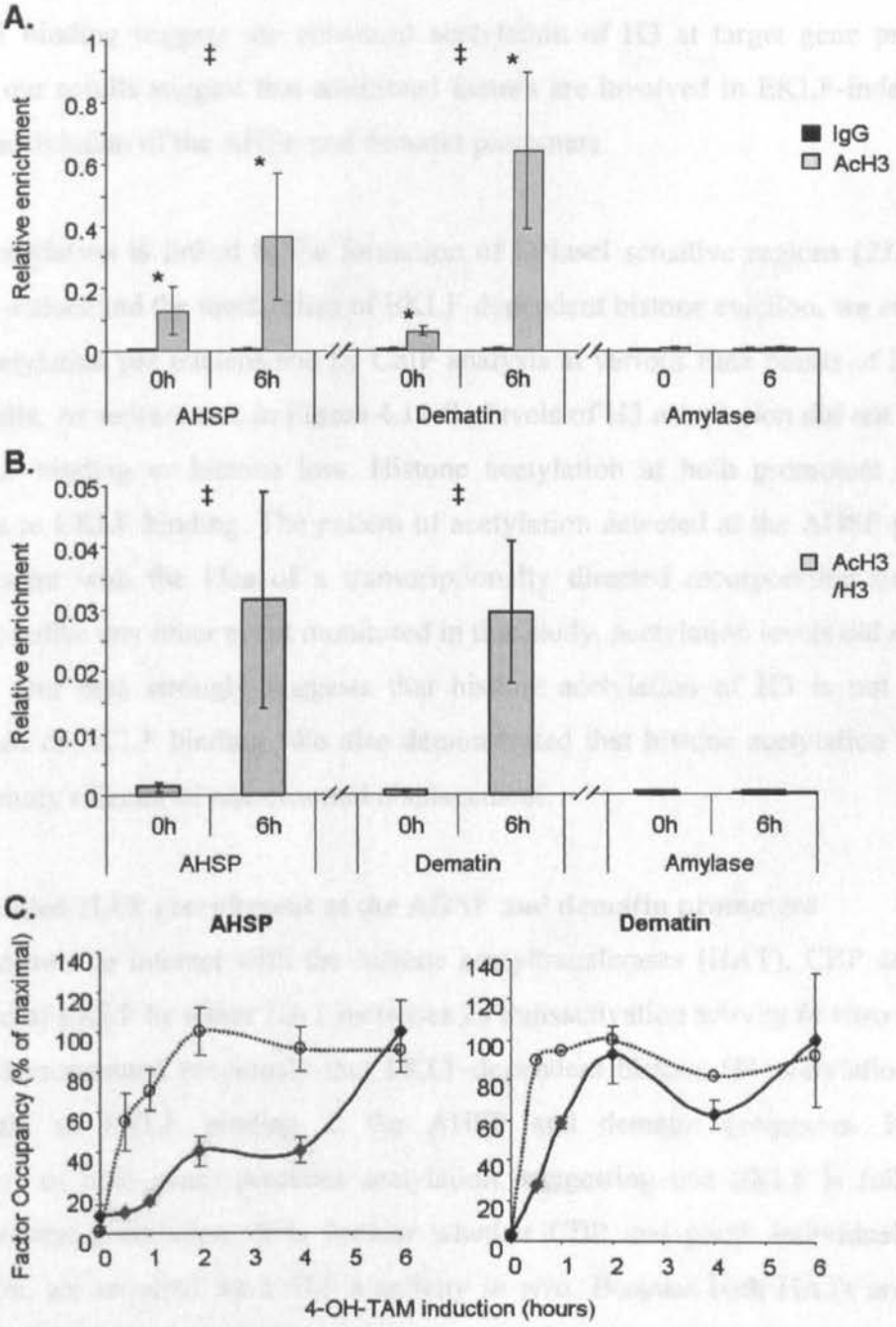

Figure 4.11. AcH3 pattern at the AHSP and Dematin genes in JH31 cells. AcH3 pattern at the AHSP and Dematin promoters respectively was determined by ChIP analysis. Relative enrichment of AcH3 prior to and 6 hrs post 4-OH-TAM treatment of JH31 cells corrected to (A). input or B). input and histone occupancy. * p value<0.05 between IgG and corresponding sample. ‡ p value<0.05 between 0h and 6hr. (C). Kinetics of acetylation of H3 corrected to overall maximal signal intensity at 0, 0.5, 1, 2 and 6 hrs post treatment of JH31 cells with 4-OH-TAM. The doted line represents binding of EKLF for comparison. •p value< 0.05. Data shown represents the average of at least 3 independent experiments (mean ± SEM).

the AcH3 ChIP by the H3 density at the promoter (Figure 4.12.B.). Our data indicated that EKLF binding triggers the enhanced acetylation of H3 at target gene promoters. However, our results suggest that additional factors are involved in EKLF-independent, low level acetylation of the AHSP and dematin promoters.

Histone acetylation is linked to the formation of DNaseI sensitive regions (*232*). In an attempt to understand the mechanism of EKLF-dependent histone eviction, we monitored histone acetylation per nucleosome by ChIP analysis at various time points of induction of JH31 cells. As represented in Figure 4.11.C., levels of H3 acetylation did not coincide with EKLF binding or histone loss. Histone acetylation at both promoters occurred subsequent to EKLF binding. The pattern of acetylation detected at the AHSP promoter was consistent with the idea of a transcriptionally directed incorporation of histone variants as unlike any other event monitored in this study, acetylation levels did not reach a plateau. Our data strongly suggests that histone acetylation of H3 is not a direct consequence of EKLF binding. We also demonstrated that histone acetylation of H3 is not the primary effector of nucleosomal displacement.

EKLF-coupled HAT recruitment at the AHSP and dematin promoters

EKLF is known to interact with the histone acetyltransferases (HAT), CBP and p300. Acetylation of EKLF by either HAT increases its transactivation activity *in vitro* (*59, 64*). We have demonstrated previously that EKLF-dependent histone H3 acetylation occurs subsequently to EKLF binding at the AHSP and dematin promoters. However, transcription of both genes precedes acetylation, suggesting that EKLF is fully active prior to histone acetylation. It is unclear whether CBP and p300, individually or in combination, are required for EKLF's activity *in vivo*. Because both HATs are closely related, involved in the transcription of many genes and most probably exhibit redundant functions at most target genes, disruption and mutations of the individual genes in mice have not allowed a deeper understanding of their involvement in erythropoiesis (*67, 233-236*).

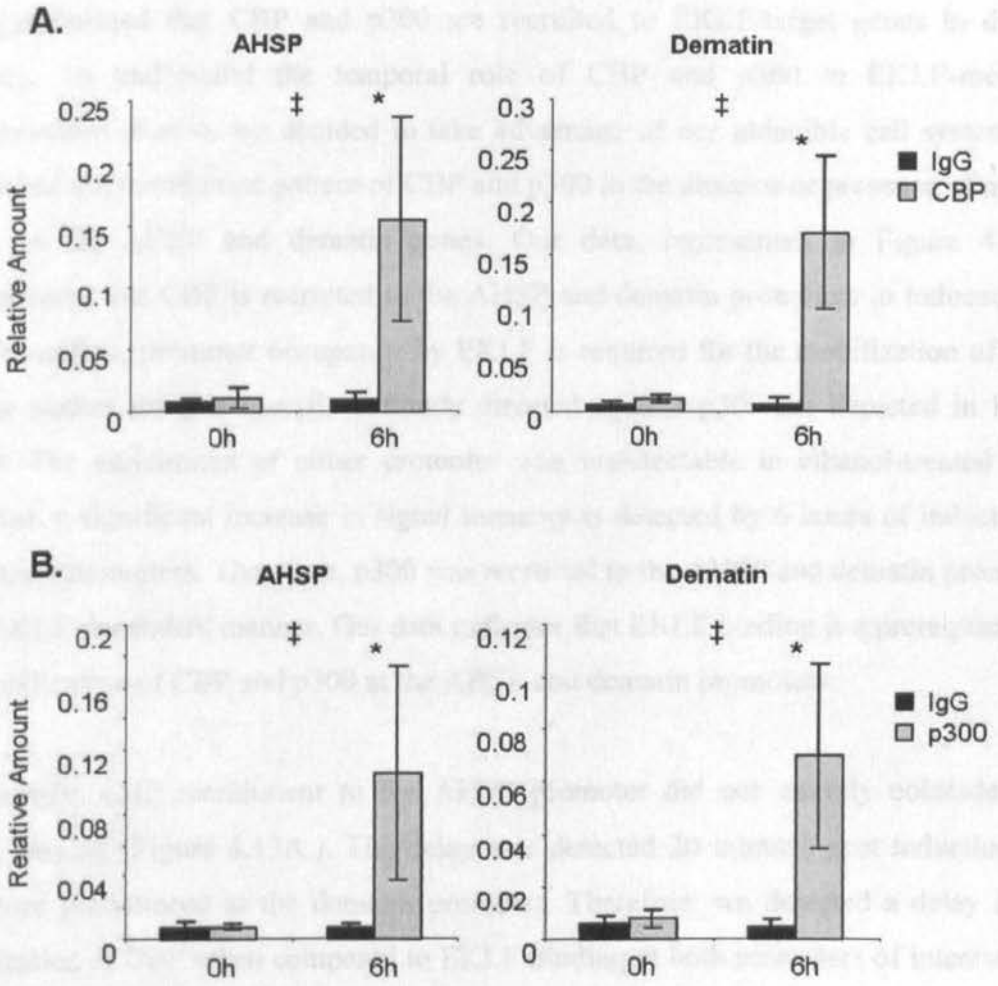

Figure 4.12. Binding of HATs EKLF co-factors CBP and p300 at the AHSP and Dematin promoters in JH31 cells. Relative enrichment of co-actor binding at the AHSP and Dematin promoters respectively as determined by ChIP analysis of (A).CBP and (B). p300 prior to, and 6hrs post treatment of JH31 cells with 4-OH-TAM. Values for each factor were corrected to input. * p value<0.05 between IgG and corresponding sample. ‡ p value<0.05 between 0h and 6hr. Data shown represents the average of at least 3 independent experiments (mean ± SEM).

We hypothesized that CBP and p300 are recruited to EKLF-target genes in distinct manners. To understand the temporal role of CBP and p300 in EKLF-mediated transactivation *in vivo*, we decided to take advantage of our inducible cell system. We established the recruitment pattern of CBP and p300 in the absence or presence of nuclear EKLF at the AHSP and dematin genes. Our data, represented in Figure 4.12.A, demonstrated that CBP is recruited to the AHSP and dematin promoters in induced cells only. Therefore, promoter occupancy by EKLF is required for the mobilization of CBP. Similar studies using a specific antibody directed against p300 are depicted in Figure 4.12.B. The enrichment of either promoter was undetectable in ethanol-treated cells. However, a significant increase in signal intensity is detected by 6 hours of induction at both target promoters. Therefore, p300 was recruited to the AHSP and dematin promoters in an EKLF-dependent manner. Our data indicates that EKLF binding is a prerequisite for the mobilization of CBP and p300 at the AHSP and dematin promoters.

Surprisingly, CBP recruitment to the AHSP promoter did not entirely coincide with EKLF binding (Figure 4.13A.). The delay was detected 30 minutes post induction and was more pronounced at the dematin promoter. Therefore, we detected a delay in the mobilization of CBP when compared to EKLF binding at both promoters of interest. The sequential recruitment of CBP is therefore a common event of EKLF mediated factor recruitment.

Because the recruitment of CBP did not exactly coincide with EKLF or the primary transcripts analysis (Figure 4.3), we hypothesized that p300 is recruited prior to CBP, at the AHSP and dematin promoters. In order to assess the kinetics of recruitment of p300, we performed p300 ChIP analysis at various time points of induction in JH31 cells. In accord with our hypothesis, p300 was recruited prior to CBP at both promoters (Figure 4.13.B). p300 is mobilized to each promoter simultaneously with EKLF. Our data

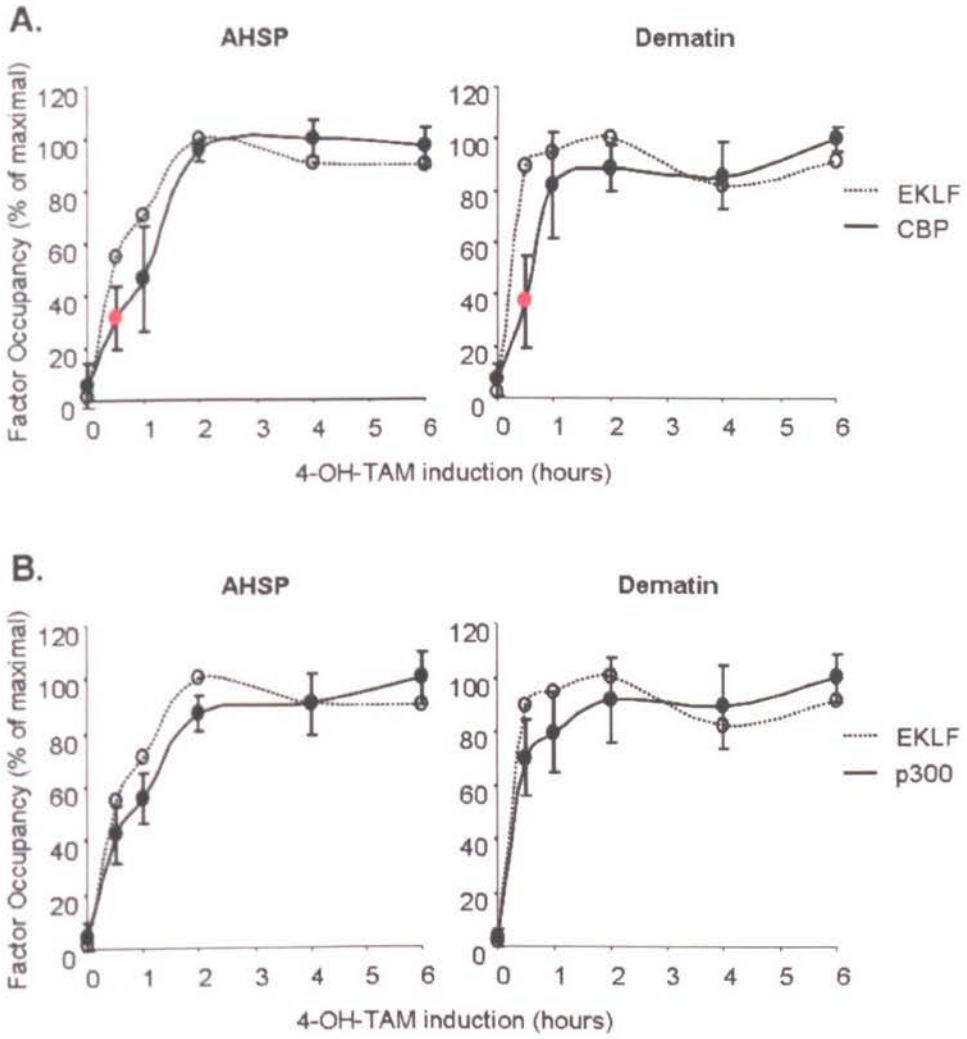

Figure 4.13. Kinetics of HATs binding at the AHSP and Dematin promoters in JH31 cells. HAT binding across the beta-globin locus was determined by ChIP analysis using an antibody raised against (A). CBP or (B). p300. Relative enrichment was corrected to overall maximal signal intensity at 0, 0.5, 1, 2 and 6 hrs post treatment of JH31 cells with 4-OH-TAM. The doted line represents binding of EKLF for comparison. •p value< 0.05. Data shown represents the average of at least 3 independent experiments (mean ± SEM).

demonstrated the lack of synchronization between the mobilization of CBP and EKLF binding. In contrast, the recruitment of p300 coincided with EKLF binding. Interestingly, our results revealed an evident separation of roles between the HATs CBP and p300 in EKLF-directed transcriptional activation. Analysis of the dynamics of HAT occupancy at the AHSP and dematin promoters allowed us to gain insight on the relationship of individual HATs with EKLF. We demonstrate the absolute correlation between p300 and EKLF binding at both promoters of interest. We also determined that recruitment of CBP, while EKLF-dependent, was not coupled to EKLF binding. We therefore established that EKLF preferentially recruits p300 over CBP. This observation strongly suggests that EKLF interacts with p300 *in vivo*, prior to or simultaneously with promoter binding. In contrast, our data clearly indicates that additional events are necessary for the mobilization of CBP to EKLF target genes.

Context-dependent recruitment of the transcription machinery at EKLF-target genes

Interestingly, the kinetics of factor recruitment at both promoters did not correlate exactly to the kinetics of transcriptional activation, suggesting that additional regulatory factors modulate the expression of each gene. The phosphorylation state of the RNA Pol-II enzyme is indicative of its activity. RNA Pol-II can be recruited to promoters in an unphosphorylated form. The activated form of the enzyme is phosphorylated at the Ser5 residue of its large subunit CTD.

In order to decipher the role of EKLF in the recruitment and the state of RNA Pol-II, we assessed total RNA Pol-II and Ser5 Pol-II promoter occupancy by ChIP analysis in our JH31 cell system. As depicted in Figure 4.14.A., no significant enrichment of either form of RNA Pol-II was detected prior to EKLF binding. A dramatic increase in signal intensity is detected 6 hours post induction for both total RNA pol-II and Ser5 Pol-II. Our data demonstrate that RNA Pol-II occupancy at the AHSP and dematin promoters requires the binding of EKLF.

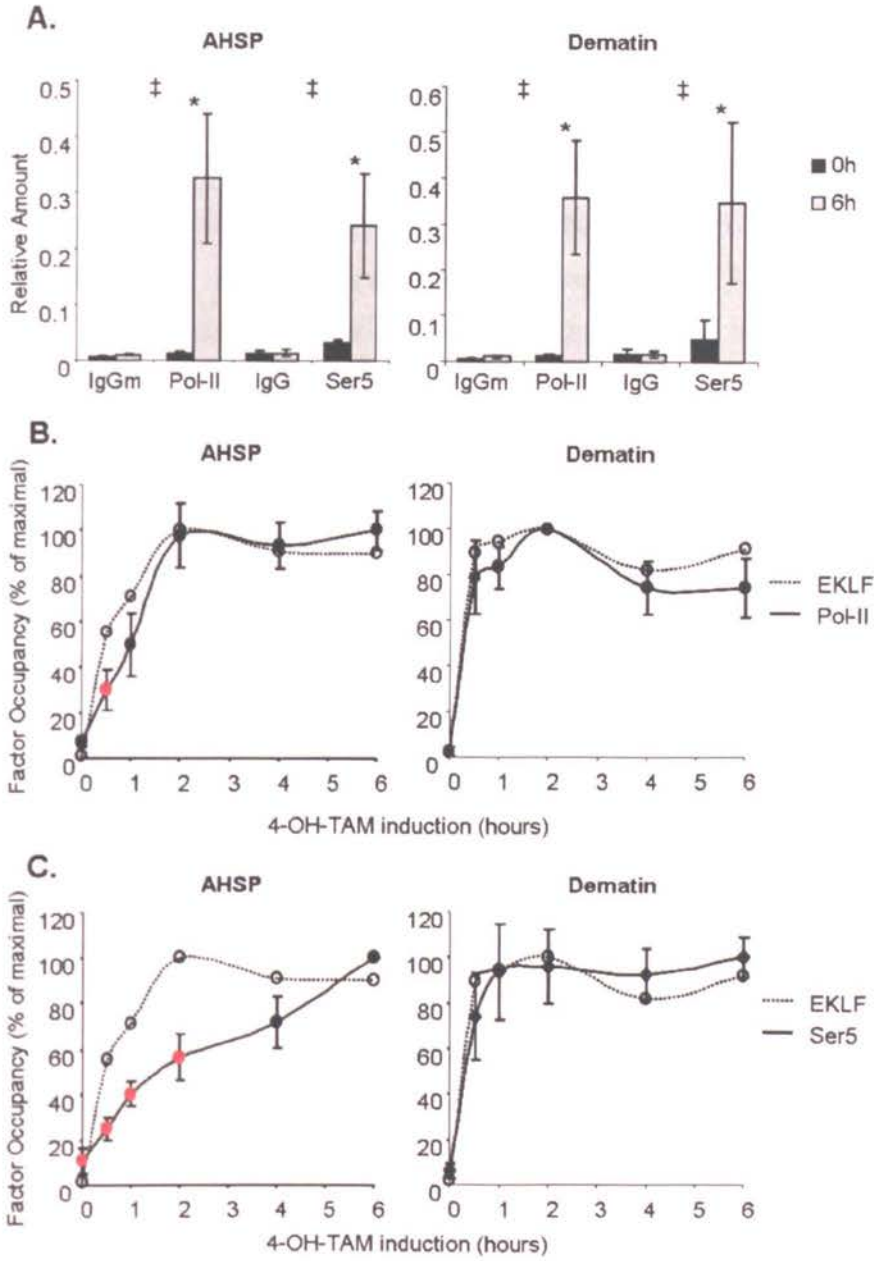

Figure 4.14. RNA Polymerase-II recruitment at the AHSP and Dematin genes in JH31 cells. RNA polymerase II binding at the AHSP and Dematin promoters respectively was determined by ChIP analysis using an antibody raised against Pol-II or Ser5Pol-II. (A). Relative enrichment of RNA Pol-II and Ser5 Pol-II prior to and 6 hrs post 4-OH-TAM treatment of JH31 cells corrected to input. * p value<0.05 between IgG and corresponding sample. ‡ p value<0.05 between 0h and 6hr. Kinetics of recruitment of (B). RNA Pol-II and (C). Ser5 Pol-II corrected to overall maximal signal intensity at 0, 0.5, 1, 2 and 6 hrs post treatment of JH31 cells with 4-OH-TAM. The doted line represents binding of EKLF for comparison. •p value< 0.05. Data shown represents the average of at least 3 independent experiments (mean ± SEM).

While it is evident that occupancy of each promoter by the transcription machinery requires the presence of EKLF, it is unclear whether EKLF and RNA Pol-II are recruited simultaneously. To resolve this issue, we applied the ChIP assay at various time points of induction and developed the temporal analysis of recruitment of total RNA Pol-II at the AHSP and dematin promoters. As illustrated in Figure 4.14.B., RNA Pol-II was recruited to the AHSP promoter with a slight delay when compared to EKLF. In contrast, RNA Pol-II recruitment at the dematin promoter was coupled to EKLF binding. These observations do not account for the kinetic differences detected between RNA Pol-II mobilization and gene transcription.

To determine whether the activation of RNA Pol-II is a sequential event to EKLF binding, we applied a similar strategy using an antibody raised against Ser5 Pol-II. Striking differences in Ser5 Pol-II mobilization were detected between the AHSP and the dematin promoter (Figure 4.14.C.). Ser5 Pol-II occupancy at the AHSP promoter was steadily progressive and did not correlate with EKLF binding. In comparison, Ser5 Pol-II is recruited to the dematin promoter in a manner that is similar to EKLF binding. Therefore, our data strongly suggests that EKLF does not recruit RNA Pol-II directly to the AHSP promoter and that additional factor(s) are involved in the activation of the enzyme. In contrast, RNA Pol-II recruitment at the dematin promoter appears coupled to EKLF binding. We therefore uncovered distinct mechanisms of transcriptional regulation of the two EKLF target genes, suggesting that RNA Pol-II recruitment is dictated by the chromatin context.

DISCUSSION

The studies in this chapter explore the principal function(s) of EKLF at non-globin target gene promoters. We uncovered common events as well as discrepancies in factor recruitment at both promoters which provide us with further insight into the direct role of EKLF in transcriptional activation. Our studies revealed a newly described chromatin remodeling mechanism for EKLF, histone eviction. Finally, in addition to providing a deeper understanding in AHSP and dematin gene regulation, we identified differences in recruitment and potentially function between the two closely related HATs CBP and p300.

EKLF-coupled mobilization of sequence-specific transcription factors and co-factors at target gene promoters

Monitoring the temporal events of factor recruitment upon EKLF localization to the nucleus, we demonstrated the critical impact of EKLF binding at target gene promoters. EKLF is required for factor occupancy, chromatin remodeling as well as histone modifications at the AHSP and dematin promoters. Based on our studies, we categorized EKLF-dependent events in the order in which they occur with regards to EKLF binding. We reveal a series of EKLF-coupled events at both studied promoters. Indeed, the recruitment of GATA-1, Ldb-1 and p300 coincides with EKLF binding at both promoters therefore indicating that the direct recruitment of all three factor constitute the primary mode of action of EKLF at target gene promoters.

Interestingly, some GATA-1 binding is detected at the promoter of both genes in the absence of EKLF suggesting that low levels of promoter bound GATA-1 are insufficient to trigger the series of events necessary for gene transcription. Indeed, none of the additional factors monitored in these studies were detectable prior to EKLF binding. The most tangible explanation is that EKLF-directed chromatin remodeling enhances GATA-1's accessibility to GATA motifs. Because GATA-1 is involved in gene activation as well as gene repression (*117, 173, 237-241*), we should consider the possibility that the

promoter bound GATA-1 detected prior to EKLF binding is part of a repressor complex represented at low levels in the absence of EKLF.

For the purpose of these studies, Ldb-1 was used as a marker of the SCL/TAL-1/LMO2/E2A/Ldb-1 complex. We report that promoter occupancy by the SCL/TAL-1 complex coincides with EKLF binding. Studies revealing that SCL/TAL-1 and GATA-1 are found to co-occupy regulatory regions of GATA-1 activated genes failed to monitor EKLF occupancy at those same sites (*117*). We hypothesize that EKLF is required for the correct formation of the SCL/TAL-1 complex at target gene promoters in combination with GATA-1.

As stated previously, the activity of EKLF is modulated by its acetylation status. Therefore, we were expecting the co-recruitment of HATs with EKLF. Indeed, we demonstrate that p300 is recruited to the dematin promoter simultaneously with EKLF. This coupled mobilization was also detected at the AHSP promoter, strongly suggesting that co-incident recruitment of p300 is a common event of EKLF binding at target promoters. Intriguingly, unlike p300, EKLF dependent mobilization of CBP is not coupled to EKLF binding. Further exploration into the significance of the recruitment of each HAT is required to reveal the potential function of CBP and p300 in EKLF-directed transcriptional activation.

Context-specific recruitment of the transcription machinery

Our studies demonstrate that chromatin context influences the accessibility and/or binding affinity of EKLF as well as the EKLF-dependent recruitment of the transcription machinery at target gene promoters. Whilst recruitment of GATA-1, Ldb-1 and p300 is reported to be co-incident with EKLF binding at the promoter of the AHSP and dematin genes, EKLF binding itself does not follow similar kinetics of recruitment at both promoters. The AHSP promoter demonstrates less sensitivity to EKLF than the dematin promoter, highlighting the importance of chromatin context for factor recruitment. Exploration into the potential limiting factors of AHSP transcription led to the discovery of the evident discrepancy between EKLF binding and the recruitment of the

transcriptional machinery. A short but significant delay in RNA polymerase II recruitment was measured.

Using a specific antibody against Ser5Pol-II, the activated form of the enzyme, we revealed that promoter occupancy of Ser5Pol-II is the limiting factor for AHSP transcription. In contrast, this rate-limiting step of gene activation is not detected at the dematin gene thereby re-enforcing the idea of context-specific gene regulation. Further support of this concept is presented in studies of the transcription factor GATA-1 and its binding partner FOG-1. A sumoylation defective mutant of GATA-1 fails to induce AHSP transcription while dematin transcription remains unperturbed (*242*). These results were recapitulated by similar studies using a mutant of GATA-1 that abrogates the interaction with FOG-1 (*242*). In addition, downregulation of FOG-1 by siRNA strategies led to a similar outcome (*60*). The mentioned studies also report that both activated genes localized to separate regions of the nucleus. It would be of great interest to explore the idea of transcription factor-specific gene activation being determined at least in part by nuclear localization (*228*).

The chromatin remodeling capability of EKLF is not limited to the recruitment of Brg1

In addition to previous studies demonstrating the requirement of EKLF for HS formation at the AHSP and beta-globin promoters, we demonstrate here that EKLF binding establishes the formation of HS at the dematin promoter (Figure 4.7.). However, studies failed to evaluate the direct action of EKLF as opposed to transcription-promoted histone eviction. We approached the issue by monitoring nucleosomal density in relation to EKLF binding and transcription. We demonstrate the immediate loss of Histone H3 upon EKLF binding at the AHSP and dematin promoter. We could not exclude entirely the role of elongating Pol-II in the apparent nucleosomal eviction; however we detected a significant time gap between maximal histone loss and maximal transcription rate at the dematin gene indicating that transcription elongation alone does not account for the totality of H3 loss measured.

These studies demonstrate rapid chromatin remodeling upon EKLF binding at target gene promoters. In an attempt to identify the effector of these structural changes of chromatin, we focused our efforts on monitoring the mobilization of the SWI/SNF complex, specifically the known binding partner of EKLF, Brg-1. Surprisingly, we report that Brg-1 recruitment at either promoter does not coincide with histone loss. Brg1 is mobilized to the promoter subsequent to histone eviction, suggesting that Brg1 is not involved in the initial chromatin remodeling of the AHSP and dematin promoters, but may facilitate maintenance of an open chromatin state. Although our data does not disprove the a priori assumption that EKLF remodels chromatin via its direct interaction with Brg1, it certainly extends the spectrum of EKLF's remodeling properties.

Indeed, our data recapitulates studies in yeast demonstrating that the recruitment of the SWI/SNF complex at the *CYC1* promoter occurs post-activation of gene transcription (*243*). Additional studies at the *RNR3* gene have highlighted the requirement of RNA Pol-II promoter occupancy for SWI/SNF recruitment (*244*). In addition, our data support an unexpected role for EKLF-recruited Brg1 in transcription elongation. However, it is surprising that chromatin remodeling, as measured by H3 loss, is detected at high levels prior to Brg1 recruitment or histone H3 acetylation. Further studies are required to evaluate the role of Brg1 in the initial EKLF-induced chromatin remodeling at target promoters. For example, posttranslational modification(s) of EKLF may be required to interact with Brg1 *in vivo*.

Differential EKLF-dependent recruitment of HATs at target gene promoters

Previous studies have explored the functional significance of EKLF interaction with HATs, using reporter constructs rather than chromatinized endogenous loci. Whilst CBP, p300 and P/CAF interact with EKLF, only CBP and p300 have the ability to acetylate EKLF and increase its transactivation activity *in vitro* (*64*). Acetylation of EKLF is suggested to alter its DNA binding affinity, thereby increasing its binding affinity for target gene promoter CACC boxes. Monitoring the mobilization of CBP and p300 at the AHSP and dematin promoter, we demonstrate the sequential recruitment of CBP in

relation to EKLF and p300. Therefore, our studies indicate that EKLF preferentially interacts with p300 over CBP *in vivo*.

It is particularly interesting that the HATs are recruited to EKLF target promoters via distinct mechanisms. Ablation studies in mice strongly indicated the non-redundancy of p300 and CBP in hematopoiesis (*67*). Developed further, the present study could extend these findings by demonstrating the involvement of each HAT in separate steps of transcription.

Model of context-specific EKLF-directed transcriptional activation

This study has allowed the distinction between molecular events coupled to EKLF binding at target promoters and subsequent events. We demonstrate that GATA-1 is not recruited to EKLF target promoters in the absence of EKLF. Therefore, EKLF plays a major role in GATA-1 dependent transcription. Our results clearly demonstrate that, similarly to GATA-1, Ldb-1 is recruited simultaneously with EKLF at the AHSP and dematin promoters. This observation is particularly significant as Ldb-1 was detected at the AHSP promoter regardless of the lack of putative E-boxes and thus potential SCL/Tal-1 binding sites. Our data is in agreement with genome-wide studies reporting Ldb-1 and GATA-1 co-occupancy at promoters of GATA-1 activated genes (*117, 245*). We extend these findings by demonstrating the co-occupancy of EKLF, GATA-1 and SCL-TAL1 at EKLF target gene promoters. In addition, we report that recruitment of Ldb-1 at EKLF target promoters does not require the presence of E-boxes.

From our studies, we were able to develop a model of the temporal events of the context-specific EKLF-directed transcription (Figure 4.15). We propose that EKLF-coupled binding of GATA-1, Ldb-1 and p300 triggers structural changes of chromatin comparable to histone eviction. A later step of transactivation includes the recruitment of CBP, RNA Pol-II and Ser5-Pol-II and finally Brg1. The finality of the formation of the transcriptional complex is detected by the establishment of histone modifications including global H3 acetylation and H3K4Me3 modification.

In conclusion, our studies increase our understanding of EKLF-directed transcription. In addition, we contributed to a better understanding of the regulation of the AHSP and dematin genes. Our studies revealed intriguing disparities in EKLF-directed chromatin remodeling processes. We therefore established a need to reconsider the conventional model of EKLF-induced chromatin remodeling.

Model of context specific EKLF-dependent transcription

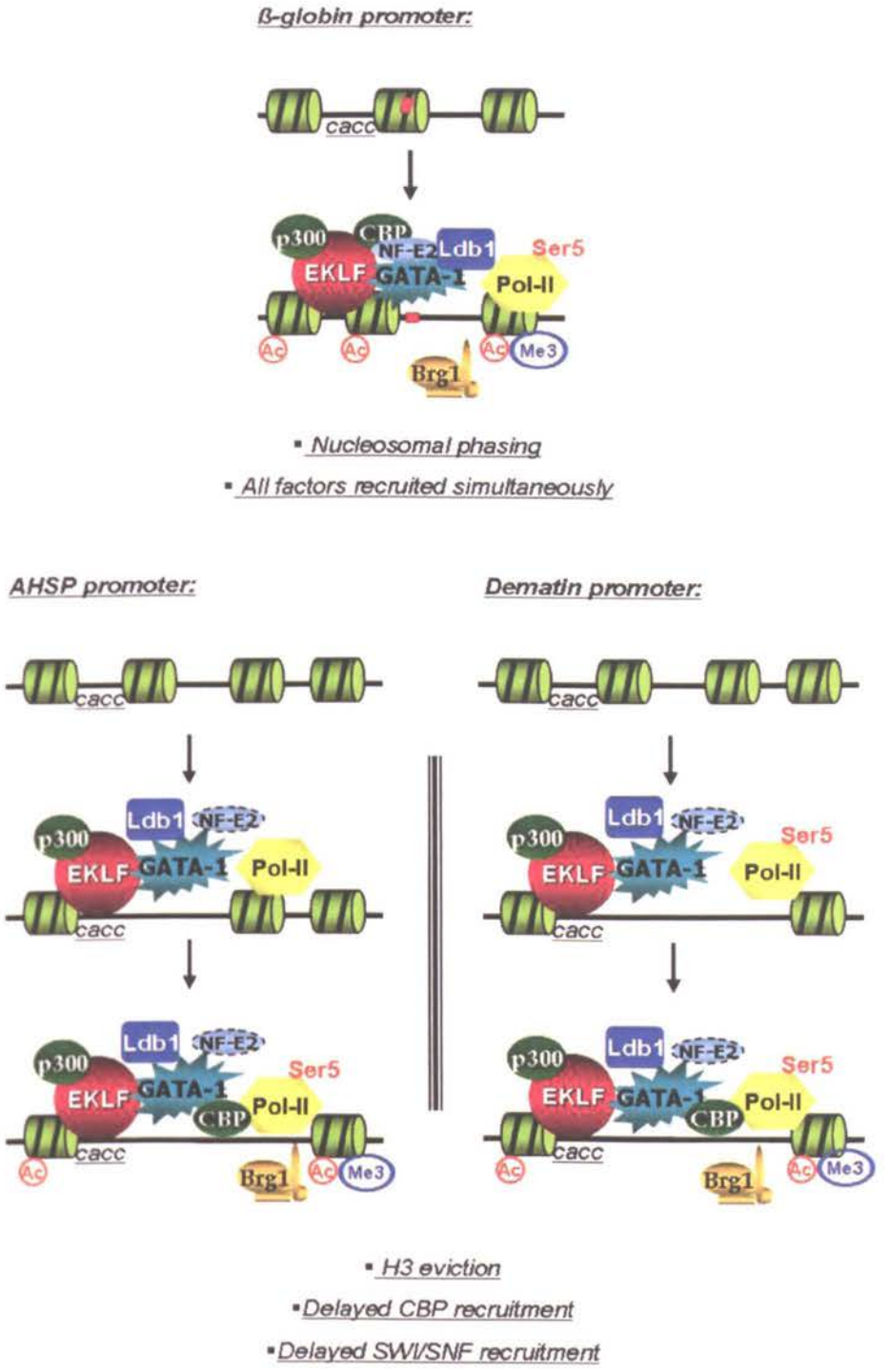

Figure 4.15. Model of EKLF context-dependent transcription.

-CHAPTER 5-

A ROLE FOR EKLF IN HEME BIOSYNTHESIS: REGULATION OF DELTA-AMINOLEVULINIC ACID DEHYDRATASE (ALAD) GENE TRANSCRIPTION

INTRODUCTION

The production of a functional hemoglobin molecule consisting of 4 globin chains, coordinated by a heme moiety is critical to the physiological function of red blood cells. Indeed, the levels of heme in erythroid cells are uniquely regulated to meet the stoichiometric proportions required to match the levels of globin chains. Therefore, mechanisms involved in the regulation of heme biosynthesis and globin chain synthesis must share common regulators.

In addition to controlling the transcription of the globin genes, the hematopoietic restricted transacting factor GATA-1 is involved in the regulation of the expression of several genes encoding enzymes of the heme biosynthesis pathway (see Figure 5.1). The most relevant GATA-1 target gene of the pathway is the ALAS2 gene. ALAS is the enzymatically rate limiting step of the heme biosynthesis pathway. Therefore, GATA-1 can be considered as a transcriptional master regulator of hemoglobin production.

Similar to GATA-1, EKLF is critical for the expression of the β-globin like genes and has been implicated in the transcriptional regulation of the genes of the α-globin loci genes (*246-247*). EKLF has also been reported to influence the regulation of heme in erythroid cells. Studies in EKLF null fetal livers and progenitor cells have demonstrated that mRNA levels of the first three enzymes of the heme biosynthesis pathway are underrepresented (*151-152*). Similar conclusions have resulted from expression studies in cells comparable to our JH31 cell system, described in chapter 3 (*151*). Because ALAS2 is the principal rate limiting enzyme of the pathway, studies have been focused on identifying the *trans*-acting factors responsible for the regulation of its expression. *In vitro* studies have reported the presence of a conserved CACC element, a potential EKLF binding site, within the promoter sequence of the ALAS2 gene (*248*). Additional research has demonstrated that EKLF can activate the expression of the ALAS2 gene in a reporter assay (*249*). Furthermore, an intronic

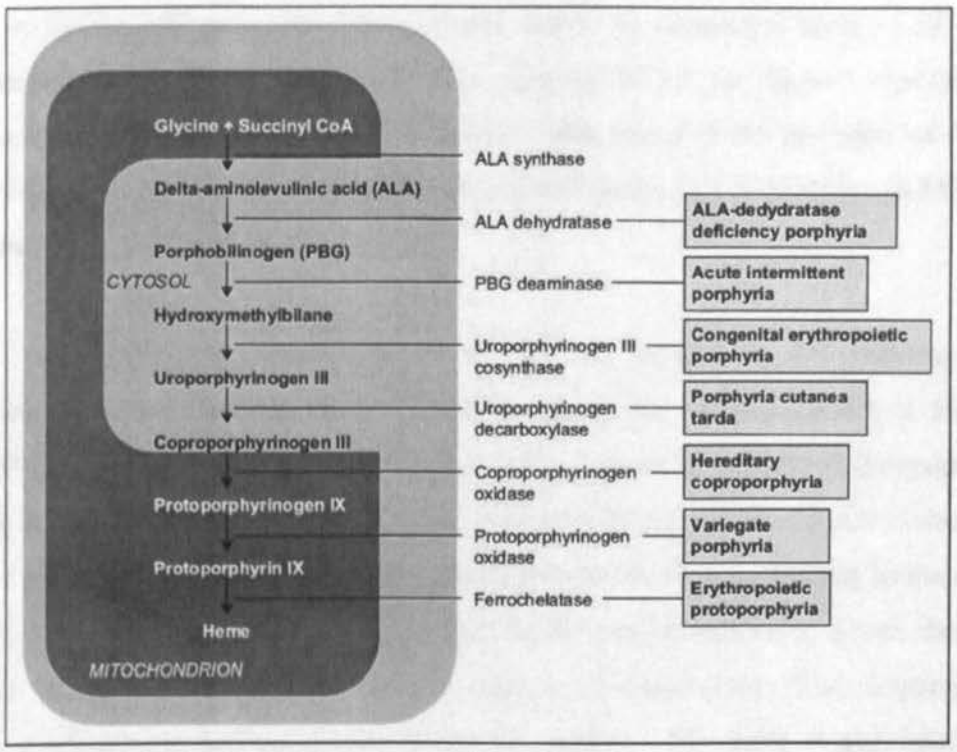

Figure 5.1. Diagram of the Heme Biosynthesis pathway. Derived from reference (*250*). Products of the pathway are orderly represented within their appropriate cellular compartment. Enzymes of the pathway catalyzing the conversion of one product to the next are orderly represented at the center. Known conditions resulting from defects in the corresponding enzymatic reaction are depicted on the right.

enhancer of the ALAS2 gene has also been reported to be dependent upon EKLF *in vitro* (*251*). However, evidence is lacking to link directly EKLF to ALAS2 transcriptional regulation *in vivo*. A conserved CACC element is also found at the promoter of the third enzyme of the pathway, porphobilinogen deaminase (PBGD) and is defective in EKLF null progenitors (*144, 152, 252*).

In EKLF null fetal livers, expression of the second enzyme in the pathway, delta-aminolevulinate dehydratase (ALAD), is defective but is not entirely abolished. However, unlike PBGD, expression of ALAD is not rescued in culture of primary null erythroblasts, indicating that high levels of ALAD expression require EKLF (*151*). ALAD is the second enzyme of the pathway, is essential although not enzymatically rate limiting in the cell due to its high level of expression. It is expressed in all mammalian cells, given the central importance of heme biosynthesis in many aspects of metabolism. Two transcripts are observed, a ubiquitous and an erythroid-specific variant. The latter is regulated by an immediate upstream promoter bearing consensus-binding sequences for GATA-1 and a conserved CACC element (Figure 5.2.) (*253*).

To date, no erythroid disease has been reported as a consequence of aberrant ALAD expression. Mutations in the protein coding sequences lead to a severe form of hepatic porphyria and spontaneous abortions in homozygotes (*254-255*). ALAD is strongly inhibited by lead and contributes to the toxicity effects in lead poisoning cases (*256-258*). Complete loss of ALAD expression in erythroid cells results in catastrophic events during ontogeny in fish (*259*).

In this study, we decided to further analyze the role of EKLF in heme biosynthesis. Using our EKLF-inducible cell system, we identified EKLF as an early regulator (within 2 hours of induction) of ALAD, but not ALAS and PGBD transcription. The latter factors appear to be regulated at later time points (>6 hours). To gain insight into the principal role of EKLF in the regulation of heme biosynthesis, we choose to dissect its role at a previously uncharacterized gene target.

A.

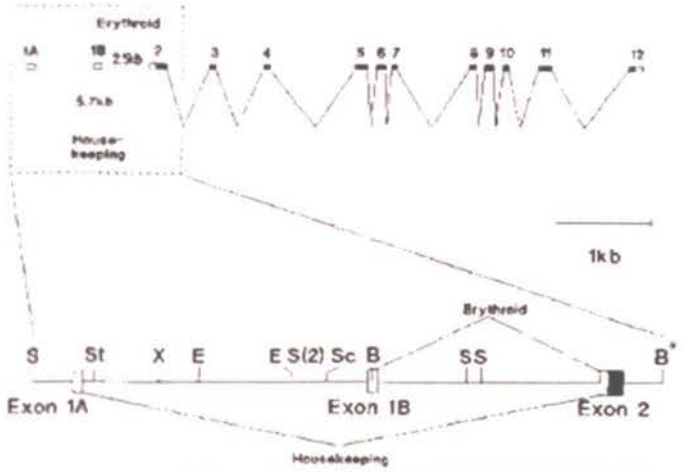

Bishop et al. NAR, 1996; 24(13): 2511-2518

B.

```
-280  TATGTCATTTTGAGCAAATAGTTGTACATCCCAGGGCAACCTCCTGGCAG
                                                   E-box
-230  ATGTGAGAGCCAAATTCTGCACAAAGAGTCTATATAGATAAACTCTCGAA
                                          GATA
-180  TGTGCTGAGTGTGTTACTTAGGAGCCAGAACATCTCTAAGGAGGCTTGGC
      ----------------------------------------------------
-130  TCTCTTGTGTCCTGTGAAGAGGCTGGCCCACCCAGGGGTGTGGTGGCAGG
                                     CACC          CACC
      ----------------------------------------------------
-80   GTTGGTCCTTGTGTGGTTCCTGATAACCTCAACCCCAGCAAGGAGGGAAA
                           GATA
      ----------------------------------
-30   GGGGATAAGGTGGGCCCTGAGCTGCTTGGGagggagctgaaggagcctga
```

C.

Figure 5.2. Structure of the mouse ALAD gene and transcription factor binding sites at the mouse ALAD erythroid promoter. (A) Structure of the mouse ALAD gene extracted from (*253*) (B) Nucleotide sequence of the mouse ALAD promoter. Positioning of nucleotides is relative the transcriptional start site in exon1B. Underlined sequences represent consensus binding sequences for GATA factors or CACC binding factors or previously undisclosed E-boxes (red). The exon 1B sequence is displayed in lower case. The broken upper line represents the region amplified for ChIP analysis. (C) Representative diagram of clustered transcription factor binding sites of the mouse ALAD promoter.

RESULTS

EKLF-dependent high-level transcription of ALAD

Studies of erythroblasts derived from EKLF-null mice have suggested strongly that EKLF is involved directly in the transcriptional regulation of ALAS2 and ALAD (*151-152*). In addition, PGBD and UROD may also be regulated, albeit in a partial manner, by this factor in erythroid cells. To test this hypothesis, we decided to take advantage of the JH31 cell system. In this cellular system, transcription of several EKLF target genes was rescued within a few hours of induction with 4-OH-Tamoxifen (see Chapters 3 and 4). Therefore, we hypothesized that monitoring the transcriptional response of the first four genes of the heme biosynthesis pathway upon 4-OH-Tamoxifen induction would provide an outstanding foundation to explore the regulation of these factors.

In initial studies, we assessed mRNA levels of ALAS2 and PBGD, given the rate limiting nature of the concentrations of these factors. As described in Figure 5.3., transcription of the ALAS2 gene did not respond to the presence of EKLF in the nucleus. In addition, the transcription of the PBGD gene increased only slightly upon induction. The detected increase corresponded to approximately 50% of the measured mRNA levels of uninduced cells. The data on ALAS, coupled with additional studies outside the scope of this thesis, suggested that the response to EKLF occurs at more distant time points, >6 hours, and required additional events that cannot occur in the transformed JH31 cell line. Because the effect of EKLF on PBGD mRNA levels was limited, we decided to not explore further the role of EKLF in PBGD transcription at this time.

Next to ALAS2, ALAD was the most affected gene of the heme biosynthesis pathway in EKLF null animals (*152*). Interestingly, unlike ALAS2, ALAD transcription increases

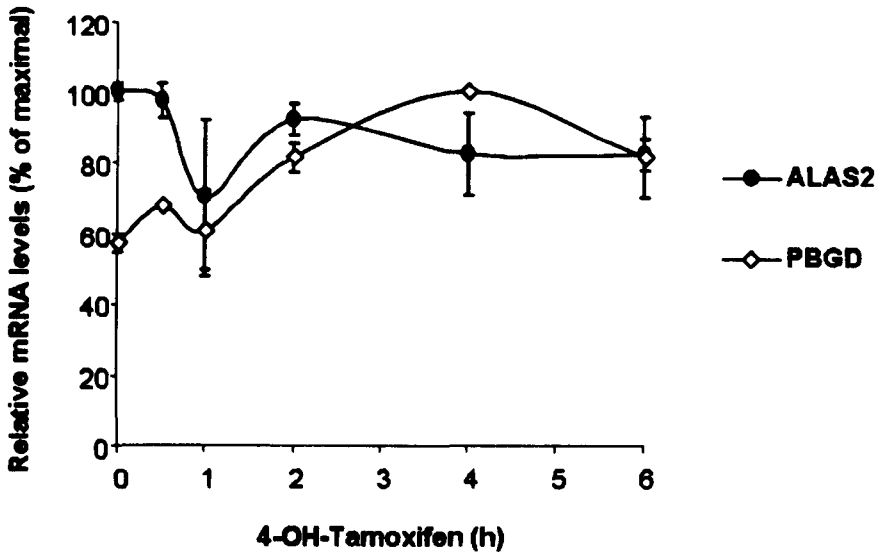

Figure 5.3. ALAS2 and PBGD mRNA levels in JH31 cells. Relative mRNA levels for ALAS2 and PBGD as determined by semi-quantitative real-time PCR. mRNA was purified at 0, 0.5, 1, 2, 4, and 6 hours after induction with 4-OH-Tamoxifen. Represented mRNA levels were corrected to HPRT mRNA levels. Data shown represents the average of at least 2 independent experiments (mean ± SEM).

significantly and rapidly upon induction and reaches a plateau by 2 hours of treatment (Figure 5.4.A.). Our data strongly suggests that ALAD was directly influenced by the presence of EKLF in the nucleus. The transcriptional response to induction was unique to ALAD as mRNA levels for the UROD gene did not increase upon induction (Figure 5.4.B.).

In order to establish that the increase in ALAD mRNA upon induction is the result of an increase in transcription efficiency as opposed to an increase in mRNA stability, we monitored the levels of primary transcripts of the ALAD gene upon induction. As shown in Figure 5.5., ALAD primary transcript levels increased significantly to reach a maximum within 30 minutes of treatment. Intriguingly, ALAD transcription gradually decreased after 30 minutes, to reach an apparent plateau by 6 hours of induction. Importantly, primary transcript levels measured at 6 hours of treatment were significantly greater than those observed prior to induction. Our data strongly suggests that the translocation of EKLF to the nucleus induces a rapid increase in the transcriptional rate of the ALAD gene. The intensity of the increase diminished over time but remains greater than in uninduced cells.

We hypothesized than EKLF is recruited to a *cis*-regulatory element of the erythroid specific promoter of the ALAD gene. To test our hypothesis, we performed a ChIP assay using an antibody directed against the HA epitope tag. As described in Figure 5.6.A., a small enrichment of the ALAD promoter with this monoclonal antiserum was detected prior to induction. However, a dramatic increase in signal intensity was observed at 6 hours post-induction. Our data clearly demonstrates that EKLF is recruited to the ALAD promoter upon induction.

Because ALAD primary transcripts gradually decreased after reaching a maximum, we decided to assess the stability of EKLF binding to the ALAD promoter. To do so, we applied the HA ChIP in JH31 cells at several time points of induction. As demonstrated in Figure 5.6.B., EKLF reached maximal occupancy at the promoter within 30 minutes of induction, which correlated with the primary transcripts results. However, unlike primary transcripts, the signal intensity did not decrease with time. Therefore, we demonstrated that

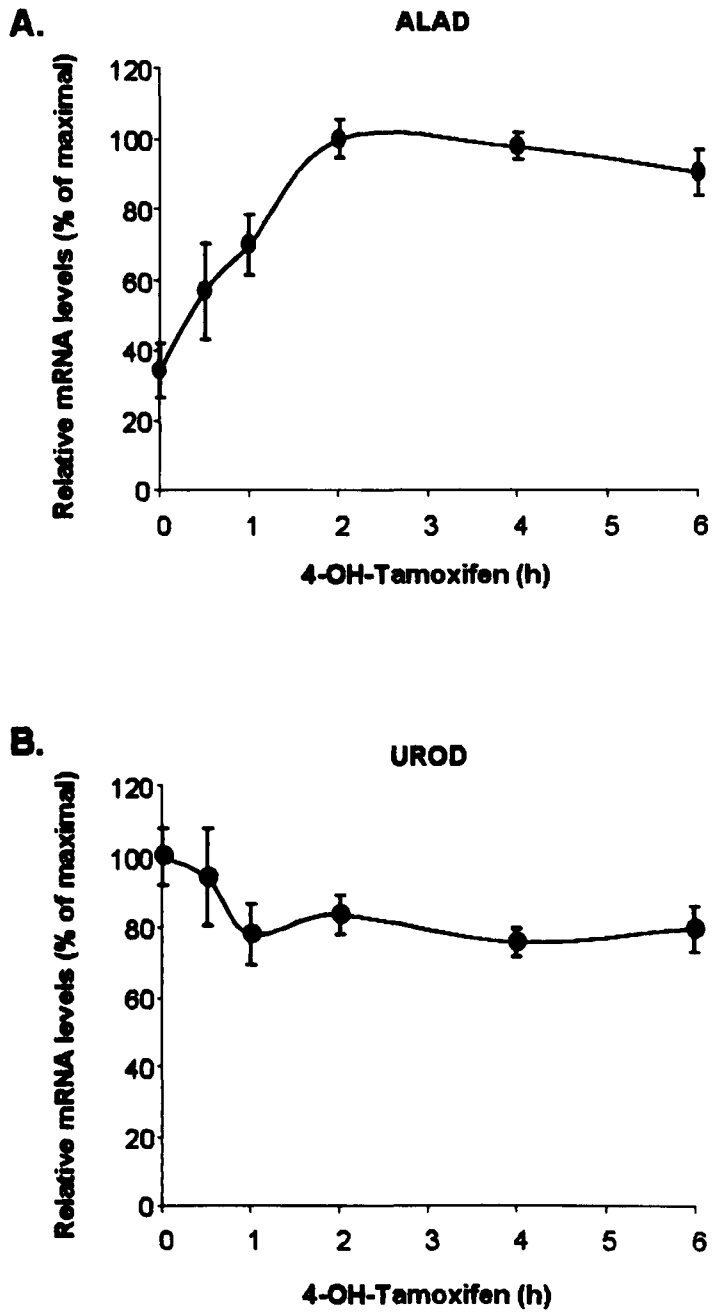

Figure 5.4. ALAD and UROD mRNA levels in JH31 cells. Relative mRNA levels for ALAD (A.) and UROD (B.) as determined by semi-quantitative real-time PCR. mRNA was purified at 0, 0.5, 1, 2, 4, and 6 hours after induction with 4-OH-Tamoxifen. Represented mRNA levels were corrected to HPRT mRNA levels. Data shown represents the average of at least 2 independent experiments (mean ± SEM).

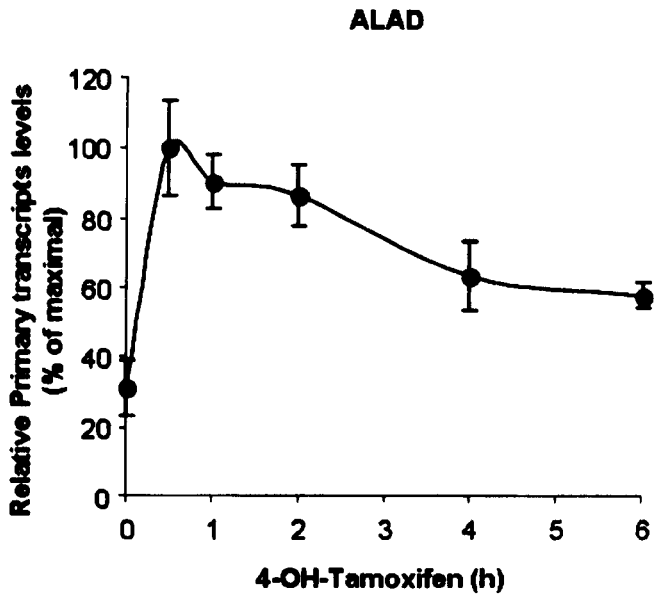

Figure 5.5. ALAD transcription in JH31 cells. Relative primary transcript levels for ALAD as determined by semi-quantitative real-time PCR. RNA was isolated at 0, 0.5, 1, 2, 4, and 6 hours after induction with 4-OH-Tamoxifen. Represented primary transcripts levels were corrected to HPRT mRNA levels. Data shown represents the average of at least 2 independent experiments (mean ± SEM).

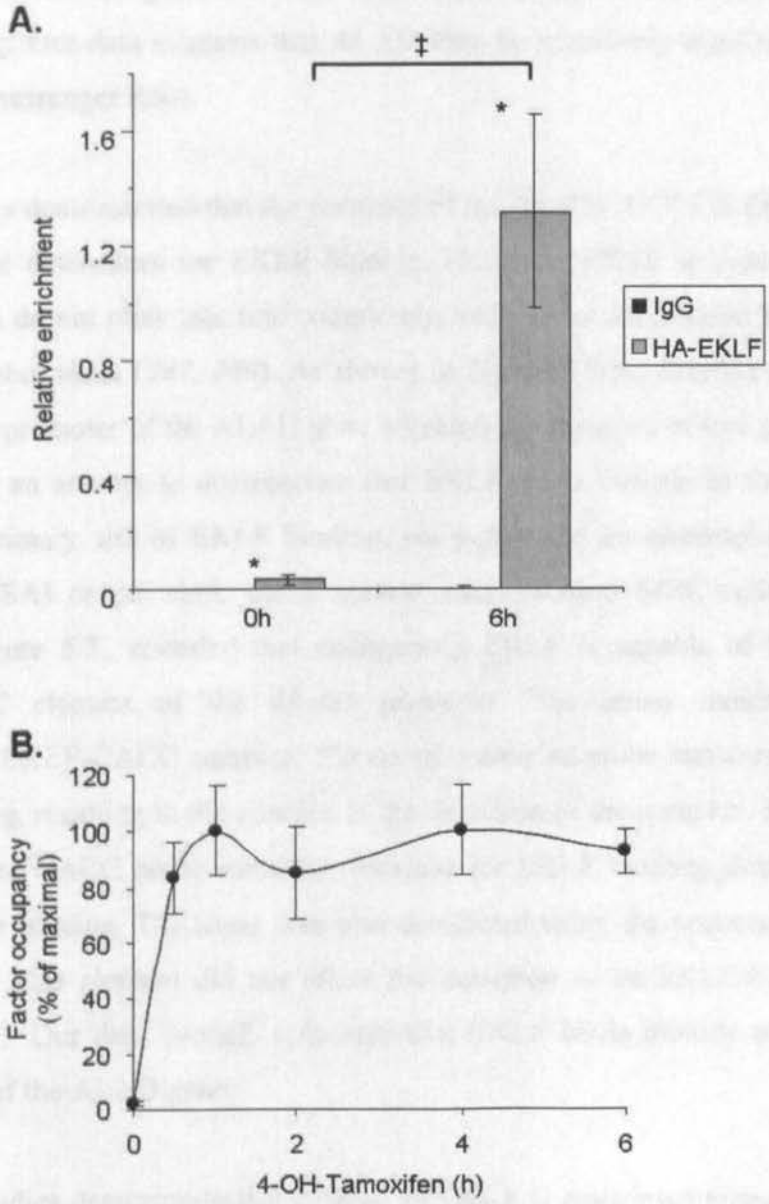

Figure 5.6. EKLF occupies the ALAD erythroid promoter *in vivo*. EKLF binding determined by ChIP analysis using an antibody raised against the HA epitope tag. (A). Relative enrichment of EKLF prior to and 6 hrs post 4-OH-TAM treatment of JH31 cells corrected to input. * p value<0.05 between IgG and corresponding sample. ‡ p value<0.05 between 0h and 6hr. (B). Kinetics of recruitment of EKLF corrected to overall maximal signal intensity at 0, 0.5, 1, 2 and 6 hrs post treatment of JH31 cells with 4-OH-TAM. Data shown represents the average of at least 3 independent experiments (mean ± SEM).

EKLF binding to the ALAD promoter was rapid and stable. The measured decrease in primary transcripts following the first 30 minutes of induction was not related to a decrease in EKLF binding. Our data suggests that ALAD may be negatively regulated to maintain stable levels of messenger RNA.

Most studies have demonstrated that the presence of the NCCNCNCCCN EKLF consensus binding sequence determines the EKLF binding. However, EKLF is capable of binding sequences which do not obey this rule completely, such as its determined binding sites at the murine α-globin locus (*247, 260*). As shown in Figure 5.2.B., detailed analysis of the mouse erythroid promoter of the ALAD gene revealed the presence of two potential EKLF binding sites. In an attempt to demonstrate that EKLF binds directly to the DNA and to determine the primary site of EKLF binding, we performed an electrophoretic mobility shift assay (EMSA) or gel shift, using nuclear extracts from MEL cells. The results, presented in Figure 5.7., revealed that endogenous EKLF is capable of binding to the proximal CACC element of the ALAD promoter. The arrow indicates the band representing the EKLF-CACC complex. Excess of unlabeled probe successfully competed for EKLF binding, resulting in the absence in the detection of the complex. In addition, the unlabeled mutated CACC probe could not compete for EKLF binding, demonstrating the specificity of the binding. The assay was also conducted using the sequence of the distal CACC element. This element did not allow the detection of an EKLF-CACC complex (data not shown). Our data strongly indicated that EKLF binds directly to the proximal CACC element of the ALAD gene.

Together, our studies demonstrate that binding of EKLF is associated temporally and in a strict manner with a dramatic increase in the transcriptional rate of the ALAD gene. Binding occurs, at least in part, via the proximal CACC box of the erythroid-specific promoter.

EKLF-mediated enhanced recruitment of GATA-1 and Ldb-1 at the ALAD promoter. The synergistic interaction of EKLF and GATA-1 *in vitro*, in addition to the reported co-occupancy of GATA-1 and the SCL/TAL-1 complex at GATA-1 activated genes prompted

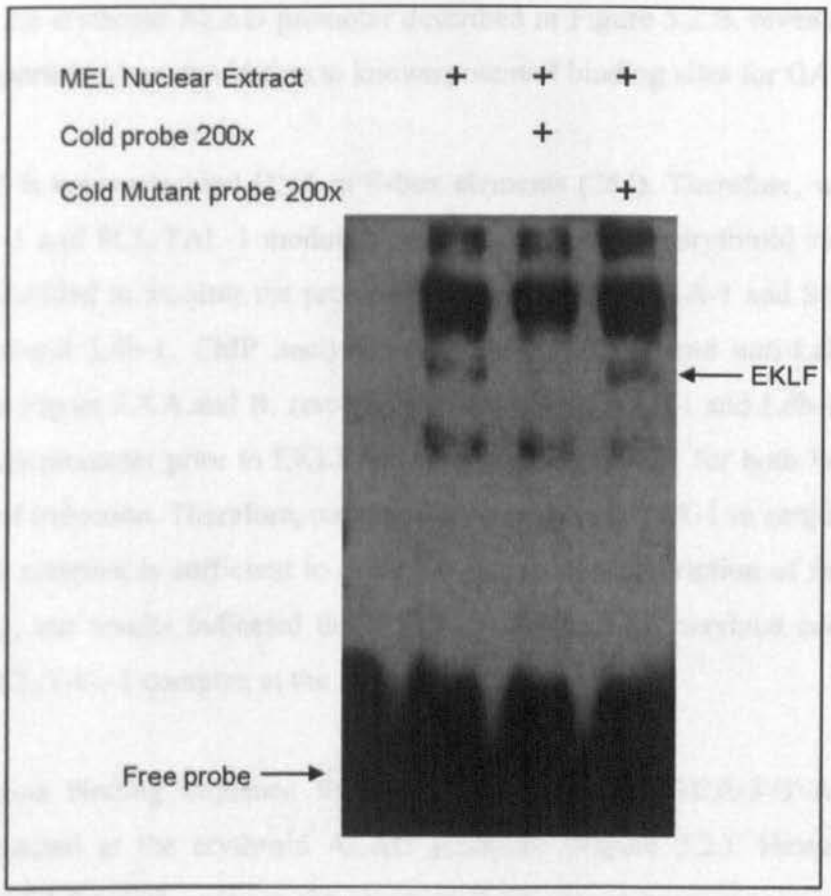

Figure 5.7. Endogenous EKLF occupies the ALAD promoter *in vitro*

EMSA using a probe specific for the proximal CACC box of the ALAD erythroid promoter. Binding specificity was confirmed with the use of a mutated probe.

us to evaluate their potential involvement in ALAD transcription (*172-173*). Detailed analysis of the erythroid ALAD promoter described in Figure 5.2.B. revealed the presence of one unreported E-box in addition to known potential binding sites for GATA-1(*253*).

SCL/TAL-1 is known to bind DNA at E-box elements (*261*). Therefore, we hypothesized that GATA-1 and SCL/TAL-1 modulate ALAD expression in erythroid cells. To test our model, we decided to monitor the promoter occupancy by GATA-1 and SCL/Tal-1 via its complex subunit Ldb-1. ChIP analysis using anti-GATA-1 and anti-Ldb-1 antibodies, described in Figure 5.8.A.and B. respectively, revealed GATA-1 and Ldb-1 co-occupancy of the ALAD promoter prior to EKLF binding. Signal intensity for both factors increased by 6 hours of induction. Therefore, our data indicated that GATA-1 in conjunction with the SCL/TAL-1 complex is sufficient to drive low levels of transcription of the ALAD gene. Interestingly, our results indicated that EKLF is required for maximal occupancy of the GATA-1-SCL/TAL-1 complex at the ALAD promoter.

The consensus binding sequence for p45NF-E2 (TGA(G/C)TCA-3'/3'-ACT(C/G)AGT) was not detected at the erythroid ALAD promoter (Figure 5.2.). However, NF-E2 is detected at EKLF-target genes in the absence of consensus binding sequences (*175, 193, 201*). Therefore, we decided to assess NF-E2 occupancy of the promoter upon induction. ChIP analysis using an antibody directed against the p45 subunit of NF-E2, we demonstrated that NF-E2 is detected at the promoter 6 hours into treatment (Figure 5.8.C.). Interestingly, unlike GATA-1 and Ldb-1, NF-E2 was not detected at the promoter prior to EKLF binding. Our results suggest that NF-E2 is recruited to the ALAD promoter in an EKLF-dependent and GATA-1-SCL/TAL-1 independent manner. The relevance of the promoter occupancy by NF-E2 as yet to be established.

In an attempt to determine the direct role of EKLF in ALAD enhanced transcription, we applied ChIP analysis at several time points of induction. This procedure allowed the visualization of the kinetics of recruitment of GATA-1, Ldb-1 and NF-E2, described in Figure 5.9.A., B., and C. respectively. Our data indicated that the recruitment of GATA-1

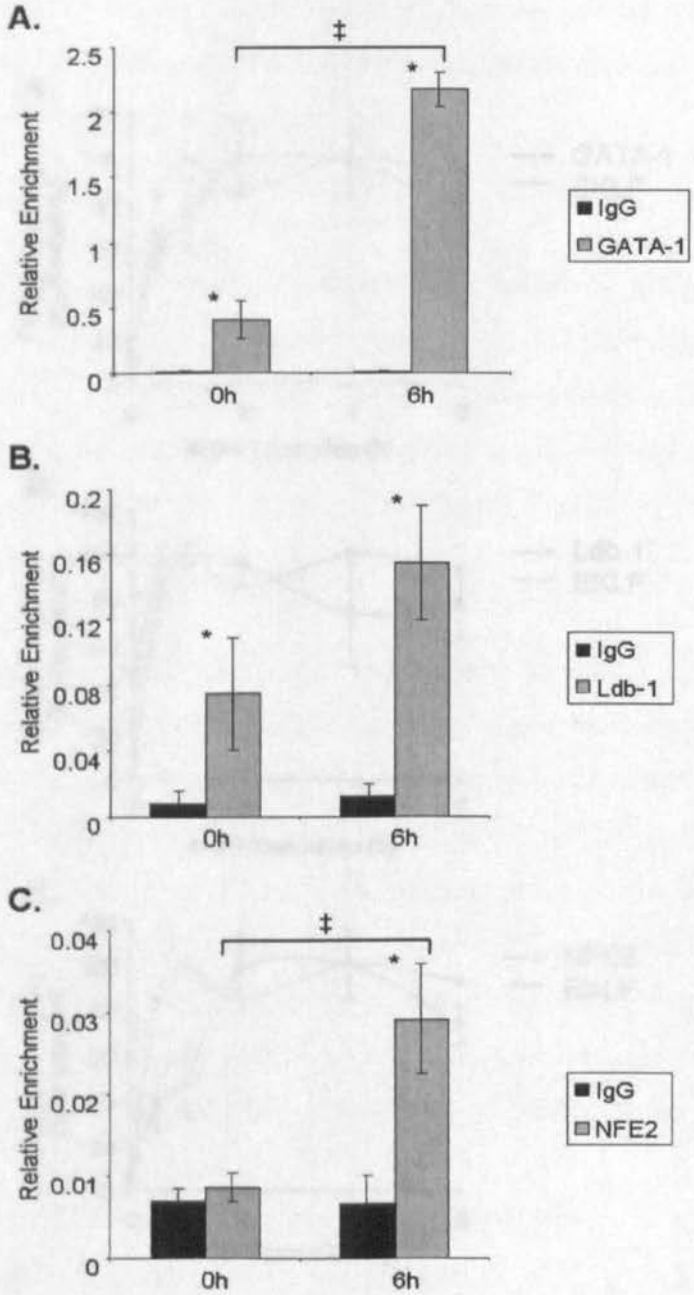

Figure 5.8. Transcription factor occupancy of the ALAD erythroid promoter in JH31 cells. RNA Pol-II and Ser5 Pol-II binding determined by ChIP analysis using an antibody rose against RNA Pol-II CTD or Ser5 Pol-II. Relative enrichment of (A). RNA Pol-II and (B) Ser5 Pol-II prior to and 6 hrs post 4-OH-TAM induction of JH31 cells corrected to input. * p value<0.05 between IgG and corresponding sample. ‡ p value<0.05 between 0h and 6hr. Data shown represents the average of at least 2 independent experiments (mean ± SEM).

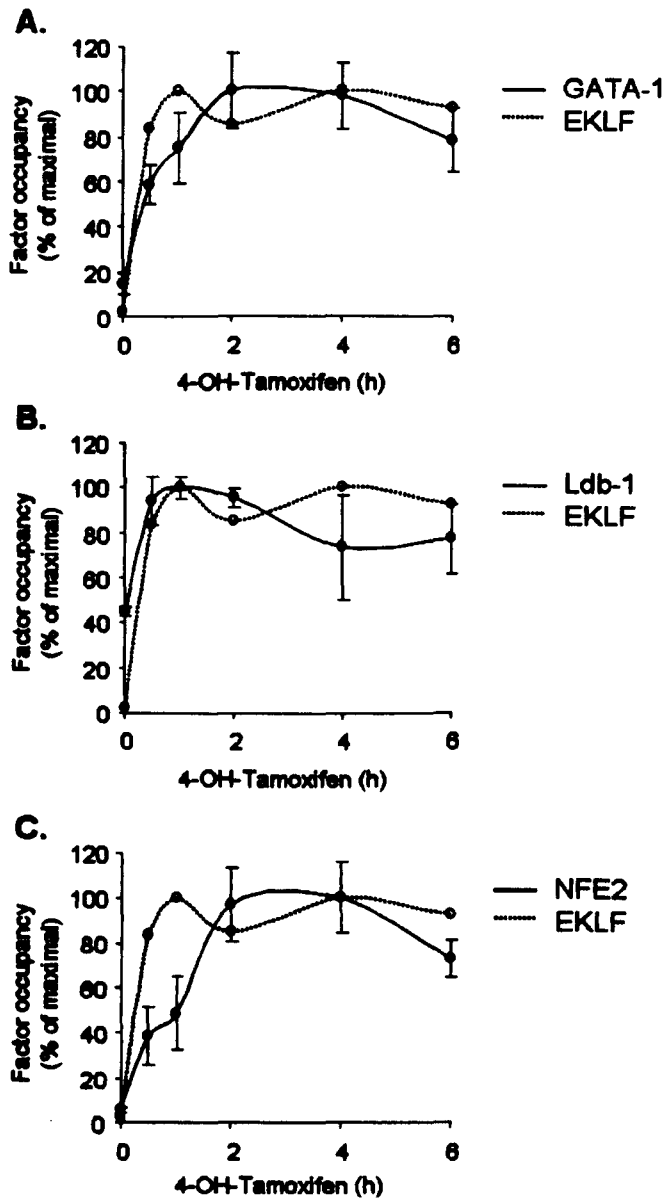

Figure 5.9. Kinetics of transcription factor recruitment at the ALAD erythroid promoter in JH31 cells. Transcription factor occupancy was determined by ChIP analysis using antibodies against GATA-1, Ldb-1 and NFE2. (Kinetics of recruitment (A)GATA-1, (B) Ldb-1 and (C) NFE2 corrected to overall maximal signal intensity at 0, 0.5, 1, 2 and 6 hrs post treatment of JH31 cells with 4-OH-TAM. The broken line represents binding of EKLF for comparison. •p value< 0.05. Data shown represents the average of at least 2 independent experiments (mean ± SEM).

and Ldb-1 to the promoter was coupled to EKLF binding. In contrast, the mobilization of NF-E2 did not follow the kinetics of EKLF binding, suggesting that additional factors are involved in the recruitment of NF-E2 to the promoter.

EKLF binding induces changes in chromatin structure at the ALAD promoter

A direct consequence of EKLF binding at other target *cis*-elements is a change in chromatin architecture, as measured by the DNaseI hypersensitivity profile of the locus (*63, 148, 162*). EKLF-mediated chromatin remodeling could account for the enhanced transcription of ALAD and the recruitment of additional factors via the consequential increase in promoter accessibility.

To address this model, we tested the DNaseI hypersensitivity profile of the ALAD gene locus in EKLF-null fetal liver cells, and in JH31 cells. As described in Figure 5.10.A., the sensitivity of the ALAD promoter to increasing concentrations of DNAseI is significantly more pronounced in wild type fetal livers when compared with EKLF-null cells. Surprisingly, the data in JH31 cells did not replicate these results. The data, represented in Figure 5.10.B., indicated that the ALAD locus was sensitive to DNaseI digestion in the absence of EKLF. Nevertheless, the sensitivity of the promoter at 6 hours post induction was significantly greater when compared to control cells. Our data indicates that EKLF is responsible for a measurable increase in DNaseI hypersensitivity at the erythroid ALAD promoter.

An additional measure of the chromatin state is defined by nucleosomal density. Using histone H3 as a marker of nucleosomes, we determined by ChIP analysis that EKLF binding induces a remarkable decrease in histone density at the ALAD promoter (Figure 5.11.A.). Application of the ChIP assay to evaluate the kinetics of this event, we demonstrated that the EKLF-directed histone loss is maximal within 30 minutes of induction. Unlike the rate of transcription (Figure 5.5.), the detected event remained constant throughout the study. This particular observation suggests that EKLF directly induces H3 eviction.

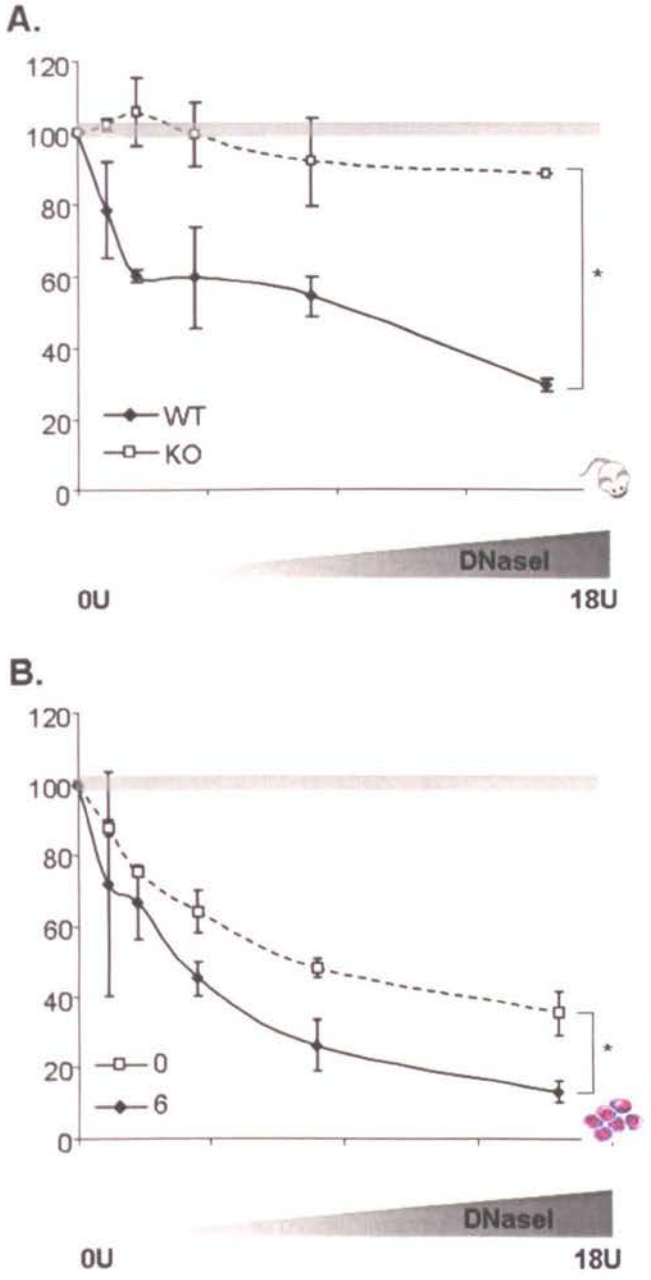

Figure 5.10. EKLF enhances HS formation at the ALAD erythroid specific promoter. DNaseI hypersensitivity assay in mice (A) and JH31 cells (B) at the ALAD erythroid promoter. *p value< 0.05. Data shown represents the average of a minimum of 2 independent experiments (mean ± SEM).

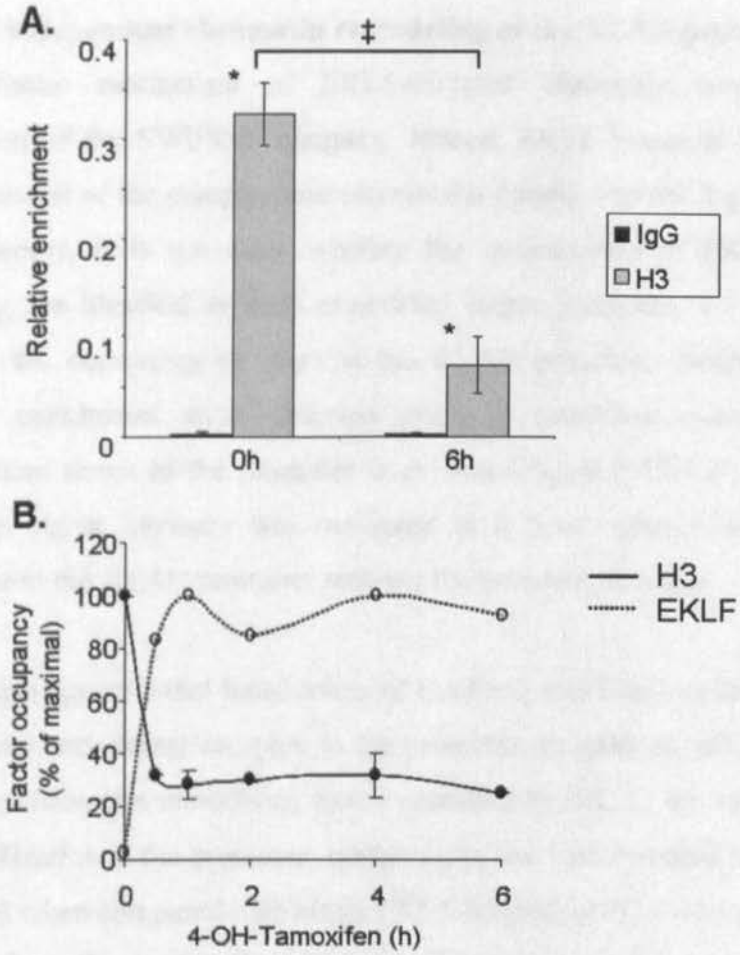

Figure 5.11. H3 density at the ALAD erythroid promoter in JH31 cells. H3 occupancy was determined by ChIP analysis. (A) Relative enrichment of H3 prior to and 6 hrs post 4-OH-TAM treatment of JH31 cells corrected to input. * p value<0.05 between IgG and corresponding sample. ‡ p value<0.05 between 0h and 6hr. (B) Kinetics of recruitment H3 corrected to overall maximal signal intensity at 0, 0.5, 1, 2 and 6 hrs post treatment of JH31 cells with 4-OH-TAM. The broken line represents binding of EKLF for comparison. •p value< 0.05. Data shown represents the average of at least 2 independent experiments (mean ± SEM).

SWI/SNF independent chromatin remodeling at the ALAD promoter.

The stochastic mechanism of EKLF-directed chromatin remodeling involves the participation of the SWI/SNF complex. Indeed, EKLF interacts directly with Brg1, the ATPase subunit of the complex and recruits the complex to the β-globin promoter (*59, 63, 262*). However, it is not clear whether the mechanisms of EKLF-directed chromatin remodeling are identical at each remodeled target promoter. To address this issue, we monitored the occupancy of Brg1 at the ALAD promoter. Surprisingly, no significant levels of enrichment were detected prior to induction even though the DNaseI hypersensitive status of the promoter is evident (Figure 5.12.A.). However, a significant increase in signal intensity was measured at 6 hours post-induction. Therefore, Brg1 recruitment to the ALAD promoter requires the presence of EKLF.

Our data also suggests that basal levels of GATA-1 and Ldb-1 combined are not sufficient to recruit the remodeling complex to the promoter. In order to validate the consensus that Brg1 is the chromatin remodeling motor recruited by EKLF, we monitored the kinetics of Brg1 mobilization at the promoter. Intriguingly, our data revealed a striking delay in Brg1 recruitment when compared with either EKLF binding or H3 eviction (Figure 5.12.B.). Our data strongly indicates that Brg1 is not recruited simultaneously with EKLF and thereby can not mediate the coincident loss of H3. However, we speculate that it may be involved in stabilizing the open conformation.

EKLF-dependent histone mark deposition at the active ALAD promoter

In addition to its chromatin remodeling potential, EKLF has been reported to induce covalent histone modifications at the β-globin promoter (*65*). Epigenetic hallmarks of active genes include H3K4Me3 and AcH3. However, little is known about the manner in which these marks are established. In an attempt to gain further insight into the mechanisms driving the deposition of histone marks, we sought to determine the relationship between EKLF binding, transcription and histone mark deposition using our inducible cell system.

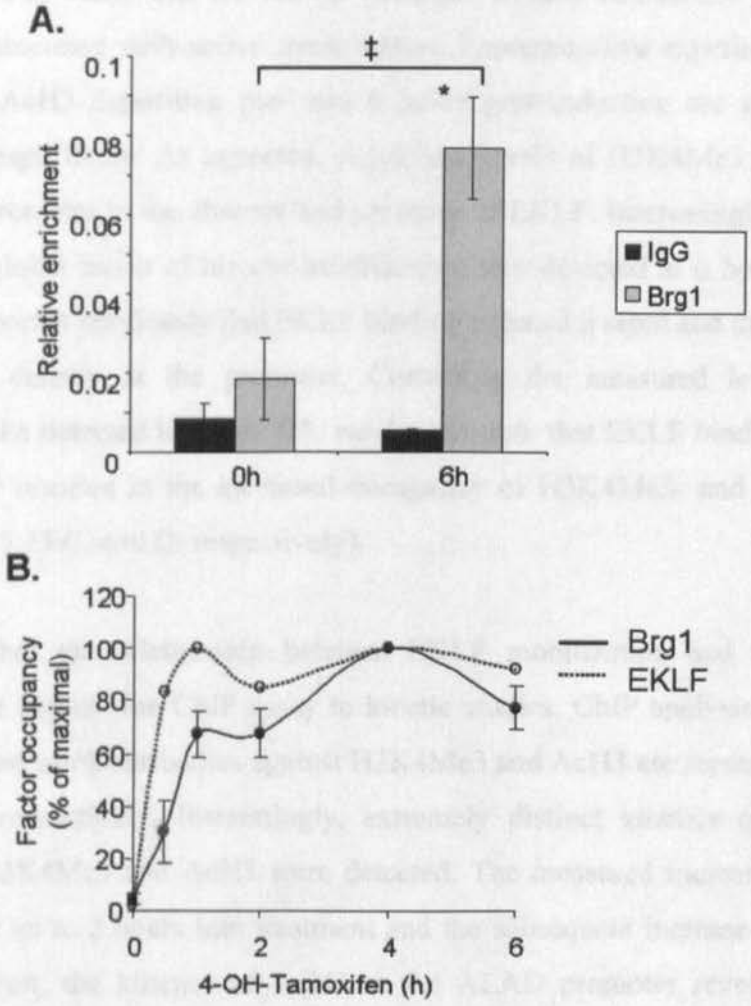

Figure 5.12. Mobilization of Brg1 at the ALAD erythroid promoter in JH31 cells. Brg1 occupancy was determined by ChIP analysis. (A) Relative enrichment of Brg1 prior to and 6 hrs post 4-OH-TAM treatment of JH31 cells corrected to input. * p value<0.05 between IgG and corresponding sample. ‡ p value<0.05 between 0h and 6hr. (B) Kinetics of recruitment Brg1 corrected to overall maximal signal intensity at 0, 0.5, 1, 2 and 6 hrs post treatment of JH31 cells with 4-OH-TAM. The broken line represents binding of EKLF for comparison. •p value< 0.05. Data shown represents the average of at least 3 independent experiments (mean ± SEM).

First, we decided to verify that the ALAD promoter already carried the covalent histone modifications associated with active transcription. Representative experiments evaluating H3K4Me3 and AcH3 deposition pre- and 6 hours post-induction are shown in Figure 5.13.A. and B respectively. As expected, significant levels of H3K4Me3 and AcH3 were detected at the promoter in the absence and presence of EKLF. Interestingly, no significant increase in the global levels of histone modification was detected at 6 hours of induction However, we reported previously that EKLF binding induced a rapid and dramatic decrease in nucleosomal density at the promoter. Correcting the measured levels of histone modification to the detected levels of H3, we demonstrate that EKLF binding at the active ALAD promoter resulted in the increased occupancy of H3K4Me3- and AcH3-modified histones (Figure 5.13.C. and D. respectively).

To explore further the relationship between EKLF mobilization and the increase in modified H3, we applied the ChIP assay to kinetic studies. ChIP analysis at several time points of induction using antibodies against H3K4Me3 and AcH3 are represented in Figure 5.13.E. and F. respectively. Interestingly, extremely distinct kinetics of histone mark deposition for H3K4Me3 and AcH3 were detected. The measured increase in H3K4Me3 was not detected up to 2 hours into treatment and the subsequent increase did not reach a plateau. In contrast, the kinetics of AcH3 at the ALAD promoter revealed that AcH3 deposition is coupled to EKLF binding.

Our data indicate that AcH3 precedes H3K4Me3 deposition at the ALAD promoter. In addition, the coincident increase of AcH3 and EKLF binding indicates that EKLF directly modulates the acetylation of H3 at the active ALAD promoter.

EKLF-dependent recruitment of CBP and enhanced mobilization of p300 at the active ALAD promoter

EKLF is known to interact *in vitro* with three HATs, namely CBP, p300 and P/CAF (*59, 64-65*). GATA-1 interacts with CBP and modulates the recruitment of CBP at GATA-1 target genes

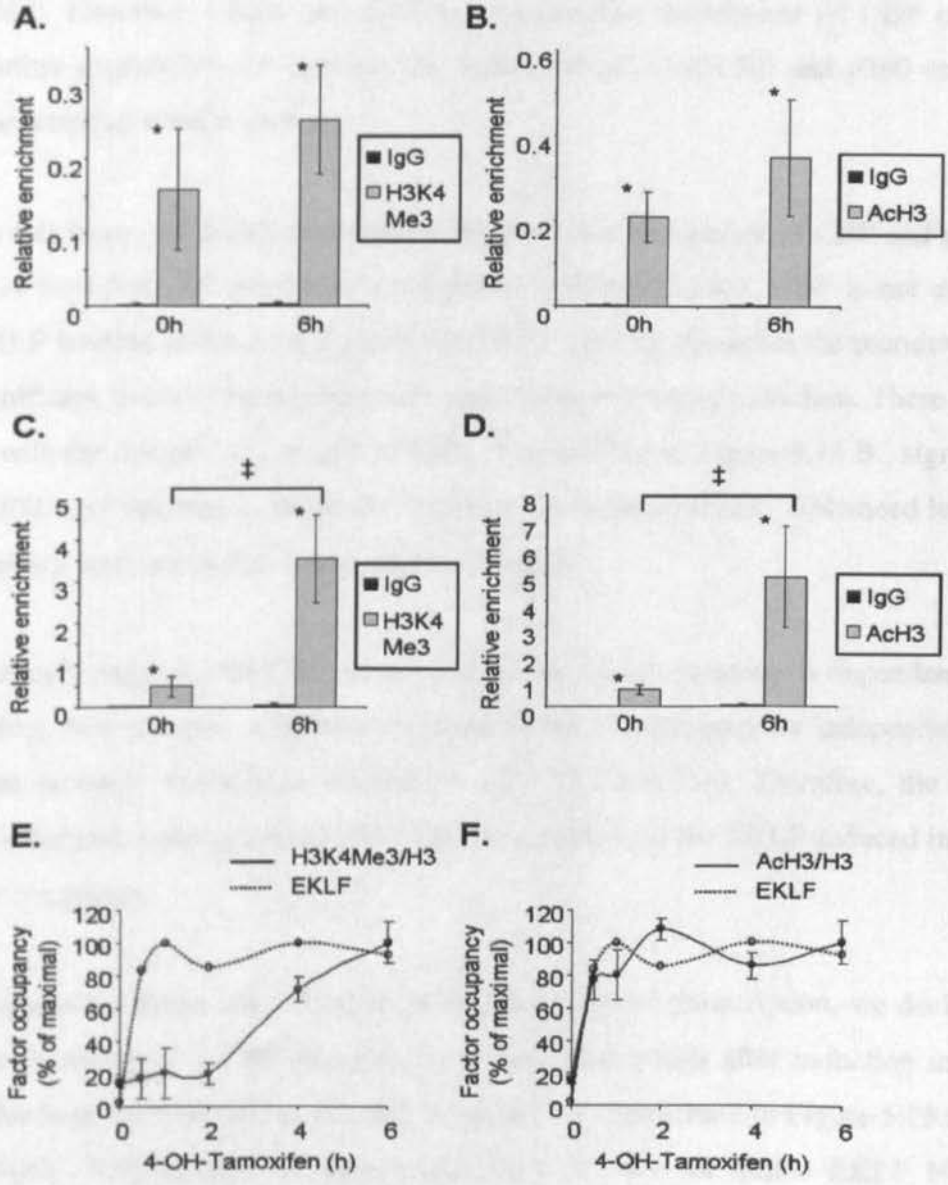

Figure 5.13. Histone modifications at the ALAD erythroid promoter in JH31 cells. H3K4Me3 and AcH3 occupancy was determined by ChIP analysis using an antibody raised against H3K4Me3 or panAcH3. Relative enrichment of (A) H3K4Me3 (C) corrected to H3 density and (B) AcH3 (D) corrected to H3 density prior to and 6 hrs post 4-OH-TAM treatment of JH31 cells corrected to input. * p value<0.05 between IgG and corresponding sample. ‡ p value<0.05 between 0h and 6hr. Kinetics of recruitment of (E) H3K4Me3 per H3 and (F) AcH3 per H3 corrected to overall maximal signal intensity at 0, 0.5, 1, 2 and 6 hrs post treatment of JH31 cells with 4-OH-TAM. The broken line represents binding of EKLF for comparison. •p value< 0.05. Data shown represents the average of at least 2 independent experiments (mean ± SEM).

(*52, 263-264*). However, EKLF and GATA-1 preferential recruitment of CBP or p300 requires further exploration. In addition, the individual roles of CBP and p300 in EKLF directed transcription remain unclear.

To address this issue, we decided to monitor the promoter occupancy of CBP and p300 at the GATA-1 bound ALAD promoter. As depicted in Figure 5.14.A, CBP is not detected prior to EKLF binding at the ALAD promoter. EKLF binding promotes the recruitment of CBP as significant levels of enrichment were detected at 6 hours of induction. These results contrasted with the detected occupancy of p300. As described in Figure 5.14.B., significant levels of p300 were detected at the ALAD promoter in uninduced cells. Enhanced levels in p300 occupancy were measured at 6 hours of induction.

Our data strongly suggests that CBP recruitment to the ALAD promoter is dependent upon EKLF binding. Interestingly, p300 was recruited to the ALAD promoter independently of EKLF, most probably through its interaction with GATA-1(*265*). Therefore, the EKLF modulated enhanced mobilization of p300 may be reflective of the EKLF-induced increase in GATA-1 occupancy.

To further assess the direct role of EKLF in ALAD-enhanced transcription, we decided to monitor the recruitment of CBP and p300 at several time points after induction in JH31 cells. Results from the CBP and p300 ChIP analyses are represented in Figure 5.15.A. and B., respectively. Surprisingly, the mobilization of CBP did not mimic EKLF binding, suggesting that the recruitment of CBP is an event independent of EKLF binding. The delay in CBP recruitment was most significant 30 minutes into treatment. Interestingly, p300 mobilization at the ALAD promoter coincided with EKLF binding. Therefore our data clearly indicates contrasting recruitment mechanisms for CBP and p300. We hypothesize that additional events are required for the mobilization of CBP to the promoter.

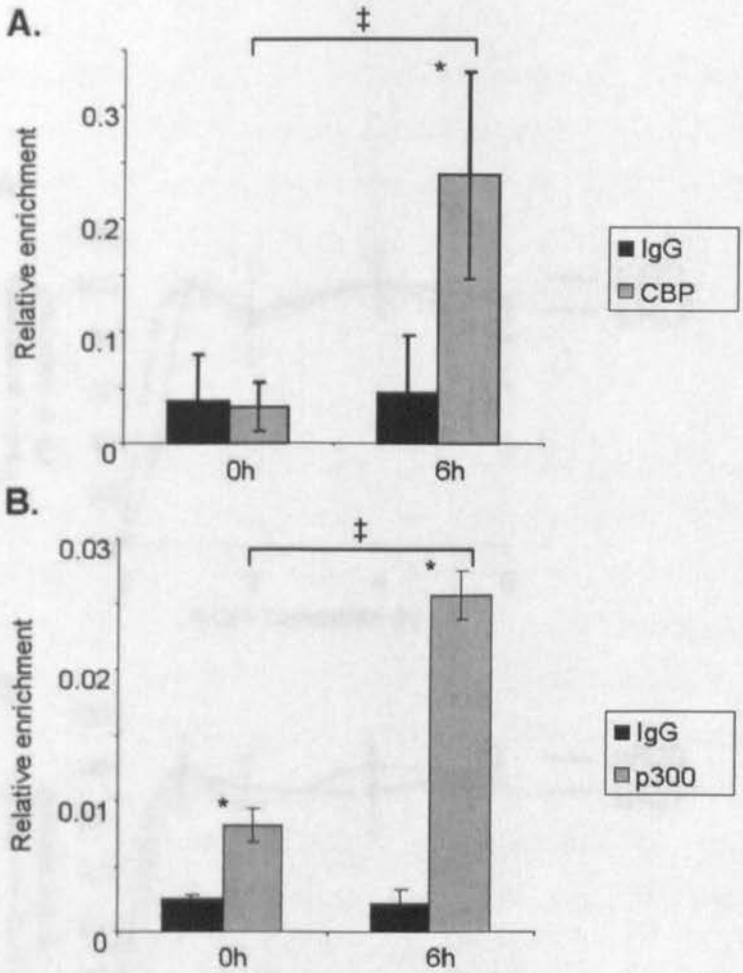

Figure 5.14. HAT occupancy of the ALAD erythroid promoter in JH31 cells. CBP and p300 binding determined by ChIP analysis using an antibody rose against CBP or p300. Relative enrichment of (A). CBP and (B) p300 prior to and 6 hrs post 4-OH-TAM induction of JH31 cells corrected to input. * p value<0.05 between IgG and corresponding sample. ‡ p value<0.05 between 0h and 6hr. Data shown represents the average of at least 3 independent experiments (mean ± SEM).

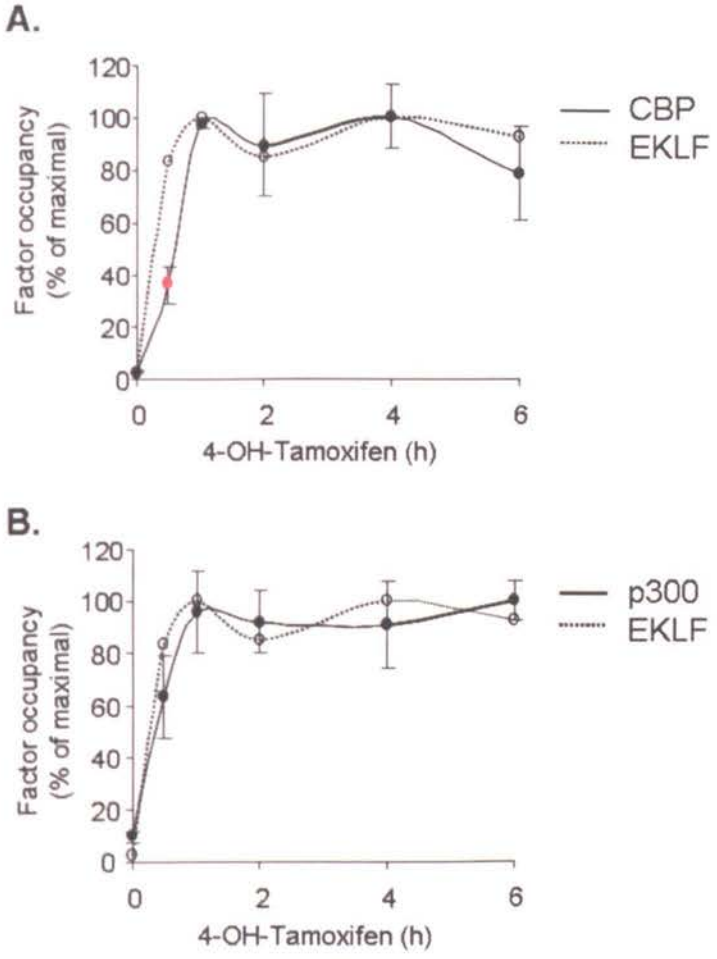

Figure 5.15. Kinetics of HAT recruitment at the ALAD erythroid promoter in JH31 cells. CBP and p300 occupancy was determined by ChIP analysis using an antibody raised against CBP and p300. Kinetics of recruitment of (A) CBP and (B) p300 corrected to overall maximal signal intensity at 0, 0.5, 1, 2 and 6 hrs post treatment of JH31 cells with 4-OH-TAM. The broken line represents binding of EKLF for comparison. •p value< 0.05. Data shown represents the average of at least 3 independent experiments (mean ± SEM).

EKLF-directed enhanced recruitment of the transcription machinery at the ALAD promoter

As mentioned previously, low levels of ALAD transcripts are detectable in EKLF-null cells. Therefore, EKLF is not essential to basal transcription of the ALAD gene. This observation contrasts with the absolute requirement for EKLF in the transcriptional activation of the β-globin, AHSP and Dematin genes (see chapter 3 and 4) (*151-152*). Therefore, we decided to explore the mechanisms by which EKLF can enhance the transcription of already active genes.

Transcription, by definition, is entirely dependent upon the presence and activity of the transcription machinery. We hypothesized that similarly to the β-globin, AHSP and Dematin genes, EKLF induces the recruitment of RNA Pol-II at the ALAD promoter. To assess the relative amounts of RNA Pol-II bound at the ALAD promoter in the absence and presence of EKLF, we performed RNA-Pol-II ChIP analysis in 4-OH-Tamoxifen induced cells and ethanol control cells. As depicted in Figure 5.16.A, significant enrichment of the promoter was detected in ethanol-treated cells, consistent with active transcription. Interestingly, RNA Pol-II occupancy increased significantly by 6 hours post-induction. Our data demonstrates that EKLF binding induces an increase in RNA Pol-II density at the promoter, thereby increasing ALAD transcription.

The activity state of the RNA Pol-II can dictate the rate of transcription. A change in the phosphorylation status of the CTD of RNA Pol-II from Ser5 to Ser2 coincides with transcription elongation. In order to evaluate the impact of EKLF binding on the phosphorylation status of the CTD of RNA Pol-II, we monitored the relative occupancy of Ser5 Pol-II at the ALAD promoter pre- and post-induction. Depicted in Figure 5.16.B., our results demonstrated significant occupancy of the activated form of Pol-II prior to induction. EKLF binding promoted a significant increase in occupancy of Ser5 Pol-II at the promoter.

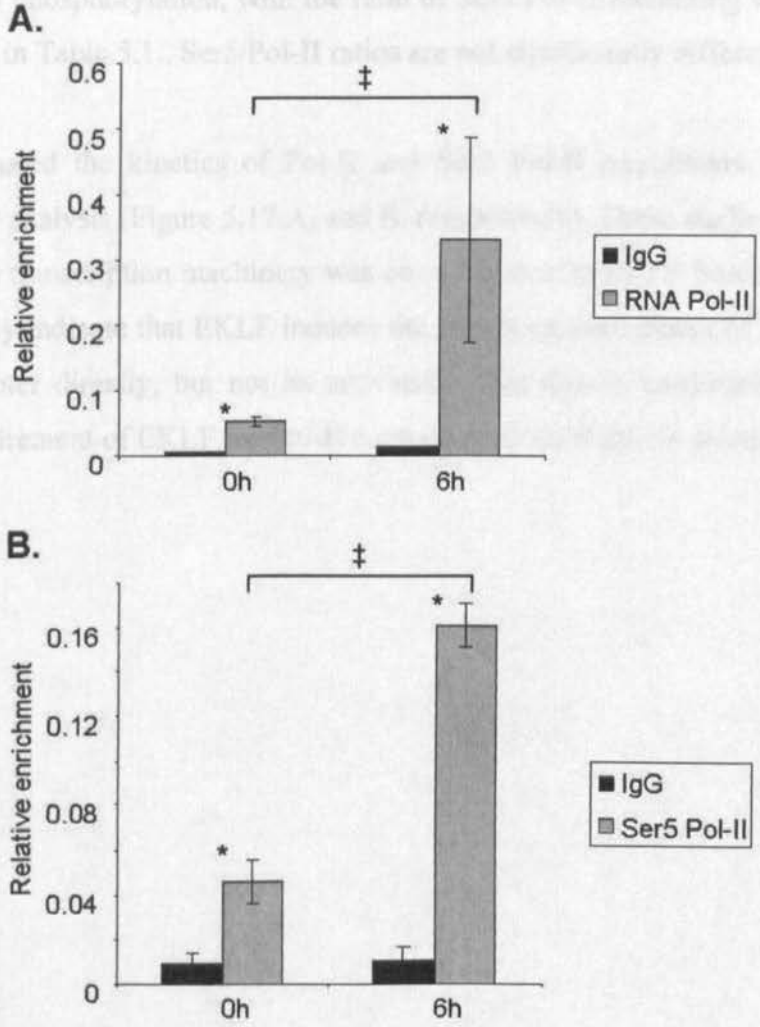

Figure 5.16. RNA Pol-II and Ser5 pol-II occupancy of the ALAD erythroid promoter in JH31 cells. RNA Pol-II and Ser5 Pol-II binding determined by ChIP analysis using an antibody rose against RNA Pol-II CTD or Ser5 Pol-II. Relative enrichment of (A). RNA Pol-II and (B) Ser5 Pol-II prior to and 6 hrs post 4-OH-TAM induction of JH31 cells corrected to input. * p value<0.05 between IgG and corresponding sample. ‡ p value<0.05 between 0h and 6hr. Data shown represents the average of at least 3 independent experiments (mean ± SEM).

One scenario to consider is that EKLF induces a significant activation of Pol-II, as measured by Ser5 phosphorylation, with the ratio of Ser5/Pol-II increasing with induction. However, as seen in Table 5.1., Ser5/Pol-II ratios are not significantly different.

Finally, we evaluated the kinetics of Pol-II and Ser5 Pol-II recruitment at the ALAD promoter by ChIP analysis (Figure 5.17.A. and B. respectively). These studies revealed that recruitment of the transcription machinery was co-incident with EKLF binding. Therefore, our results strongly indicate that EKLF induces the enhanced recruitment of RNA Pol-II at the ALAD promoter directly, but not its activation. Our data is consistent with studies reporting the requirement of EKLF for Pol-II occupancy at the β-globin promoter (*65*).

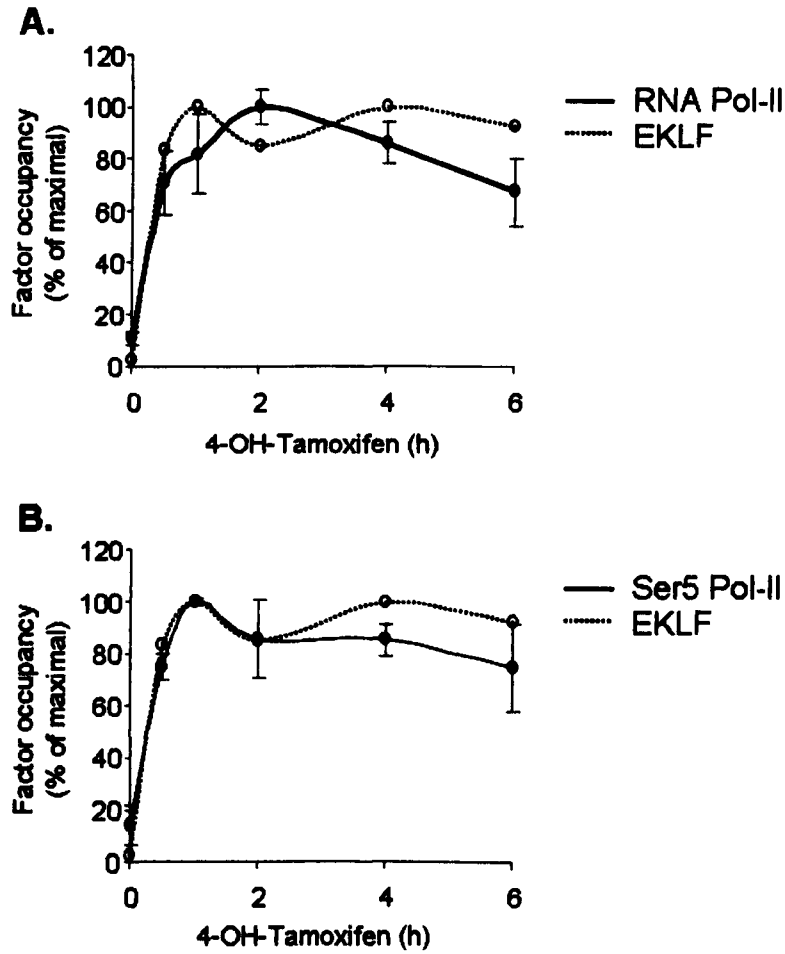

Figure 5.17. Kinetics of RNA Pol-II and Ser5 Pol-II recruitment at the ALAD erythroid promoter in JH31 cells. RNA Pol-II and Ser5 Pol-II binding determined by ChIP analysis using an antibody raised against RNA Pol-II CTD and Ser5 Pol-II. Kinetics of recruitment of (A). RNA Pol-II or (B) Ser5 Pol-II corrected to overall maximal signal intensity at 0, 0.5, 1, 2 and 6 hrs post treatment of JH31 cells with 4-OH-TAM. The broken line represents binding of EKLF for comparison. Data shown represents the average of at least 3 independent experiments (mean ± SEM).

DISCUSSION

EKLF is involved in the regulation of the Heme Biosynthesis pathway

A role for EKLF in the regulation of the genes encoding the first two to four enzymes of the heme biosynthesis pathway was suggested in previous studies (*151-152*). Fetal liver erythroblasts of EKLF-null mice display low levels of mRNA for ALAS2, ALAD, PBGD and UROD. However, culture of EKLF null erythroid progenitors revealed that only the expression of ALAS2 and ALAD is significantly affected by the ablation of EKLF. Although these studies made compelling statements about the potential role of EKLF in the regulation of the heme biosynthesis pathway, no further studies have been reported to date.

In the presented work, we explore the impact of EKLF expression on the transcription of these first four heme pathway enzymes. Taking advantage of our inducible cell system, we monitored the levels of gene expression upon EKLF translocalization to the nucleus. We demonstrated that EKLF significantly induces an increase in ALAD mRNA levels by enhancing the transcriptional rate of the ALAD gene. Our studies determined that EKLF binds to the erythroid promoter of the ALAD gene *in vitro* and *in vivo*.

Because transcription of the ALAD gene does not truly require EKLF, we demonstrated that EKLF acts as an enhancing factor. Intriguingly, primary transcript levels decreased after reaching a peak on induction. The decrease in the transcriptional rate did not correlate with the persistent EKLF promoter occupancy or the stable levels of mRNA. Therefore, ALAD expression is regulated at the transcriptional levels by both activating as well as repressing mechanisms. This observation emphasizes on the complexity of the regulatory mechanisms of the heme biosynthesis pathway. In addition, because actively stabilized mRNA levels were 2.5 fold greater than levels in uninduced cells, we conclude that ALAD deficiency in EKLF null erythrocytes contributes to the anemic phenotype. Although it is currently unclear what the role ALAD plays in this phenotype, it is interesting to note that it has been implicated in the regulation of proteosome metabolism, suggesting a critical function in degradative processes in the differentiating erythroblast (*266*).

The role of EKLF as a co-factor involves enhanced factor recruitment

EKLF has been shown to be a critical factor at all genes of the α- and β-globin gene loci. In the case of the α- and γ-globin genes, it functions to enhance rather than establish transcriptional initiation (*246-247*). Additional studies at similar non-globin EKLF-responsive genes have not been initiated to date, leaving a gap in our understanding of EKLF in the regulation of the erythroid program. In the present study, to gain further knowledge into the basic mode of action of EKLF we sought to determine the molecular events triggered by EKLF in this context. Using our EKLF-inducible cell system, we monitored the recruitment of the transcription machinery, transcription factors and co-factors known to participate in EKLF-directed transcriptional activation. Our data strongly indicates that the EKLF-induced events are similar whether EKLF is essential for gene transcription or partially required.

These common events include the coupled enhanced recruitment of the transcription machinery but not the activation of RNA Pol-II. In addition, optimal recruitment of the well characterized transcription factor GATA-1, the SCL/TAL1 complex member Ldb-1 as well as the HAT p300 is coincident with EKLF binding. EKLF is known to physically interact with GATA-1 and p300; however the mechanism by which RNA Pol-II in addition to Ldb-1, and thus SCL/TAL-1, is recruited may require further investigation.

Surprisingly, NF-E2 promoter occupancy was strictly dependent upon EKLF binding. Our data suggest that low levels of GATA-1-SCL/TAL-1-Ldb-1 complex promoter occupancy are insufficient to induce the recruitment of NF-E2. Intriguingly, NF-E2 mobilization was not coupled to EKLF binding. Therefore, our data indicates that the mobilization of NF-E2 at the activated ALAD promoter necessitates additional events sequential to EKLF binding. The functional relevance of NF-E2 recruitment in the transcriptional regulation of the ALAD gene as yet to be determined.

Interestingly, although strictly dependent upon EKLF binding, the mobilization of CBP and Brg1 do not occur with the same tempo as EKLF binding. Again, our data suggests a) these

factors do not initiate chromatin modifications, and b) may be required for stabilization of the open chromatin structure induced by EKLF binding.

EKLF enhances structural and covalent modifications of the chromatin.

EKLF has been extensively studied as an inducer of chromatin remodeling at the β-globin locus (*47, 162*). However, there is no evidence to suggest that EKLF modulates structural changes of chromatin at already active genes. Exploring this problem, we determined that, in JH31 cells, EKLF binding induces a moderate increase in the sensitivity to DNaseI digestion of the already hypersensitive promoter. Surprisingly, these results did not correlate with results from similar studies in EKLF-null fetal livers. In EKLF null mice, the erythroid specific promoter is resistant to DNaseI digestion. This observation is contradictory with expression studies. However, these results can be explained as EKLF-null fetal livers contain a majority of hepatocytes in which the erythroid-specific promoter is not active. Therefore, the DNaseI hypersensitivity results from EKLF-null fetal livers most probably represented the status of the erythroid specific promoter in fetal hepatocytes as opposed to erythroid cells.

In order to confirm the DNaseI data, we monitored the nucleosome density at the erythroid specific ALAD promoter in JH31 cells. We demonstrate that EKLF binding induces a rapid coincidental decrease in H3 occupancy at the promoter, indicating that EKLF binding results in the structural reconfiguration of the promoter. Therefore, we conclude that de novo EKLF binding promotes differing chromatin remodeling events at silenced versus already active genes.

Most of the studies of EKLF chromatin remodeling properties revolve around its physical interaction with the SWI/SNF subunit Brg1 (*59, 63, 148, 262*). One particular study explored the role of EKLF as a co-factor of γ-globin gene activation (*246*). These studies suggested that promoter occupancy by EKLF was required for efficient loading of Brg1 to the γ-promoter (*246*). Although these studies strongly hinted towards the direct recruitment of Brg1 via its interaction with EKLF, they presented major flaws. These studies failed to assess the protein levels of critical regulators of γ-globin expression. The Brg1 paralog Brm

is not expressed in erythroid cells (*143*). In addition, the SWI/SNF complex is involved in the transcription of a multitude of genes. Therefore, it is likely that the non activation of the γ-promoter in cells expressing extremely low levels of Brg1 was the consequence of the down-regulated expression of essential γ-globin inducers. Potential factors would include GATA-1 which successfully co-immunoprecipitates with Brg1 (*143*).

Taking advantage of our inducible cell system, we decided to further investigate the role of Brg1 in EKLF-directed chromatin remodeling. Surprisingly, we demonstrate that the EKLF-dependent recruitment of Brg1 contradicts the kinetics of H3 loss. The mobilization of Brg1 was detected as a subsequent event of EKLF binding and H3 eviction. Therefore, it is highly unlikely that Brg1 was involved in the reported H3 eviction. In addition, we demonstrate that Brg1 mobilization to the promoter requires additional events to EKLF binding. Our studies significantly deepen the knowledge of the mechanism of action of EKLF at already active genes. This factor induces similar events to those reported when EKLF acts as a transcription factor at silent genes including the recruitment of the transcription machinery, the transcription factor GATA-1 and NF-E2 in addition to the co-factors CBP, p300 and Brg1. We demonstrated that EKLF binding increases the accessibility of the promoter to DNA binding factors via eviction of H3. In addition, we determine that EKLF directly modulates the transcription rate of ALAD, rendering this study the first report of the direct involvement of EKLF in the regulation of the heme biosynthesis pathway.

-CHAPTER 6-

SUMMARY AND GENERAL DISCUSSION

Throughout the presented studies, we sought to determine the true role of EKLF at target *cis*-regulatory regions. Taking advantage of our EKLF-inducible erythroblast cell line system, we determined the role of this factor in modifying the chromatin architecture of target genes, its interaction with a variety of known interacting proteins, and the kinetics of recruitment of erythroid transcription factor and basal transcription machinery complex at 6 EKLF-dependent regulatory elements.

The combination of studies of molecular events across the β-globin locus, the downstream AHSP promoter, in addition to the erythroid specific Dematin and ALAD promoters uncovered a series of common elements of EKLF-mediated transactivation. These events include the recruitment of GATA-1, Ldb-1 and NF-E2 along with the mobilization of the known EKLF co-binding partners CBP, p300 and Brg1. In addition, EKLF binding promotes an increase in RNA Pol-II occupancy at each studied promoter as well as structural and covalent modifications of the chromatin that are associated with active transcription.

We have determined that at the β-globin locus, EKLF and associated factors are recruited preferentially to the β-globin LCR, suggesting that the LCR serves as a docking element for transcription factors and co-factors in addition to RNA Pol-II. Importantly, we determined that the recruitment of Ldb-1 constitutes the first event at the β-promoter upon EKLF translocalization to the nucleus.

Most importantly, the combined kinetic analyses of EKLF-directed transcriptional events allowed us to distinguish between EKLF-coupled and sequential events. Interestingly, with the exception of Ldb-1 at the β-globin promoter, GATA-1, Ldb-1 and p300 mobilization is coupled to EKLF binding at each target element. Therefore, we have defined the prevalent mode of action of EKLF which is not influenced by the chromatin context or EKLF's own degree of influence on the transcription of the target gene.

We describe a previously unreported mechanism of EKLF-directed chromatin remodeling which does not directly involve the SWI/SNF complex. Although EKLF

induces chromatin remodeling events at each target gene promoter, context-dependent EKLF coupled H3 eviction contrasts with the sequential recruitment of Brg1. Furthermore, our studies unveiled distinct mechanisms in the mobilization of the closely related CBP and p300 histone acetyl transferases at EKLF target regions. The recruitment of CBP is subsequent to EKLF binding and correlates with Brg1 mobilization at each target promoter.

In addition, our work reveal that the deposition of histone modifications commonly associated with activated genes is subsequent to transcriptional activation and does not coincide with a transcriptional plateau.

In summary, our studies led to the discovery of several novel aspects of EKLF-directed transcription. These new findings not only increase our knowledge of EKLF role and function but further broaden conservative notions of basic transcriptional events.

Further insights into the regulation of the β–globin gene transcription

Our studies demonstrate the EKLF-coupled nature of the mobilization and enhanced recruitment of the GATA-1 and SCL/TAL-1 complexes. It remains difficult to distinguish specifically between GATA-1- and EKLF-directed events. EKLF has been postulated to have at least three separate functions *in vivo*. Studies from our group, described in Chapter 3, and others have shown that GATA-1 is found at the HS3 and HS2 in the absence of EKLF (*61*). In addition, we detect GATA-1 at the ALAD gene in the absence of EKLF (see Chapter 5). However, we demonstrate a significant increase in promoter- and enhancer-bound GATA-1 coincident with EKLF binding. Importantly, we measured significant changes in the configuration of the chromatin upon EKLF binding. These observations correlate with the general hypothesis of EKLF action that binding promotes structural changes of chromatin resulting in increased DNA accessibility to tissue-specific and general transcription factors.

The laboratory has recently developed a tool that if used appropriately would allow us to partially address this issue. The Δ221 EKLF mutant is a truncated form of EKLF that

retains chromatin remodeling and DNA binding capabilities, reside in the carboxyl terminal amino acids 221-376, but has no transactivation activity (aa 1-220)(*148*).The development of Δ221 knock-in mice, and stable cell lines, will allow us to dissect the relevance of chromatin remodeling in factor recruitment across the β-globin locus. The proposed studies would allow us to assess directly the impact of EKLF-directed chromatin remodeling and may provide an ideal system to separate EKLF- from GATA-1-directed events.

This information is critical to the understanding of not only promoter events but also the mechanisms of long distance communication between enhancers and promoters. The manner in which communication is established between the LCR and globin gene promoters is not yet fully understood. Suggested mechanisms include linking (*267*) , tracking (*195*), looping (*268*) and combinations of any of the three (*201, 269*).

To date there is compelling evidence favoring the looping hypothesis. The establishment of the Chromosome Conformation Capture assay, or 3C, has allowed the evaluation of the physical proximity between *cis*-elements (*205*). The technique was developed in erythroid cells and detected the clustering of the HSs of the LCR with the active globin gene promoter. The assay has since then been applied to other loci containing cell-type specific HSs and revealed that clustering of *cis*-elements over large distances is not restricted to the β-globin gene locus (*270-272*). Additional evidence for the critical role of *cis*-element clustering at the β-globin locus derived from studies in GATA-1 as well as EKLF depleted erythroid cells. EKLF is required for proper formation of the active chromatin hub (ACH) (*150*) as well as GATA-1 (*273*), adding to their multiple coincident roles in globin gene regulation. Non DNA-binding factors have also been involved in promoting/maintaining ACH formation and include FOG-1 (*273*) and Ldb1 (*122*). It is likely that "looping" at the β-globin gene locus requires some form of linking. Using the work presented in Chapter 3 as a foundation, we propose to dissect the role of EKLF at the β-promoter and at the enhancer in the absence of ACH formation.

We reported in our studies that the monitored events at the β-major promoter are synchronized with EKLF binding with the exception of the early occupancy of Ldb-1. A homodimerization defective mutant of Ldb-1 has been reported recently to prevent the "looping" between the enhancer and the promoter of the protein 4.2 gene (*213*). In these same studies, protein 4.2 expression decreased with enforced Ldb-1 expression, indicating that high amounts of Ldb-1 triggers a quenching effect, thereby disrupting the communication between the enhancer of the promoter.

Therefore, we propose Ldb-1 as an ideal target to disrupt ACH formation at the β-globin promoter. This strategy will be used towards the investigation of the distinct roles of EKLF at the LCR and the β-globin promoter in the absence of LCR: promoter communication. This study will also assess our hypothesis that the LCR serves as a partially EKLF-dependent docking element for sequence-specific transcription factors and co-factors, in addition to the already established transcription machinery.

EKLF and GATA-1-SCL/TAL-1-LMO2-Ldb-1 complex anchoring at target *cis*-regulatory elements.

GATA-1 and EKLF induce the maturation of erythrocytes in 4-OH-Tamoxifen inducible cell lines (*111, 155*). Recent unpublished studies combined EKLF ChIP-seq analysis, using an mouse expressing the HA-tagged full-length EKLF, with microarray profiles from inducible GATA-1 ER cells (G1E)(*173*). The mentioned studies utilized G1E cells as a guide of differential gene expression in maturating erythroid cells and linked EKLF to the active expression of genes controlling the cell cycle as well as Stat3 and Bcl-XL.

However, these studies failed to associate EKLF occupancy directly with GATA-1 induced gene activation and repression. Given that EKLF cooperates synergistically with GATA-1 to induce expression of a reporter gene *in vitro* (*274*), and that we demonstrated the EKLF-dependent optimal mobilization of the GATA-1-SCL/TAL-1 complex at each studied target, it would be interesting to compare and contrast DNA binding profiles from ChIP-seq analysis of EKLF and GATA-1. Such analysis would allow us to determine whether EKLF co-occupies with GATA-1 at each activated developmental specific gene

and whether all EKLF target genes share dependency for both factors. We propose the attractive hypothesis that EKLF represents the developmental counterpart of GATA-1 complexes in GATA-1 dependent transcription. EKLF has also been implicated in transcriptional repression (*275-277*). However, little is known about EKLF-repressed genes. The proposed studies would be extremely useful in the identification of those genes in erythroid cells as well as to assess the EKLF and GATA-1 cooperation in gene repression.

In addition to the downregulation of genes encoding components of the hemoglobin heteromeric complex, EKLF-null mice display severe defects in the expression of erythroid membrane genes. Parallel studies using the data from ChIP-seq analysis would help identify the role of EKLF in the expression of membrane proteins. Expression of Ankyrin, β-spectrin, AE1 and ADD2 is limited in EKLF null cells (*152*). However, the erythroid promoter of Ankyrin and β-spectrin proves to be fully active in the absence of EKLF and does not bind EKLF (*221, 278-279*). EKLF is required to establish the clustering of the β-globin promoter and the LCR (*150*). Recent work at the large *CFTR* gene locus implicates intronic enhancers in the looping of *cis*-regulatory elements (*280*). Membrane protein genes are often composed of multiple exons spread over long distances. Studies have suggested the presence of an EKLF-dependent intronic enhancer at the Dematin gene in addition to multiple conserved stretches of intronic sequence containing CACC boxes (*151*). Preliminary studies in our laboratory further support a role of EKLF at this intronic enhancer. We propose to evaluate the role of EKLF at intronic enhancers of large genes encoding membrane-associated proteins.

Distinct roles of the closely related HAT proteins CBP and p300 in erythroid cells

Our data clearly demonstrates that CBP and Brg1 recruitment is sequential to EKLF binding at all three promoters studied outside of the β-globin locus. Studies suggest that acetylation of lysine 288 of EKLF increases its affinity for CBP and Brg1 in vitro (*65*). It is therefore plausible that the observed delay in the mobilization of CBP and Brg1 reflects the acetylation status of EKLF. Mice homozygous for mutations in the KIX domain of p300 display defects in hematopoiesis which include anemia (*235*).

Throughout our studies, we demonstrate that p300 is recruited simultaneously with EKLF at target gene promoters. We propose that acetylation of EKLF by p300 is the rate limiting factor in the recruitment of CBP and Brg-1 and that the recruitment of p300 to EKLF target genes involves its KIX domain. Further exploration into the role of p300 in EKLF-directed transcription is required. This work would include the identification of the domains of p300 responsible for its interaction with EKLF and GATA-1. We expect that the down regulation of p300 protein levels by shRNA strategies would disrupt EKLF-directed transcription at a majority of target genes.

A novel mechanism of EKLF-directed chromatin remodeling

The physical interaction of EKLF with the SWI/SNF catalytic subunit Brg1 has long been established (*59, 63*). SWI/SNF nucleosomal remodeling at the human β-globin promoter *in vitro* requires the presence of EKLF as well as an intact HS2 element (*63, 262*). Our studies extended these findings and revealed the EKLF-coupled nature of the recruitment of Brg1 at the β-globin promoter.

However, the investigation into the role of EKLF at loci devoid of a long distance enhancer led to the novel finding of an apparent Brg1-independent EKLF-directed H3 eviction at target promoters. To further validate our findings, we need to establish that the process of elongation is not responsible for the detected H3 eviction at target gene promoters. Preliminary data indicates that H3 eviction is not detected at transcribed regions of the Dematin gene. We propose to monitor EKLF-binding and the associated H3 eviction in JH31 cells treated with the elongation inhibitor 5,6-dichloro-1-β-D-ribofuranosylbenzimidazole (DRB). DRB is an inhibitor of the CDK7 TFIIH-associated kinases, CKI and CKII, which are required for the phosphorylation of RNA Pol-II at the Ser5 residue of its CTD (*281-283*). Therefore, blocking the early stages of elongation prior to EKLF-translocalization, we expect to detect H3 eviction upon EKLF binding at the Dematin promoter. Because H3 eviction is maximal within the first 30 minutes of induction of JH31 cells with 4-OH-Tamoxifen, we do not expect its requirement for *de novo* synthesis of auxiliary proteins.

To further verify our hypothesis that the EKLF-induced chromatin remodeling does not involve Brg1 at target genes located outside of the β-globin locus, we propose to use shRNA strategies to abrogate the protein expression of Brg1. We predict that binding of EKLF to target gene promoters will result in H3 eviction in the absence of Brg1. Preliminary data indicates that efficient transfection of shBrg1 constructs leads to cell death. Using the green fluorescent protein to monitor the transfection and transduction efficiency, we were not able to recover a sufficient amount of cells to carry out experiments. The amount of GFP positive cells following shBrg1 transductions was significantly reduced within 24 hours post transduction when compared with vector control cells.

To address this technical issue, we are currently evaluating a catalytic mutant of Brg1 in the JH31 system. Brg-1 null mice succumb at a peri-implantation stage of development (*284*). However, mice homozygous for a mutation in the catalytic core of Brg1, develop further and die at mid-gestation suggesting that chromatin remodeling is not the sole role of Brg1 (*47*). The mutated protein assembles in SWI/SNF complexes and maintains full ATPase activity but its nucleosomal remodeling property is severely impeded. The Brg1 mutant mice display severe anemia and a dramatic decrease in β-globin expression due to inefficient chromatin remodeling at the β-globin LCR. These results are consistent with previous studies implicating the chromatin remodeling role Brg1 in the expression of the β-globin gene (*59, 63, 262*). Studies in Brg1 mutant mice failed to evaluate the expression as well as the promoter accessibility of additional EKLF target genes.

To directly assess the chromatin status of EKLF target genes in the Brg1 mutant mice, we will determine the function of Brg1 at target genes that are remodeled by alternate mechanisms. Our preliminary observations suggest that Brg1 travels with elongating RNA Pol-II, a result consistent with that of others (*57, 285*). Indeed both Brg1 and its paralog Brm may regulate the transcriptional rate through interactions with the spliceosome (*56, 58, 229*). Thus, our studies suggest that Brg1 has a role in transcription elongation control and/or splicing events, independent of nucleosomal remodeling.

The mechanisms of EKLF-directed H3 eviction, identified by us for the first time, need to be elucidated. As demonstrated throughout this work, GATA-1 recruitment to EKLF target gene is coupled to EKLF binding. Therefore, it is likely that the chromatin remodeling factors responsible for EKLF-directed histone eviction co-purify with EKLF-GATA-1 complexes. The purification of GATA-1 complexes in erythroid cells demonstrated that GATA-1 co-purifies with the chromatin remodeling proteins snf2h and ACF1 (*286*). Therefore, it is reasonable to assess their individual interaction with EKLF.

The Potential role of EKLF in the nuclear localization of target loci.

Recent studies in erythroid cells have focused on the localization of active genes within the nucleus. The detection of hyperphosphorylated RNA Pol-II nuclear foci has raised the notion of transcription nodes or 'factories' (*287-288*). The formation of such structures depends upon transcription initiation, but their maintenance does not require active transcription (*289*). Active tissue –restricted genes in erythroid cells preferentially share transcription factories containing specific transcription factors (*228*). These studies highlight the potential role of EKLF in mediating such preferential associated interactions, but EKLF mechanism of action in this process remains unclear.

In the aforementioned study, the Hbb and Hba genes were used as reference anchors of factory association. The β- and α- globin locus are regulated by well-defined upstream enhancers. In addition, the β-globin LCR is required for the association of the locus to transcription factories (*290*). We report in Chapter 3 the EKLF-independent nature of Pol-II, and more particularly Ser5 Pol-II occupancy at the LCR. Our data correlates with and extends findings in GATA-1 ER cells, where LCR Pol-II occupancy is demonstrated to be unperturbed by the combined absence of GATA-1, FOG-1 and EKLF (*61*). Therefore, the LCR element appears to be a principal determinant in the establishment of, or localization of the locus in, Pol-II factories.

All evidence suggests a need for further investigation into the role of EKLF at enhancer elements in order to truly assess the mechanisms behind the EKLF-mediated multi-gene assignment to EKLF-Pol-II factories. We propose that EKLF-mediated factor recruitment

to, or remodeling of, the LCR alone is sufficient to trigger the preferential sharing of erythroid genes in nuclear structures containing high concentrations of RNA Pol-II, HATs and chromatin remodelers.

-REFERENCES-

1. Orkin, S. H. (2000) Diversification of haematopoietic stem cells to specific lineages, *Nat Rev Genet 1*, 57-64.
2. Orkin, S. H., and Zon, L. I. (2008) Hematopoiesis: an evolving paradigm for stem cell biology, *Cell 132*, 631-644.
3. Lemoli, R. M., Fortuna, A., Fogli, M., Motta, M. R., Rizzi, S., Benini, C., and Tura, S. (1994) Stem cell factor (c-kit ligand) enhances the interleukin-9-dependent proliferation of human CD34+ and CD34+CD33-DR- cells, *Exp Hematol 22*, 919-923.
4. Muta, K., Krantz, S. B., Bondurant, M. C., and Wickrema, A. (1994) Distinct roles of erythropoietin, insulin-like growth factor I, and stem cell factor in the development of erythroid progenitor cells, *J Clin Invest 94*, 34-43.
5. Panzenbock, B., Bartunek, P., Mapara, M. Y., and Zenke, M. (1998) Growth and differentiation of human stem cell factor/erythropoietin-dependent erythroid progenitor cells in vitro, *Blood 92*, 3658-3668.
6. Nienhuis, G. S. a. A. W. (1994) Hemoglobin switching: G. Stamatoyannopoulos, A.W. Nienhuis, P.W. Majerus and H. Varmus, Editors,, *The Molecular Basis of Blood Diseases, Philadelphia, PA, Saunders*, p. 107.
7. Dzierzak, E., and Speck, N. A. (2008) Of lineage and legacy: the development of mammalian hematopoietic stem cells, *Nat Immunol 9*, 129-136.
8. Tsiftsoglou, A. S., Vizirianakis, I. S., and Strouboulis, J. (2009) Erythropoiesis: model systems, molecular regulators, and developmental programs, *IUBMB Life 61*, 800-830.
9. McGrath, K. E., Kingsley, P. D., Koniski, A. D., Porter, R. L., Bushnell, T. P., and Palis, J. (2008) Enucleation of primitive erythroid cells generates a transient population of "pyrenocytes" in the mammalian fetus, *Blood 111*, 2409-2417.
10. Palis, J. (2008) Ontogeny of erythropoiesis, *Curr Opin Hematol 15*, 155-161.
11. Mohandas, N., and Evans, E. (1994) Mechanical properties of the red cell membrane in relation to molecular structure and genetic defects, *Annu Rev Biophys Biomol Struct 23*, 787-818.
12. Salomao, M., Zhang, X., Yang, Y., Lee, S., Hartwig, J. H., Chasis, J. A., Mohandas, N., and An, X. (2008) Protein 4.1R-dependent multiprotein complex: new insights into the structural organization of the red blood cell membrane, *Proc Natl Acad Sci U S A 105*, 8026-8031.
13. Derick, L. H., Liu, S. C., Chishti, A. H., and Palek, J. (1992) Protein immunolocalization in the spread erythrocyte membrane skeleton, *Eur J Cell Biol 57*, 317-320.
14. Mohandas, N. (1992) Molecular basis for red cell membrane viscoelastic properties, *Biochem Soc Trans 20*, 776-782.

15. Mohandas, N., and Chasis, J. A. (1993) Red blood cell deformability, membrane material properties and shape: regulation by transmembrane, skeletal and cytosolic proteins and lipids, *Semin Hematol 30*, 171-192.
16. Mathai, J. C., Mori, S., Smith, B. L., Preston, G. M., Mohandas, N., Collins, M., van Zijl, P. C., Zeidel, M. L., and Agre, P. (1996) Functional analysis of aquaporin-1 deficient red cells. The Colton-null phenotype, *J Biol Chem 271*, 1309-1313.
17. Gilligan, D. M., Lozovatsky, L., Gwynn, B., Brugnara, C., Mohandas, N., and Peters, L. L. (1999) Targeted disruption of the beta adducin gene (Add2) causes red blood cell spherocytosis in mice, *Proc Natl Acad Sci U S A 96*, 10717-10722.
18. Peters, L. L., Jindel, H. K., Gwynn, B., Korsgren, C., John, K. M., Lux, S. E., Mohandas, N., Cohen, C. M., Cho, M. R., Golan, D. E., and Brugnara, C. (1999) Mild spherocytosis and altered red cell ion transport in protein 4. 2-null mice, *J Clin Invest 103*, 1527-1537.
19. An, X., and Mohandas, N. (2008) Disorders of red cell membrane, *Br J Haematol 141*, 367-375.
20. Kihm, A. J., Kong, Y., Hong, W., Russell, J. E., Rouda, S., Adachi, K., Simon, M. C., Blobel, G. A., and Weiss, M. J. (2002) An abundant erythroid protein that stabilizes free alpha-haemoglobin, *Nature 417*, 758-763.
21. Mohandas, N., and Gallagher, P. G. (2008) Red cell membrane: past, present, and future, *Blood 112*, 3939-3948.
22. Kong, Y., Zhou, S., Kihm, A. J., Katein, A. M., Yu, X., Gell, D. A., Mackay, J. P., Adachi, K., Foster-Brown, L., Louden, C. S., Gow, A. J., and Weiss, M. J. (2004) Loss of alpha-hemoglobin-stabilizing protein impairs erythropoiesis and exacerbates beta-thalassemia, *J Clin Invest 114*, 1457-1466.
23. Bird, G. W. (1972) The haemoglobinopathies, *Br Med J 1*, 363-368.
24. Bank, A. (2007) AHSP: a novel hemoglobin helper, *J Clin Invest 117*, 1746-1749.
25. Albright, S. R., and Tjian, R. (2000) TAFs revisited: more data reveal new twists and confirm old ideas, *Gene 242*, 1-13.
26. Struhl, K. (1999) Fundamentally different logic of gene regulation in eukaryotes and prokaryotes, *Cell 98*, 1-4.
27. Owen-Hughes, T., and Workman, J. L. (1994) Experimental analysis of chromatin function in transcription control, *Crit Rev Eukaryot Gene Expr 4*, 403-441.
28. Juven-Gershon, T., Hsu, J. Y., and Kadonaga, J. T. (2006) Perspectives on the RNA polymerase II core promoter, *Biochem Soc Trans 34*, 1047-1050.
29. Martin, D. I. (2001) Transcriptional enhancers--on/off gene regulation as an adaptation to silencing in higher eukaryotic nuclei, *Trends Genet 17*, 444-448.
30. Blackwood, E. M., and Kadonaga, J. T. (1998) Going the distance: a current view of enhancer action, *Science 281*, 60-63.
31. Pazin, M. J., Bhargava, P., Geiduschek, E. P., and Kadonaga, J. T. (1997) Nucleosome mobility and the maintenance of nucleosome positioning, *Science 276*, 809-812.
32. Steger, D. J., and Workman, J. L. (1996) Remodeling chromatin structures for transcription: what happens to the histones?, *Bioessays 18*, 875-884.

33. Grosveld, F., Antoniou, M., van Assendelft, G. B., de Boer, E., Hurst, J., Kollias, G., MacFarlane, F., and Wrighton, N. (1987) The regulation of expression of human beta-globin genes, *Prog Clin Biol Res 251*, 133-144.
34. Dillon, N., and Sabbattini, P. (2000) Functional gene expression domains: defining the functional unit of eukaryotic gene regulation, *Bioessays 22*, 657-665.
35. Festenstein, R., Tolaini, M., Corbella, P., Mamalaki, C., Parrington, J., Fox, M., Miliou, A., Jones, M., and Kioussis, D. (1996) Locus control region function and heterochromatin-induced position effect variegation, *Science 271*, 1123-1125.
36. Milot, E., Strouboulis, J., Trimborn, T., Wijgerde, M., de Boer, E., Langeveld, A., Tan-Un, K., Vergeer, W., Yannoutsos, N., Grosveld, F., and Fraser, P. (1996) Heterochromatin effects on the frequency and duration of LCR-mediated gene transcription, *Cell 87*, 105-114.
37. Bonifer, C. (2000) Developmental regulation of eukaryotic gene loci: which cis-regulatory information is required?, *Trends Genet 16*, 310-315.
38. Li, Q., Peterson, K. R., Fang, X., and Stamatoyannopoulos, G. (2002) Locus control regions, *Blood 100*, 3077-3086.
39. Bell, A. C., West, A. G., and Felsenfeld, G. (1999) The protein CTCF is required for the enhancer blocking activity of vertebrate insulators, *Cell 98*, 387-396.
40. Wai, A. W., Gillemans, N., Raguz-Bolognesi, S., Pruzina, S., Zafarana, G., Meijer, D., Philipsen, S., and Grosveld, F. (2003) HS5 of the human beta-globin locus control region: a developmental stage-specific border in erythroid cells, *EMBO J 22*, 4489-4500.
41. Chung, J. H., Whiteley, M., and Felsenfeld, G. (1993) A 5' element of the chicken beta-globin domain serves as an insulator in human erythroid cells and protects against position effect in Drosophila, *Cell 74*, 505-514.
42. Woychik, N. A., and Hampsey, M. (2002) The RNA polymerase II machinery: structure illuminates function, *Cell 108*, 453-463.
43. Hartzog, G. A. (2003) Transcription elongation by RNA polymerase II, *Curr Opin Genet Dev 13*, 119-126.
44. Sterner, D. E., and Berger, S. L. (2000) Acetylation of histones and transcription-related factors, *Microbiol Mol Biol Rev 64*, 435-459.
45. Becker, P. B., and Horz, W. (2002) ATP-dependent nucleosome remodeling, *Annu Rev Biochem 71*, 247-273.
46. Quinn, J., Fyrberg, A. M., Ganster, R. W., Schmidt, M. C., and Peterson, C. L. (1996) DNA-binding properties of the yeast SWI/SNF complex, *Nature 379*, 844-847.
47. Bultman, S. J., Gebuhr, T. C., and Magnuson, T. (2005) A Brg1 mutation that uncouples ATPase activity from chromatin remodeling reveals an essential role for SWI/SNF-related complexes in beta-globin expression and erythroid development, *Genes Dev 19*, 2849-2861.
48. Kingston, R. E., and Narlikar, G. J. (1999) ATP-dependent remodeling and acetylation as regulators of chromatin fluidity, *Genes Dev 13*, 2339-2352.
49. Kim, S. I., Bresnick, E. H., and Bultman, S. J. (2009) BRG1 directly regulates nucleosome structure and chromatin looping of the alpha globin locus to activate transcription, *Nucleic Acids Res 37*, 6019-6027.

50. Schnitzler, G., Sif, S., and Kingston, R. E. (1998) Human SWI/SNF interconverts a nucleosome between its base state and a stable remodeled state, *Cell 94*, 17-27.
51. Tong, J. K., Hassig, C. A., Schnitzler, G. R., Kingston, R. E., and Schreiber, S. L. (1998) Chromatin deacetylation by an ATP-dependent nucleosome remodelling complex, *Nature 395*, 917-921.
52. Kim, S. I., Bultman, S. J., Kiefer, C. M., Dean, A., and Bresnick, E. H. (2009) BRG1 requirement for long-range interaction of a locus control region with a downstream promoter, *Proc Natl Acad Sci U S A 106*, 2259-2264.
53. Gunawardena, R. W., Fox, S. R., Siddiqui, H., and Knudsen, E. S. (2007) SWI/SNF activity is required for the repression of deoxyribonucleotide triphosphate metabolic enzymes via the recruitment of mSin3B, *J Biol Chem 282*, 20116-20123.
54. Bryant, G. O., Prabhu, V., Floer, M., Wang, X., Spagna, D., Schreiber, D., and Ptashne, M. (2008) Activator control of nucleosome occupancy in activation and repression of transcription, *PLoS Biol 6*, 2928-2939.
55. Corey, L. L., Weirich, C. S., Benjamin, I. J., and Kingston, R. E. (2003) Localized recruitment of a chromatin-remodeling activity by an activator in vivo drives transcriptional elongation, *Genes Dev 17*, 1392-1401.
56. Batsche, E., Yaniv, M., and Muchardt, C. (2006) The human SWI/SNF subunit Brm is a regulator of alternative splicing, *Nat Struct Mol Biol 13*, 22-29.
57. Schwabish, M. A., and Struhl, K. (2007) The Swi/Snf complex is important for histone eviction during transcriptional activation and RNA polymerase II elongation in vivo, *Mol Cell Biol 27*, 6987-6995.
58. Tyagi, A., Ryme, J., Brodin, D., Ostlund Farrants, A. K., and Visa, N. (2009) SWI/SNF associates with nascent pre-mRNPs and regulates alternative pre-mRNA processing, *PLoS Genet 5*, e1000470.
59. Zhang, W., Kadam, S., Emerson, B. M., and Bieker, J. J. (2001) Site-specific acetylation by p300 or CREB binding protein regulates erythroid Kruppel-like factor transcriptional activity via its interaction with the SWI-SNF complex, *Mol Cell Biol 21*, 2413-2422.
60. Pope, N. J., and Bresnick, E. H. (2010) Differential coregulator requirements for function of the hematopoietic transcription factor GATA-1 at endogenous loci, *Nucleic Acids Res*.
61. Kim, S. I., Bultman, S. J., Jing, H., Blobel, G. A., and Bresnick, E. H. (2007) Dissecting molecular steps in chromatin domain activation during hematopoietic differentiation, *Mol Cell Biol 27*, 4551-4565.
62. Pal, S., Cantor, A. B., Johnson, K. D., Moran, T. B., Boyer, M. E., Orkin, S. H., and Bresnick, E. H. (2004) Coregulator-dependent facilitation of chromatin occupancy by GATA-1, *Proc Natl Acad Sci U S A 101*, 980-985.
63. Armstrong, J. A., Bieker, J. J., and Emerson, B. M. (1998) A SWI/SNF-related chromatin remodeling complex, E-RC1, is required for tissue-specific transcriptional regulation by EKLF in vitro, *Cell 95*, 93-104.
64. Zhang, W., and Bieker, J. J. (1998) Acetylation and modulation of erythroid Kruppel-like factor (EKLF) activity by interaction with histone acetyltransferases, *Proc Natl Acad Sci U S A 95*, 9855-9860.

65. Sengupta, T., Chen, K., Milot, E., and Bieker, J. J. (2008) Acetylation of EKLF is essential for epigenetic modification and transcriptional activation of the beta-globin locus, *Mol Cell Biol 28*, 6160-6170.
66. Oliveira, A. M., Abel, T., Brindle, P. K., and Wood, M. A. (2006) Differential role for CBP and p300 CREB-binding domain in motor skill learning, *Behav Neurosci 120*, 724-729.
67. Kasper, L. H., Fukuyama, T., Biesen, M. A., Boussouar, F., Tong, C., de Pauw, A., Murray, P. J., van Deursen, J. M., and Brindle, P. K. (2006) Conditional knockout mice reveal distinct functions for the global transcriptional coactivators CBP and p300 in T-cell development, *Mol Cell Biol 26*, 789-809.
68. Kang-Decker, N., Tong, C., Boussouar, F., Baker, D. J., Xu, W., Leontovich, A. A., Taylor, W. R., Brindle, P. K., and van Deursen, J. M. (2004) Loss of CBP causes T cell lymphomagenesis in synergy with p27Kip1 insufficiency, *Cancer Cell 5*, 177-189.
69. Han, L., Lu, J., Pan, L., Wang, X., Shao, Y., Han, S., and Huang, B. (2006) Histone acetyltransferase p300 regulates the transcription of human erythroid-specific 5-aminolevulinate synthase gene, *Biochem Biophys Res Commun 348*, 799-806.
70. Oudet, P., Gross-Bellard, M., and Chambon, P. (1975) Electron microscopic and biochemical evidence that chromatin structure is a repeating unit, *Cell 4*, 281-300.
71. Luger, K., Mader, A. W., Richmond, R. K., Sargent, D. F., and Richmond, T. J. (1997) Crystal structure of the nucleosome core particle at 2.8 A resolution, *Nature 389*, 251-260.
72. Horn, P. J., and Peterson, C. L. (2002) Molecular biology. Chromatin higher order folding--wrapping up transcription, *Science 297*, 1824-1827.
73. Talbert, P. B., and Henikoff, S. (2010) Histone variants--ancient wrap artists of the epigenome, *Nat Rev Mol Cell Biol 11*, 264-275.
74. Bell, O., and Schubeler, D. (2009) Chromatin: sub out the replacement, *Curr Biol 19*, R545-547.
75. Tremethick, D. J. (2007) Higher-order structures of chromatin: the elusive 30 nm fiber, *Cell 128*, 651-654.
76. Pennings, S., Meersseman, G., and Bradbury, E. M. (1994) Linker histones H1 and H5 prevent the mobility of positioned nucleosomes, *Proc Natl Acad Sci U S A 91*, 10275-10279.
77. Kim, A., and Dean, A. (2003) A human globin enhancer causes both discrete and widespread alterations in chromatin structure, *Mol Cell Biol 23*, 8099-8109.
78. Bresnick, E. H., Bustin, M., Marsaud, V., Richard-Foy, H., and Hager, G. L. (1992) The transcriptionally-active MMTV promoter is depleted of histone H1, *Nucleic Acids Res 20*, 273-278.
79. O'Neill, T. E., Meersseman, G., Pennings, S., and Bradbury, E. M. (1995) Deposition of histone H1 onto reconstituted nucleosome arrays inhibits both initiation and elongation of transcripts by T7 RNA polymerase, *Nucleic Acids Res 23*, 1075-1082.
80. Francis, N. J., Kingston, R. E., and Woodcock, C. L. (2004) Chromatin compaction by a polycomb group protein complex, *Science 306*, 1574-1577.

81. Tse, C., Sera, T., Wolffe, A. P., and Hansen, J. C. (1998) Disruption of higher-order folding by core histone acetylation dramatically enhances transcription of nucleosomal arrays by RNA polymerase III, *Mol Cell Biol 18*, 4629-4638.
82. Cheng, X., and Blumenthal, R. M. (2010) Coordinated chromatin control: structural and functional linkage of DNA and histone methylation, *Biochemistry 49*, 2999-3008.
83. Jenuwein, T., and Allis, C. D. (2001) Translating the histone code, *Science 293*, 1074-1080.
84. Quina, A. S., Buschbeck, M., and Di Croce, L. (2006) Chromatin structure and epigenetics, *Biochem Pharmacol 72*, 1563-1569.
85. Kouzarides, T. (2007) Chromatin modifications and their function, *Cell 128*, 693-705.
86. van Ingen, H., van Schaik, F. M., Wienk, H., Ballering, J., Rehmann, H., Dechesne, A. C., Kruijzer, J. A., Liskamp, R. M., Timmers, H. T., and Boelens, R. (2008) Structural insight into the recognition of the H3K4me3 mark by the TFIID subunit TAF3, *Structure 16*, 1245-1256.
87. Li, H., Ilin, S., Wang, W., Duncan, E. M., Wysocka, J., Allis, C. D., and Patel, D. J. (2006) Molecular basis for site-specific read-out of histone H3K4me3 by the BPTF PHD finger of NURF, *Nature 442*, 91-95.
88. Wysocka, J., Swigut, T., Xiao, H., Milne, T. A., Kwon, S. Y., Landry, J., Kauer, M., Tackett, A. J., Chait, B. T., Badenhorst, P., Wu, C., and Allis, C. D. (2006) A PHD finger of NURF couples histone H3 lysine 4 trimethylation with chromatin remodelling, *Nature 442*, 86-90.
89. Mujtaba, S., Zeng, L., and Zhou, M. M. (2007) Structure and acetyl-lysine recognition of the bromodomain, *Oncogene 26*, 5521-5527.
90. Campos, E. I., and Reinberg, D. (2009) Histones: annotating chromatin, *Annu Rev Genet 43*, 559-599.
91. Zhang, Y., Wu, W., Cheng, Y., King, D. C., Harris, R. S., Taylor, J., Chiaromonte, F., and Hardison, R. C. (2009) Primary sequence and epigenetic determinants of in vivo occupancy of genomic DNA by GATA1, *Nucleic Acids Res 37*, 7024-7038.
92. Cheng, Y., Wu, W., Kumar, S. A., Yu, D., Deng, W., Tripic, T., King, D. C., Chen, K. B., Zhang, Y., Drautz, D., Giardine, B., Schuster, S. C., Miller, W., Chiaromonte, F., Blobel, G. A., Weiss, M. J., and Hardison, R. C. (2009) Erythroid GATA1 function revealed by genome-wide analysis of transcription factor occupancy, histone modifications, and mRNA expression, *Genome Res 19*, 2172-2184.
93. Zhang, L., Dai, Y., Peng, W., Lu, J., Zhang, Y., and Wang, L. (2009) Genome-wide analysis of histone H3 lysine 4 trimethylation in peripheral blood mononuclear cells of minimal change nephrotic syndrome patients, *Am J Nephrol 30*, 505-513.
94. Robertson, A. G., Bilenky, M., Tam, A., Zhao, Y., Zeng, T., Thiessen, N., Cezard, T., Fejes, A. P., Wederell, E. D., Cullum, R., Euskirchen, G., Krzywinski, M., Birol, I., Snyder, M., Hoodless, P. A., Hirst, M., Marra, M. A., and Jones, S. J. (2008) Genome-wide relationship between histone H3 lysine 4 mono- and tri-methylation and transcription factor binding, *Genome Res 18*, 1906-1917.

95. Orford, K., Kharchenko, P., Lai, W., Dao, M. C., Worhunsky, D. J., Ferro, A., Janzen, V., Park, P. J., and Scadden, D. T. (2008) Differential H3K4 methylation identifies developmentally poised hematopoietic genes, *Dev Cell 14*, 798-809.
96. Vastenhouw, N. L., Zhang, Y., Woods, I. G., Imam, F., Regev, A., Liu, X. S., Rinn, J., and Schier, A. F. (2010) Chromatin signature of embryonic pluripotency is established during genome activation, *Nature 464*, 922-926.
97. McEwen, K. R., and Ferguson-Smith, A. C. (2010) Distinguishing epigenetic marks of developmental and imprinting regulation, *Epigenetics Chromatin 3*, 2.
98. Zon, L. I., Yamaguchi, Y., Yee, K., Albee, E. A., Kimura, A., Bennett, J. C., Orkin, S. H., and Ackerman, S. J. (1993) Expression of mRNA for the GATA-binding proteins in human eosinophils and basophils: potential role in gene transcription, *Blood 81*, 3234-3241.
99. Evans, T., Reitman, M., and Felsenfeld, G. (1988) An erythrocyte-specific DNA-binding factor recognizes a regulatory sequence common to all chicken globin genes, *Proc Natl Acad Sci U S A 85*, 5976-5980.
100. Orkin, S. H. (1992) GATA-binding transcription factors in hematopoietic cells, *Blood 80*, 575-581.
101. Weiss, M. J., and Orkin, S. H. (1995) GATA transcription factors: key regulators of hematopoiesis, *Exp Hematol 23*, 99-107.
102. Wall, L., deBoer, E., and Grosveld, F. (1988) The human beta-globin gene 3' enhancer contains multiple binding sites for an erythroid-specific protein, *Genes Dev 2*, 1089-1100.
103. Fujiwara, Y., Browne, C. P., Cunniff, K., Goff, S. C., and Orkin, S. H. (1996) Arrested development of embryonic red cell precursors in mouse embryos lacking transcription factor GATA-1, *Proc Natl Acad Sci U S A 93*, 12355-12358.
104. Phillips, J. D., Steensma, D. P., Pulsipher, M. A., Spangrude, G. J., and Kushner, J. P. (2007) Congenital erythropoietic porphyria due to a mutation in GATA1: the first trans-acting mutation causative for a human porphyria, *Blood 109*, 2618-2621.
105. Majewski, I. J., Metcalf, D., Mielke, L. A., Krebs, D. L., Ellis, S., Carpinelli, M. R., Mifsud, S., Di Rago, L., Corbin, J., Nicola, N. A., Hilton, D. J., and Alexander, W. S. (2006) A mutation in the translation initiation codon of Gata-1 disrupts megakaryocyte maturation and causes thrombocytopenia, *Proc Natl Acad Sci U S A 103*, 14146-14151.
106. Kitajima, K., Zheng, J., Yen, H., Sugiyama, D., and Nakano, T. (2006) Multipotential differentiation ability of GATA-1-null erythroid-committed cells, *Genes Dev 20*, 654-659.
107. Woo, A. J., Moran, T. B., Schindler, Y. L., Choe, S. K., Langer, N. B., Sullivan, M. R., Fujiwara, Y., Paw, B. H., and Cantor, A. B. (2008) Identification of ZBP-89 as a novel GATA-1-associated transcription factor involved in megakaryocytic and erythroid development, *Mol Cell Biol 28*, 2675-2689.
108. Shimizu, R., Ohneda, K., Engel, J. D., Trainor, C. D., and Yamamoto, M. (2004) Transgenic rescue of GATA-1-deficient mice with GATA-1 lacking a FOG-1 association site phenocopies patients with X-linked thrombocytopenia, *Blood 103*, 2560-2567.

109. Chang, A. N., Cantor, A. B., Fujiwara, Y., Lodish, M. B., Droho, S., Crispino, J. D., and Orkin, S. H. (2002) GATA-factor dependence of the multitype zinc-finger protein FOG-1 for its essential role in megakaryopoiesis, *Proc Natl Acad Sci U S A 99*, 9237-9242.
110. Lowry, J. A., and Mackay, J. P. (2006) GATA-1: one protein, many partners, *Int J Biochem Cell Biol 38*, 6-11.
111. Welch, J. J., Watts, J. A., Vakoc, C. R., Yao, Y., Wang, H., Hardison, R. C., Blobel, G. A., Chodosh, L. A., and Weiss, M. J. (2004) Global regulation of erythroid gene expression by transcription factor GATA-1, *Blood 104*, 3136-3147.
112. Cantor, A. B., and Orkin, S. H. (2002) Transcriptional regulation of erythropoiesis: an affair involving multiple partners, *Oncogene 21*, 3368-3376.
113. Kim, S. I., and Bresnick, E. H. (2007) Transcriptional control of erythropoiesis: emerging mechanisms and principles, *Oncogene 26*, 6777-6794.
114. Porcher, C., Swat, W., Rockwell, K., Fujiwara, Y., Alt, F. W., and Orkin, S. H. (1996) The T cell leukemia oncoprotein SCL/tal-1 is essential for development of all hematopoietic lineages, *Cell 86*, 47-57.
115. Robb, L., Lyons, I., Li, R., Hartley, L., Kontgen, F., Harvey, R. P., Metcalf, D., and Begley, C. G. (1995) Absence of yolk sac hematopoiesis from mice with a targeted disruption of the scl gene, *Proc Natl Acad Sci U S A 92*, 7075-7079.
116. Shivdasani, R. A., Mayer, E. L., and Orkin, S. H. (1995) Absence of blood formation in mice lacking the T-cell leukaemia oncoprotein tal-1/SCL, *Nature 373*, 432-434.
117. Tripic, T., Deng, W., Cheng, Y., Zhang, Y., Vakoc, C. R., Gregory, G. D., Hardison, R. C., and Blobel, G. A. (2009) SCL and associated proteins distinguish active from repressive GATA transcription factor complexes, *Blood 113*, 2191-2201.
118. Warren, A. J., Colledge, W. H., Carlton, M. B., Evans, M. J., Smith, A. J., and Rabbitts, T. H. (1994) The oncogenic cysteine-rich LIM domain protein rbtn2 is essential for erythroid development, *Cell 78*, 45-57.
119. Mead, P. E., Kelley, C. M., Hahn, P. S., Piedad, O., and Zon, L. I. (1998) SCL specifies hematopoietic mesoderm in Xenopus embryos, *Development 125*, 2611-2620.
120. Mead, P. E., Deconinck, A. E., Huber, T. L., Orkin, S. H., and Zon, L. I. (2001) Primitive erythropoiesis in the Xenopus embryo: the synergistic role of LMO-2, SCL and GATA-binding proteins, *Development 128*, 2301-2308.
121. Meier, N., Krpic, S., Rodriguez, P., Strouboulis, J., Monti, M., Krijgsveld, J., Gering, M., Patient, R., Hostert, A., and Grosveld, F. (2006) Novel binding partners of Ldb1 are required for haematopoietic development, *Development 133*, 4913-4923.
122. Song, S. H., Hou, C., and Dean, A. (2007) A positive role for NLI/Ldb1 in long-range beta-globin locus control region function, *Mol Cell 28*, 810-822.
123. Andrews, N. C., Kotkow, K. J., Ney, P. A., Erdjument-Bromage, H., Tempst, P., and Orkin, S. H. (1993) The ubiquitous subunit of erythroid transcription factor NF-E2 is a small basic-leucine zipper protein related to the v-maf oncogene, *Proc Natl Acad Sci U S A 90*, 11488-11492.

124. Chan, J. Y., Han, X. L., and Kan, Y. W. (1993) Isolation of cDNA encoding the human NF-E2 protein, *Proc Natl Acad Sci U S A 90*, 11366-11370.
125. Andrews, N. C., Erdjument-Bromage, H., Davidson, M. B., Tempst, P., and Orkin, S. H. (1993) Erythroid transcription factor NF-E2 is a haematopoietic-specific basic-leucine zipper protein, *Nature 362*, 722-728.
126. Lu, S. J., Rowan, S., Bani, M. R., and Ben-David, Y. (1994) Retroviral integration within the Fli-2 locus results in inactivation of the erythroid transcription factor NF-E2 in Friend erythroleukemias: evidence that NF-E2 is essential for globin expression, *Proc Natl Acad Sci U S A 91*, 8398-8402.
127. Shivdasani, R. A., Rosenblatt, M. F., Zucker-Franklin, D., Jackson, C. W., Hunt, P., Saris, C. J., and Orkin, S. H. (1995) Transcription factor NF-E2 is required for platelet formation independent of the actions of thrombopoietin/MGDF in megakaryocyte development, *Cell 81*, 695-704.
128. Peters, L. L., Andrews, N. C., Eicher, E. M., Davidson, M. B., Orkin, S. H., and Lux, S. E. (1993) Mouse microcytic anaemia caused by a defect in the gene encoding the globin enhancer-binding protein NF-E2, *Nature 362*, 768-770.
129. Shivdasani, R. A., and Orkin, S. H. (1995) Erythropoiesis and globin gene expression in mice lacking the transcription factor NF-E2, *Proc Natl Acad Sci U S A 92*, 8690-8694.
130. Andrews, N. C. (1998) The NF-E2 transcription factor, *Int J Biochem Cell Biol 30*, 429-432.
131. Bieker, J. J. (1996) Isolation, genomic structure, and expression of human erythroid Kruppel-like factor (EKLF), *DNA Cell Biol 15*, 347-352.
132. Friend, C. (1957) Leukemia of adult mice caused by a transmissible agent, *Ann N Y Acad Sci 68*, 522-532.
133. Jenkins, N. A., Gilbert, D. J., Copeland, N. G., Gruzglin, E., and Bieker, J. J. (1998) Erythroid Kruppel-like transcription factor (Eklf) maps to a region of mouse chromosome 8 syntenic with human chromosome 19, *Mamm Genome 9*, 174-176.
134. van Ree, J. H., Roskrow, M. A., Becher, A. M., McNall, R., Valentine, V. A., Jane, S. M., and Cunningham, J. M. (1997) The human erythroid-specific transcription factor EKLF localizes to chromosome 19p13.12-p13.13, *Genomics 39*, 393-395.
135. Miller, I. J., and Bieker, J. J. (1993) A novel, erythroid cell-specific murine transcription factor that binds to the CACCC element and is related to the Kruppel family of nuclear proteins, *Mol Cell Biol 13*, 2776-2786.
136. Quadrini, K. J., and Bieker, J. J. (2002) Kruppel-like zinc fingers bind to nuclear import proteins and are required for efficient nuclear localization of erythroid Kruppel-like factor, *J Biol Chem 277*, 32243-32252.
137. Pandya, K., and Townes, T. M. (2002) Basic residues within the Kruppel zinc finger DNA binding domains are the critical nuclear localization determinants of EKLF/KLF-1, *J Biol Chem 277*, 16304-16312.
138. Frontelo, P., Manwani, D., Galdass, M., Karsunky, H., Lohmann, F., Gallagher, P. G., and Bieker, J. J. (2007) Novel role for EKLF in megakaryocyte lineage commitment, *Blood 110*, 3871-3880.

139. Southwood, C. M., Downs, K. M., and Bieker, J. J. (1996) Erythroid Kruppel-like factor exhibits an early and sequentially localized pattern of expression during mammalian erythroid ontogeny, *Dev Dyn 206*, 248-259.
140. Anderson, K. P., Crable, S. C., and Lingrel, J. B. (2000) The GATA-E box-GATA motif in the EKLF promoter is required for in vivo expression, *Blood 95*, 1652-1655.
141. Adelman, C. A., Chattopadhyay, S., and Bieker, J. J. (2002) The BMP/BMPR/Smad pathway directs expression of the erythroid-specific EKLF and GATA1 transcription factors during embryoid body differentiation in serum-free media, *Development 129*, 539-549.
142. Ouyang, L., Chen, X., and Bieker, J. J. (1998) Regulation of erythroid Kruppel-like factor (EKLF) transcriptional activity by phosphorylation of a protein kinase casein kinase II site within its interaction domain, *J Biol Chem 273*, 23019-23025.
143. Kadam, S., McAlpine, G. S., Phelan, M. L., Kingston, R. E., Jones, K. A., and Emerson, B. M. (2000) Functional selectivity of recombinant mammalian SWI/SNF subunits, *Genes Dev 14*, 2441-2451.
144. Perkins, A. C., Sharpe, A. H., and Orkin, S. H. (1995) Lethal beta-thalassaemia in mice lacking the erythroid CACCC-transcription factor EKLF, *Nature 375*, 318-322.
145. Nuez, B., Michalovich, D., Bygrave, A., Ploemacher, R., and Grosveld, F. (1995) Defective haematopoiesis in fetal liver resulting from inactivation of the EKLF gene, *Nature 375*, 316-318.
146. Chen, X., and Bieker, J. J. (1996) Erythroid Kruppel-like factor (EKLF) contains a multifunctional transcriptional activation domain important for inter- and intramolecular interactions, *EMBO J 15*, 5888-5896.
147. Wijgerde, M., Gribnau, J., Trimborn, T., Nuez, B., Philipsen, S., Grosveld, F., and Fraser, P. (1996) The role of EKLF in human beta-globin gene competition, *Genes Dev 10*, 2894-2902.
148. Brown, R. C., Pattison, S., van Ree, J., Coghill, E., Perkins, A., Jane, S. M., and Cunningham, J. M. (2002) Distinct domains of erythroid Kruppel-like factor modulate chromatin remodeling and transactivation at the endogenous beta-globin gene promoter, *Mol Cell Biol 22*, 161-170.
149. Dekker, J., Rippe, K., Dekker, M., and Kleckner, N. (2002) Capturing chromosome conformation, *Science 295*, 1306-1311.
150. Drissen, R., Palstra, R. J., Gillemans, N., Splinter, E., Grosveld, F., Philipsen, S., and de Laat, W. (2004) The active spatial organization of the beta-globin locus requires the transcription factor EKLF, *Genes Dev 18*, 2485-2490.
151. Hodge, D., Coghill, E., Keys, J., Maguire, T., Hartmann, B., McDowall, A., Weiss, M., Grimmond, S., and Perkins, A. (2006) A global role for EKLF in definitive and primitive erythropoiesis, *Blood 107*, 3359-3370.
152. Drissen, R., von Lindern, M., Kolbus, A., Driegen, S., Steinlein, P., Beug, H., Grosveld, F., and Philipsen, S. (2005) The erythroid phenotype of EKLF-null mice: defects in hemoglobin metabolism and membrane stability, *Mol Cell Biol 25*, 5205-5214.

153. Keys, J. R., Tallack, M. R., Hodge, D. J., Cridland, S. O., David, R., and Perkins, A. C. (2007) Genomic organisation and regulation of murine alpha haemoglobin stabilising protein by erythroid Kruppel-like factor, *Br J Haematol 136*, 150-157.
154. Funnell, A. P., Maloney, C. A., Thompson, L. J., Keys, J., Tallack, M., Perkins, A. C., and Crossley, M. (2007) Erythroid Kruppel-like factor directly activates the basic Kruppel-like factor gene in erythroid cells, *Mol Cell Biol 27*, 2777-2790.
155. Coghill, E., Eccleston, S., Fox, V., Cerruti, L., Brown, C., Cunningham, J., Jane, S., and Perkins, A. (2001) Erythroid Kruppel-like factor (EKLF) coordinates erythroid cell proliferation and hemoglobinization in cell lines derived from EKLF null mice, *Blood 97*, 1861-1868.
156. Andrews, N. C., and Faller, D. V. (1991) A rapid micropreparation technique for extraction of DNA-binding proteins from limiting numbers of mammalian cells, *Nucleic Acids Res 19*, 2499.
157. Boyd, K. E., and Farnham, P. J. (1999) Coexamination of site-specific transcription factor binding and promoter activity in living cells, *Mol Cell Biol 19*, 8393-8399.
158. Boyd, K. E., Wells, J., Gutman, J., Bartley, S. M., and Farnham, P. J. (1998) c-Myc target gene specificity is determined by a post-DNAbinding mechanism, *Proc Natl Acad Sci U S A 95*, 13887-13892.
159. Forsberg, E. C., Downs, K. M., and Bresnick, E. H. (2000) Direct interaction of NF-E2 with hypersensitive site 2 of the beta-globin locus control region in living cells, *Blood 96*, 334-339.
160. Forsberg, E. C., Downs, K. M., Christensen, H. M., Im, H., Nuzzi, P. A., and Bresnick, E. H. (2000) Developmentally dynamic histone acetylation pattern of a tissue-specific chromatin domain, *Proc Natl Acad Sci U S A 97*, 14494-14499.
161. Kiekhaefer, C. M., Grass, J. A., Johnson, K. D., Boyer, M. E., and Bresnick, E. H. (2002) Hematopoietic-specific activators establish an overlapping pattern of histone acetylation and methylation within a mammalian chromatin domain, *Proc Natl Acad Sci U S A 99*, 14309-14314.
162. Pilon, A. M., Nilson, D. G., Zhou, D., Sangerman, J., Townes, T. M., Bodine, D. M., and Gallagher, P. G. (2006) Alterations in expression and chromatin configuration of the alpha hemoglobin-stabilizing protein gene in erythroid Kruppel-like factor-deficient mice, *Mol Cell Biol 26*, 4368-4377.
163. Splinter, E., Heath, H., Kooren, J., Palstra, R. J., Klous, P., Grosveld, F., Galjart, N., and de Laat, W. (2006) CTCF mediates long-range chromatin looping and local histone modification in the beta-globin locus, *Genes Dev 20*, 2349-2354.
164. Johnson, K. D., and Bresnick, E. H. (2002) Dissecting long-range transcriptional mechanisms by chromatin immunoprecipitation, *Methods 26*, 27-36.
165. McArthur, M., Gerum, S., and Stamatoyannopoulos, G. (2001) Quantification of DNaseI-sensitivity by real-time PCR: quantitative analysis of DNaseI-hypersensitivity of the mouse beta-globin LCR, *J Mol Biol 313*, 27-34.
166. Faustino, P., Lavinha, J., Marini, M. G., and Moi, P. (1996) beta-Thalassemia mutation at -90C-->T impairs the interaction of the proximal CACCC box with both erythroid and nonerythroid factors, *Blood 88*, 3248-3249.

167. Moi, P., Faa, V., Marini, M. G., Asunis, I., Ibba, G., Cao, A., and Rosatelli, M. C. (2004) A novel silent beta-thalassemia mutation in the distal CACCC box affects the binding and responsiveness to EKLF, *Br J Haematol 126*, 881-884.
168. Kulozik, A. E., Bellan-Koch, A., Bail, S., Kohne, E., and Kleihauer, E. (1991) Thalassemia intermedia: moderate reduction of beta globin gene transcriptional activity by a novel mutation of the proximal CACCC promoter element, *Blood 77*, 2054-2058.
169. Bender, M. A., Bulger, M., Close, J., and Groudine, M. (2000) Beta-globin gene switching and DNase I sensitivity of the endogenous beta-globin locus in mice do not require the locus control region, *Mol Cell 5*, 387-393.
170. Hu, X., Bulger, M., Bender, M. A., Fields, J., Groudine, M., and Fiering, S. (2006) Deletion of the core region of 5' HS2 of the mouse beta-globin locus control region reveals a distinct effect in comparison with human beta-globin transgenes, *Blood 107*, 821-826.
171. Fang, X., Sun, J., Xiang, P., Yu, M., Navas, P. A., Peterson, K. R., Stamatoyannopoulos, G., and Li, Q. (2005) Synergistic and additive properties of the beta-globin locus control region (LCR) revealed by 5'HS3 deletion mutations: implication for LCR chromatin architecture, *Mol Cell Biol 25*, 7033-7041.
172. Merika, M., and Orkin, S. H. (1995) Functional synergy and physical interactions of the erythroid transcription factor GATA-1 with the Kruppel family proteins Sp1 and EKLF, *Mol Cell Biol 15*, 2437-2447.
173. Yu, M., Riva, L., Xie, H., Schindler, Y., Moran, T. B., Cheng, Y., Yu, D., Hardison, R., Weiss, M. J., Orkin, S. H., Bernstein, B. E., Fraenkel, E., and Cantor, A. B. (2009) Insights into GATA-1-mediated gene activation versus repression via genome-wide chromatin occupancy analysis, *Mol Cell 36*, 682-695.
174. Sawado, T., Halow, J., Bender, M. A., and Groudine, M. (2003) The beta -globin locus control region (LCR) functions primarily by enhancing the transition from transcription initiation to elongation, *Genes Dev 17*, 1009-1018.
175. Sawado, T., Igarashi, K., and Groudine, M. (2001) Activation of beta-major globin gene transcription is associated with recruitment of NF-E2 to the beta-globin LCR and gene promoter, *Proc Natl Acad Sci U S A 98*, 10226-10231.
176. Pomerantz, O., Goodwin, A. J., Joyce, T., and Lowrey, C. H. (1998) Conserved elements containing NF-E2 and tandem GATA binding sites are required for erythroid-specific chromatin structure reorganization within the human beta-globin locus control region, *Nucleic Acids Res 26*, 5684-5691.
177. Goodwin, A. J., McInerney, J. M., Glander, M. A., Pomerantz, O., and Lowrey, C. H. (2001) In vivo formation of a human beta-globin locus control region core element requires binding sites for multiple factors including GATA-1, NF-E2, erythroid Kruppel-like factor, and Sp1, *J Biol Chem 276*, 26883-26892.
178. Onishi, Y., and Kiyama, R. (2003) Interaction of NF-E2 in the human beta-globin locus control region before chromatin remodeling, *J Biol Chem 278*, 8163-8171.
179. Kurdistani, S. K., and Grunstein, M. (2003) Histone acetylation and deacetylation in yeast, *Nat Rev Mol Cell Biol 4*, 276-284.
180. Felsenfeld, G., and Groudine, M. (2003) Controlling the double helix, *Nature 421*, 448-453.

181. Kurdistani, S. K., Tavazoie, S., and Grunstein, M. (2004) Mapping global histone acetylation patterns to gene expression, *Cell 117*, 721-733.
182. Fromm, G., de Vries, C., Byron, R., Fields, J., Fiering, S., Groudine, M., Bender, M. A., Palis, J., and Bulger, M. (2009) Histone hyperacetylation within the beta-globin locus is context-dependent and precedes high-level gene expression, *Blood 114*, 3479-3488.
183. Shilatifard, A. (2008) Molecular implementation and physiological roles for histone H3 lysine 4 (H3K4) methylation, *Curr Opin Cell Biol 20*, 341-348.
184. Eissenberg, J. C., and Shilatifard, A. (2010) Histone H3 lysine 4 (H3K4) methylation in development and differentiation, *Dev Biol 339*, 240-249.
185. Heintzman, N. D., Stuart, R. K., Hon, G., Fu, Y., Ching, C. W., Hawkins, R. D., Barrera, L. O., Van Calcar, S., Qu, C., Ching, K. A., Wang, W., Weng, Z., Green, R. D., Crawford, G. E., and Ren, B. (2007) Distinct and predictive chromatin signatures of transcriptional promoters and enhancers in the human genome, *Nat Genet 39*, 311-318.
186. Lee, D. Y., Hayes, J. J., Pruss, D., and Wolffe, A. P. (1993) A positive role for histone acetylation in transcription factor access to nucleosomal DNA, *Cell 72*, 73-84.
187. Cruickshank, M. N., Besant, P., and Ulgiati, D. (2010) The impact of histone post-translational modifications on developmental gene regulation, *Amino Acids*.
188. Hung, H. L., Kim, A. Y., Hong, W., Rakowski, C., and Blobel, G. A. (2001) Stimulation of NF-E2 DNA binding by CREB-binding protein (CBP)-mediated acetylation, *J Biol Chem 276*, 10715-10721.
189. Takahashi, T., Suwabe, N., Dai, P., Yamamoto, M., Ishii, S., and Nakano, T. (2000) Inhibitory interaction of c-Myb and GATA-1 via transcriptional co-activator CBP, *Oncogene 19*, 134-140.
190. Gribnau, J., Diderich, K., Pruzina, S., Calzolari, R., and Fraser, P. (2000) Intergenic transcription and developmental remodeling of chromatin subdomains in the human beta-globin locus, *Mol Cell 5*, 377-386.
191. Levings, P. P., and Bungert, J. (2002) The human beta-globin locus control region, *Eur J Biochem 269*, 1589-1599.
192. Levings, P. P., Zhou, Z., Vieira, K. F., Crusselle-Davis, V. J., and Bungert, J. (2006) Recruitment of transcription complexes to the beta-globin locus control region and transcription of hypersensitive site 3 prior to erythroid differentiation of murine embryonic stem cells, *FEBS J 273*, 746-755.
193. Johnson, K. D., Christensen, H. M., Zhao, B., and Bresnick, E. H. (2001) Distinct mechanisms control RNA polymerase II recruitment to a tissue-specific locus control region and a downstream promoter, *Mol Cell 8*, 465-471.
194. Johnson, K. D., Grass, J. A., Boyer, M. E., Kiekhaefer, C. M., Blobel, G. A., Weiss, M. J., and Bresnick, E. H. (2002) Cooperative activities of hematopoietic regulators recruit RNA polymerase II to a tissue-specific chromatin domain, *Proc Natl Acad Sci U S A 99*, 11760-11765.
195. Johnson, K. D., Grass, J. A., Park, C., Im, H., Choi, K., and Bresnick, E. H. (2003) Highly restricted localization of RNA polymerase II within a locus control region of a tissue-specific chromatin domain, *Mol Cell Biol 23*, 6484-6493.

196. Tang, Y., Liu, D. P., and Liang, C. C. (2002) Further understanding of the beta-globin locus regulation at the molecular level: looping or linking models?, *Genes Cells 7*, 889-900.
197. Engel, J. D., and Tanimoto, K. (2000) Looping, linking, and chromatin activity: new insights into beta-globin locus regulation, *Cell 100*, 499-502.
198. Lin, P. S., Marshall, N. F., and Dahmus, M. E. (2002) CTD phosphatase: role in RNA polymerase II cycling and the regulation of transcript elongation, *Prog Nucleic Acid Res Mol Biol 72*, 333-365.
199. Komarnitsky, P., Cho, E. J., and Buratowski, S. (2000) Different phosphorylated forms of RNA polymerase II and associated mRNA processing factors during transcription, *Genes Dev 14*, 2452-2460.
200. Bottardi, S., Ross, J., Pierre-Charles, N., Blank, V., and Milot, E. (2006) Lineage-specific activators affect beta-globin locus chromatin in multipotent hematopoietic progenitors, *EMBO J 25*, 3586-3595.
201. Demers, C., Chaturvedi, C. P., Ranish, J. A., Juban, G., Lai, P., Morle, F., Aebersold, R., Dilworth, F. J., Groudine, M., and Brand, M. (2007) Activator-mediated recruitment of the MLL2 methyltransferase complex to the beta-globin locus, *Mol Cell 27*, 573-584.
202. Tewari, R., Gillemans, N., Wijgerde, M., Nuez, B., von Lindern, M., Grosveld, F., and Philipsen, S. (1998) Erythroid Kruppel-like factor (EKLF) is active in primitive and definitive erythroid cells and is required for the function of 5'HS3 of the beta-globin locus control region, *EMBO J 17*, 2334-2341.
203. Jia, C. P., Huang, S. Z., Yan, J. B., Xiao, Y. P., Ren, Z. R., and Zeng, Y. T. (2003) Effects of human locus control region elements HS2 and HS3 on human beta-globin gene expression in transgenic mouse, *Blood Cells Mol Dis 31*, 360-369.
204. Sun, J., Brand, M., Zenke, Y., Tashiro, S., Groudine, M., and Igarashi, K. (2004) Heme regulates the dynamic exchange of Bach1 and NF-E2-related factors in the Maf transcription factor network, *Proc Natl Acad Sci U S A 101*, 1461-1466.
205. Tolhuis, B., Palstra, R. J., Splinter, E., Grosveld, F., and de Laat, W. (2002) Looping and interaction between hypersensitive sites in the active beta-globin locus, *Mol Cell 10*, 1453-1465.
206. Ross, J., Bottardi, S., Bourgoin, V., Wollenschlaeger, A., Drobetsky, E., Trudel, M., and Milot, E. (2009) Differential requirement of a distal regulatory region for pre-initiation complex formation at globin gene promoters, *Nucleic Acids Res 37*, 5295-5308.
207. Palstra, R. J., Tolhuis, B., Splinter, E., Nijmeijer, R., Grosveld, F., and de Laat, W. (2003) The beta-globin nuclear compartment in development and erythroid differentiation, *Nat Genet 35*, 190-194.
208. Jackson, D. A., McDowell, J. C., and Dean, A. (2003) Beta-globin locus control region HS2 and HS3 interact structurally and functionally, *Nucleic Acids Res 31*, 1180-1190.
209. Yu, X., Kong, Y., Dore, L. C., Abdulmalik, O., Katein, A. M., Zhou, S., Choi, J. K., Gell, D., Mackay, J. P., Gow, A. J., and Weiss, M. J. (2007) An erythroid chaperone that facilitates folding of alpha-globin subunits for hemoglobin synthesis, *J Clin Invest 117*, 1856-1865.

210. Chen, H., Khan, A. A., Liu, F., Gilligan, D. M., Peters, L. L., Messick, J., Haschek-Hock, W. M., Li, X., Ostafin, A. E., and Chishti, A. H. (2007) Combined deletion of mouse dematin-headpiece and beta-adducin exerts a novel effect on the spectrin-actin junctions leading to erythrocyte fragility and hemolytic anemia, *J Biol Chem 282*, 4124-4135.
211. Anderson, K. P., Crable, S. C., and Lingrel, J. B. (1998) Multiple proteins binding to a GATA-E box-GATA motif regulate the erythroid Kruppel-like factor (EKLF) gene, *J Biol Chem 273*, 14347-14354.
212. Karacay, B., and Chang, L. S. (1999) Induction of erythrocyte protein 4.2 gene expression during differentiation of murine erythroleukemia cells, *Genomics 59*, 6-17.
213. Xu, Z., Huang, S., Chang, L. S., Agulnick, A. D., and Brandt, S. J. (2003) Identification of a TAL1 target gene reveals a positive role for the LIM domain-binding protein Ldb1 in erythroid gene expression and differentiation, *Mol Cell Biol 23*, 7585-7599.
214. Azim, A. C., Knoll, J. H., Beggs, A. H., and Chishti, A. H. (1995) Isoform cloning, actin binding, and chromosomal localization of human erythroid dematin, a member of the villin superfamily, *J Biol Chem 270*, 17407-17413.
215. Khanna, R., Chang, S. H., Andrabi, S., Azam, M., Kim, A., Rivera, A., Brugnara, C., Low, P. S., Liu, S. C., and Chishti, A. H. (2002) Headpiece domain of dematin is required for the stability of the erythrocyte membrane, *Proc Natl Acad Sci U S A 99*, 6637-6642.
216. Mohseni, M., and Chishti, A. H. (2008) The headpiece domain of dematin regulates cell shape, motility, and wound healing by modulating RhoA activation, *Mol Cell Biol 28*, 4712-4718.
217. Mohseni, M., and Chishti, A. H. (2009) Regulatory models of RhoA suppression by dematin, a cytoskeletal adaptor protein, *Cell Adh Migr 3*, 191-194.
218. Khan, A. A., Hanada, T., Mohseni, M., Jeong, J. J., Zeng, L., Gaetani, M., Li, D., Reed, B. C., Speicher, D. W., and Chishti, A. H. (2008) Dematin and adducin provide a novel link between the spectrin cytoskeleton and human erythrocyte membrane by directly interacting with glucose transporter-1, *J Biol Chem 283*, 14600-14609.
219. Sahr, K. E., Daniels, B. P., and Hanspal, M. (1996) Identification of the proximal erythroid promoter region of the mouse anion exchanger gene, *Blood 88*, 4500-4509.
220. Gallagher, P. G., and Forget, B. G. (1998) An alternate promoter directs expression of a truncated, muscle-specific isoform of the human ankyrin 1 gene, *J Biol Chem 273*, 1339-1348.
221. Gallagher, P. G., Sabatino, D. E., Romana, M., Cline, A. P., Garrett, L. J., Bodine, D. M., and Forget, B. G. (1999) A human beta-spectrin gene promoter directs high level expression in erythroid but not muscle or neural cells, *J Biol Chem 274*, 6062-6073.
222. Yenerel, M. N., Sundell, I. B., Weese, J., Bulger, M., and Gilligan, D. M. (2005) Expression of adducin genes during erythropoiesis: a novel erythroid promoter for ADD2, *Exp Hematol 33*, 758-766.

223. Azim, A. C., Kim, A. C., Lutchman, M., Andrabi, S., Peters, L. L., and Chishti, A. H. (1999) cDNA sequence, genomic structure, and expression of the mouse dematin gene (Epb4.9), *Mamm Genome 10*, 1026-1029.
224. Williams, P. P., and Gallagher, J. E. (1978) Preparation and long-term cultivation of porcine tracheal and lung organ cultures by alternate exposure to gaseous and liquid medium phases, *In Vitro 14*, 686-696.
225. Gell, D., Kong, Y., Eaton, S. A., Weiss, M. J., and Mackay, J. P. (2002) Biophysical characterization of the alpha-globin binding protein alpha-hemoglobin stabilizing protein, *J Biol Chem 277*, 40602-40609.
226. Kooren, J., Palstra, R. J., Klous, P., Splinter, E., von Lindern, M., Grosveld, F., and de Laat, W. (2007) Beta-globin active chromatin Hub formation in differentiating erythroid cells and in p45 NF-E2 knock-out mice, *J Biol Chem 282*, 16544-16552.
227. Osborne, C. S., Chakalova, L., Brown, K. E., Carter, D., Horton, A., Debrand, E., Goyenechea, B., Mitchell, J. A., Lopes, S., Reik, W., and Fraser, P. (2004) Active genes dynamically colocalize to shared sites of ongoing transcription, *Nat Genet 36*, 1065-1071.
228. Schoenfelder, S., Sexton, T., Chakalova, L., Cope, N. F., Horton, A., Andrews, S., Kurukuti, S., Mitchell, J. A., Umlauf, D., Dimitrova, D. S., Eskiw, C. H., Luo, Y., Wei, C. L., Ruan, Y., Bieker, J. J., and Fraser, P. (2010) Preferential associations between co-regulated genes reveal a transcriptional interactome in erythroid cells, *Nat Genet 42*, 53-61.
229. Ito, T., Watanabe, H., Yamamichi, N., Kondo, S., Tando, T., Haraguchi, T., Mizutani, T., Sakurai, K., Fujita, S., Izumi, T., Isobe, T., and Iba, H. (2008) Brm transactivates the telomerase reverse transcriptase (TERT) gene and modulates the splicing patterns of its transcripts in concert with p54(nrb), *Biochem J 411*, 201-209.
230. Shen, W., Xu, C., Huang, W., Zhang, J., Carlson, J. E., Tu, X., Wu, J., and Shi, Y. (2007) Solution structure of human Brg1 bromodomain and its specific binding to acetylated histone tails, *Biochemistry 46*, 2100-2110.
231. Subtil-Rodriguez, A., and Reyes, J. C. (2010) BRG1 helps RNA polymerase II to overcome a nucleosomal barrier during elongation, in vivo, *EMBO Rep 11*, 751-757.
232. Anderson, J. D., Lowary, P. T., and Widom, J. (2001) Effects of histone acetylation on the equilibrium accessibility of nucleosomal DNA target sites, *J Mol Biol 307*, 977-985.
233. Yao, T. P., Oh, S. P., Fuchs, M., Zhou, N. D., Ch'ng, L. E., Newsome, D., Bronson, R. T., Li, E., Livingston, D. M., and Eckner, R. (1998) Gene dosage-dependent embryonic development and proliferation defects in mice lacking the transcriptional integrator p300, *Cell 93*, 361-372.
234. Xu, W., Fukuyama, T., Ney, P. A., Wang, D., Rehg, J., Boyd, K., van Deursen, J. M., and Brindle, P. K. (2006) Global transcriptional coactivators CREB-binding protein and p300 are highly essential collectively but not individually in peripheral B cells, *Blood 107*, 4407-4416.

235. Kasper, L. H., Boussouar, F., Ney, P. A., Jackson, C. W., Rehg, J., van Deursen, J. M., and Brindle, P. K. (2002) A transcription-factor-binding surface of coactivator p300 is required for haematopoiesis, *Nature 419*, 738-743.
236. Bedford, D. C., Kasper, L. H., Fukuyama, T., and Brindle, P. K. (2010) Target gene context influences the transcriptional requirement for the KAT3 family of CBP and p300 histone acetyltransferases, *Epigenetics 5*, 9-15.
237. Whitelaw, E., Tsai, S. F., Hogben, P., and Orkin, S. H. (1990) Regulated expression of globin chains and the erythroid transcription factor GATA-1 during erythropoiesis in the developing mouse, *Mol Cell Biol 10*, 6596-6606.
238. Zon, L. I., Youssoufian, H., Mather, C., Lodish, H. F., and Orkin, S. H. (1991) Activation of the erythropoietin receptor promoter by transcription factor GATA-1, *Proc Natl Acad Sci U S A 88*, 10638-10641.
239. Miccio, A., Wang, Y., Hong, W., Gregory, G. D., Wang, H., Yu, X., Choi, J. K., Shelat, S., Tong, W., Poncz, M., and Blobel, G. A. (2010) NuRD mediates activating and repressive functions of GATA-1 and FOG-1 during blood development, *EMBO J 29*, 442-456.
240. Im, H., Grass, J. A., Johnson, K. D., Kim, S. I., Boyer, M. E., Imbalzano, A. N., Bieker, J. J., and Bresnick, E. H. (2005) Chromatin domain activation via GATA-1 utilization of a small subset of dispersed GATA motifs within a broad chromosomal region, *Proc Natl Acad Sci U S A 102*, 17065-17070.
241. Nerlov, C., Querfurth, E., Kulessa, H., and Graf, T. (2000) GATA-1 interacts with the myeloid PU.1 transcription factor and represses PU.1-dependent transcription, *Blood 95*, 2543-2551.
242. Lee, H. Y., Johnson, K. D., Fujiwara, T., Boyer, M. E., Kim, S. I., and Bresnick, E. H. (2009) Controlling hematopoiesis through sumoylation-dependent regulation of a GATA factor, *Mol Cell 36*, 984-995.
243. Zhang, L., Fletcher, A. G., Cheung, V., Winston, F., and Stargell, L. A. (2008) Spn1 regulates the recruitment of Spt6 and the Swi/Snf complex during transcriptional activation by RNA polymerase II, *Mol Cell Biol 28*, 1393-1403.
244. Sharma, V. M., Li, B., and Reese, J. C. (2003) SWI/SNF-dependent chromatin remodeling of RNR3 requires TAF(II)s and the general transcription machinery, *Genes Dev 17*, 502-515.
245. Soler, E., Andrieu-Soler, C., de Boer, E., Bryne, J. C., Thongjuea, S., Stadhouders, R., Palstra, R. J., Stevens, M., Kockx, C., van Ijcken, W., Hou, J., Steinhoff, C., Rijkers, E., Lenhard, B., and Grosveld, F. (2010) The genome-wide dynamics of the binding of Ldb1 complexes during erythroid differentiation, *Genes Dev 24*, 277-289.
246. Perrine, S. P., Mankidy, R., Boosalis, M. S., Bieker, J. J., and Faller, D. V. (2009) Erythroid Kruppel-like factor (EKLF) is recruited to the gamma-globin gene promoter as a co-activator and is required for gamma-globin gene induction by short-chain fatty acid derivatives, *Eur J Haematol 82*, 466-476.
247. Shyu, Y. C., Wen, S. C., Lee, T. L., Chen, X., Hsu, C. T., Chen, H., Chen, R. L., Hwang, J. L., and Shen, C. K. (2006) Chromatin-binding in vivo of the erythroid kruppel-like factor, EKLF, in the murine globin loci, *Cell Res 16*, 347-355.

248. Surinya, K. H., Cox, T. C., and May, B. K. (1997) Transcriptional regulation of the human erythroid 5-aminolevulinate synthase gene. Identification of promoter elements and role of regulatory proteins, *J Biol Chem 272*, 26585-26594.
249. Kramer, M. F., Gunaratne, P., and Ferreira, G. C. (2000) Transcriptional regulation of the murine erythroid-specific 5-aminolevulinate synthase gene, *Gene 247*, 153-166.
250. Poblete-Gutierrez, P., Wiederholt, T., Merk, H. F., and Frank, J. (2006) The porphyrias: clinical presentation, diagnosis and treatment, *Eur J Dermatol 16*, 230-240.
251. Surinya, K. H., Cox, T. C., and May, B. K. (1998) Identification and characterization of a conserved erythroid-specific enhancer located in intron 8 of the human 5-aminolevulinate synthase 2 gene, *J Biol Chem 273*, 16798-16809.
252. Porcher, C., Pitiot, G., Plumb, M., Lowe, S., de Verneuil, H., and Grandchamp, B. (1991) Characterization of hypersensitive sites, protein-binding motifs, and regulatory elements in both promoters of the mouse porphobilinogen deaminase gene, *J Biol Chem 266*, 10562-10569.
253. Bishop, T. R., Miller, M. W., Beall, J., Zon, L. I., and Dierks, P. (1996) Genetic regulation of delta-aminolevulinate dehydratase during erythropoiesis, *Nucleic Acids Res 24*, 2511-2518.
254. Jaffe, E. K., and Stith, L. (2007) ALAD porphyria is a conformational disease, *Am J Hum Genet 80*, 329-337.
255. Sassa, S. (1998) ALAD porphyria, *Semin Liver Dis 18*, 95-101.
256. Kelada, S. N., Shelton, E., Kaufmann, R. B., and Khoury, M. J. (2001) Delta-aminolevulinic acid dehydratase genotype and lead toxicity: a HuGE review, *Am J Epidemiol 154*, 1-13.
257. Oskarsson, A., and Hellstrom-Lindahl, E. (1988) Increased lead uptake and inhibition of ALAD-activity in isolated rat hepatocytes incubated with lead-diethyldithiocarbamate complex, *Chem Biol Interact 67*, 59-70.
258. Bergdahl, I. A., Grubb, A., Schutz, A., Desnick, R. J., Wetmur, J. G., Sassa, S., and Skerfving, S. (1997) Lead binding to delta-aminolevulinic acid dehydratase (ALAD) in human erythrocytes, *Pharmacol Toxicol 81*, 153-158.
259. Sakamoto, D., Kudo, H., Inohaya, K., Yokoi, H., Narita, T., Naruse, K., Mitani, H., Araki, K., Shima, A., Ishikawa, Y., Imai, Y., and Kudo, A. (2004) A mutation in the gene for delta-aminolevulinic acid dehydratase (ALAD) causes hypochromic anemia in the medaka, Oryzias latipes, *Mech Dev 121*, 747-752.
260. Pilon, A. M., Ajay, S. S., Abaan, H. O., Margulies, E. H., Gallagher, P. G., and Bodine, D. M. (2009) Genome-Wide ChIP-Seq Reveals a Dramatic Shift in the EKLF Binding Profile Between Erythroid Progenitors and Erythroblasts, *ASH Annual Meeting Abstracts 114*, 565-.
261. Nielsen, A. L., Norby, P. L., Pedersen, F. S., and Jorgensen, P. (1996) E-box sequence and context-dependent TAL1/SCL modulation of basic helix-loop-helix protein-mediated transcriptional activation, *J Biol Chem 271*, 31463-31469.
262. Lee, C. H., Murphy, M. R., Lee, J. S., and Chung, J. H. (1999) Targeting a SWI/SNF-related chromatin remodeling complex to the beta-globin promoter in erythroid cells, *Proc Natl Acad Sci U S A 96*, 12311-12315.

263. Cho, Y., Song, S. H., Lee, J. J., Choi, N., Kim, C. G., Dean, A., and Kim, A. (2008) The role of transcriptional activator GATA-1 at human beta-globin HS2, *Nucleic Acids Res 36*, 4521-4528.
264. Blobel, G. A., Nakajima, T., Eckner, R., Montminy, M., and Orkin, S. H. (1998) CREB-binding protein cooperates with transcription factor GATA-1 and is required for erythroid differentiation, *Proc Natl Acad Sci U S A 95*, 2061-2066.
265. Boyes, J., Byfield, P., Nakatani, Y., and Ogryzko, V. (1998) Regulation of activity of the transcription factor GATA-1 by acetylation, *Nature 396*, 594-598.
266. Guo, G. G., Gu, M., and Etlinger, J. D. (1994) 240-kDa proteasome inhibitor (CF-2) is identical to delta-aminolevulinic acid dehydratase, *J Biol Chem 269*, 12399-12402.
267. Bulger, M., and Groudine, M. (1999) Looping versus linking: toward a model for long-distance gene activation, *Genes Dev 13*, 2465-2477.
268. de Laat, W., and Grosveld, F. (2003) Spatial organization of gene expression: the active chromatin hub, *Chromosome Res 11*, 447-459.
269. Zhu, X., Ling, J., Zhang, L., Pi, W., Wu, M., and Tuan, D. (2007) A facilitated tracking and transcription mechanism of long-range enhancer function, *Nucleic Acids Res 35*, 5532-5544.
270. Liu, Z., and Garrard, W. T. (2005) Long-range interactions between three transcriptional enhancers, active Vkappa gene promoters, and a 3' boundary sequence spanning 46 kilobases, *Mol Cell Biol 25*, 3220-3231.
271. Zhou, G. L., Xin, L., Song, W., Di, L. J., Liu, G., Wu, X. S., Liu, D. P., and Liang, C. C. (2006) Active chromatin hub of the mouse alpha-globin locus forms in a transcription factory of clustered housekeeping genes, *Mol Cell Biol 26*, 5096-5105.
272. Lee, G. R., Spilianakis, C. G., and Flavell, R. A. (2005) Hypersensitive site 7 of the TH2 locus control region is essential for expressing TH2 cytokine genes and for long-range intrachromosomal interactions, *Nat Immunol 6*, 42-48.
273. Vakoc, C. R., Letting, D. L., Gheldof, N., Sawado, T., Bender, M. A., Groudine, M., Weiss, M. J., Dekker, J., and Blobel, G. A. (2005) Proximity among distant regulatory elements at the beta-globin locus requires GATA-1 and FOG-1, *Mol Cell 17*, 453-462.
274. Fischer, K. D., Haese, A., and Nowock, J. (1993) Cooperation of GATA-1 and Sp1 can result in synergistic transcriptional activation or interference, *J Biol Chem 268*, 23915-23923.
275. Siatecka, M., Xue, L., and Bieker, J. J. (2007) Sumoylation of EKLF promotes transcriptional repression and is involved in inhibition of megakaryopoiesis, *Mol Cell Biol 27*, 8547-8560.
276. Chen, X., and Bieker, J. J. (2004) Stage-specific repression by the EKLF transcriptional activator, *Mol Cell Biol 24*, 10416-10424.
277. Chen, X., and Bieker, J. J. (2001) Unanticipated repression function linked to erythroid Kruppel-like factor, *Mol Cell Biol 21*, 3118-3125.
278. Persons, D. A., Allay, E. R., Sabatino, D. E., Kelly, P., Bodine, D. M., and Nienhuis, A. W. (2001) Functional requirements for phenotypic correction of murine beta-thalassemia: implications for human gene therapy, *Blood 97*, 3275-3282.

279. Gallagher, P. G., Romana, M., Tse, W. T., Lux, S. E., and Forget, B. G. (2000) The human ankyrin-1 gene is selectively transcribed in erythroid cell lines despite the presence of a housekeeping-like promoter, *Blood 96*, 1136-1143.
280. Ott, C. J., Blackledge, N. P., Kerschner, J. L., Leir, S. H., Crawford, G. E., Cotton, C. U., and Harris, A. (2009) Intronic enhancers coordinate epithelial-specific looping of the active CFTR locus, *Proc Natl Acad Sci U S A 106*, 19934-19939.
281. Dubois, M. F., Bellier, S., Seo, S. J., and Bensaude, O. (1994) Phosphorylation of the RNA polymerase II largest subunit during heat shock and inhibition of transcription in HeLa cells, *J Cell Physiol 158*, 417-426.
282. Yankulov, K., Yamashita, K., Roy, R., Egly, J. M., and Bentley, D. L. (1995) The transcriptional elongation inhibitor 5,6-dichloro-1-beta-D-ribofuranosylbenzimidazole inhibits transcription factor IIH-associated protein kinase, *J Biol Chem 270*, 23922-23925.
283. Zandomeni, R., Mittleman, B., Bunick, D., Ackerman, S., and Weinmann, R. (1982) Mechanism of action of dichloro-beta-D-ribofuranosylbenzimidazole: effect on in vitro transcription, *Proc Natl Acad Sci U S A 79*, 3167-3170.
284. Bultman, S., Gebuhr, T., Yee, D., La Mantia, C., Nicholson, J., Gilliam, A., Randazzo, F., Metzger, D., Chambon, P., Crabtree, G., and Magnuson, T. (2000) A Brg1 null mutation in the mouse reveals functional differences among mammalian SWI/SNF complexes, *Mol Cell 6*, 1287-1295.
285. Sullivan, E. K., Weirich, C. S., Guyon, J. R., Sif, S., and Kingston, R. E. (2001) Transcriptional activation domains of human heat shock factor 1 recruit human SWI/SNF, *Mol Cell Biol 21*, 5826-5837.
286. Rodriguez, P., Bonte, E., Krijgsveld, J., Kolodziej, K. E., Guyot, B., Heck, A. J., Vyas, P., de Boer, E., Grosveld, F., and Strouboulis, J. (2005) GATA-1 forms distinct activating and repressive complexes in erythroid cells, *EMBO J 24*, 2354-2366.
287. Iborra, F. J., Pombo, A., Jackson, D. A., and Cook, P. R. (1996) Active RNA polymerases are localized within discrete transcription "factories' in human nuclei, *J Cell Sci 109 (Pt 6)*, 1427-1436.
288. Eskiw, C. H., Rapp, A., Carter, D. R., and Cook, P. R. (2008) RNA polymerase II activity is located on the surface of protein-rich transcription factories, *J Cell Sci 121*, 1999-2007.
289. Mitchell, J. A., and Fraser, P. (2008) Transcription factories are nuclear subcompartments that remain in the absence of transcription, *Genes Dev 22*, 20-25.
290. Ragoczy, T., Bender, M. A., Telling, A., Byron, R., and Groudine, M. (2006) The locus control region is required for association of the murine beta-globin locus with engaged transcription factories during erythroid maturation, *Genes Dev 20*, 1447-1457.

-APPENDIX-

	0h	0.5h	1h	2h	4h	6h
HA	1.801369	64.7339	80.13987	97.50142	86.37124	73.45061
adjusted	1.84753	66.39277	82.19353	99.99999	88.58459	75.33286
avedev	1.24327	12.47907	10.82557	3.843898	6.989009	11.08893
GATA-1	14.90633	60.80924	82.92504	99.99991	92.61134	81.06512
adjusted	14.90634	60.80929	82.92512	100	92.61142	81.06519
avedev	6.117265	15.44815	11.2811	5.89E-05	5.555293	11.6245
NFE2	29.50108	41.52324	69.3297	80.14161	83.94628	85.08529
adjusted	34.67236	48.8019	81.48259	94.18974	98.66133	100
avedev	6.811413	7.155626	15.48496	13.63184	10.70206	19.88727
Ldb1	18.04724	58.71782	77.19904	98.84354	97.8461	84.39962
adjusted	18.25839	59.40481	78.10226	100	98.99089	85.38709
avedev	5.016028	5.258073	5.174976	1.559647	2.179604	7.018557
H3	98.53901	81.84337	74.14601	80.06199	71.74614	51.74013
adjusted	100	83.05682	75.24533	81.24903	72.80989	52.50726
avedev	2.057614	13.57317	7.957061	9.696354	19.11535	10.44102
CBP	9.084053	52.09659	79.11228	89.23442	95.57848	86.19895
adjusted	9.504287	54.50661	82.77206	93.36246	100	90.18657
avedev	7.967019	15.85751	12.26624	12.56864	6.665447	5.602623
p300	5.984702	52.13617	68.42648	90.32072	87.09362	87.3239
adjusted	6.626056	57.72338	75.75945	100	96.42706	96.68203
avedev	3.877463	9.152849	17.18601	9.74266	12.51815	13.53211
Brg1	13.80573	36.14627	54.5207	73.8947	93.57664	76.84953
adjusted	14.75339	38.62746	58.26315	78.96704	100	82.12469
avedev	12.78694	10.90812	6.821963	8.398992	10.98097	16.1693
Pol-II	15.95052	36.34266	58.96351	92.56333	83.12579	71.03676
adjusted	17.23201	39.26248	63.70072	99.99999	89.80423	76.74396
avedev	5.661191	10.55942	16.08684	10.7126	17.84768	2.168136
Ser5 pol-II	61.32248	73.55018	95.15289	90.22864	74.47872	96.89833
adjusted	63.28539	75.90449	98.19869	93.11681	76.86275	100
avedev	11.73774	11.12053	3.335871	5.455349	9.944048	4.268225
AcH3	52.65018	72.57671	52.17655	70.03081	47.38695	100.0001
adjusted	52.65012	72.57664	52.17649	70.03074	47.3869	100
avedev	20.09764	18.28221	8.268873	2.660102	16.66891	1.37E-05

APPENDIX A.1. Data set summary of ChIP studies at the HS2 region

	0h	0.5h	1h	2h	4h	6h
HA	9.586668	53.87302	78.41537	94.45023	81.72498	89.34918
adjusted	10.14997	57.03853	83.02295	100	86.52703	94.59922
avedev	2.599608	7.354256	14.44883	7.8343	19.34888	0.93448
GATA-1	44.30199	59.14166	75.66742	98.00204	100.0001	83.54654
adjusted	44.30195	59.1416	75.66735	98.00194	100	83.54645
avedev	1.890815	10.808	15.6753	1.331986	2.94E-05	9.154681
Nfe2	37.28682	31.09978	51.80281	77.11973	100.0003	87.24628
adjusted	37.28671	31.09969	51.80265	77.11949	100	87.24602
avedev	10.47532	4.208289	6.593663	5.206588	0.001325	6.392977
Ldb1	63.31544	75.00245	87.52408	82.84914	88.95931	86.75062
adjusted	71.17348	84.31097	98.38665	93.1315	100	97.51719
avedev	6.911983	2.917645	3.370524	12.73152	6.654355	8.607567
H3	82.61668	84.21346	68.72063	86.941	87.90027	67.72048
adjusted	93.98911	95.80569	78.18022	98.90868	100	77.0424
avedev		17.95939	2.135855	0.339942	13.76533	19.46381
CBP	22.78603	40.37351	81.74094	92.45624	94.20667	81.72991
adjusted	24.18728	42.85631	86.76767	98.14192	100	86.75597
avedev	1.700882	10.53969	7.336623	8.007129	8.199061	10.76815
p300	25.954	45.2605	55.8216	95.50993	95.73766	88.13926
adjusted	27.10952	47.27558	58.30687	99.7622	100.0001	92.06338
avedev	6.925466	6.51978	11.19451	3.753328	5.341917	10.30206
Brg1	22.34441	30.14391	52.54015	73.05471	99.99768	76.48899
adjusted	22.34493	30.14461	52.54137	73.0564	100	76.49076
avedev	6.889092	8.798016	10.68907	11.27477	0.00329	15.16332
Pol-II	49.75441	39.06325	43.19915	78.2017	96.07987	74.04873
adjusted	51.78443	40.65706	44.96171	81.39239	100	77.06997
avedev	9.550974	10.62317	9.725943	15.58926	6.119773	14.66831
Ser5 pol-II	53.05448	57.11941	77.58418	94.58562	75.3002	84.04767
adjusted	56.09149	60.38911	82.02534	100	79.61062	88.85883
avedev	14.80071	10.11037	5.789696	4.97697	7.592902	22.48747
AcH3	54.22936	84.77571	55.09682	81.35893	58.89413	63.28937
adjusted	63.96804	100	64.99128	95.96962	69.47053	74.65508
avedev	32.72243	11.97223	9.56497	14.65915	13.13722	28.86882
H3K4Me3	33.79542	29.64089	37.85183	44.57541	47.41548	100.0009
adjusted	33.79511	29.64063	37.85149	44.57501	47.41505	100
avedev	8.396097	2.963162	9.040302	6.911267	7.061064	0.00386

APPENDIX A.2. Data set summary of ChIP studies at the HS3 region

	0h	0.5h	1h	2h	4h	6h
HA	7.538155	30.64144	44.27151	79.472	92.19904	91.29061
corrected	8.175959	33.23401	48.01732	86.19613	100	99.01471
avedev	4.113254	13.55086	14.85934	13.17444	9.489323	8.710201
GATA-1	22.8986	51.35952	67.97138	86.52927	99.9964	86.44928
corrected	22.89943	51.36137	67.97382	86.53238	100	86.45239
avedev	1.835455	10.67273	12.19006	16.85254	0	9.034348
NFE2	7.834034	37.04693	70.57414	86.23684	85.69313	83.45628
corrected	9.084325	42.95952	81.83757	100	99.36951	96.77567
avedev	3.921877	18.46	29.42635	13.25243	13.73191	15.09056
Ldb1	7.722885	71.69493	74.88747	91.52521	77.5489	87.28156
corrected	8.437987	78.33353	81.82169	100	84.72955	95.36341
avedev	8.513687	8.077687	4.689047	8.474782	9.500666	12.72039
H3	88.93475	89.03317	74.88781	81.13196	70.64882	53.56638
corrected	99.88946	100	84.11226	91.12555	79.35112	60.16452
avedev	12.42828	12.31775	9.460875	14.42065	15.5068	10.50499
p300	14.94397	25.08986	39.72406	84.07849	97.1329	84.61337
corrected	14.94391	25.08976	39.7239	84.07816	97.13251	84.61303
avedev	4.728752	6.086935	5.560615	11.53381	2.868277	15.38614
CBP	9.08231	17.83641	58.54303	73.30746	95.65528	83.98711
corrected	9.082468	17.83673	58.54405	73.30874	95.65694	83.98857
avedev	6.054873	9.94522	3.296853	14.49896	6.513026	10.6761
Brg1	2.714785	23.39652	36.04299	68.22202	99.99997	79.94198
corrected	2.714786	23.39652	36.043	68.22204	100	79.942
avedev	1.809857	13.5444	18.83759	8.130003	0.000245	2.410179
Pol-II	12.82944	17.33204	21.77835	60.95066	92.90869	74.79753
corrected	13.80866	18.65491	23.4406	65.60276	100	80.5065
avedev	5.905082	8.863585	2.219495	13.0688	9.455796	16.80155
Ser5 Pol-II	6.164933	34.69103	34.52872	60.69423	74.47463	91.08362
corrected	6.768432	38.08701	37.90881	66.63573	81.76512	100
avedev	8.219911	14.37047	3.472405	15.0257	17.00666	11.89277
AcH3	33.5304	47.59911	50.21884	75.35248	56.96904	93.21142
corrected	35.97241	51.06575	53.87627	80.84039	61.11809	100
avedev	10.89589	8.880998	8.40925	16.4318	21.42774	9.051318
	11.68943	9.527801	9.021695	17.62853	22.98832	9.710524
H3K4Me3	7.992003	9.078222	4.936811	21.32247	49.25114	99.98835
corrected	7.992934	9.07928	4.937386	21.32495	49.25688	100
avedev	3.615397	5.050803	0.889904	7.452708	20.3381	0.008524

APPENDIX A.3. Data set summary of ChIP studies at the β-globin promoter.

	0h	0.5h	1h	2h	4h	6h
HA	1.094794	50.54814	64.94824	91.84516	83.5941	82.71194
corrected	1.192	55.03626	70.71493	100	91.01634	90.05585
avedev	0.602851	14.27959	10.27074	11.83843	11.34565	10.68417
GATA-1	3.966226	56.05695	69.22608	89.88552	92.84612	80.32731
corrected	4.271827	60.37619	74.56002	96.81129	100	86.51661
avedev	2.135914	8.85055	13.88096	14.11003	10.27329	8.616599
NFE2	1.660242	41.2257	46.16263	83.79044	95.73261	99.9926
corrected	1.660365	41.22875	46.16604	83.79664	95.73969	100
avedev	1.110608	16.37835	15.0634	13.85113	4.280134	0.008316
Ldb1	5.133656	55.34218	77.02542	88.4495	96.37491	81.6407
corrected	5.326756	57.42385	79.92269	91.77648	100	84.71157
avedev	3.699216	9.293302	5.303084	15.97975	4.027461	10.04994
H3	99.99998	58.86597	47.51612	41.78259	30.26461	17.47812
corrected	100	58.86598	47.51613	41.7826	30.26461	17.47812
avedev	2.77E-05	11.62762	8.781506	8.711058	8.283937	6.220828
CBP	5.334963	29.3867	43.69075	89.81762	94.12344	91.22305
corrected	5.668049	31.22145	46.41857	95.42534	100	96.91852
avedev	8.588855	12.10509	20.06483	3.814779	7.492013	7.459074
p300	4.075442	39.23637	51.82684	81.06883	84.31561	93.10785
corrected	4.37712	42.14078	55.66324	87.06981	90.55693	100
avedev	5.363379	10.72338	9.725522	6.777482	11.23285	9.870444
Brg1	5.472131	21.73601	38.12208	62.29688	94.33946	86.74127
corrected	5.800469	23.04021	40.40947	66.0348	100	91.9459
avedev	3.859898	3.20878	10.68988	10.50763	9.616667	10.73668
Pol-II	6.845833	27.88026	46.67346	91.54212	87.44558	93.62055
corrected	7.312319	29.78007	49.85387	97.77994	93.40426	100
avedev	5.290794	14.50033	14.96499	7.228101	16.21899	10.45477
Ser5 Pol-II	10.79451	24.86443	39.95909	56.22588	71.67653	100.0001
corrected	10.7945	24.86441	39.95905	56.22582	71.67646	100
avedev	5.868574	5.25432	5.443505	10.34769	11.31471	0.00021
AcH3	44.17246	30.57684	37.02087	84.35553	61.14743	86.95733
corrected	50.79785	35.16304	42.57361	97.00796	70.31889	100
avedev	31.22161	1.665082	3.109674	17.98771	10.94898	14.99832

APPENDIX A.4. Data set summary of ChIP studies at the AHSP promoter.

	0h	0.5h	1h	2h	4h	6h
HA	2.178882	81.59286	86.04248	91.30288	74.77829	83.70748
corrected	2.386433	89.36504	94.23851	100	81.90135	91.6811
avedev	1.378527	2.130289	9.108335	8.835576	7.832378	15.0789
GATA-1	15.96204	81.55729	92.54212	93.25762	87.60105	79.06476
corrected	17.11607	87.45376	99.23277	100	93.93447	84.78102
avedev	3.855578	3.340108	8.046089	9.639588	2.655377	7.470544
NFE2	4.253755	30.7132	34.42788	75.63888	72.48621	76.88613
corrected	5.623768	40.60504	45.51612	100	95.83195	101.649
avedev	5.623768	18.60883	16.99249	32.206	18.75939	30.56324
Ldb1	6.085546	78.61565	87.19915	80.57887	86.34437	82.67758
corrected	6.978905	90.15644	100	92.40786	99.01974	94.81466
avedev	4.22071	20.23945	28.02844	13.70988	10.29233	9.97077
H3	100	41.38305	28.29416	29.56148	33.22295	23.83587
corrected	100	41.38305	28.29416	29.56148	33.22295	23.83587
avedev	9.62E-06	9.904533	3.326602	6.54826	6.080241	3.262332
AcH3	8.796415	36.2717	52.42269	86.26665	65.85564	75.18095
corrected	10.19677	42.04603	60.7682	100	76.33963	87.1495
avedev	5.050674	1.928358	2.931772	15.91987	8.689899	28.77047
p300	3.063039	64.75715	73.30456	84.59278	82.27232	92.34577
corrected	3.316926	70.12469	79.38057	91.60444	89.09164	100.0001
avedev	3.418897	14.09578	14.96608	16.13624	15.57003	9.157767
CBP	6.809514	35.70582	78.65172	84.74838	82.47004	96.04713
corrected	7.089771	37.17535	81.88876	88.23633	85.86423	100.0001
avedev	6.363612	18.02145	20.20743	8.729432	12.97623	4.938959
BRG1	2.691094	32.12184	71.68598	82.42187	90.81762	97.61342
corrected	2.756889	32.9072	73.43865	84.43703	93.03804	100
avedev	2.573262	7.546258	5.716407	20.6152	9.406944	2.493511
Pol-II	2.792433	78.73503	83.35292	99.99998	74.542	74.42116
corrected	2.792433	78.73505	83.35294	100	74.54202	74.42117
avedev	1.776766	16.18026	9.294555	0.000166	11.44626	12.89387
Ser5 pol-II	5.296753	64.28375	81.2993	83.29443	80.19123	86.79473
corrected	6.10262	74.06412	93.66848	95.96715	92.39182	100
avedev	3.038747	19.16302	20.69233	16.16652	11.15372	8.592889

APPENDIX A.5. Data set summary of ChIP studies at the Dematin ECRa region

	0h	0.5h	1h	2h	4h	6h
HA	1.971385	74.23606	89.22086	75.95166	89.16561	82.29505
corrected	2.210925	83.25638	100.062	85.18044	100	92.29461
avedev	0.87132	12.95164	16.11851	16.73371	16.02204	8.195167
GATA-1	12.59857	52.08124	66.59194	88.87467	86.77321	69.67586
corrected	14.17566	58.60076	74.92792	100	97.63547	78.39788
avedev	4.530445	8.750941	15.5005	16.69072	14.88248	14.46745
NFE2	4.783618	31.79932	40.24304	80.11256	82.40126	60.13299
corrected	5.805273	38.59082	48.8379	97.2225	100	72.97581
avedev	0.102959	18.86185	5.986158	24.13428	21.36503	9.775457
Ldb1	43.01186	89.90017	95.24103	91.03584	69.96209	73.47252
corrected	45.16106	94.39227	100	95.58468	73.45794	77.14377
avedev	1.892036	10.60429	4.996774	4.122825	23.28512	15.30197
H3	99.99993	31.63482	27.93421	29.66799	31.70372	24.82695
corrected	99.99993	31.63482	27.93421	29.66799	31.70372	24.82695
avedev	7.1E-06	0.145936	5.807918	0.567373	8.07633	0.240998
CBP	2.51144	33.25803	89.17239	81.83348	91.67375	71.65713
corrected	2.748445	36.3966	97.58761	89.55613	100.325	78.41943
avedev	0.219699	7.190121	1.726928	19.81657	12.10979	17.88011
p300	8.972353	58.88899	89.07806	85.28103	84.60688	92.84946
corrected	9.663333	63.42416	95.93816	91.84871	91.12264	100
avedev	2.361416	15.59708	15.68408	11.96816	16.57847	7.584591
Brg1	4.73853	30.21163	67.50849	67.90881	100	77.28299
corrected	4.73853	30.21163	67.50849	67.90881	100	77.28299
avedev	2.622737	12.20899	8.386771	8.977647	0.000131	8.24521
Pol-II	10.66212	67.59202	78.17496	95.37888	82.18821	64.06117
corrected	11.1787	70.86686	81.96254	100	86.17024	67.16495
avedev	2.567234	12.22593	15.25501	6.459995	7.757476	12.96191
Ser5 pol-II	14.1007	74.16175	98.80309	84.96077	84.55882	74.09659
corrected	14.27152	75.06016	100	85.98999	85.58318	74.9942
avedev	7.202087	4.856617	1.615009	15.22143	6.089624	16.86163
AcH3	46.16839	70.71847	64.7774	93.18568	78.49635	71.87629
corrected	49.54457	75.88994	69.51441	100.0001	84.2366	77.13242
avedev	7.845485	9.774375	11.41876	7.312457	8.878268	15.28971
H3K4Me3	57.16928	21.44326	22.54404	23.37301	89.14859	97.73779
corrected	58.4925	21.93957	23.06584	23.914	91.212	100
avedev	13.79414	4.148905	2.686797	1.041811	14.80317	1.618678

APPENDIX A.6. Data set summary of ChIP studies at the ALAD promoter

Antibody	HA	Ldb1
	58.0117	83.81146
	16.14494	62.32712
	31.62581	68.94621
	8.2303	
	20.12108	
	46.65012	
	33.70613	
Total number of ChIPs	3	8
p value =		**0.003071**

APPENDIX A.7. Significance of the detected kinetic differences at the β-globin promoter. p values determined using the Student T test associated to the % occupancy of a factor in relation to EKLF's occupancy at t=0.5h.

A.

Antibody	HA	CBP	Brg1	Ser5
	60.20587	39.1133	23.10258	22.8575
	70.80481	9.945059	15.68172	20.1539
	36.41355	29.40741	23.76299	18.44609
	31.89496	20.34403	24.39674	25.78238
	53.42151	48.1237		37.0823
Total number of ChIPs	5	5	4	5
p value =		0.032647	0.005629	0.006174

B.

Antibody	HA	CBP	Brg1	Ser5
	65.46466	28.7985	31.01471	26.35031
	73.17677	14.45085	47.27998	42.48518
	50.40829	67.36006	54.1761	48.29174
	51.18866	40.60864	20.17227	42.58529
	67.82928	67.23572	37.96732	40.08291
	81.62177			
Total number of ChIPs	6	5	5	5
p value =		0.04235	0.00354	0.001892

C.

Antibody	HA	Brg1	Ser5
	99.99979	56.63161	40.77666
	99.99991	77.84986	71.13295
	99.99999	48.13647	67.18807
	75.64803	66.56956	51.28359
	100		50.74813
	75.4232		
Total number of ChIPs	6	4	5
p value =		0.003472	0.000592

APPENDIX A.8. Significance of the detected kinetic differences at the AHSP promoter. p values determined using the Student T test associated to the % occupancy of a factor in relation to EKLF's occupancy at A. t=0.5h, B. t=1h and C. t=2h.

Antibody	HA	CBP	p300	Brg1
	83.54732	75.94584	69.08292	42.85459
	78.67533	11.8036	98.67636	20.45102
	82.55592	20.26272	77.2082	36.12141
		45.28929	66.12857	
		31.77843	64.3133	
			62.18324	
			38.7385	
			35.17535	
Total number of ChIPs	3	8	5	3
p value =		0.012542	0.089886	0.001026

APPENDIX A.9. Significance of the detected kinetic differences at the Dematin promoter. p values determined using the Student T test associated to the % occupancy of a factor in relation to EKLF's occupancy at t=0.5h.

Antibody	HA	CBP	Brg1
	84.9405	17.75952	48.52512
	65.91952	39.84948	19.60566
	51.99365	26.66657	23.15009
Total number of ChIPs	3	8	5
p value =		**0.013198**	**0.00894**

APPENDIX A.10. Significance of the detected kinetic differences at the ALAD promoter. p values determined using the Student T test associated to the % occupancy of a factor in relation to EKLF's occupancy at t=0.5h.

-ABBREVIATIONS-

3C	Chromosome Conformation Capture
4-OH-TAM	4-Hydroxy-Tamoxifen
aa	Amino acid
ACF1	ATP-utilizing chromatin assembly and remodeling factor
ACH	Active Chromatin Hub
AcH3	Acetylated Histone H3
ADD2	Adducin beta
AHSP	Alpha Hemoglobin Stabalizing Protein
ALAD	Aminolevulinate Dehydratase
ALAS2	Aminolevulinic Acid Synthase
Avedev	Average Deviation
BKLF	Bovine Krüppel Like Factor
bp	Base pair
Brg1	Brahma related gene 1
Brm	Brahma
CBP	CREB binding protein
cDNA	Complementary Deoxyribose Nucleic Acid
ChIP	Chromatin Immunoprecipitation
ChIP-Seq	Chromatin Immunoprecipitation Sequencing
CTCF	CCCTC-binding factor
CTD	Carboxyl Terminal Domain
cyc1	Cytochrome c1
DNA	Deoxyribose Nucleic Acid
DNaseI	Deoxyribonuclease 1
E2A	transcription Factor 3 (tcf3)
EKLF	Erythroid Krüppel-Like Factor
EMSA	Electrophoretic Mobility Shift Assay
EPO	Erythropoietin
ER	Estrogen Response element
ERC-1	EKLF coactivator remodeling complex 1
ES cells	Embryonic Stem cells
ETO2	Eight Twenty-One 2
EtOH	Ethanol
FOG-1	Friend Of GATA-1
G1E	GATA-1 estrogen response cells
GAPDH	Glyceraldehyde-3-phosphate Dehydrogenase
GATA-1	GATA binding factor 1
GFP	Green Fluorescent Protein
Glut-1	Glucose Transporter 1

GTF	General Transcription Factor
H3	Histone H3
H3K4Me1	Monomethylated Lysine 4 of Histone H3
H3K4Me2	Dimethylated Lysine 4 of Histone H3
H3K4Me3	Trimethylated Lysine 4 of Histone H3
HA	Hemagglutin A
HAT	Histone Acetyl Transferase
HDAC	Histone Deacetylase
HMT	Histone Methyl Tramsferase
HPRT	Hypoxanthine Phosphoribosyltransferase
HRP	Horseradish Peroxidase
HS	Hypersensitive Site
HS2	Hypersensitive Site 2
HS3	Hypersensitive Site 3
HSC	Hematopoietic Stem Cells
ivr5	Intervening region 5
Kb	Kilo base
KD	Kilo Dalton
KO	Knock Out
LCR	Locus Control Region
Ldb1 (Clim2/NLI)	LIM domain binding 1
LMO2	LIM domain only 2
Mel	Murine Erythroleukemia cells
MEP	Megakaryocyte-Erythroid Progenitor
mRNA	Messenger Ribonucleic Acid
NF-E2	Nuclear Factor Erythroid-derived 2
Nf-M	Neurofilament Medium chain
NLS	Nuclear Localization Signal
NuRD	Nucleosome Remodelling and Histone Deacetylation
P/CAF	p300/CREB associated factor
P2(E)	Promoter 2 Erythroid
p300 (EP300)	E1A binding protein
PBGD/hmbs	Porphobilinogen Deaminase / hydroxymethylbilane synthase
PCR	Polymerase Chain Reaction
RhoGTPase	Rhodopsin Guanosine Triphosphatase
RNA	Ribonucleic Acid
RNA Pol-II	Ribonucleic Acid Polymerase 2
Rnase	Ribonuclease
RNR3	Ribonucleic Acid Ribosomal 3
SCL/TAL-1	Stem Cell Leukemia /T-cell acute lymphocytic leukemia protein 1
SEM	Standard Error of the Mean
Ser5 Pol-II	Ribonucleic Acid Polymerase 2 phosphorylated on Ser5 residue of the carboxy terminal domain
sHRP	Streptavidin-conjugated Horseradish Peroxidase

SWI/SNF	SWItch/sucrose nonfermentable
TF	Transcription factor
UROD	Uroporphyrinogen Decarboxylase
WT	Wild Type
ZBP89	Zinc finger DNA-binding protein 89

-ACCOMPLISHMENTS-

POSTER PRESENTIONS

- 17th Hemoglobin Switching meeting held in Oxford (UK) in September 2010

  "Context-specific EKLF-mediated chromatin remodeling"

  Aurelie Desgardin, Tatiana Abramova, Eun-Hee Shim, John M. Cunningham
- 3rd Annual Pediatrics research Day held at the University of Chicago in May 2009

  "EKLF-mediated transcriptional activation of the β-globin gene in erythroid cells"

  Aurelie Desgardin, Tatiana Abramova, Eun-Hee Shim, John M. Cunningham.
- 2nd Annual Pediatrics Research Day held at the University of Chicago in May 2008

  "Context-specific EKLF-mediated chromatin remodeling"

  Aurelie Desgardin, Tatiana Abramova, Eun-Hee Shim, John M. Cunningham.

ORAL PRESENTATIONS

- Blood (51st American Society of Hematology (ASH) Annual Meeting Abstracts), Nov 2009; **114**: 461.

  "Context-Specific KLF-1 Mediated Transcriptional Activation at the Alpha Hemoglobin-Stabilizing Protein and Dematin Promoters in Erythroid Cells."

  Aurelie Desgardin, Valerie M. Jansen, Eun-Hee Shim, Tatiana Abramova, Shaji Ramachandran, Stephen Jane, and John M Cunningham

ADDITIONAL ABSTRACTS

- Blood (48th American Society of Hematology (ASH) Annual Meeting Abstracts), Nov 2006; **108**: 365.

  "Context-Specific Roles for Erythroid Krüppel-Like Factor (EKLF) in Co-Ordinate High Level Expression of the Murine α- and β-Globin Genes."
  Valerie M. Jansen, Shaji Ramachandran, Aurelie Desgardin, Jin He, Vishwas Parekh, Stephen M. Jane, and John M. Cunningham
- Blood (50th American Society of Hematology (ASH) Annual Meeting Abstracts), Nov 2008; **112**: 132.

  "Altered Erythroid and Megakaryocytic Differentiation in Mice Expressing a Unique Chromatin Remodeling Domain of Erythroid Krüppel-Like Factor (EKLF)"
  Valerie Jansen, Tatiana Abramova, Eun-Hee Shim, Shaji Ramachandran, Aurelie Desgardin, Vishwas Parekh, Stephen Jane and John Cunningham.

HONORS AND AWARDS

- "Best poster presentation/abstract by a student" award received in conjunction with the 2nd Annual Pediatrics Research Day held at the University of Chicago in May 2008

  "Context-specific EKLF-mediated chromatin remodeling"
  Aurelie Desgardin, Tatiana Abramova, Eun-Hee Shim, John M. Cunningham.

PUBLICATIONS

- *"Context-specific EKLF-mediated chromatin remodeling"*
  Aurelie Desgardin, Tatiana Abramova, Eun-Hee Shim, John M. Cunningham.
  Manuscript in writing

- *"EKLF regulates the expression of the ALAD gene in erythroid cells"*
  Aurelie Desgardin, Tatiana Abramova, Eun-Hee Shim, John M. Cunningham.
  Manuscript in writing